Reaction and Transport Processes Controlling In Situ Chemical Oxidation of DNAPLs

SERDP Project CU-1290

Final Report

Submitted to:

Strategic Environmental Research and Development Program

Prepared by:

Principal Investigators:	Robert L. Siegrist, Ph.D., P.E. Michelle Crimi, Ph.D. Junko Munakata-Marr, Ph.D. Tissa Illangasekare, Ph.D., P.E.
Research Staff:	Kathryn Lowe, M.S. Sheila Van Cuyk, Ph.D.
Research Students:	Pamela Dugan Jeff Heiderscheidt Shannon Jackson Ben Petri Jason Sahl Sarah Seitz

Colorado School of Mines
Environmental Science and Engineering Division
Center for Experimental Study of Subsurface Environmental Processes
Golden, Colorado 80401-1887

November 1, 2006

REPORT DOCUMENTATION PAGE

Form Approved
OMB No. 0704-0188

PLEASE DO NOT RETURN YOUR FORM TO THE ABOVE ORGANIZATION.

1. REPORT DATE *(DD-MM-YYYY)*	2. REPORT TYPE	3. DATES COVERED *(From - To)*
01-11-2006	Final Project Report	September 2002 - June 2006

4. TITLE AND SUBTITLE
"Reaction and Transport Processes Controlling In Situ Chemical Oxidation of DNAPLs"

5a. CONTRACT NUMBER
DACA72-02-C-0012

5b. GRANT NUMBER

5c. PROGRAM ELEMENT NUMBER

6. AUTHOR(S)
Siegrist, Robert L.; Crimi, Michelle L.; Munakata-Marr, Junko; Illangasekare, Tissa; Dugan, Pamela; Heiderscheidt, Jeff; Jackson, Shannon; Petri, Ben; Sahl, Jason; Seitz, Sarah; Lowe, Kathryn; Van Cuyk, Sheila

5d. PROJECT NUMBER
CU-1290

5e. TASK NUMBER

5f. WORK UNIT NUMBER

7. PERFORMING ORGANIZATION NAME(S) AND ADDRESS(ES)
Colorado School of Mines, Environmental Science and Engineering, Center for Experimental Study of Subsurface Environmental Processes, 206 Coolbaugh Hall, Golden, Colorado, 80401-1887

8. PERFORMING ORGANIZATION REPORT NUMBER

9. SPONSORING/MONITORING AGENCY NAME(S) AND ADDRESS(ES)
Strategic Environmental Research and Development Program (SERDP) with funds administered via the U.S. Army Corps of Engineers, 420 So. 18th Street, Omaha, Nebraska, 68102-2586

10. SPONSOR/MONITOR'S ACRONYM(S)
SERDP; USACOE

11. SPONSOR/MONITOR'S REPORT NUMBER(S)
CU-1290

12. DISTRIBUTION/AVAILABILITY STATEMENT
This is a final report document provided in accordance with SERDP final reporting.

13. SUPPLEMENTARY NOTES

14. ABSTRACT
In situ chemical oxidation involves the introduction of chemical oxidants into the subsurface to destroy organic contaminants in soil and ground water, with the goal being to reduce the mass, mobility, and/or toxicity of contamination. The objective of this project was to quantify the pore/interfacial scale DNAPL reactions and porous media transport processes that govern the delivery of oxidant to a DNAPL-water interface and degradation of the DNAPL. In this project, an integrated set of tasks were carried out involving a comparative analysis focused on contrasting oxidant types (permanganate and catalyzed hydrogen peroxide) and oxidant application methods (low to high dose concentrations and delivery densities) to treat a mixture of tetrachloroethene (PCE) and trichloroethene (TCE) DNAPL present in mass levels and distributions under conditions representative of a range of subsurface environmental settings. The research also addressed the potential secondary effects of applications of ISCO, as well as the coupling of ISCO with pre- and post-ISCO treatment operations.

15. SUBJECT TERMS
Remediation of contaminated sites, groundwater cleanup, dense nonaqueous phase liquids, coupling chemical and biological methods, partitioning tracer test methods, human health and environmental risk reduction

16. SECURITY CLASSIFICATION OF:			17. LIMITATION OF ABSTRACT	18. NUMBER OF PAGES	19a. NAME OF RESPONSIBLE PERSON
a. REPORT	b. ABSTRACT	c. THIS PAGE			Dr. Robert L. Siegrist
					19b. TELEPHONE NUMBER *(Include area code)* 303-384-2158

Reset

Standard Form 298 (Rev. 8/98)
Prescribed by ANSI Std. Z39.18

TABLE OF CONTENTS

List of Figures iv

List of Tables vi

Acknowledgements viii

Acronyms and Abbreviations ix

Executive Summary xiv

Chapter 1. Introduction 1-1
- 1.1. Project Purpose and Scope 1-1
- 1.2. Background and Motivations 1-1
  - 1.2.1. DNAPL Contamination at DOD Sites 1-1
  - 1.2.2. Evolution of ISCO and its Application to DNAPL Sites 1-2
  - 1.2.3. Knowledge Gaps Concerning ISCO Applied to DNAPL Sites at the Start of Project CU-1290 1-8
- 1.3. Project Approach 1-9
- 1.4. Organization of This Report 1-10
- 1.5. References 1-10

Chapter 2. Background Theory and Relevant Prior Research Findings 2-1
- 2.1. Introduction 2-1
- 2.2. DNAPL Behavior and Application of ISCO 2-2
  - 2.2.1. DNAPL Movement and Entrapment in the Subsurface 2-2
  - 2.2.2. Remediation of DNAPL Source Zones and Plumes 2-3
- 2.3. Chemical Oxidation for Remediation of DNAPLs 2-5
  - 2.3.1. Introduction 2-5
  - 2.3.2. Oxidation of Aqueous Phase PCE and TCE 2-6
  - 2.3.3. ISCO-Enhanced Degradation of DNAPL-Phase PCE and TCE 2-9
- 2.4. Oxidant Persistence and Stability in the Subsurface 2-21
  - 2.4.1. Introduction 2-21
  - 2.4.2. Natural Oxidant Demand for Permanganate 2-21
  - 2.4.3. Persistence and Stability of Hydrogen Peroxide 2-23
- 2.5. ISCO Effects on Subsurface Permeability 2-24
  - 2.5.1. Introduction 2-24
  - 2.5.2. Effects of Permanganate on Subsurface Permeability 2-24
- 2.6. Application of ISCO to Low Permeability Zones 2-26
  - 2.6.1. Introduction 2-26
  - 2.6.2. DNAPL Contamination in Low Permeability Media 2-26
  - 2.6.3. Diffusion in LPM Zones 2-27
  - 2.6.4. ISCO Application to Sites with LPM 2-28
- 2.7. Mathematical Modeling and Computer Code Development for ISCO 2-29
  - 2.7.1. Introduction 2-29
  - 2.7.2. Mathematical Modeling 2-29
  - 2.7.3. Numerical Modeling of ISCO 2-31
- 2.8. Coupling ISCO with Other Remediation Methods 2-32
  - 2.8.1. Coupling ISCO with Bioremediation 2-32
  - 2.8.2. Coupling of ISCO with Surfactant Enhanced Aquifer Restoration 2-36

2.9. Partitioning Tracers for Performance Assessment at ISCO Sites 2-40
2.9.1. Introduction 2-40
2.9.2. Application of Partitioning Tracers at ISCO Sites 2-40
2.10. References 2-44

Chapter 3. Materials and Methods 3-1
3.1. Specific Experimental Objectives and Approaches 3-1
3.1.1. Bench-Scale Kinetic and DNAPL Degradation Studies 3-1
3.1.2. Bench-Scale Studies of Porous Media Effects on Oxidation Reactions 3-1
3.1.3. Upscaling Reactive Transport During ISCO: Experimental and Modeling Studies 3-1
3.1.4. Experimental Evaluation of Coupling of ISCO 3-2
3.1.5. Evaluation of Partitioning Tracer Test (PTT) Methods for Site Characterization and Performance Monitoring 3-2
3.2. Materials and Methods Common to Multiple Experimental Studies 3-2
3.2.1. Conceptual Model Used for Experimental Design 3-2
3.2.2. Porous Media Types Used in Investigations 3-3
3.2.3. Ground Water Types Used in Investigations 3-4
3.2.4. Properties of Key Reagents Used in this Study 3-4
3.2.5. Quantitative Analytical Methods 3-5
3.2.6. Common Data Analysis Techniques 3-7
3.3. Bench-Scale Kinetic and DNAPL Degradation Studies 3-7
3.3.1. Aqueous Phase Vial Reactor Studies 3-7
3.3.2. Multiple Phase Vial Reactor Studies 3-8
3.4. Bench-Scale Studies of Porous Media Effects on Oxidation Reactions 3-9
3.4.1. Zero Headspace Reactor Studies 3-9
3.4.2. Natural Oxidant Demand Studies for Diffusion Cell Core Design 3-11
3.4.3. Catalyzed Hydrogen Peroxide Stabilization Studies 3-11
3.4.4. Diffusion Cell Studies 3-11
3.5. Upscaling Reactive Transport During ISCO: Experimental and Modeling Studies 3-13
3.5.1. One-Dimensional Flow-Through Tube Reactor Experiments 3-13
3.5.2. Two-Dimensional Flow Cell Studies 3-16
3.5.3. Two-Dimensional Intermediate-Scale Tank Studies 3-17
3.5.4. Two-Dimensional Large-Scale Tank Experiments 3-19
3.5.5. Development of a Model for DNAPL Remediation Using Permanganate 3-21
3.6. Experimental Evaluation of Coupling ISCO with Other Remediation Technologies 3-22
3.6.1. Screening Tests for Coupling Surfactants and Cosolvents with ISCO 3-23
3.6.2. Upscaling Experimental Evaluation of Coupling ISCO with Surfactant Flushing in 2-D Flow Cell Experiments 3-23
3.6.3. Microbial Culture Preparation for Evaluation of Coupling ISCO with Bioremediation 3-24
3.6.4. Evaluation of Permanganate Oxidation Impacts on Contaminant Degrading Cultures using 1-D Column Studies 3-24
3.6.5. Anaerobic Batch Microcosm Studies 3-26
3.7. Experimental Investigation of Partitioning Tracer Test (PTT) Methods for Performance Evaluation at ISCO Treated Sites 3-26
3.7.1. Batch Studies of Interactions Between Oxidants and Partitioning Tracers 3-27
3.7.2. Upscaling PTT Application to 1-D and 2-D Systems 3-27
3.8. References 3-28

Chapter 4. Results and Discussion 4-1
4.1. Introduction 4-1
4.2. Bench Scale Kinetic and DNAPL Degradation Studies 4-1
4.2.1. Aqueous Phase Vial Reactor Experiments 4-1
4.2.2. Multiple Phase Vial Reactor Experiments (MVRs) 4-7
4.3. Bench-Scale Studies of Porous Media Effects on Oxidation Reactions 4-13
4.3.1. Zero Headspace Reactor Studies 4-13
4.3.2. Diffusion Cell Studies 4-14
4.4. Upscaling Reaction and Transport During ISCO: Experimental and Modeling Studies 4-22
4.4.1. Flow-Through Tube Reactor Studies 4-22
4.4.2. Two-Dimensional Flow Cell Studies 4-27
4.4.3. Two-Dimensional Intermediate-Scale Tank Experiments 4-29
4.4.4. Large-Scale Tank Experiments 4-34
4.4.5. Evaluation of the CORT3D Model for Performance Prediction and Evaluation of ISCO Using Permanganate 4-37
4.5. Experimental Evaluation of Coupling ISCO with Other Remediation Technologies 4-46
4.5.1. Coupling ISCO with Surfactant/Cosolvent Flushing 4-46
4.5.2. Coupling ISCO with Bioremediation 4-53
4.6. Experimental Investigation of Partitioning Tracer Test (PTT) Methods for Performance Evaluation at ISCO Treated Sites 4-60
4.6.1. Batch Studies of Interactions Between Oxidants and Partitioning Tracers 4-60
4.6.2. Evaluation of Partitioning Tracer Methods in a 2-D Flow Cell for Remediation Performance Assessment 4-65
4.7. Summary of Major Findings Common to Multiple Research Elements 4-65
4.7.1. Oxidant Type 4-65
4.7.2. Oxidant Concentration and Subsurface Delivery 4-66
4.7.3. Subsurface Environmental Characteristics 4-67
4.7.4. Coupling ISCO with other Remediation Methods 4-69
4.8. Practical Implications 4-70
4.8.1. General Implications 4-70
4.8.2. Site-Specific Implications 4-72
4.9. References 4-75

Chapter 5. Summary, Conclusions and Recommendations 5-1
5.1. Summary and Conclusions 5-1
5.2. Recommendations 5-4

Appendix A. Supplementary Experimental Studies A-1

Appendix B. List of Technical Publications B-1

Appendix C. Other Technical Material C-1

LIST OF FIGURES

1.1. Illustration of a DNAPL source zone leading to long-term contamination of subsurface soil and ground water. 1-2
1.2. Illustration of in situ chemical oxidation where injection wells or direct-push probes are used to deliver oxidants into the subsurface to cleanup soil and ground water contamination 1-6

2.1. Macro- and micro-scale features of in situ chemical oxidation for DNAPL sites 2-1
2.2. Conceptual model of a DNAPL site 2-3
2.3. Thin film model for DNAPL dissolution 2-9
2.4. Thin film model with chemical oxidation 2-14
2.5. Conceptual models for permanganate depletion by NOD 2-21

3.1. Conceptual model for design of experiments to evaluate ISCO applied to DNAPL sites 3-3
3.2. ZHR experimental apparatus 3-10
3.3. 1-D diffusion cell apparatus 3-12
3.4. FTR apparatus 3-14
3.5. 2-D cell apparatus 3-16
3.6. 2-D Intermediate-scale tank apparatus 3-18
3.7. 2-D Large-scale tank experimental apparatus at CSM 3-20

4.1. Relationships between TOC and COD with oxidant and media demand 4-8
4.2. Permanganate concentrations vs. time for sandy loam LPM 4-15
4.3. Comparison of NOD for different LPM and oxidant concentrations 4-15
4.4. Sandy loam CHP stabilization results 4-17
4.5. Effluent chamber bromide concentrations from 1D diffusion cell runs 4-18
4.6. Observation of permanganate breakthrough in cores A and B 4-20
4.7. Soil core dissection diagram 4-21
4.8. Conceptualization of mass transfer enhancement mechanism 4-25
4.9. Plot of $SR_{post\text{-}ox}$ vs. mass fraction depleted 4-26
4.10. PCE concentration distributions during the intermediate-scale tank experiments during select time points 4-30
4.11. Mass depletion data from the intermediate-scale tank study 4-31
4.12. Plot of MnO_2 distribution across the tank 4-33
4.13. Change in head drop across source zones during oxidation 4-33
4.14. Photographs of the heterogeneous large-scale 2-D experiments: (a) experiment 1, and (b) experiment 2 4-34
4.15. Plots of PCE mass flux vs. time from large-scale tank experiments: (a) experiment 1, and (b) experiment 2 4-35
4.16. PCE source zone DNAPL saturation profile from large-tank oxidation experiments 4-36
4.17. Application of the CORT3D model to data from Schroth *et al.* (2001) 4-38
4.18. Comparison of simulated and observed results for 1-D PCE oxidation – low oxidant concentration: (a) PCE concentration vs. time, and (b) chloride concentration vs. time 4-39
4.19. Comparison of simulated and observed results for 1-D PCE oxidation – High oxidant concentration 4-40
4.20. Comparison of simulations and observed results using varied mass transfer fitting parameters to account for mass transfer enhancement due to oxidation 4-41
4.21. Comparison of simulations and observed results accounting for changes in permeability resultant of MnO_2 precipitation 4-41

4.22. Comparison of simulations and observed results considering the impact of slow NOD 4-42
4.23. Simulated and observed permanganate transport in 1-D NOD column tests 4-42
4.24. Evaluation of the impact of NOD on oxidant transport simulation results 4-43
4.25. Comparison of design parameters for optimized oxidation 4-44
4.26. Comparison of high velocity oxidant injection simulations 4-45
4.27. Comparison of time and pore volumes needed to treat a hypothetical DNAPL source zone 4-46
4.28. Photo of surfactant solution color change after reaction with CHP 4-47
4.29. Hydrogen peroxide remaining after contacting residual concentrations of surfactant 4-48
4.30. Example data of oxidant degradation versus surfactant concentration 4-50
4.31. Results of short- and longer-term reaction of three different surfactants with $KMnO_4$ (5000 mg/L) 4-52
4.32. Manganese dioxide fronts observed during anaerobic column studies 4-56
4.33. Manganese dioxide concentrations (mg-Mn as MnO_2/kg-dry sand) in each dissected column 4-57
4.34. Time to activity rebound vs. hours of oxidant application 4-58
4.35. Chloroethene data from NTC batch microcosm study 4-58
4.36. Total PCE mass in Mines Park batch microcosms 4-59

LIST OF TABLES

1.1. General features of the three common ISCO technologies (information as of 2001) 1-3
1.2. Representative list of organics treated by chemical oxidants as of 2001 1-4
1.3. Examples of studies exploring ISCO treatment of DNAPLs and a summary of the observations made as of 2001 1-7
1.4. Reader's guide for the final report from SERDP project CU-1290 1-11

2.1. Gilland-Sherwood mass transfer correlations for NAPL-water systems 2-11
2.2. Laboratory studies of permanganate oxidation of DNAPLs 2-17
2.3. Field studies of in situ chemical oxidation using permanganate 2-20
2.4. Processes important to capture during numerical modeling of ISCO 2-32
2.5. Summary of research concerning the effects of ISCO on subsurface bioprocesses 2-37
2.6. Examples of field experiences with use of SEAR to remediate NAPL sites 2-39
2.7. Examples of recent field applications of SEAR and ISCO 2-40

3.1. Properties of porous media utilized in this study 3-4
3.2. Properties of ground water sources used in this study 3-5
3.3. Sources and properties of main reagents used in this study 3-5
3.4. Analytical method summaries 3-6
3.5. Experimental conditions tested in VRs 3-8
3.6. Experimental conditions tested in MVRs 3-9
3.7. ZHR study conditions. 3-10
3.8. Experimental conditions for 1-D oxidant diffusion cell studies 3-12
3.9. FTR experimental conditions 3-15
3.10. 2-D flow cell experimental conditions 3-17
3.11. Conditions of the large-scale tank ISCO investigation 3-20
3.12. NTC field site CORT3D simulation conditions 3-22
3.13. Anaerobic column study conditions 3-25
3.14. Conditions of anaerobic batch microcosm studies 3-26
3.15. Tracers evaluated during batch studies 3-28

4.1. Efficiency and effectiveness terms from vial reactor (VR) experiments 4-2
4.2. Statistically significant findings from permanganate VR studies 4-3
4.3. Statistically significant findings from CHP VR studies 4-4
4.4. System chemistry data for aqueous vial reactor (VR) experiments 4-6
4.5. Efficiency and effectiveness results from the MVR experiments 4-9
4.6. Statistically significant findings from permanganate MVR studies 4-10
4.7. Statistically significant findings from CHP MVR studies 4-12
4.8. Bromide diffusion rate in LPM diffusion cells 4-19
4.9. Oxidant and TOC results from diffusion cell soil core analysis 4-21
4.10. Summary data from the FTR trials 4-23
4.11. Efficiency and effectiveness results obtained during 2-D cell studies 4-29
4.12. Large-scale tank oxidation performance summary 4-35
4.13. Compatibility of surfactants and cosolvents with permanganate 4-49
4.14. Permanganate remaining after a 3-hr or 24-hr period of reaction of 3.5-wt.% surfactant with 5000 mg/L $KMnO_4$ 4-51
4.15. Permanganate remaining after a 24-hr period of reaction of 0.5- to 1.0-wt% surfactant with 5000 mg/L $KMnO_4$ 4-52
4.16. Average concentrations of chloroethenes from the anaerobic column experiments 4-54

4.17. Observations that indicate performance of the KB-1 culture during oxidation 4-55
4.18. Dechlorination rates in batch microcosm studies 4-60
4.19. Partitioning tracer K_{NW} values in water, without oxidation 4-61
4.20. K_{NW} values for Group 1 tracers after exposure to permanganate 4-62
4.21. Example data of tracer mass loss after exposure to 5.0 mg/L $KMnO_4$ 4-62
4.22. Batch tests of MnO_2 film formation impacts to K_{NW} values for Group 1 tracers 4-64
4.23. Batch tests of MnO_2 film formation impacts to K_{NW} values for Group 4 tracers 4-64
4.24. Summary of key implications for different aspects of ISCO application 4-72

ACKNOWLEDGEMENTS

The research described in this final project report was supported by the U.S. Department of Defense, through the Strategic Environmental Research and Development Program (SERDP). Dr. Andrea Leeson and other SERDP staff are gratefully acknowledged for their assistance and support.

An ISCO Expert Panel formed by SERDP to provide oversight and guidance for the portfolio of project concerning in situ chemical oxidation has provided valuable review and input to the project. Panel members included:

Dr. Marvin Unger (Chair) – HydroGeoLogic, Inc., Phoenix, Arizona
Dr. Dick Brown – ERM, Ewing, New Jersey
Mr. Michael C. Marley - XDD, LLC, Stratham, New Hampshire
Mr. Bob Norris – Brown and Caldwell, Inc., Denver, Colorado
Dr. Ian Osgerby – U.S. Army Corps of Engineers, New England District, Concord, Massachusetts

The project described herein was completed in collaboration with several other SERDP projects under the ISCO Initiative within the SERDP/ESTCP Program. Collaboration among the varied projects proved valuable to advancing the science and engineering of ISCO. In addition, the project described herein was completed in cooperation with another SERDP project carried out at CSM, that being CU-1294. The close collaboration between projects CU-1290 and CU-1294 provided very important synergies and greatly aided the accomplishment of an ambitious array of experimental and modeling studies.

During the course of this SERDP project, experimental and modeling studies were completed in support of full-scale application of ISCO for remediation of a contaminated site at the Navy Training Center (NTC) in Orlando, Florida. Mike Singletary of the Southern Division Naval Facilities Engineering Command in Charleston, South Carolina and Tom Palaia of CH2M Hill in Englewood, Colorado are acknowledged for their collaborative efforts.

ACRONYMS, ABBREVIATIONS, AND SYMBOLS

ACRONYMS AND ABBREVIATIONS

APHA	-	American Public Health Association
ASTM	-	American Society for Testing and Materials
bgs	-	below ground surface
Br^-	-	bromide ion
^oC	-	degrees celsius
C	-	concentration
CBD	-	cannot be determined
Cl^-	-	chloride ion
CHP	-	catalyzed hydrogen peroxide
cm	-	centimeter
CMC	-	critical micelle concentration
COD	-	chemical oxidant demand
CORT3D	-	Chemical Oxidation Reactive Transport in 3D
CSM	-	Colorado School of Mines
D_{eff}	-	effective diffusion coefficient
DCE	-	dichloroethene
1,1-DCE	-	1,1-dichloroethene
cis-1,2-DCE	-	*cis*-1,2-dichloroethene
DI	-	deionized water
DNAPL	-	dense nonaqueous phase liquid
1-D	-	one dimensional
2-D	-	two dimensional
3-D	-	three dimensional
DO	-	dissolved oxygen
DOC	-	dissolved organic carbon
DOD	-	Department of Defense
DOE	-	Department of Energy
ECD	-	electron capture detector
Eh	-	redox potential
eqn.	-	equation
EPA	-	Environmental Protection Agency
ESTCP	-	Environmental Security Technology Certification Program
Fe	-	iron
FID	-	flame ionization detector
FTR	-	flow-through tube reactor
f_{oc}	-	fractional organic carbon content
g	-	gram
G	-	gravity
GAC	-	granular activated carbon
GTP	-	ganglia-to-pool ratio
GC	-	gas chromatography
GW	-	groundwater
HA	-	humic acid
HPLC	-	high pressure liquid chromatography
hr	-	hour
H_2O_2	-	hydrogen peroxide

I	-	ionic strength
IC	-	ion chromatography
ICP-AES	-	inductively-coupled plasma atomic emissions spectroscopy
ID	-	internal diameter
IFT	-	interfacial tension
ISCO	-	in situ chemical oxidation
^{o}K	-	degrees Kelvin
kg	-	kilogram
Ksat	-	hydraulic conductivity
$KMnO_4$	-	potassium permanganate
L	-	liter
lb	-	pound
LNAPL	-	light nonaqueous phase liquid
LPM	-	low permeability media
m	-	meter
M	-	mass
	-	molar
MCL	-	maximum contaminant level
MDL	-	method detection limit
MDR	-	mass depletion rate
mg	-	milligram
min	-	minutes
mL	-	milliliter
mm	-	millimeter
mM	-	millimolar
mon	-	months
MnO_2	-	manganese dioxide
MnO_4^-	-	permanganate anion
Mn^{+2}	-	manganese ion
MVR	-	multiphase vial reactor
MW	-	molecular weight
NAPL	-	nonaqueous phase liquid
nd or ND	-	nondetectable
nm	-	nanometer
NOD	-	natural oxidant demand
NOM	-	natural organic matter
NPL	-	national priorities list
NRC	-	National Research Council
O_3	-	ozone
OH*	-	hydroxyl radical
PAH	-	polyaromatic hydrocarbon
PCB	-	polychlorinated biphenyl
PCE	-	tetrachloroethene
PCP	-	pentachlorophenol
PID	-	photoionization detector
ppb	-	parts per billion
ppm	-	part per million
psi	-	pounds per square inch
PTT	-	partitioning tracer test
PV	-	pore volume
RCRA	-	Resource Conservation and Recovery Act

Re	-	Reynolds number
REV	-	representative elemental volume
rpm	-	revolutions per minute
s	-	second
S	-	specific surface area of the media
S_o	-	specific surface area of an idealized capillary bundle
SD	-	standard deviation
SEM	-	scanning electron microscope
SERDP	-	Strategic Environmental Research and Development Program
SOD	-	soil oxidant demand
SVOC	-	semi-volatile organic compounds
T	-	time
$t_{1/2}$	-	reaction half life
T	-	temperature
TCA	-	1,1,1-trichloroethane
TCE	-	trichloroethene
TCLP	-	toxicity characteristic leaching procedure
TDS	-	total dissolved solids
TOC	-	total organic carbon
TPH	-	total petroleum hydrocarbons
trans-1,2-DCE	-	trans-1,2-dichloroethene
TSS	-	total suspended solids
v	-	Darcy groundwater velocity
VC	-	vinyl chloride
VOC	-	volatile organic compound
VR	-	vial reactor
wt.	-	weight
XRD	-	x-ray diffraction
ZHR	-	zero headspace reactor

SYMBOLS

α, β	-	empirical constants
δ	-	soil constrictivity factor
	-	theoretical stagnant film thickness for DNAPL dissolution
ξ	-	rate-limiting mass transfer coefficient
λ	-	linear sorption coefficient
ϕ	-	soil porosity
ϕ_{eff}	-	effective soil porosity
λ	-	linear sorption coefficient
μ_w	-	aqueous dynamic viscosity
θ_n	-	volumetric DNAPL content
θ_w	-	volumetric water content
ρ_B	-	soil bulk density
ρ_w	-	water density
τ	-	soil tortuosity factor
τ_s	-	soil tortuosity factor
τ_f	-	characteristic time of fluid motion
τ_m	-	characteristic time of DNAPL mass transfer
τ_r	-	characteristic time of chemical reaction

ξ	-	rate-limiting mass transfer coefficient
A_{nw}	-	DNAPL-water interfacial surface area
c_∞	-	steady-state bulk solution concentration of contaminant
c^*	-	aqueous solubility limit of contaminant
C_i	-	concentration of species *i*
d_{50}	-	median grain size diameter
dc/dx	-	concentration gradient
dc/dt	-	change in concentration per time
$Da(I)$	-	First Damkohler number [-]
$Da(II)$	-	Second Damkohler number
D_e	-	effective aqueous phase diffusion coefficient
D_m	-	molecular diffusion coefficient in water
D_x	-	longitudinal dispersion coefficient
D_y	-	transverse dispersion coefficient
i	-	component *i*
j	-	component *j*
J_a	-	mass flux per unit area
k_1	-	1st-order reaction rate constant
k_2	-	2nd-order oxidation reaction rate constant
k_L	-	intrinsic mass transfer coefficient
k_L^*	-	intrinsic mass transfer coefficient with chemical reaction
k_{La}	-	lumped mass transfer (NAPL dissolution) coefficient
k_{nod_f}	-	1st-order oxidation rate constant for fast NOD
k_{nod_s}	-	1st-order oxidation rate constant for slow NOD
$k_{r,w}$	-	relative aqueous permeability
K_s	-	saturated hydraulic conductivity
MW_i	-	molecular weight of component i
q	-	Darcy groundwater velocity
Re	-	Reynolds number
Sc	-	Schmidt number
Sh	-	Sherwood number [-]
S_{mno2}	-	MnO_2(s) pseudo-saturation
S_n	-	DNAPL saturation
$S_{r,w}$	-	irreducible water saturation
t	-	time
$t_{1/2}$	-	reaction half life
U_{in}	-	soil uniformity index
$\bar{v}$	-	linear pore groundwater velocity
$\bar{v}_x$	-	linear pore groundwater velocity in the x-direction
V	-	volume of interest
X^0_i	-	initial mass fraction of component i in soil
X_i	-	mass fraction of component i in soil
X_{sorb}	-	mass fraction of sorbed contaminant in the soil
$Y_{i/j}$	-	stoichiometric ratio of component i to component j

d_{50}	-	median grain size diameter
D_e	-	effective aqueous phase diffusion coefficient
D_m	-	molecular diffusion coefficient in water
i	-	component, i
J	-	mass flux
K	-	mass transfer coefficient
k_{La}	-	1st-order NAPL dissolution rate constant
k^*_{La}	-	maximum 1st-order NAPL dissolution rate constant
K_{NW}	-	NAPL-water partition coefficient
K_{org}	-	organic contaminant oxidation rate
K_{ox}	-	oxidant depletion rate
k_2	-	2nd-order reaction rate constant
MW_i	-	molecular weight of component, $_i$
U_{in}	-	soil uniformity index
X_{MnO2}	-	mass fraction of MnO_2(s) precipitates in soil
X_{napl}	-	mass fraction of NAPL in soil
X^0_{napl}	-	initial mass fraction of NAPL in soil
X_{sorb}	-	mass fraction of sorbed contaminant in the soil

EXECUTIVE SUMMARY

In situ chemical oxidation (ISCO) involves the introduction of chemical oxidants into the subsurface to destroy organic contaminants in soil and groundwater, with the goal being to reduce the mass, mobility, and/or toxicity of contamination. ISCO is rapidly emerging as a viable technology for the remediation of sites contaminated with low levels of chlorinated solvents and petrochemicals, and there is great interest in applying it to sites contaminated by dense nonaqueous phase liquids (DNAPLs). Successful application of ISCO requires knowledge of oxidation processes for free phase and residual DNAPLs, the stability and reactivity of oxidants during transport in the subsurface, the subsurface effects on oxidant fate and DNAPL destruction, and the potential for coupling ISCO with pre- or post-ISCO remedial methods. The objective of SERDP project CU-1290, which is described herein, was to quantify the pore/interfacial scale DNAPL reactions and porous media transport processes that govern the delivery of oxidant to a DNAPL-water interface and degradation of the DNAPL. This project was completed by a team of faculty, staff, and students at the Colorado School of Mines (CSM). An integrated set of tasks were carried out involving a comparative analysis focused on contrasting oxidant types (permanganate and catalyzed hydrogen peroxide) and oxidant application methods (low to high dose concentrations and delivery densities) to treat a mixture of tetrachloroethene (PCE) and trichloroethene (TCE) DNAPL present in mass levels and distributions under conditions representative of a range of subsurface environmental settings. The research also addressed the potential secondary effects of applications of ISCO, as well as the coupling of ISCO with pre- and post-ISCO treatment operations.

Based on the results of this CSM research, for the application of ISCO using potassium permanganate or catalyzed hydrogen peroxide for remediation of PCE or TCE DNAPL contamination, quantitative understanding has been improved and mathematical expressions and a numerical model have been developed and/or tested through the following efforts:

- Bench-scale studies involving aqueous phase vial reactors (VRs) were used to determine how dissolved phase reaction kinetics for PCE and TCE are affected by the composition of the bulk aqueous phase (i.e., oxidant type and concentration and natural organic matter (NOM), mineralogy, pH). Additional studies conducted in multiphase vial reactors (MVRs) investigated the impact of ISCO on TCE and PCE DNAPL mass transfer rates as a function of aqueous phase compositions. A series of response variables were developed to evaluate the efficiency and effectiveness of ISCO under the varied phase compositions investigated.
- Bench-scale studies involving zero headspace reactors (ZHRs) and 1-D diffusion cells were used to determine the effects of porous media of varying properties on oxidant transport and degradation of DNAPLs (e.g., PCE vs. TCE at different mass levels, presence and composition of NOM, oxidant type and loading). During these studies, it was necessary to evaluate the oxidant persistence in porous media (i.e., natural oxidant demand (NOD) or oxidant decomposition) and determine if catalyzed hydrogen peroxide (CHP) could be readily stabilized to promote subsurface transport.
- Bench and intermediate-scale flow-through studies were used to evaluate the reaction and transport processes for ISCO systems of varied designs when used to treat different DNAPL mass levels and entrapment architectures. Bench scale 1-D flow-through tube reactors (FTRs) and 2-D flow cells were utilized.
- Several intermediate-scale and large-scale 2-D tank systems were used to investigate complex DNAPL entrapment architectures and complex heterogeneous flow fields to determine impacts to DNAPL mass depletion and mass flux in an associated ground water plume. These experiments enabled the testing of a new model, CORT3D, that was developed as part of this project, as well as in cooperation with SERDP project CU-1294: “Mass Transfer from Entrapped DNAPL

Sources Undergoing Remediation: Characterization Methods and Prediction Tools." CORT3D was developed to simulate permanganate ISCO including oxidation chemistry, multiple rate-limited NOD fractions, DNAPL mass transfer, and changes in porous media flow properties resulting from permanganate oxidation.

- Batch and flow-through experiments were completed to evaluate the viability and effectiveness of coupling ISCO with other remediation technologies. Studies were conducted to investigate the feasibility and design considerations of coupling ISCO with both anaerobic and aerobic bioremediation technologies, utilizing batch microcosm studies and 1-D column experiments. Experimentation also investigated coupling ISCO with surfactant and cosolvent remediation.
- A final aspect of the project included experiments designed to evaluate whether partitioning tracer test (PTT) methods provide a viable way to measure DNAPL mass removals after ISCO has been applied to a DNAPL site.

The results of this research provide new insights into the effective application of ISCO for sites contaminated with DNAPLs as well as point out important limitations. Listed below are several generalized findings while further details may be found in the body of this report and other project publications.

- CHP was found to have very fast rates of reaction, and subsequently fast rates of oxidant decomposition. As such, the oxidant persistence as evaluated in these studies was poor. This was found to hold true in all systems of varying experimental scale that evaluated the use of CHP. In general, systems that provided effective contact of CHP with the contaminant appeared to be highly efficient with regard to contaminant destruction and oxidant use (i.e., relative treatment efficiency (RTE) values in the VRs, MVRs and ZHRs). However, the effectiveness (rate and extent) of contaminant mass depletion by CHP was generally lower than in equivalent permanganate systems in every experimental series CHP was evaluated in (VRs, MVRs, ZHRs, diffusion cells, 2-D flow cells).
- Permanganate was much more effective in reducing DNAPL contaminant mass in the experimental systems evaluated. Due to the reduced reactivity of permanganate, advective and diffusive transport of oxidant is possible, as evidenced in all experimental transport studies (e.g., 1-D diffusion cells, FTRs, 2-D cells).
- Oxidant concentration can interact strongly with the velocity of oxidant delivery into a porous media system. A common theme among the experiments that evaluated multiple velocities was that higher velocities led to more effective remediation performance, evidenced by increased DNAPL mass depletion, and frequently reduced adverse impacts and enhanced potential for bio-coupling. However, higher oxidant concentrations can promote diffusive transport of oxidant into low permeability media, and be more time-efficient from a site flushing perspective as fewer pore volumes may be required to destroy a given DNAPL contaminant source.
- Natural oxidant demand (permanganate) and oxidant decomposition (peroxide) increased with increasing complexity of porous media (e.g., higher reduced mineral content, NOM, or clay/silt particle fractions, increasing oxidant concentration, and increased contact time). NOD and oxidant decomposition challenge both advective and diffusive oxidant transport. Site-specific characterization is critical, but difficult to accomplish in a simple, meaningful manner.
- TCE was found to be depleted and destroyed faster than PCE in every experimental system that evaluated both DNAPL types (VRs, MVRs, ZHRs, diffusion cells and FTRs). This is likely due to the order of magnitude higher solubility of TCE versus PCE, as well the faster kinetic rate of reaction between TCE over PCE in permanganate systems. Moreover, DNAPL present in the

subsurface as residual ganglia are highly amenable to depletion and destruction by oxidant flushing. However, when pooled DNAPL was present, oxidation effectiveness was more variable. Mass transfer was observed to be enhanced from residuals by permanganate oxidation of aqueous phase contaminants, as well as by other potential impacts to mass transfer processes, based on FTR and CORT3D modeling study results.

- The role of natural organic matter and certain minerals (i.e., goethite) present in the subsurface can complicate the understanding of ISCO efficiency and effectiveness. For example, the results of this study revealed that the role of NOM in porous media during ISCO has a more complex effect on remediation performance than simply increasing natural oxidant demand.

- Coupling ISCO with anaerobic reductive dechlorination for destruction of contaminants such as TCE and PCE is a viable approach. Coupling ISCO with surfactant enhanced aquifer restoration and use of PTT test methods appears viable, but only with careful evaluation and design to ensure that the oxidant-surfactant and oxidant-PTT systems are compatible.

This fundamental and applied research completed during the course of SERDP project CU-1290 provides a knowledge base for the future development of guidance on the principles and practices of ISCO so that it can be selected as a preferred remedy when appropriate and can be implemented to reliably achieve performance goals. Decision aids and design tools will enable cost-effective implementation of ISCO for remediation of DNAPLs at a given site, using ISCO either as a stand-alone method or by coupling it with a pre- or post-ISCO operation. This guidance is being developed by the CSM project team under the follow-on ESTCP project, ER-0623: "In Situ Chemical Oxidation for Remediation of Groundwater: Technology Practices Manual".

CHAPTER 1

INTRODUCTION

1.1. PROJECT PURPOSE AND SCOPE

In situ chemical oxidation (ISCO) is rapidly emerging as a viable technology for the remediation of sites contaminated by organic chemicals. ISCO has been used extensively for in situ treatment of low levels of chlorinated solvents and petrochemicals, and there is great interest in applying it to sites contaminated by dense nonaqueous phase liquids (DNAPL). Successful application of ISCO requires knowledge of oxidation processes for free phase and residual DNAPLs, the stability and reactivity of oxidants during transport in the subsurface, the subsurface effects on oxidant fate and DNAPL destruction, and the potential for coupling ISCO with pre- or post-ISCO remedial methods. To further the understanding and advance the standard of practice for application of ISCO to DNAPL sites, experimental and modeling studies were carried out at the Colorado School of Mines (CSM). These studies were completed with funding provided by the DOD Strategic Environmental Research and Development Program (SERDP) through project CU-1290: "Reaction and Transport Processes Controlling In Situ Chemical Oxidation of DNAPLs". The objective of this project was to quantify the pore/interfacial scale DNAPL reactions and porous media transport processes that govern the delivery of oxidant to a DNAPL-water interface and degradation of the DNAPL in situ. The fundamental research completed during this project was needed to provide a knowledge base for the future development of guidance on the principles and practices of ISCO so that it can be selected as a preferred remedy when appropriate, either as a stand-alone method or combined with other remediation technologies.

1.2. BACKGROUND AND MOTIVATION

1.2.1. DNAPL Contamination at DOD Sites

Dense non-aqueous phase liquid (DNAPL) contamination represents a major environmental problem for many hazardous waste sites throughout the United States, including Department of Defense (DOD) and Department of Energy (DOE) sites (Kavanaugh *et al.* 2003, GAO 2005). Common DNAPLs include trichloroethene (TCE), tetrachloroethene (PCE), chloroform, and carbon tetrachloride. DNAPLs present a long-term problem due to their chemical properties, including low solubility and high density, which can result in release of high concentrations to ground water over extensive time frames. Contamination of subsurface soils and ground water can present unacceptable risks to human health and environmental quality (e.g., increased cancer risk through ingestion of contaminated drinking water or inhalation of vapors) (Figure 1.1). An early method of ground water cleanup was simply pumping the ground water and treating it above-ground. But experiences with this approach revealed it to have severe limitations and high costs (Mackay and Cherry 1989, USEPA 1999). Major research and development efforts have been directed at finding alternative remedies that can clean up ground water and eliminate risks or reduce them to an acceptable level (NRC 1994, 1997).

In the U.S. today, there are still an estimated 30,000 to 50,000 sites with ground water contamination (excluding petroleum contamination from underground storage tanks) (Kavanaugh *et al.* 2003). About 80% of the sites are contaminated with organic chemicals, and of these, 60% likely have DNAPLs present. The cleanup costs for 15,000 to 25,000 sites with DNAPLs is known to be significant when conventional ground water pumping and treatment systems are employed. The median cost to operate a ground water pump and treat system is on the order of $180,000 per year with a range of $30,000 to $4,000,000. For all sites, the annual costs are $2.7 to 4.5 billion dollars per year. Assuming a 30-year life and a 5 to 10% interest rate, life-cycle costs of "cleanup" could range from $50 to $100

billion dollars. Many now conclude that clean up based on ground water pump and treat alone is *hopeless* and alternative technologies and approaches are needed (Kavanaugh *et al.* 2003).

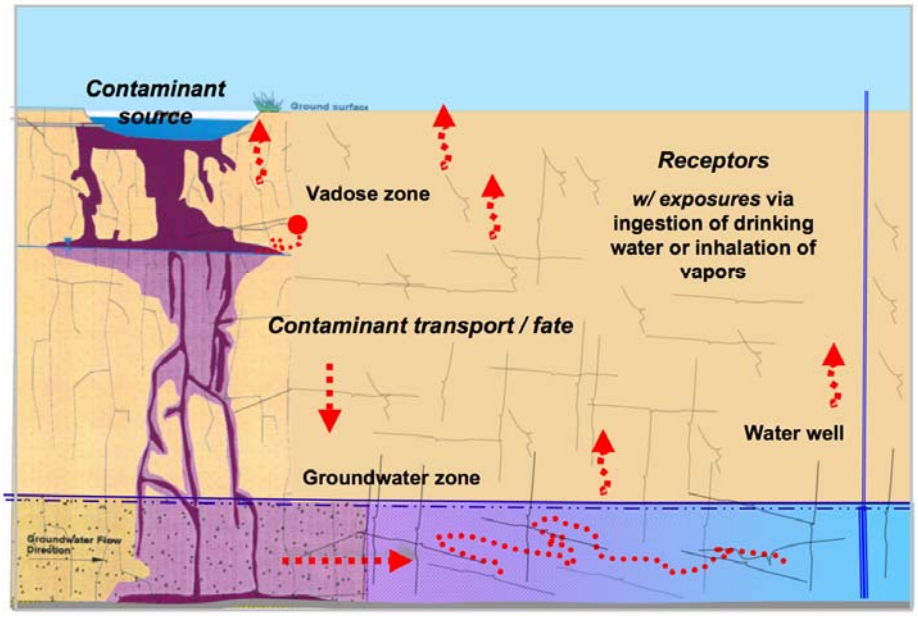

Figure 1.1. Illustration of a DNAPL source zone leading to long-term contamination of subsurface soil and ground water.

Recent efforts have increasingly focused on source zone treatment of DNAPL contamination to reduce the volume and mass available for dissolution to ground water. A variety of in situ technologies have been developed and demonstrated and, to varying degrees, utilized for cleanup of DNAPL contaminated sites, including: (1) thermally enhanced recovery, (2) surfactant/cosolvent flushing, (3) chemical oxidation and reduction, and (4) bioremediation.

1.2.2. Evolution of ISCO and its Application to DNAPL Sites

1.2.2.1. Introduction. The project described in this report is focused on the use of ISCO for remediation of sites contaminated with PCE and TCE DNAPLs. ISCO involves the introduction of chemical oxidants (e.g., catalyzed H_2O_2 (also known as modified Fenton's reagent), potassium and sodium permanganate ($KMnO_4$, $NaMnO_4$), sodium persulfate ($Na_2S_2O_8$), and ozone (O_3)) into the subsurface to destroy organic contaminants in soil and ground water, with the goal being to reduce the mass, mobility, and/or toxicity of contamination (Table 1-1) (e.g., USEPA 1998, ESTCP 1999, Yin and Allen 1999, Siegrist *et al.* 2000a,b, 2001, ITRC 2001, 2005). ISCO has been used extensively for in situ treatment of low levels of chlorinated solvents and petrochemicals, and there is great interest in applying it to sites contaminated by DNAPLs. Successful application of ISCO requires knowledge of oxidation processes for free phase and residual DNAPLs, the stability and reactivity of oxidants during transport in the subsurface, the subsurface effects on oxidant fate and DNAPL destruction, and the potential for coupling ISCO with pre- or post-ISCO remedial methods.

SERDP project CU-1290 was initiated in 2002 to advance the science and engineering of ISCO applied to DNAPL sites. Highlights of the state-of-knowledge available at the start of the project described herein are provided below.

Table 1.1. General features of the three common ISCO technologies (information as of 2002 when CU-1290 was initiated).

Features	H_2O_2 and Fenton's reagent	Ozone	$KMnO_4$ or $NaMnO_4$
Oxidant Characteristics:			
Form -	Liquid	Gas	Liquid or solid
Point of generation -	Offsite, shipped onsite	Onsite during use	Offsite, shipped onsite
Quantities available -	Small to large	Small to large	Small to large
ISCO Design:			
Delivery Methods -	GW wells, soil probes	GW sparge wells	GW wells, soil probes, fractures
Dose concentrations -	5 to 50 wt.% H_2O_2	Variable	0.02 to 4.0 wt.% MnO_4^-
Single / multiple dosing -	Multiple is common	Multiple	Single and multiple
Amendments -	Fe^{+2} and acid	Often ozone in air	None
Subsurface transport -	Advection	Advection	Advection and diffusion
Rate reaction / transport -	High or very high	Very high	Moderate to high
Companion technol. -	None required	Soil vapor extraction	None required
ISCO Effectiveness:			
Susceptible organics -	BTEX, PAHs, phenols, alkenes	BTEX, PAHs, phenols, alkenes	BTEX, PAHs, alkenes
Difficult to treat organics -	Some alkanes, PCBs	Alkanes, PCBs	Alkanes, PCBs
Oxidation of NAPLs -	Direct oxidation possible	Direct oxidation possible	Direct oxidation possible
Reaction products -	Organic acids, salts, O_2, CO_2	Organic acids, salts, O_2, CO_2	Organic acids, salts, MnO_2, CO_2
	Substantial gas evolution	Minimal gas evolution	Minimal gas evolution
Subsurface Effects on ISCO:			
Effect of NOM -	Demand for oxidant	Demand for oxidant	Demand for oxidant
Effect of pH -	Most effective in acidic pH	Most effective in acidic pH	Effective over pH 3.5 to 12
Effect of temperature -	Reduced rate at lower temp.	Reduced rate at lower temp.	Reduced rate at lower temp.
Effect of ionic strength -	Limited effects	Limited effects	Limited effects
ISCO Effects on Subsurface:			
pH -	Lowered if inadeq. buffering	Lowered if inadeq. buffering	Lowered if inadeq. buffering
Temperature -	Minor to high increase	Minor to high increase	None to minor increase
Metal mobility -	Potential for redox metals	Potential for redox metals	Potential for redox/CEC metals
Permeability loss -	Gas evolution and colloids	Gas evolution and colloids	MnO_2 colloid genesis
Microbiology -	Short-term perturbations (?)	Short-term perturbations (?)	Short-term perturbations (?)

1.2.2.2. In Situ Oxidation of Organic Chemicals. Chemical oxidation to destroy organic contaminants in water has been utilized for decades in the municipal and industrial water and waste treatment industry. Chemical oxidation was most often accomplished with the use of hydrogen peroxide (H_2O_2), modified Fenton's reagent (H_2O_2 plus Fe^{+2} to yield free radicals such as hydroxyl radicals, OH*), or ozone (O_3). Implemented in tank-based reactors, chemical oxidation was increasingly used for *ex situ* treatment of individual organics in water (Hoigne and Bador 1983, Barbeni *et al.* 1987, Bowers *et al.* 1989, Watts and Smith 1991, Venkatadri and Peters 1993). Subsequently, research began to explore H_2O_2 and modified Fenton's reagent oxidation in soil and ground water environments (Watts *et al.* 1990, Watts and Smith 1991, Watts *et al.* 1991, Tyre *et al.* 1991, Ravikumar and Gurol 1994, Gates and Siegrist 1993, Gates and Siegrist 1995, Watts *et al.* 1997).

Research was also initiated with alternative oxidants such as ozone (Bellamy *et al.* 1991, Nelson and Brown 1994, Marvin *et al.* 1998) and potassium permanganate ($KMnO_4$) (Vella *et al.* 1990, Vella and Veronda 1994, Gates *et al.* 1995, Schnarr *et al.* 1998, West *et al.* 1998a,b, Siegrist *et al.* 1998a,b,c, Huang *et al.* 1999, 2000, Siegrist *et al.* 1999, Yan and Schwartz 1996, 1999, Urynowicz and Siegrist 2000). As of the start of project CU-1290 in 2002, a wide variety of organic contaminants in soil and ground water have been successfully oxidized by hydrogen peroxide (including Fenton's reagent), ozone, and permanganate oxidants (Table 1.2).

Alternative methods of oxidant delivery used in the field have included permeation by vertical injection probes (e.g., Jerome *et al.* 1997, Siegrist *et al.* 1998c, Moes *et al.* 2000), deep soil mixing (e.g., Cline *et al.* 1997), flushing by vertical and horizontal ground water wells (e.g., Schnarr *et al.* 1998, West *et al.* 1998a,b, Lowe *et al.* 2002), and reactive zone emplacement by hydraulic fracturing (e.g., Siegrist *et al.* 1999a) (Figure 1.2).

Table 1.2. Representative list of organics treated by chemical oxidants (information as of 2002 when CU-1290 was initiated).

Organic contaminant	Media treated	Oxidant	References
Trichloroethene	Water (spiked)	H_2O_2	Bellamy *et al.* 1991
	Silica sand (spiked)	H_2O_2	Ravikumar and Gurol 1994
	Silty clay soil (spiked)	H_2O_2	Gates and Siegrist 1995
	Sand & clay soils (spiked)	H_2O_2 /$KMnO_4$	Gates *et al.*1995, Gates-Anderson *et al.* 2001
	Ground water (spiked)	$KMnO_4$	Case 1997, Yan and Schwartz 1999
	Ground water (field site)	$KMnO_4$	West *et al.* 1998a,b, Schnarr *et al.* 1998
	Ground water (field site)	$NaMnO_4$	Lowe *et al.* 2002
	Silty clay soil (field site)	$KMnO_4$	Siegrist *et al.* 1999
Tetrachloroethene	Water (spiked)	H_2O_2	Bellamy *et al.* 1991
	Silica sand (spiked)	H_2O_2	Leung *et al.* 1992
	Sand, clay soils (spiked)	H_2O_2 /$KMnO_4$	Gates *et al.*1995, Gates-Anderson *et al.* 2001
	Ground water (field site)	$KMnO_4$	Schnarr *et al.* 1998
	Ground water (spiked)	$KMnO_4$	Yan and Schwartz 1996
	Ground water (field site)	Ozone	Dreiling *et al.* 1998
trans-1,2-DCE	Water (spiked)	H_2O_2	Bellamy *et al.* 1991
Carbon tetrachloride	Water (spiked)	H_2O_2	Bellamy *et al.* 1991
Pentachlorophenol	Silica sand (spiked)	H_2O_2	Ravikumar and Gurol 1994
	Natural soil (spiked)	H_2O_2	Watts *et al.* 1990
2,4-dichlorophenol, dinitro-o-cresol	Water (spiked)	H_2O_2	Bowers *et al.* 1989
Trifluralin, hexadecane, dieldrin	Soil (spiked)	H_2O_2	Tyre *et al.* 1991
Phenols	Water (spiked)	$KMnO_4$	Vella *et al.* 1990
Naphthalene, phenanthrene, pyrene	Clay , sandy soils (spiked)	H_2O_2 /$KMnO_4$	Gates *et al.*1995, Gates-Anderson *et al.* 2001
Octachlorodibenzo(p)dioxin	Soil (spiked)	H_2O_2	Watts *et al.* 1991
Motor oil / diesel fuel	Soil (field site)	H_2O_2	Watts 1992
PAHs and pentachlorophenol	Soil and GW (field site)	Ozone	Marvin *et al.* 1998
BTEX and TPH	Soil and GW (field site)	Ozone	USEPA 1998

For ISCO application, modified Fenton's reagent and, more recently, $KMnO_4$, have been the subject of an extensive research and growing field applications. Highlights of the relevant facets of the knowledge base at the start of this project in 2002 are given in Tables 1.2 and 1.3 while some brief remarks are made below.

During the 1990's, laboratory studies were initially focused on H_2O_2 or Fenton's Reagent (H_2O_2 plus Fe^{+2}) and most often for *ex situ* treatment of dissolved organics in water (Barbeni *et al.* 1987, Bowers *et al.* 1989, Watts and Smith 1991, Bellamy *et al.* 1991, Venkatadri and Peters 1993) (Table 1.2). Subsequent research began to explore peroxide oxidants in soil environments (Watts *et al.* 1990, Watts and Smith 1991, Watts *et al.* 1991, Tyre *et al.* 1991, Ravikumar and Gurol 1994, Gates and Siegrist 1993, 1995, Watts *et al.* 1997). Research was also initiated with alternative oxidants such as ozone (Nelson and Brown 1994, Marvin *et al.* 1998) and $KMnO_4$ (Vella *et al.* 1990, Vella and Veronda 1994, Gates *et al.* 1995, Schnarr *et al.* 1998, West *et al.* 1998a,b, Siegrist *et al.* 1998a,b, 1999). Results of early laboratory studies provided insight into the oxidation chemistry of a few common organics such as TCE in ground water and soils. Oxidation using H_2O_2 in the presence of native or supplemental Fe^{+2} produces Fenton's reagent, which yields free radicals that can rapidly degrade a variety of organics compounds (Table 1.1). Oxidation using permanganate (typically as $KMnO_4$ but also as $NaMnO_4$) can include destruction of

many organics by direct electron transfer or free radical oxidation (Table 1.1). Oxidation of TCE by peroxide and permanganate can yield intermediate organic acids but with excess oxidant, can ultimately produce CO_2, acid, and salts (Equation 1-1 and 1-2). Permanganates also can generate MnO_2 precipitates (Equation 1-2). While a variety of complex reactions can occur when oxidants are applied in situ, the following simplified stoichiometric equations are insightful:

$$3H_2O_2 + C_2HCl_3 \text{ ---> } 2CO_2 + 2H_2O + 3Cl^- + 3H^+ \quad (1\text{-}1)$$

$$2KMnO_4 + C_2HCl_3 \text{ ---> } 2CO_2 + 2MnO_{2(s)} + 2K^+ + 3Cl^- + H^+ \quad (1\text{-}2)$$

Both oxidants yield salts and CO_2 gas. However, permanganate oxidants yield manganese oxide (MnO_2) particles. While the character and features of these particles will depend on the environmental conditions, Siegrist *et al.* (2002) recently observed a relationship between particle production and the oxidant dose concentration and type, TCE concentration, pre-existing particles >0.45 um, and reaction time:

$$\text{Particles} = 0.0089\ (MnO_4^-\ \text{dose}) + 2.14\ (\text{TCE conc.}) + 0.197\ (\text{ambient filterable particles}) \quad (1\text{-}3)$$

where all concentrations are in mg/L. The constant, 2.14, compares with the stoichiometric data of Equation 2 which indicates that for TCE oxidation, 1.32 g of MnO_2 are produced when 1.81 g of MnO_4^- reacts with 1 g of C_2HCl_3 (per Eqn. 1-2). This relationship suggests that the presence of ambient filterable particles in the ground water increases the net production of particles beyond that of just the MnO_2 alone. While peroxide or Fenton's reagent don't produce particles as a reaction product (Equation 1-1), they can generate particles by shearing off colloids from the soil and sediment matrix. Also, while not shown in Equations 1-1 or 1-2, oxidation reactions with different organics can either yield acidity as shown or in some cases, alkalinity (e.g., MnO_4^- reaction with DCE). Both oxidative reactions are extremely rapid and follow 2nd-order kinetics overall with respect to the concentration of the oxidant and the reductants in the system and can be represented by pseudo- 1st order kinetics under a given oxidant loading. The Fenton's reaction is strongly exothermic and can evolve substantial gas and heat while the permanganate reaction is more moderate. Peroxide-based oxidation is most effective under very acidic pH (e.g., pH 2 to 4) and becomes ineffective under alkaline conditions, while MnO_4^- is effective over a much wider pH range (pH 3 to 12).

Based on early promising laboratory and pilot-test results, field-scale applications increased rapidly and as of about 2001, ISCO systems deployed at more than 40 sites in the U.S. including delivery of Fenton's reagent or permanganate by vertical injection probes (e.g., Jerome *et al.* 1997, Siegrist *et al.* 1998c, Moes *et al.* 2000), deep soil mixing (e.g., Cline *et al.* 1997, Gardner *et al.* 1998), vertical and horizontal ground water wells (e.g., Schnarr *et al.* 1998, West *et al.* 1998a,b, Lowe *et al.* 2002), and reactive zone emplacement by hydraulic fracturing (e.g., Siegrist *et al.* 1999) (Table 2.3). Some of these field applications have yielded encouraging results with respect to reducing the mass of COCs in soil and ground water. However, there have been reports of unexpectedly poor *in situ* treatment performance often associated with (1) poor uniformity of oxidant delivery caused by a deficient delivery method or site heterogeneities, (2) excessive oxidant consumption by natural soil materials, (3) presence of DNAPL residuals, and/or (4) problems with treatment produced particles and permeability loss.

Laboratory research began to focus on some of the issues and concerns observed in field applications. Key issues affecting performance with respect to ISCO as applied to sites with the pervasive TCE and PCE DNAPLs have been the subject of considerable recent and ongoing research, the objectives of which have been to:

- Define the unproductive oxidant demand due to NOM and other reductants (e.g., Case 1997, Li *et al.* 1997, Sherman *et al.* 1998, Tarr and Lindsey 1998, Siegrist *et al.* 2000),

- Determine the particle genesis and potential permeability loss that occurs during ISCO (e.g., Wiesner *et al.* 1996, Siegrist *et al.* 2000, Li and Schwartz 2000, Reitsma and Marshall 2000),
- Elucidate the processes occurring at the sorbed- or DNAPL-water interface when an oxidant was present in the bulk aqueous phase (e.g., Li *et al.* 1997, Watts *et al.* 1997, Urynowicz 2000, Li and Schwartz 2000, Rietsma and Marshall 2000),
- Evaluate the degradation of DNAPLs present in porous media during flushing with oxidant solutions and assessing the changes in DNAPL degradability due to interfacial resistance, changes in permeability due to particle genesis and gas evolution (e.g., Urynowicz 2000, Li and Schwartz 2000, Reitsma and Marshall 2000, Chambers *et al.* 2000), and
- Assess the effects of ISCO on subsurface biogeochemical properties including changes in metal mobility (Chambers *et al.* 2000, IT Corp 2000, Siegrist *et al.* 2000).

While these research efforts have begun to provide insight and to advance the science and engineering of ISCO, at the start of this project there were still significant gaps in the state-of-knowledge that precluded rational and reliable design, particularly for sites contaminated with DNAPLs.

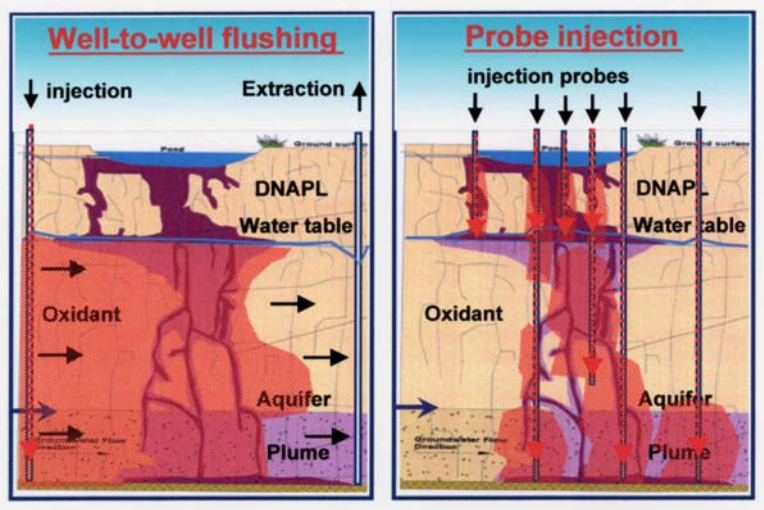

Figure 1.2. Illustration of in situ chemical oxidation where injection wells or direct-push probes are used to deliver oxidants into the subsurface to cleanup soil and ground water contamination.

1.2.2.3. Coupling of ISCO with Pre- and Post-ISCO Remediation Options. The coupling of compatible *in situ* treatment technologies is a logical remediation approach particularly for more heavily contaminated source areas and plumes as well as DNAPL residuals. For source areas with high concentrations and DNAPL residuals, if there is adequate permeability and limited heterogeneity, high mass removal efficiencies can be achieved by flushing with surfactants/cosolvents (Palmer and Fish 1992, Jafvert 1996, Fountain 1997, Roote 1997, Jackson and Mariner 1998) or by thermal methods (Davis 1997, Davis and Udell 1998). Air sparging may also be used for this purpose. Field tests of surfactant enhanced recovery and air sparging have been completed at controlled release cells at the NETTS site at Dover AFB. Unfortunately, while these methods can achieve high mass recovery efficiencies of DNAPLs (e.g., 95% or more), there are still appreciable levels of residual contaminants in the subsurface (e.g., 1000 mg/kg range) which can continue to sustain concentrations above risk based action levels. In addition, the residuals may have an altered mobility due to treatment-induced changes in the contaminant and/or the subsurface and thus the residuals may be of great concern. Coupling a treatment strategy

involving first mass recovery followed by a lower-level oxidant flush could cost-effectively reduce the residual mass and enable achievement of clean up goals such as maximum contaminant levels (MCLs) in ground water. However this approach was not explored in any detail as of 2002 when project CU-1290 was initiated.

Table 1.3. Examples of studies exploring ISCO treatment of DNAPLs and a summary of the observations made as of 2002.

Study type	Observation(s)
~ DNAPL Degradation Effectiveness ~	
Lab study of TCE DNAPL destruction by $KMnO_4$ based on dose concentration and flow-velocity (Urynowicz 2000, Urynowicz and Siegrist 2000)	Observed degradation enhancement due to oxidation but development of an interfacial film (MnO_2) reduced rates. Suggested importance of DNAPL-water interface vs. mass.
Laboratory tank studies with TCE or PCE DNAPL examining degradation as affected by heterogeneity (Reitsma and Marshall 2000, Li and Schwartz 2000)	Observed permeability loss due to particle production and gas evolution and incomplete DNAPL mass destruction due to film formation around the DNAPL.
~ Permeability Effects ~	
Field study of permanganate ISCO of DNAPL examining impact on permeability (Mott-Smith *et al.* 2000)	No significant formation plugging or decreased injection flow rates.
Field measurements of effects of Fenton's oxidation of DNAPL contamination (Levin *et al.* 2000)	Clean-up goals were reached with no noted mobilization of contaminants.
Field studies of permanganate ISCO noting pre- and post-treatment hydraulic conductivity. (Lowe *et al.* 2000, Siegrist *et al.* 2000)	Similar ISCO applications at the same site demonstrated no permeability loss with low TCE/oxidant conditions, yet significant well pressure build-up occurred under high TCE and high oxidant conditions.
Laboratory 1 and 2-D studies examining flushing efficiencies of aquifer materials following permanganate oxidation. (Li and Schwartz 2000)	The tendency to develop preferential flow paths was promoted by MnO_2 precipitation in zones of higher DNAPL saturation or as CO_2 bubbles are trapped in porous media.
~ pH Effects ~	
Field measurements of pH effects of permanganate oxidation of TCE. (Siegrist *et al.* 1999, West *et al.* 2001)	pH depression was found following oxidation with low TCE and oxidant concentrations. An increase in pH was noted following oxidant flushing to treat TCE DNAPL residuals.
Pilot-scale treatability study using $NaMnO_4$ to treat TCE in both DNAPL and aqueous phases. (Huang *et al.* 2000)	The pH dropped notably within 2 d, then increased beyond the initial pH within 10 d and was sustained high. The rise in pH was attributed to permanganate side reactions.
~ Oxidant Comparisons ~	
Laboratory studies to compare applicability of three oxidants for treatment of varied contaminants. (Oberle and Schroder 2000)	Fenton's and permanganate had much greater impact on reduction of organics than peroxide. Fenton's could destroy more contaminant types than permanganate, but was impacted by reaction pH.
Laboratory studies comparing permanganate and Fenton's Reagent for treatment of contaminant mixtures. (Coons *et al.* 2000)	Both were successful in treating mixtures. Permanganate was (generally) more effective at treating soils and Fenton's was more effective at treating ground water.
~ Treatment-Induced Toxicity ~	
Field application of permanganate ISCO by oxidant flushing at a DOE site in Ohio. (Lowe *et al.* 2003)	No measured oxidation-induced toxicity.
Laboratory and field scale testing of permanganate oxidation of explosives. (Clayton *et al.*, IT Corp and SM Stollar Corp 2000)	Measured toxicity effect in oxidized samples potentially due to oxidant itself.

Another coupling strategy involves combining ISCO with post-ISCO bioremediation. At some sites, one or more of the organics in a mixture are recalcitrant to biodegradation due to their original concentrations or chemical forms. Use of a pretreatment step involving ISCO could enhance subsequent biodegradation. However, strong chemical oxidants are known to be potentially toxic to microorganisms. Precipitates such as iron hydroxides and manganese oxides formed during chemical oxidation have also raised treatment concerns. Despite these concerns, numerous studies have verified the capacity of chemical pre-treatment with oxidants such as peroxide, Fenton's reagent, and ozone to enhance subsequent biodegradation of organics in water or wastewater (Scott and Ollis 1995). In most of these studies, the oxidants were removed and solution conditions such as pH modified prior to the biodegradation measurements.

More recently, simultaneous chemical and biological oxidation were studied in a system with Fenton reactions and the pure culture *Xanthobacter flavus* FB71; toxic effects of Fenton reactions were observed in peroxide-acclimated bacteria, with greatest PCE degradation occurring at optimal concentrations of peroxide, Fe(II) and initial cell numbers (Büyüksönmez *et al.* 1998, Büyüksönmez *et al.* 1999). An additional twist on this approach is the use of a single microorganism to produce both Fe(II) and peroxide as a microbially driven Fenton reaction, as demonstrated by McKinzi and DiChristina using *Shewanella putrefaciens* strain 200 and pentachlorophenol (PCP) (McKinzi and DiChristina 1999). Few studies have carefully investigated the effect of chemical oxidation on soil microbial activities or communities. For example, Fenton's reagent has been applied to PCB congeners (Aronstein and Rice, 1995) and TCE, PCP and toluene (Carberry and Benzing 1991) prior to biodegradation in acclimated planktonic soil cultures and soil/sediment slurries, respectively, but in both cases the organics were oxidized in the absence of the microorganisms ultimately responsible for biodegradation. Similarly, ozonation has been shown to increase biodegradation of pesticides in silt loam/sand materials, but again ozonation was applied to a liquid stream that was subsequently applied to the soil (Somich *et al.* 1988, Somich *et al.* 1990).

Biocoupling can also be employed for redox sensitive metals to alter metal mobility. Some metals are mobile at high redox potentials but sorbed or precipitated under reducing conditions (e.g., mobile Cr^{+6} vs. immobile Cr^{+3}) while for others it is just the opposite (e.g., immobile As^{+5} vs. mobile As^{+3}). Chemical oxidation can alter reducing conditions that are often present in contaminated subsurface regions by elevating Eh and reducing pH (Palmer and Puls 1994, Evanko and Dzombak 1997). This can affect the mobility and fate of redox metals. In some cases, natural or engineered bioprocesses can be exploited to reverse or counter a redox mobilization effect. For example, prior work has demonstrated biologically mediated reduction of Cr^{+6} to Cr^{+3} (Horitsu *et al.* 1987, Zhang *et al.* 1996) and uranium U^{+6} to U^{+3} (Lovley 1991, Lovley *et al.* 1991, Gorby and Lovley 1992, Francis *et al.* 1994).

1.2.3. Knowledge Gaps Concerning ISCO Applied to DNAPLs at the Start of Project CU-1290

In 2002, much was known about ISCO, but there were still considerable gaps in understanding regarding the reaction and transport processes that control its effective application for in situ remediation in general and in particular for sites with DNAPLs. As a result, field-scale applications continue to be plagued by uncertain or poor *in situ* treatment performance often attributed to poor uniformity of oxidant delivery caused by a deficient delivery method or site heterogeneity, excessive oxidant consumption by natural subsurface materials, presence of DNAPLs and incomplete degradation, and/or problems with treatment produced particles causing well and formation permeability loss.

While there is a theoretical basis for enhanced degradation of DNAPLs due to chemical oxidation, few fundamental and applied studies had been completed as of 2002. As a result, understanding was limited with respect to key facets that span from the reaction processes for chemical oxidants in a bulk aqueous phase in contact with a DNAPL phase, to the oxidant delivery and transport processes for a subsurface region where DNAPLs may be present in unknown distributions as dispersed

ganglia or entrapped pools. Results from relatively uncontrolled and nonrepresentative laboratory pilot tests (e.g., with DNAPLs in 1-D columns of homogenous sand) or uncontrolled field applications (where DNAPLs are thought to exist but information regarding mass and distribution before and after ISCO is unknown), have provided some insight, but they have been of limited value for fundamental understanding and furthering the standard of practice for ISCO and DNAPL sites. Also, research into ISCO coupled with other remedies such as pre-ISCO mass recovery by surfactant/cosolvent flushing or post-ISCO bioremediation was limited or nonexistent. Similarly, there was no experimental evidence of the utility and validity of partitioning tracer techniques, advocated for defining DNAPL mass and assessing treatment efficiency, to sites treated by ISCO.

1.3. PROJECT APPROACH

The ultimate goal of the project was to increase the level of understanding such that one can better know when and how to cost-effectively remediate DNAPL sites using ISCO as a stand-alone method or by coupling ISCO with a pre- or post-ISCO operation. To accomplish this goal, the project was designed and carried out by a collaborative team involving faculty, staff, and students at the Colorado School of Mines. The project scope included literature review and analysis, laboratory experimentation using batch- and 1-D and 2-D flow-through apparatus, and development and refinement of mathematical models and completion of lab- and field-scale model simulations. The project scope included comparative experimental and modeling studies to evaluate both potassium permanganate ($KMnO_4$) and catalyzed hydrogen peroxide (H_2O_2) oxidants and the pore/interfacial scale DNAPL degradation reactions and the transport processes governing delivery of oxidant to the DNAPL-water interfaces.

The SERDP project described in this report was enabled by other research recently completed or ongoing at CSM. Existing facilities and methodologies were employed and coordination was achieved with ongoing research. This was critical to accomplishing the breadth of experimental and modeling studies completed through the following set of inter-related tasks:

Task 1: Bench-scale studies were used to define (series 1) the dissolved phase reaction kinetics for DNAPLs affected by bulk aqueous phase composition, and (series 2) the DNAPL degradation achieved as a function of DNAPL mass/surface area and cross-flow velocity.

Task 2: Bench-scale studies involving slurry reactors (series 1) and diffusion cells (series 2) were used to determine the effects of porous media of varying properties on the natural oxidant demand (NOD) and the degradation of DNAPLs under flow regimes spanning very high to zero advection. This task also explored the potential for coupling ISCO with surfactant/ cosolvent recovery or natural attenuation through examination of reactions of oxidants with DNAPLs in the presence of surfactants/cosolvents and assessment of effects on microbial/biomass activities.

Task 3: Intermediate scale studies were conducted in 1-D columns and 2-D transport cells to evaluate the reaction and transport processes including the effects of ISCO on different DNAPL mass and distribution characteristics in subsurface conditions of varying heterogeneity.

Task 4: This task evaluated the coupling of ISCO with pre-treatment and post-treatment operations to most cost-effectively achieve a desired endpoint using 1-D and 2-D systems to examine the interaction of surfactants/cosolvents with oxidants and DNAPLs, partitioning tracer behavior before and after ISCO, and changes in biomass and activity levels due to ISCO.

Task 5: Task 5 involved preparation of project reports and papers documenting the work completed and providing recommendations regarding the process principles and implications of ISCO applied for remediation of DNAPL contaminated sites.

1.4. ORGANIZATION OF THIS REPORT

A substantial body of research results was produced during this project through experimental work and modeling efforts. This report describes the methods and results of the research completed to quantify the pore/interfacial scale DNAPL reactions and porous media transport processes that govern the delivery of oxidant to a DNAPL-water interface and degradation of the DNAPL. The report chapters provide a summary of the various facets of the project while detailed information on some components of the effort is provided in other publications as noted in Table 1.4 and Appendix B.

In addition to the information contained in this project report, additional details regarding the work have been disseminated through the following means:

- Published CSM student M.S. theses and Ph.D. dissertations (Jackson 2004, Seitz 2004, Sahl 2005, Heiderscheidt 2005, Petri 2006, Dugan 2006),
- Conference presentations and proceedings abstracts and papers (Crimi *et al.* 2002, Crimi and Siegrist 2003, Crimi *et al.* 2004a,b, Crimi *et al.* 2005a,b, Crimi and Taylor 2005, Dugan *et al.* 2004a,b, Heiderscheidt *et al.* 2004, Petri *et al.* 2004, Petri *et al.* 2005, Sahl *et al.* 2004a,b, Sahl *et al.* 2005, Seitz *et al.* 2003, Seitz *et al.* 2004a,b, Siegrist 2002, Siegrist 2003, Siegrist *et al.* 2004, Siegrist 2005a,b, Siegrist 2006a,b, Taylor *et al.* 2002),
- Journal articles (Haselow *et al.* 2003, Crimi and Siegrist 2005, Sahl and Munakata-Marr 2006, Sahl *et al.* 2006), and
- Forthcoming publications.

1.5. REFERENCES

Barbeni, M., C. Nfinero, E. Pelizzetti, E. Borgarello, and N. Serpon (1987). Chemical Degradation of Chlorophenols with Fenton's Reagent. *Chemosphere*, 16:2225-37.

Bellamy, W.D., P.A. Hickman, and N. Ziemba (1991). Treatment of VOC-contaminated Ground Water by Hydrogen Peroxide and Ozone Oxidation. *Research Journal WPCF*, 63:120-28.

Bowers, A.R., P. Gaddipati, W.W. Eckenfelder, and R.M. Monsen (1989). Treatment of Toxic or Refractory Wastewaters with Hydrogen Peroxide. *Water Science and Technology*, 21:477-86.

Büyüksönmez, F., T. F. Hess, *et al.* (1999). Optimization of Simultaneous Chemical and Biological Mineralization of Perchloroethylene. *Applied and Environmental Microbiology*, 65(6):2784-2788.

Büyüksönmez, F., T. F. Hess, *et al.* (1998). Toxic Effects of Modified Fenton Reactions on *Xanthobacter flavus* FB71. *Applied and Environmental Microbiology*, 64(10):3759-3764.

Carberry, J.B., and T. M. Benzing (1991). Peroxide Pre-oxidation of Recalcitrant Toxic Waste to Enhance Biodegradation. *Water Science and Technology*, 23:367-376.

Case, T.L. (1997). Reactive Permanganate Grouts for Horizontal Permeable Barriers and In Situ Treatment of Ground Water. M.S. Thesis, Colorado School of Mines, Golden, CO.

Chambers, J., A. Leavitt, C. Walti, C.G. Schreier, and J. Melby (2000). Treatability Study – Fate of Chromium During Oxidation of Chlorinated Solvents. In: Wickramanayake, G.B., A.R. Gavaskar, and A.S.C. Chen (ed.). Chemical Oxidation and Reactive Barriers. Battelle Press, Columbus, OH. pp. 57-66.

Cline, S.R., O.R. West, N.E. Korte, F.G. Gardner, R.L. Siegrist, and J.L. Baker (1997). $KMnO_4$ Chemical Oxidation and Deep Soil Mixing for Soil Treatment. *Geotechnical News*, December. pp. 25-28.

Table 1.4. Reader's guide for the final report from SERDP project CU-1290.

Project task or research element	Student M.S. theses or Ph.D. dissertations	Journal papers and selected conference presentations, published abstracts and proceedings papers
Bench scale kinetic and DNAPL degradation studies: vial reactors and multiphase vial reactor	Jackson 2004	Crimi *et al.* 2002, 2004a, Crimi and Siegrist 2005
Bench-scale studies of porous media effects on oxidation reactions: zero headspace reactors, 1-D diffusion cells	Seitz 2004	Crimi and Siegrist 2005, Seitz *et al.* 2004a,b
Upscaling reaction/transport experiments: flow-through tube reactors, 2-D flow-through cells, 2-D tanks	Heiderscheidt 2005, Petri 2006	Petri *et al.* 2004, Crimi *et al.* 2005a, Petri *et al.* 2005, Petri *et al.* 2007
Experimental evaluation of coupling ISCO with post-ISCO bioremediation: batch microcosms, 1-D columns	Sahl 2005	Sahl *et al.* 2004a,b, Sahl and Munakata-Marr 2006, Sahl *et al.* 2006
Experimental evaluation of coupling ISCO with pre-ISCO surfactant/ cosolvent flushing: batch vial reactors, 2-D flow-through cells	Dugan 2006	Dugan *et al.* 2004b, 2005a
Experimental studies of the compatibility of partitioning tracers and ISCO: batch vial reactors, 2-D flow-through cells	Dugan 2006	Dugan *et al.* 2004b, 2005b
Mathematical modeling	Heiderscheidt 2005, Petri 2006	Heiderscheidt *et al.* 2004,
Project presentations and research information dissemination		Siegrist *et al.* 2004, Siegrist 2005a,b, 2006a,b

Coons, D.E., M.T. Balba, C. Lin, S. Schrocci, and A. Weston (2000). Remediation of Chlorinated Compounds by Chemical Oxidation. In: G.B. Wickramanayake, A.R. Gavaskar, A.S.C. Chen (ed.). Chemical Oxidation and Reactive Barriers: Remediation of Chlorinated and Recalcitrant Compounds. Battelle Press. Columbus, OH. pp. 161-168.

Crimi, M.L., S. Taylor, and R.L. Siegrist (2002). Effects of Porous Media Type on Natural Oxidant Demand and DNAPL Degradation During In Situ Chemical Oxidation. 2nd Intern. Conf. on Oxidation and Reduction Technologies for In Situ Treatment of Soil and Ground Water. Nov. 17, 2002, Toronto, Ontario.

Crimi, M.L., and R.L. Siegrist (2003). Bench-Scale Studies of Reaction Processes Controlling In Situ Chemical Oxidation (ISCO) of DNAPLs. 6th Intern. Symp. and Exhibition on Environmental Contamination in Central and Eastern Europe and the Commonwealth of Independent States. Sept. 1, 2003, Prague, Czech Republic.

Crimi, M.L., R.L. Siegrist, and S. Jackson (2004a). Chemical Oxidation of Aqueous-Phase vs. DNAPL-Phase Contaminants. Battelle's 4th Intern. Conf. on Remediation of Chlorinated and Recalcitrant Compounds. May 24, 2004, Monterey, CA.

Crimi M., R.L. Siegrist, S. Jackson, S. Seitz, T.A. Palaia, and M.A. Singletary (2004b). Optimization of Field Scale Permanganate Injection for PCE Treatment. 3rd Intern. Conf. on Oxidation and Reduction Technologies for In Situ Treatment of Soil and Ground Water. October 2004, San Diego, CA.

Crimi M., S. Seitz, J. Sahl, J. Kopp, J. Heiderscheidt, P. Dugan, B. Petri, and R.L. Siegrist (2005a). ISCO of DNAPLs: Applicability Based on 2-Dimensional Transport Studies of DNAPL Entrapment and Oxidant Delivery Techniques. The 21st Annual Intern. Conf. on Soils, Sediments, and Water. Oct. 17-21, 2005, Amherst, MA.

Crimi, M.L., P. Block, B., and McGinnis (2005a). Experimental Evaluation of the Use of Activated Persulfate to Destroy Lindane. The 4th Intern. Conf. on Oxidation and Reduction Technologies for In Situ Treatment of Soil and Ground Water. Oct. 23-27, 2005, Chicago, IL.

Crimi, M.L., and J. Taylor (2005). Remediation Protocol for Oxidative Destruction of BTEX Contaminants. The 1st Intern. Conf. on Challenges in Site Remediation: Proper Site Characterization, Technology Selection and Testing, and Performance Monitoring. Oct. 23-27, 2005, Chicago, IL.

Crimi, M.L. and R.L. Siegrist (2005). Factors Affecting Effectiveness and Efficiency of DNAPL Destruction Using Potassium Permanganate and Catalyzed Hydrogen Peroxide. *Journal of Environmental Engineering*, 131(12):1724-1732.

Davis, E.L. (1997). How Heat Can Enhance *In Situ* Soil and Aquifer Remediation: Important Chemical Properties and Guidance on Choosing the Appropriate Technique. Ground Water Issue Paper, EPA/540/S-97/502, U.S. EPA. April.

Davis, E.L., and K. Udell (1998). Mechanisms of In Situ Thermal Remediation. Pres. at Conference on In Situ Thermal Treatment. U.S. EPA Technology Innovation Office. December 16, 1998, Atlanta.

Dugan, P.J., R.L. Siegrist, M.L. Crimi, and C.E Divine (2004a). Coupling Flushing Reagents with Oxidants: Effects on Remediation and Characterization. Battelle's 4th Intern. Conf. on Remediation of Chlorinated and Recalcitrant Compounds. May 24, 2004, Monterey, CA.

Dugan, P.J., R.L. Siegrist, M.L. Crimi, and C.E. Divine (2004b). Coupling Surfactants/Cosolvents with Oxidants: Effects on Remediation and Performance Assessment. 3rd Intern. Conf. on Oxidation and Reduction Technologies for In Situ Treatment of Soil and Ground Water. Oct. 2004, San Diego, CA.

Dugan, P.J., R.L. Siegrist, and M.L. Crimi (2005a). Coupling Surfactants/Cosolvents with Permanganate for DNAPL Removal: Comparison of Co-Injection and Sequential Application. 4th Intern. Conf. on Oxidation and Reduction Technologies for In Situ Treatment of Soil and Ground Water. Oct. 23-27, 2005, Chicago, IL.

Dugan, P.J., R.L. Siegrist, and M.L. Crimi (2005b). Partitioning Tracer Tests: Effects on Performance Assessment after Coupling Surfactant with Oxidant for DNAPL Remediation. 4th Intern. Conf. on Oxidation and Reduction Technologies for In Situ Treatment of Soil and Ground Water. Oct. 23-27, 2005, Chicago, IL.

Dugan, P. (2006). Coupling In Situ Technologies for DNAPL Remediation and Viability of the PITT for Post-Remediation Performance Assessment. Ph.D. dissertation, Environmental Science and Engineering Division, Colorado School of Mines, Golden, CO. December 2006.

Evanko, C.R., and D.A. Dzombak (1997). Remediation of metals-contaminated soils and ground water. Technology Evaluation Report, TE-97-01. Ground Water Remediation Technologies Analysis Center, Pittsburgh, PA.

ESTCP (1999). Technology Status Review: In Situ Oxidation. DOD Environmental Security Technology Certification Program. http://www.estcp.gov.

Fountain, J.C. (1997). The Role of Field Trials in Development and Feasibility Assessment of Surfactant-Enhanced Aquifer Remediation. *Water Environment Research*, 69(2):188-195.

Francis, A.J., C.J. Dodge, F. Lu, G.P. Halada, and C.R. Clayton (1994). XPS and XANES Studies of Uranium Reduction by *Clostridium sp. Environmental Science and Technology*, 28(4):636-639.

GAO (2005). United States Government Accountability Office (GAO) Report to Congressional Committees. Ground Water Contamination: DOD uses and Develops a Range of Remediation Technologies to Clean Up Military Sites. GAO-55-666. Washington, D.C.

Gardner, F.G., N.E. Korte, J. Strong-Gunderson, R.L. Siegrist, O.R. West, S.R. Cline, and J. Baker (1998). Implementation of Deep Soil Mixing at the Kansas City Plant. Final project report by Oak Ridge National Laboratory for the Environmental Restoration Program at the DOE Kansas City Plant. ORNL/TM-13532.

Gates, D.D., and R.L. Siegrist (1993). Laboratory Evaluation of Chemical Oxidation Using Hydrogen Peroxide. Report from The X-231B Project for In Situ Treatment by Physicochemical Processes Coupled with Soil Mixing. Oak Ridge National Laboratory. ORNL/TM-12259.

Gates, D.D., and R.L. Siegrist (1995a). In Situ Chemical Oxidation of Trichloroethylene Using Hydrogen Peroxide. *Journal of Environmental Engineering*, 121(9): 639-644.

Gates, D.D., R.L. Siegrist and S.R. Cline (1995b). Chemical Oxidation of Contaminants in Clay or Sandy Soil. Proceedings of ASCE National Conference on Environmental Engineering. Am. Soc. of Civil Eng., Pittsburgh, PA.

Gates, D.D., R.L. Siegrist, and S.R. Cline (2001). A Comparison of Potassium Permanganate and Hydrogen Peroxide as Chemical Oxidants for Organically Contaminated Soils. *Journal of Environmental Engineering*, 127(4):337-347.

Gorby, Y.A., and D.R. Lovley (1992). Enzymatic Uranium Precipitation. *Environmental Science and Technology*, 26:205-207.

Haselow, J.S., R.L. Siegrist, M.L. Crimi, and T. Jarosch (2003). Estimating the Total Oxidant Demand for In Situ Chemical Oxidation Design. *Remediation Journal*, 13(4):5-16.

Heiderscheidt J.L., T.H. Illangasekare, R.L. Siegrist, and M.L. Crimi (2004). Use of Chemical Oxidation to Reduce Rate-limited Matrix Diffusion of PCE from Low Permeability Materials and Effects on Natural Oxidant Demand. 3rd Intern. Conf. on Oxidation and Reduction Technologies for In Situ Treatment of Soil and Ground Water. Oct. 2004, San Diego, CA.

Heiderscheidt, J.L. (2005). DNAPL Source Zone Depletion During In Situ Chemical Oxidation (ISCO): Experimental and Modeling Studies. Ph.D. dissertation, Environmental Science and Engineering Division, Colorado School of Mines, Golden, CO. August 2005.

Horitsu, H.S., S. Futo, Y. Miyaza, S. Ogai, and K. Kawai (1987). Enzymatic Reduction of Hexavalent Chromium by Chromium Tolerant *Pseudomonas Ambigua G-1*. *Agric. Biol. Chem.*, 51:2417-2420.

Hoigne, J., and H. Bador (1983). Rate Constants of Reaction of Ozone with Organic and Inorganic Compounds in Water. *Water Research*, 17:173.

Huang, K., G.E., Hoag, P. Chheda, B.A. Woody, and G.M. Dobbs (1999). Kinetic Study of Oxidation of Trichloroethylene by Potassium Permanganate. *Environmental Engineering Science*, 16(4):265-274.

Huang, K., P. Chheda, G.E. Hoag, B.A. Woody, and G.M. Dobbs (2000). Pilot-scale Study of In Situ Chemical Oxidation of Trichloroethene with Sodium Permanganate. In: G.B. Wickramanayake, A.R. Gavaskar, A.S.C. Chen (ed.). Chemical Oxidation and Reactive Barriers: Remediation of Chlorinated and Recalcitrant Compounds. Battelle Press. Columbus, OH. pp. 145-152.

IT Corporation and SM Stollar Corp (2000). Implementation Report of Remediation Technology Screening and Treatability Testing of Possible Remediation Technologies for the Pantex Perched Aquifer. October, 2000. DOE Pantex Plant, Amarillo, Texas.

ITRC (2001). Technical and Regulatory Guidance for In Situ Chemical Oxidation of Contaminated Soil and Ground Water (ISCO-1). The Interstate Technology & Regulatory Cooperation Work Group In Situ Chemical Oxidation Work Team, Interstate Technology & Regulatory Council (ITRC).

ITRC (2005). Technical and Regulatory Guidance for In Situ Chemical Oxidation of Contaminated Soil and Ground Water, 2nd Edition (ISCO-2). The Interstate Technology & Regulatory Council In Situ Chemical Oxidation Team, Interstate Technology & Regulatory Council (ITRC).

Kavanaugh, M.C., P.S.C. Rao, L. Abriola, J. Cherry, G. Destouni, R. Falta, D. Major, J. Mercer, C. Newell, T. Sale, S. Shoemaker, R.L. Siegrist, G. Teutsch, and K. Udell (2003). The DNAPL Cleanup Challenge: Source Removal or Long Term Management. Report of an Expert Panel to the U.S. EPA National Risk Management Laboratory and Technology Innovation Office. EPA/600/R-03/143, December 2003.

Jackson, S.F. (2004). Comparative Evaluation of Potassium Permanganate and Catalyzed Hydrogen Peroxide During In Situ Chemical Oxidation of DNAPLs. M.S. Thesis, Environmental Science and Engineering Division, Colorado School of Mines, Golden, CO. January 2004.

Jackson, R.E., and P.E. Mariner (1998). Surfactant-Enhanced Remediation of DNAPL Contaminated Alluvium. Proc. Intern. Conf. on Decontamination and Decommissioning and Nuclear and Hazardous Waste Management. September 13-18, 1998, Denver, CO. American Nuclear Society, La Grange Park, IL.

Jafvert, C.T. (1996). Surfactants/Cosolvents - Technology Evaluation Report. TE-96-02. Ground Water Remediation Technologies Analysis Center. Pittsburgh, PA.

Jerome, K.M., B. Riha and B.B. Looney (1997). Demonstration of In Situ Oxidation of DNAPL Using the Geo-Cleanse Technology. WSRC-TR-97-00283. Westinghouse Savannah River Company, Aiken, SC.

Levin, R., E. Kellar, J. Wilson, L. Ware, J. Findley, and J. Baehr (2000). Full-Scale Soil Remediation of Chlorinated Solvents by In Situ Chemical Oxidation. In: G.B. Wickramanayake, A.R. Gavaskar, A.S.C. Chen (ed.). Chemical Oxidation and Reactive Barriers: Remediation of Chlorinated and Recalcitrant Compounds. Battelle Press. Columbus, OH. pp. 153-160.

Leung, S.W., R.J. Watts and G.C. Miller (1992). Degradation of Perchloroethylene by Fenton's Reagent: Speciation and Pathway. *Journal Environmental Quality*, 21:377-81.

Li, X.D., and F.W. Schwartz (2000). Efficiency Problems Related to Permanganate Oxidation Schemes. In: Wickramanayake, G.B., A.R. Gavaskar, and A.S.C. Chen (eds.). Chemical Oxidation and Reactive Barriers. Battelle Press, Columbus, OH. pp. 41-48.

Lovley, D.R. 1991. Dissimilitory Fe(III) and Mn(IV) Reduction. *Microbiological Reviews*, 55:259-287.

Lovley, D.R., E.J.P. Phillips, Y. Gorby, and E.R. Landa. 1991. Microbial Reduction of Uranium. *Nature*, 350:413-416.

Lowe, K.S., F.G. Gardner, and R.L. Siegrist (2002). Field Pilot Test of In Situ Chemical Oxidation through Recirculation Using Vertical Wells. *Ground Water Monitoring and Remediation*, Winter issue. pp. 106-115.

MacKay, D.M., and J.A. Cherry (1989). Ground Water Contamination: Limits of Pump-and-Treat Remediation. *Environmental Science and Technology*, 23:630-636.

Marvin, B.K., C.H. Nelson, W. Clayton, K.M. Sullivan, and G. Skladany (1998). In Situ Chemical Oxidation of Pentachlorophenol and Polycyclic Aromatic Hydrocarbons: From Laboratory Tests to Field Demonstration. Proc. 1st Intern. Conf. Remediation of Chlorinated and Recalcitrant Compounds. May 1998, Monterey, CA.

McKinzi, A.M., and T. J. DiChristina (1999). Microbially Driven Fenton Reaction for Transformation of Pentachlorophenol. *Environmental Science and Technology*, 33(11):1886-1891.

Moes, M., C. Peabody, R. Siegrist, and M. Urynowicz (2000). Permanganate Injection for Source Zone Treatment of TCE DNAPL. In: Wickramanayake, G.B., A.R. Gavaskar, and A.S.C. Chen (ed.). Chemical Oxidation and Reactive Barriers. Battelle Press, Columbus, OH. pp. 117-124.

Mott-Smith, E., W.C. Leonard, R. Lewis, W.S. Clayton, J. Ramirez, and R. Brown (2000). In Situ Oxidation of DNAPL Using Permanganate: IDC Cape Canaveral demonstration. In: Wickramanayake, G.B., A.R. Gavaskar, and A.S.C. Chen (eds.). Chemical Oxidation and Reactive Barriers. Battelle Press, Columbus, OH. pp.125-134.

National Research Council (NRC) (1994). Alternatives for Ground Water Cleanup. National Academy Press, Washington, D.C.

National Research Council (NRC) (1997). Innovations in Ground Water and Soil Cleanup. National Academy Press, Washington, D.C.

Nelson, C.H., and R.A. Brown (1994). Adapting Ozonation for Soil and Ground Water Cleanup. *Chemical Engineering.* McGraw-Hill, Inc.

Oberle, D.W., and D.L. Schroder (2000). Design Considerations for In Situ Chemical Oxidation. In: G.B. Wickramanayake, A.R. Gavaskar, A.S.C. Chen (ed.). Chemical Oxidation and Reactive Barriers: Remediation of Chlorinated and Recalcitrant Compounds. Battelle Press. Columbus, OH. pp. 91-100.

Palmer, C.D., and W. Fish (1992). Chemical Enhancements to Pump and Treat Remediation. U.S. EPA publication EPA/540/2-91-010.

Palmer, C.D., and R. W. Puls (1994). Natural Attenuation of Hexavalent Chromium in Ground Water and Soils. U.S. EPA Ground Water Issue paper, EPA/540/S-94/505.

Petri, B.G., R.L Siegrist, and M.L. Crimi (2004). Mass Transfer Impacts of Oxidant Flushing Parameters During In Situ Chemical Oxidation of Dense Nonaqueous Phase Liquids. 3rd Intern. Conf. on Oxidation and Reduction Technologies for In Situ Treatment of Soil and. Oct. 2004, San Diego, CA.

Petri, B.G., R.L. Siegrist, and M.L. Crimi (2005). Impacts of Permanganate Flushing Parameters on Mass Transfer from Dense Nonaqueous Phase Liquid Residuals. The 4th Intern. Conf. on Oxidation and Reduction Technologies for In Situ Treatment of Soil and Ground Water. Oct. 23-27, Chicago, IL.

Petri, B.G. (2006). Impacts of Subsurface Permanganate Delivery Parameters on Dense Nonaqueous Phase Liquid Mass Depletion Rates. M.S. thesis, Environmental Science and Engineering Division, Colorado School of Mines, Golden, CO. January 2006.

Petri, B.G., R.L. Siegrist, and M.L. Crimi (2007). Effects of Groundwater Velocity and Permanganate Concentration on DNAPL Mass Depletion Rates During In Situ Chemical Oxidation. *Journal of Environmental Engineering*, in review.

Ravikmur, J.X., and M. Gurol (1994). Chemical Oxidation of Chlorinated Organics by Hydrogen Peroxide in the Presence of Sand. *Environmental Science and Technology*, 28:394-400.

Reitsma, S., and M. Marshall (2000). Experimental Study of Oxidation of Pooled NAPL. In: Wickramanayake, G.B., A.R. Gavaskar, and A.S.C. Chen (ed.). Chemical Oxidation and Reactive Barriers. Battelle Press, Columbus, OH. pp. 25-32.

Roote, D.S. (1997). In Situ Flushing - Technology Overview Report. TO-97-02. Ground Water Remediation Technologies Analysis Center. Pittsburgh, PA.

Sahl, J., S. Van Cuyk, M.L. Crimi, J. Munakata-Marr, and R.L. Siegrist (2004a). Impact of Chemical Oxidation on Microbial Communities in Contaminated Ground Water Aquifer Sediments. Battelle's 4th Intern. Conf. on Remediation of Chlorinated and Recalcitrant Compounds. May 24, Monterey, CA.

Sahl J., J. Munakata-Marr, M.L. Crimi, and R.L. Siegrist (2004b). Coupling In Situ Chemical Oxidation (ISCO) with Bioremediation for DNAPL Treatment. 3rd Intern. Conf. on Oxidation and Reduction Technologies for In Situ Treatment of Soil and Ground Water. Oct. 2004, San Diego, CA.

Sahl, J. (2005). Coupling In Situ Chemical Oxidation (ISCO) with Bioremediation Processes in the Treatment of Dense Non-aqueous Phase Liquids (DNAPLs). M.S. thesis, Environmental Science and Engineering Division, Colorado School of Mines, Golden, CO. April 2005.

Sahl, J., M.L. Crimi, J. Munakata-Marr, and R.L. Siegrist (2005). The Impact of In Situ Chemical Oxidation on Bioremediation Processes in the Treatment of Chloroethenes. 4th Intern. Conf. on Oxidation and Reduction Technologies for In Situ Treatment of Soil and Ground Water. Oct. 23-27, 2005, Chicago, IL.

Sahl, J., and J. Munakata-Marr (2006). The Effects of In Situ Chemical Oxidation on Microbial Processes: A Review. *Remediation Journal*, 16(3):57-70.

Sahl, J., J. Munakata-Marr, M.L. Crimi, and R.L. Siegrist (2006). Coupling Permanganate Oxidation with Microbial Dechlorination of Tetrachoroethene. *Water Environment Research*, accepted and in press.

Schnarr, M., C. Truax, G. Farquhar, E. Hood, T. Gonully, and B. Stickney (1998). Laboratory and Controlled Field Experimentation Using Potassium Permanganate to Remediate Trichloroethylene and Perchloroethylene DNAPLs in Porous Media. *Journal of Contaminant Hydrology*, 29:205-224.

Scott, J.P., and D. F. Ollis (1995). Integration of Chemical and Biological Oxidation Processes for Water Treatment: Review and Recommendations. *Environmental Progress*, 14(2):88-103.

Seitz, S.J., M.L. Crimi, and R.L. Siegrist (2003). Diffusive Mass Transport Limitations for In Situ Chemical Oxidation (ISCO) of DNAPLs. 6th Intern. Symp. and Exhibition on Environmental Contamination in Central and Eastern Europe and the Commonwealth of Independent States. Sept. 1, 2003, Prague, Czech Republic.

Seitz, S.J. (2004). Experimental Evaluation of Mass Transfer and Matrix Interactions During In Situ Chemical Oxidation Relying on Diffusive Transport. M.S. thesis, Environmental Science and Engineering Division, Colorado School of Mines, Golden, CO. December 2004.

Seitz, S.J., M.L. Crimi, and R.L. Siegrist (2004a). Diffusive Transport During In Situ Chemical Oxidation (ISCO) of DNAPL Sites. Battelle's 4th Intern. Conf. on Remediation of Chlorinated and Recalcitrant Compounds. May 24, 2004, Monterey, CA.

Seitz, S., M.L. Crimi, and R.L. Siegrist (2004b). In Situ Chemical Oxidation Applicability at DNAPL Sites with Diffusion-Dominated Low Permeability Media. The 3rd Intern. Conf. on Oxidation and Reduction Technologies for In Situ Treatment of Soil and Ground Water. Oct. 2004, San Diego, CA.

Siegrist, R.L., K.S. Lowe, L.D. Murdoch, W.W. Slack, and T.C. Houk (1998a). X-231A Demonstration of In Situ Remediation of DNAPL Compounds in Low Permeability Media by Soil Fracturing with Thermally Enhanced Mass Recovery or Reactive Barrier Destruction. Oak Ridge National Laboratory Report. ORNL/TM-13534.

Siegrist, R.L., K.S. Lowe, L.C. Murdoch, T.L. Case, D.A. Pickering, and T.C. Houk (1998b). Horizontal Treatment Barriers of Fracture-Emplaced Iron and Permanganate Particles. NATO/CCMS Pilot Study Special Session on Treatment Walls and Permeable Reactive Barriers. EPA 542-R-98-003. May 1998. pp. 77-82.

Siegrist, R.L., K.S. Lowe, D.R. Smuin, O.R. West, J.S. Gunderson, N.E. Korte, D.A. Pickering, and T.C. Houk (1998c). Permeation Dispersal of Reactive Fluids for In Situ Remediation: Field Studies. Project Report prepared by Oak Ridge National Laboratory for the U.S. DOE Office of Science & Technology. ORNL/TM-13596.

Siegrist, R.L., K.S. Lowe, L.C. Murdoch, T.L. Case, and D.A. Pickering (1999). In Situ Oxidation by Fracture Emplaced Reactive Solids. *Journal of Environmental Engineering*, 125(5):429-440.

Siegrist, R.L., M.A. Urynowicz, and O.R. West (2000a). An Overview of In Situ Chemical Oxidation Technology Features and Applications. EPA/625/R-99/012. U.S. EPA ORD, Washington, DC. pp. 61-69.

Siegrist, R.L., M.A. Urynowicz, and O.R. West (2000b). In Situ Chemical Oxidation for Remediation of Contaminated Soil and Ground Water. *Ground Water Currents.* Issue No. 37, U.S. EPA Office of Solid Waste and Emergency Response, EPA 542-N-00-006, September 2000. http://www.epa.gov/tio.

Siegrist R.L., M.A. Urynowicz, O.R. West, M.L. Crimi, K.S. Lowe (2001). Principles and Practices of In Situ Chemical Oxidation Using Permanganate. Battelle Press, Columbus Ohio. 336 p.

Siegrist, R.L. (2002). Fundamentals of In Situ Chemical Oxidation. USEPA workshop on In Situ Treatment of Ground Water Contaminated with Non-aqueous Phase Liquids. Dec. 10, 2002, Chicago, IL.

Siegrist, R.L., M.A. Urynowicz, M.L. Crimi, and K.S. Lowe (2002). Genesis and Effects of Particles Produced During In Situ Chemical Oxidation Using Permanganate. *Journal of Environmental Engineering*, 128(11):1068:1079.

Siegrist, R.L. (2003). In Situ Chemical Oxidation (ISCO): Principles and Practices for Source Zone Treatment. Invited presentation to NRC Committee on Source Removal of Contaminants in the Subsurface. Apr. 14, 2003, Washington, D.C.

Siegrist, R.L., M.L. Crimi, N. Thomson, and R. Watts (2004). In Situ Chemical Oxidation for DNAPL Source Zone Treatment. SERDP/ESTCP Symposium on Meeting DOD's Environmental Challenges. Dec. 2, 2004, Washington, D.C.

Siegrist, R.L. (2005a). In Situ Chemical Oxidation for DNAPL Source Zone Treatment. Invited seminar presentation, Danish Technical University. Jan. 2005, Lynnby, Denmark.

Siegrist, R.L. (2005b). Remediation of Contaminated Sites Using In Situ Chemical Oxidation and Coupled Technologies. Invited seminar presentation, Kasekart University. Mar. 2005, Bangkok, Thailand.

Siegrist, R.L. (2006a). Site Remediation Using Chemical Oxidation Techniques. Invited presentation at the NATO/CCMS Pilot Study meeting, "Prevention and Remediation in Selected Industrial Sectors: Small Sites in Urban Areas." June 4-7, 2006, Athens, Greece.

Siegrist, R.L. (2006b). Chemical Oxidation for Clean Up of Contaminated Ground Water. Invited presentation at the NATO Advanced Research Workshop, "Environmental Security Threats in Urban Settings", June 8-9, 2006, Athens, Greece.

Somich, C.J., P. C. Kearney, *et al.* (1988). Enhanced Soil Degradation of Alachlor by Treatment with Ultraviolet Light and Ozone. *Journal of Agricultural and Food Chemistry*, 36(6):1322-1326.

Somich, C.J., M. T. Muldoon, *et al.* (1990). On-site Treatment of Pesticide Waste and Rinsate Using Ozone and Biologically Active Soil. *Environmental Science and Technology*, 24(5):745-749.

Taylor, S., M.L. Crimi, and R.L. Siegrist (2002). Comparative Evaluation of Contaminant Degradation Kinetics and Efficiency During In Situ Chemical Oxidation of DNAPLS. 2nd Intern. Conf. on Oxidation and Reduction Technologies for In Situ Treatment of Soil and Ground Water. Nov. 17, 2002, Toronto, Ontario.

Tyre, B.W., Watts, R.J., and Miller, G.C. (1991). Treatment of Four Biorefractory Contaminants in Soils Using Catalyzed Hydrogen Peroxide. *Journal of Environmental Quality***,** 20:832-38.

Urynowicz, M.A. 2000 (2000). Reaction Kinetics and Mass Transfer During In Situ Oxidation of Dissolved and DNAPL - Trichloroethylene with Permanganate. Ph.D. dissertation, Environmental Science and Engineering Division, Colorado School of Mines. May.

Urynowicz, M.A., and R.L. Siegrist (2000). Chemical Degradation of TCE DNAPL by Permanganate. In: Wickramanayake, G.B., A.R. Gavaskar, and A.S.C. Chen (ed.). Chemical Oxidation and Reactive Barriers. Battelle Press, Columbus, OH. pp. 75-82.

USEPA (1998). In Situ Remediation Technology: In Situ Chemical Oxidation. EPA 542-R-98-008. Office of Solid Waste and Emergency Response. Washington, D.C.

USEPA (1999). Ground Water Cleanup: Overview of Operating Experience at 28 Sites. EPA 542-R-99-006. Office of Solid Waste and Emergency Response. Washington, D.C.

Vella, P.A., G. Deshinsky, J.E. Boll, J. Munder, and W.M. Joyce (1990). Treatment of Low Level Phenols with Potassium Permanganate. *Research Journal WPCF*, 62(7):907-14.

Vella, P.A., and B. Veronda (1994). Oxidation of Trichloroethylene: A Comparison of Potassium Permanganate and Fenton's Reagent. 3rd Intern. Symposium on Chemical Oxidation. In: In Situ Chemical Oxidation for the Nineties. Technomic Publishing Co., Inc. Lancaster, PA. Vol. 3, pp. 62-73.

Venkatadri, R., and R.W. Peters (1993). Chemical Oxidation Technologies: Ultraviolet Light/Hydrogen Peroxide, Fenton's Reagent, and Titanium Dioxide Assisted Photocatalysis. *Journal of Hazardous Waste and Hazardous Materials*, 10(2):107-149.

Watts, R.J., R.A. Rausch, S.W. Leung, and M.D. Udell (1990). Treatment of Pentachlorophenol Contaminated Soils Using Fenton's Reagent. *Journal of Hazardous Waste and Hazardous Materials*, 7:335-45.

Watts, R.J., S.W. Leung, and M.D. Udell (1991). Treatment of Contaminated Soils Using Catalyzed Hydrogen Peroxide. Proceeding to the First International Symposium on Chemical Oxidation. Technomic, Nashville, TN.

Watts, R.J., and B.R. Smith (1991). Catalyzed Hydrogen Peroxide Treatment of Octachlorobidenzo-p-dioxin (OCCD) in Surface Soils. *Chemosphere*, 23:949-55.

Watts, R.J., M.D. Udell, and R.M. Monsen (1993). Use of Iron Minerals in Optimizing the Peroxide Treatment of Contaminated Soils. *Water Environment Research*, 65:839-44.

Watts, R.J., A.P. Jones, P. Chen, and A. Kenny (1997). Mineral-Catalyzed Fenton-Like Oxidation of Sorbed Chlorobenzenes. *Water Environment Research*, 69:269-275.

West, O.R., S.R. Cline, W.L. Holden, F.G. Gardner, B.M. Schlosser, J.E. Thate, D.A. Pickering, and T.C. Houk (1998a). A Full-Scale Field Demonstration of In Situ Chemical Oxidation through Recirculation at the X-701B Site. Oak Ridge National Laboratory Report, ORNL/TM-13556.

West, O.R., S.R. Cline, R.L. Siegrist, T.C. Houk, W.L. Holden, F.G. Gardner, and R.M. Schlosser (1998b). A Field-Scale Test of In Situ Chemical Oxidation through Recirculation. Proc. Spectrum '98 International Conference on Nuclear and Hazardous Waste Management. Denver, Colorado, Sept. 13-18, pp. 1051-1057.

West, O.R., R.L. Siegrist, S.R. Cline, and F.G. Gardner (2001). The Effects of In Situ Chemical Oxidation through Recirculation (ISCOR) on Aquifer Contamination, Hydrogeology and Geochemistry. Oak Ridge National Laboratory Report, ORNL/TM-13556.

Wiesner, M.R., M.C. Grant, and S.R. Hutchins (1996). Reduced Permeability in Ground Water Remediation Systems: Role of Mobilized Colloids and Injected Chemicals. *Environmental Science and Technology*, (30):3184-3191.

Yan, Y.E., and F.W. Schwartz (1996). Oxidation of Chlorinated Solvents by Permanganate. Proc. Intern. Conf. on Remediation of Chlorinated and Recalcitrant Compounds, Ohio: Battelle Press. pp. 403-408.

Yan, Y.E., and F.W. Schwartz (1999). Oxidative Degradation and Kinetics of Chlorinated Ethylenes by Potassium Permanganate. *Journal of Contaminant Hydrology*, 37,:343-365.

Yin, Y., and H.E. Allen (1999). In Situ Chemical Treatment. Ground Water Remedation Technology Analysis Center, Technology Evaluation Report, TE-99-01. July, 1999.

Zhang, C., S. Liu, J. Logan, R. Maxumber, and T.J. Phelps (1996). Enhancement of Fe(III), Co(III), and Cr(VI) Reduction at Elevated Temperatures and by a Thermophilic Bacterium. *Applied Biochemistry and Biotechnology*, 57/58:923-932.

CHAPTER 2

BACKGROUND THEORY AND RELEVANT PRIOR RESEARCH FINDINGS

2.1 INTRODUCTION

The degradation of DNAPL residuals by ISCO has a theoretical basis, but the cost-effective realization depends on several inter-related processes and interactions as depicted in Figure 2.1 and listed below:

- Susceptibility of DNAPL organics to oxidative destruction,
- Rate and extent of mass transfer at the DNAPL-water interface,
- Ability to deliver and transport an oxidant in the subsurface,
- Effects of subsurface conditions on ISCO reactions, and
- ISCO effects on subsurface permeability and biogeochemistry.

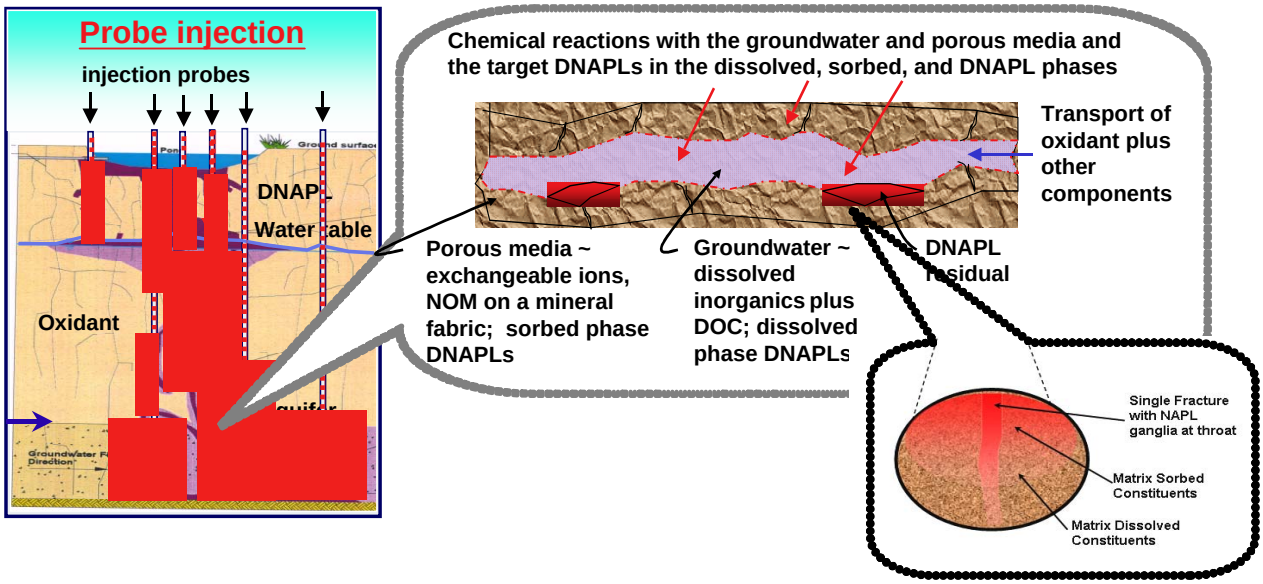

Figure 2.1. Macro- and micro-scale features of in situ chemical oxidation for DNAPL sites.

This chapter provides a summary of background theory and selected findings of more recent research concerning in situ chemical oxidation and the application of ISCO for remediation of DNAPL source zones. This chapter highlights various aspects of the science and technology of ISCO that were addressed as the objectives of SERDP project CU-1290 were accomplished. Presented first is a synopsis of DNAPL behavior in the subsurface followed by more detailed coverage of key ISCO issues, including: chemical oxidation of aqueous phase PCE and TCE, application of chemical oxidants to DNAPL phase PCE and TCE, oxidant persistence and oxidant-subsurface interactions, effects of ISCO on microbial processes, coupling ISCO with surfactant/cosolvent flushing, compatibility of ISCO with partitioning tracers, and upscaling and mathematical modeling. The information presented in this chapter is derived in large part from the M.S. theses and Ph.D. dissertations completed by graduate students at CSM with support provided by SERDP through project CU-1290 (Jackson 2004, Seitz 2004, Sahl 2005, Heiderscheidt 2005, Petri 2006, Dugan 2006).

2.2. DNAPL BEHAVIOR AND APPLICATION OF ISCO

2.2.1. DNAPL Movement and Entrapment in the Subsurface

When a DNAPL is released into a subsurface environment, it can migrate downward by density driven advection through the saturated and unsaturated zones of an aquifer. This downward flow is ultimately controlled by factors such as interfacial tension, viscosity and capillary pressures within the porous media (Mercer and Cohen 1990). Heterogeneities in the saturated zone greatly influence the entrapment architecture as DNAPL pools on low permeability lenses, and layering in the subsurface increases the horizontal spreading of the contaminant (Schwille 1988, Mercer and Cohen 1990, Illangasekare *et al.* 1995a,b). Downward movement of the DNAPL is continuous until the source of the spill ceases, at which time DNAPL movement becomes unstable and leaves behind discontinuous zones of residual saturation as well as agglomerated pools which form in depressions on low permeability layers (see Figure 2.2) (Oostrom *et al.* 1999a). The residual saturation zones are caused by droplets of DNAPL, which are trapped by capillary forces within the porous media. These droplets are highly heterogeneous in shape and size, and range from large numbers of small relatively simple shapes, to large complex ganglia with multiple fingers (Conrad *et al.* 1992). Pools represent areas where DNAPL has agglomerated into a large mass and has effectively saturated the porous media (Illangasekare *et al.* 1995, Oostrom *et al.* 1999a). The primary difference between residual DNAPL and pooled DNAPL is that residuals, due to the large number of fine droplets, contain a small mass of contaminant with a large NAPL-water interfacial area, while pools contain large amounts of DNAPL with comparatively small interfacial areas. DNAPL mass transfer occurs at this interfacial area, and thus is highly dependent on the configuration of the DNAPL (Miller *et al.* 1990, Powers *et al.* 1994a, 1994b, Soerens *et al.* 1998, Oostrom *et al.* 1999b, Saenton 2003).

Understanding DNAPL sites is particularly problematic for several reasons. Because DNAPLs are denser than water, they can migrate deeply into aquifers, leaving behind large zones of residual saturation, as well as pond on top of low permeability layers, resulting in complex contaminant entrapment architectures (e.g. Mercer and Cohen 1990, Illangasekare *et al.* 1995a,b, Oostrom *et al.* 1999a). DNAPLs dissolve into groundwater at the interface between the immiscible organic contaminant and the bulk aqueous phase. The architecture of this interface, the solubility limit of the DNAPL, as well as the groundwater flow velocity across this interface are among the key factors that determine the dissolution rate (mass transfer) of contaminant into the groundwater phase (e.g. Miller *et al.* 1990, Imhoff *et al.* 1993, Seagren and Moore 2003).

Because of their low aqueous solubility and the low flow velocities found in most aquifers, mass transfer rates are slow and DNAPLs in the subsurface are persistent sources of contamination which can last for decades or even centuries before the DNAPL phase is depleted by natural dissolution alone. As DNAPLs slowly dissolve, they form dissolved-phase plumes down-gradient of the source architecture (Rivett *et al.* 2001). These plumes form the primary threat to human health from a DNAPL site, as they have the potential to migrate away from the source zone and contaminate drinking water supply wells. Remediation goals at a typical DNAPL site ultimately seek to reduce risk by containing, removing or destroying contaminant source zones, thus preventing contaminant plumes from migrating and threatening human health.

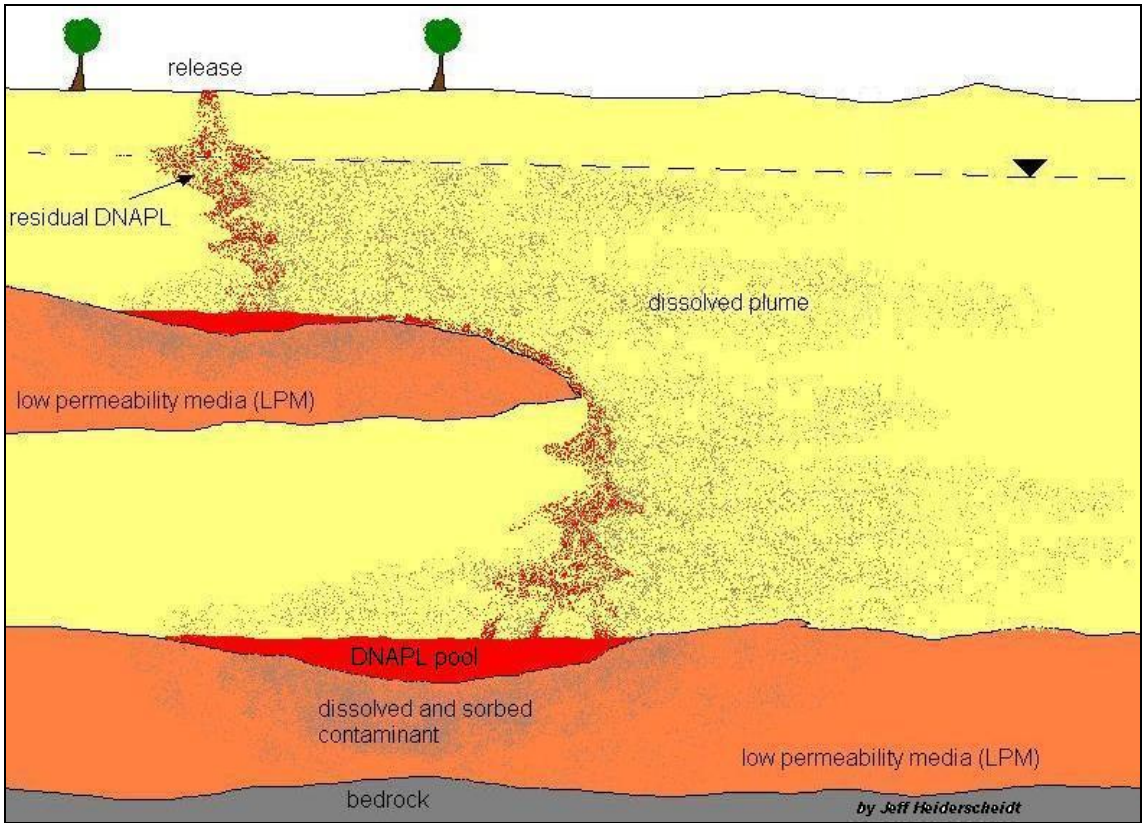

Figure 2.2. Conceptual model of a DNAPL site.

2.2.2. Remediation of DNAPL Source Zones and Plumes

2.2.2.1. Challenges of DNAPLs in Source Zones. DNAPLs present a challenging source zone because of the complex nature of their movement through the subsurface. The interplay of viscous, gravitational, and capillary forces, in conjunction with physical soil heterogeneities (large and small), can result in a non-uniform and unpredictable contaminant distribution vertically and laterally (Illangasekare *et al.* 1995a,b, Kueper and Frind 1991, Schwille 1988). The unstable distribution behavior (e.g., fingering), even in a relatively homogeneous porous media, was demonstrated in 3-D tank experiments by Held and Illangasekare (1995a,b). As the main body of DNAPL migrates, residual DNAPL is left behind as disconnected blobs and ganglia partially filling the pore space. Capillary forces hold this DNAPL residual in place, such that even relatively large hydraulic gradients cannot further mobilize it (Kueper *et al.* 2003). Additionally, there may be regions of pooled or high saturation DNAPL where the DNAPL fills a large fraction of the soil pore space.

In recent years, there has been increased emphasis and research into DNAPL source depletion. Traditional pump-and-treat systems are not able to substantially reduce the source mass and become long-term containment systems. Source depletion technologies like surfactant/co-solvent flushing, thermal

treatment, and chemical oxidation offer the potential to drastically reduce DNAPL source mass, decreasing mass flux of contaminant into the aqueous phase and decreasing the lifetime of the contamination (Stroo *et al.* 2003, USEPA 2003). Unfortunately, source depletion efforts can be challenged by subsurface heterogeneities, imprecise knowledge of source locations, and effects of the effort on source zone distribution or subsurface hydrogeologic conditions (Freeze and McWhorter 1997, ITRC 2002, Marvin *et al.* 2002, Siegrist and Lowe 1996, USEPA 2003). Feenstra and Cherry (1996) pointed out that actual free-phase DNAPL has not been found at most sites strongly suspected of having DNAPL contamination. In many cases, the existence of a DNAPL source can only be inferred from indirect evidence such as aqueous contaminant concentrations exceeding 1% of the aqueous solubility of the chemical (USEPA 1992, USEPA 2003).

2.2.2.2. Challenges of Low Permeability Media and Site Heterogeneity. Another challenge is that sand aquifers frequently have silty or clayey LPM below or within them (Mackay and Cherry 1989). These confining or low permeability layers may contain or develop fractures, which facilitate DNAPL migration into or through the layer. DNAPL within these fractures can dissolve and diffuse into the layer matrix relatively quickly (Siegrist and Lowe 1996). Observations at sites contaminated with DNAPL products suggest a significant fraction of dissolved chemical may diffuse into LPM, which acts as a sink for relatively high amounts of contaminant mass in the dissolved and sorbed phases (Ball *et al.* 1997, Johnson and Pankow 1992, Liu and Ball 2002, Mackay and Cherry 1989). Johnson *et al.* (1989) studied an extremely low permeability clay liner beneath a 5-year old hazardous waste dump containing DNAPLs and found that organic contaminants (including TCE) had diffused 15-20 cm into the liner in only five years. LPM consisting of or containing clay can be especially challenging because clays tend to have higher porosity and greater potential for organic contaminants to sorb to the soil particles than the surrounding aquifer (Mackay and Cherry 1989).

Lenses of low permeability media (LPM) provide additional challenges as secondary sources. Mackay and Cherry (1989) pointed out that sand aquifers contaminated by DNAPLs frequently have silty or clayey LPM strata below or within them, with permeabilities 10^3 - 10^6 times lower than surrounding sand. Diffusion of aqueous phase components into LPM, and subsequent diffusion out of the LPM after the DNAPL source is depleted is a particularly challenging remediation problem (Liu and Ball 2002). In many cases, pure-phase contaminant entered the aquifer and has had several to many years of close contact with LPM, resulting in diffusion of a substantial mass of dissolved contaminant into the LPM. For example, Freeze and McWhorter (1997) show that for a typical fractured clay LPM, 50-100% of the original DNAPL mass can end up in the LPM matrix, depending on the fracture sizes, either dissolved or sorbed to soil particles. Subsequently, even if the pure-phase contaminant is removed from the aquifer, the dissolved contaminant in the LPM will continue to diffuse out and remain a source of groundwater contamination, potentially well above MCLs, for years to come (Johnson and Pankow 1992, Lee and Chrysikopoulos 1998, Wilking 2004).

Schwille (1988) presented experimental and modeling results demonstrating the significant effect that site heterogeneity has on DNAPL migration and trapping resulting in complex, persistent source zones. Figure 2.2 depicts a generic site conceptual model of a groundwater system contaminated by DNAPLs. Even in a relatively homogeneous soil (light color in Figure 2.2) micro-scale heterogeneities typically exist, resulting in large zones of residual saturation (Dekker and Abriola 2000a, USEPA 2004). When initially released into the environment, DNAPLs sink below the water table, spreading laterally upon contact with finer grained layers (Illangasekare *et al.* 1995a,b, Kueper *et al.* 1989, Pinder and Abriola 1986). Lateral spreading results from the finer grained layer forming a capillary barrier with a higher entry pressure. In addition to this lateral spreading on top of finer grained layers, some DNAPL may enter the finer grained material as a result of fingering due to pore-scale heterogeneities at the interface of the two layers (Held and Illangasekare 1995a,b, Kueper and Frind 1991a, Kueper and Frind 1991b, Poulson and Kueper 1992). On the other hand, the presence of coarser grained lenses, especially

when overlying LPM lenses, can act as a trap of sorts, resulting in high DNAPL saturations or pooling (Illangasekare *et al.* 1995b).

A field experiment at the Borden site by Kueper *et al.* (1993) confirmed that PCE DNAPL released into soil generated a complex source zone. Further, in that case when the PCE encountered grain size variations causing lateral migration, the resulting horizontal pools tended to be relatively thin. Parker *et al.* (2003) carried out extensive soil coring and water sampling at five sites with DNAPL contaminated sandy aquifers. The five sites were typical of many DNAPL contaminated sites in that the contamination occurred several decades or more ago. Three of the sites actually had free phase DNAPL in monitoring wells. Results of the sampling by Parker *et al.* (2003) demonstrated the difficulty in locating actual subsurface DNAPL source zones, and showed that remaining DNAPL in these aged sites occurs in sporadic, thin layers. The thin layers of DNAPL were only reliably identifiable by taking continuous soil cores, sub-sampling them on small (5 cm or less) vertical intervals, and applying a hydrophobic red dye (Sudan IV) to the cores which gave a visual indicator that DNAPL was present.

In addition to creating complex distribution of contaminant mass that is difficult to locate and characterize, site heterogeneity also makes removal of the contaminant source more challenging. Traditional source removal techniques often rely on groundwater flow to remove the contaminant. However, groundwater flow through source zones of high DNAPL saturation is greatly reduced by the reduction in effective permeability due to DNAPL filling most of the pore space (Powers *et al.* 1998, Saba and Illangasekare 2000). Oostrum *et al.* (1999b) and Taylor *et al.* (2001) both performed 2-D tank experiments of surfactant flushing of DNAPLs in heterogeneous systems. Results from both studies showed that surfactants can be effective for residuals and entrapped ganglia, but did not considerably reduce DNAPL mass from highly saturated DNAPL pools overlying LPM due to flow bypassing. Similarly, the modeling work of Saenton *et al.* (2002) showed that the effectiveness of mass removal by surfactant flushing depends on the aquifer heterogeneity, which controls the DNAPL entrapment and surfactant delivery to the locations of entrapped DNAPLs. Flow bypassing reduces the delivery efficiency of the surfactant, prolonging the time to achieve the desired remediation end-point. In some extreme cases, the injected surfactant completely bypassed the NAPL source zones. Further, Soga *et al.* (2004) reviewed source depletion technologies and performed numerical simulations demonstrating that soil heterogeneity and complexity of DNAPL source zone morphology are critical factors controlling source reduction effectiveness.

Similarly, ground water flow through regions or strata of LPM is often negligible compared to flow around the LPM. Diffusion is the dominant transport mechanism in LPM, so groundwater carrying the treating chemicals cannot easily access the LPM zones (Dekker and Abriola 2000b, Stroo *et al.* 2003). Consequently, once the DNAPL phase source is depleted by an aggressive source removal technology (or even by natural dissolution), plume concentrations are likely to rebound as diffused mass is returned from the LPM regions back into the surrounding, higher permeability flow zone (Freeze and McWhorter 1997, Liu and Ball 2002, Parker *et al.* 1994, Parker *et al.* 1997, Polak *et al.* 2003, Reynolds and Kueper 2002).

2.3. CHEMICAL OXIDATION FOR REMEDIATION OF DNAPLS

2.3.1. Introduction

During this SERDP project, various research elements were focused on chemical oxidation of PCE and TCE (aqueous phase only or with a DNAPL phase present as well) using either potassium permanganate or catalyzed hydrogen peroxide. When ISCO is used for source zones with DNAPL present as suspended residuals or pools, chemical oxidation in the aqueous phase near the interface can impact the mass transfer and the rate and extent of DNAPL depletion and degradation. As a basis for experimental design and interpretation of results obtained, CSM team members summarized the background theory and

relevant published literature, excerpts of which are included in this section. The following definitions of terminology are provided for clarity in the subsequent discussions.

- Mass transfer – This is the process of converting contaminant mass from one phase to another (e.g. NAPL phase to aqueous phase).
- Dissolution – This is the specific mass transfer process of DNAPL dissolving into the aqueous phase.
- DNAPL mass depletion - This is the process of removing DNAPL mass from a subsurface system. The *rate* of DNAPL mass depletion is the rate at which DNAPL mass is being removed from the system. This rate is not equivalent to the lumped mass transfer coefficient (k_La), which is a value that is used to model DNAPL dissolution.
- Mass flux – This is the flow of contaminant mass across a control plane. Under the 1-D conditions of the experimental work completed by Petri (2006) or the 2-D conditions within the tank experiments completed by Heidersheidt (2005), the control plane is simply the vertical cross section perpendicular to the ground water flow field downstream from the DNAPL source zone.
- DNAPL degradation – This is the process (e.g., chemical oxidation) or processes (e.g., mass transfer and chemical oxidation) that contribute to destruction of the DNAPL.

This section provides a summary of relevant theory and experimental findings concerning the oxidation of PCE and TCE in an aqueous phase with or without a DNAPL phase being present within the aqueous phase. The following text is based on the literature reviews completed during the project by Jackson (2004), Seitz (2004), Heiderscheidt (2005), Petri (2006), *et al.* CSM team members. Note that the interaction of the two oxidants with soil matrix components is discussed in a subsequent section.

2.3.2. Oxidation of Aqueous Phase PCE and TCE

2.3.2.1. Oxidation of PCE and TCE with Permanganate. A number of studies have been performed that investigated the kinetics, mechanisms and pathways for oxidation of TCE and PCE by permanganate (Hood *et al.* 2000, Urynowicz 2000, Yan and Schwartz 2000, Huang *et al.* 2002). Permanganate ion (MnO_4^-) is a strong oxidant that is capable of attacking chlorinated ethenes through direct electron transfer. Manganese can be reduced from Mn^{+7} to Mn^{+2} (Eqn. 2.1), Mn^{+4} (Eqn. 2.2), or Mn^{+6} (Eqn. 2.3), with the number of electrons transferred dependent on the pH of the system (Siegrist *et al.* 2001). The strongest permanganate reduction occurs under low pH as the most electrons are transferred.

$$MnO_4^- + 8H^+ + 5e^- \Rightarrow Mn^{+2} + 4H_2O \qquad (pH < 3.5) \qquad (2.1)$$

$$MnO_4^- + 2H_2O + 3e^- \Rightarrow MnO_2(s) + 4OH^- \qquad (3.5 < pH < 12) \qquad (2.2)$$

$$MnO_4^- + e^- \Rightarrow MnO_4^{-2} \qquad (pH > 12) \qquad (2.3)$$

Oxidation of TCE and PCE by electron transfer proceeds as given by Equations 2.4 and 2.5 respectively.

$$C_2HCl_3 + 8OH^- \Rightarrow 2CO_2 + 4H_2O + H^+ + 3Cl^- + 6e^- \qquad (2.4)$$

$$C_2Cl_4 + 3H_2O + OH^- \Rightarrow 2CO_2 + 7H^+ + 4Cl^- + 4e^- \qquad (2.5)$$

Under most environmental conditions, the subsurface pH is between 3.5 and 12, and thus Equation 2.2 is the favored reaction for reduction of permanganate, with the production of manganese oxide solids (MnO_2) as a reaction byproduct (Siegrist *et al.* 2001). Combining the oxidation reaction stoichiometries in Equations 2.4 and 2.5 with the reduction of permanganate given by Equation 2.2, gives the complete reaction stoichiometries for oxidation of TCE and PCE by permanganate (Eqns. 2.6 and 2.7, respectively) (Siegrist *et al.* 2001).

$$2MnO_4^- + C_2HCl_3 \Rightarrow 2MnO_2(s) + 2CO_2 + H^+ + 3Cl^- \quad (2.6)$$

$$4MnO_4^- + 3C_2Cl_4 + 4H_2O \Rightarrow 4MnO_2(s) + 6CO_2 + 8H^+ + 12Cl^- \quad (2.7)$$

These stoichiometries provide a theoretical basis for the complete destruction of TCE and PCE by permanganate. If the reaction goes to completion, the byproducts are considered non-toxic, and thus desirable from a remediation standpoint. It should be noted that the reactions given by Equations 2.6 and 2.7 produce protons and thus a significant pH drop is possible in unbuffered systems, such as clean silica sand aquifers. This can impact the reaction stoichiometry if the oxidation reaction causes the pH to drop below 3.5. The reaction stoichiometries for pH below 3.5 are derived from combining Equation 2.1 with Equations 2.4 and 2.5 to yield Equations 2.8 and 2.9.

$$6MnO_4^- + 5C_2HCl_3 + 3H^+ \Rightarrow 6Mn^{2+} + 10CO_2 + 15Cl^- + 4H_2O \quad (2.8)$$

$$4MnO_4^- + 5C_2Cl_4 + 4H_2O \Rightarrow 4Mn^{2+} + 10CO_2 + 20Cl^- + 8H^+ \quad (2.9)$$

The overall kinetics of the oxidation reaction for both TCE and PCE by permanganate have been found to be second-order. Reported second-order rate constants for TCE degradation with permanganate are 0.67 ± 0.03 M^{-1} s^{-1} (Yan and Schwartz 1999) and 0.88 ± 0.07 M^{-1} s^{-1} (Urynowicz 2000), and for PCE are 0.035 ± 0.004 M^{-1} s^{-1} (Huang *et al.* 2002) and 0.041 ± 0.001 M^{-1} s^{-1} (2.45 ± 0.65 M^{-1} min^{-1}) (Hood *et al.* 2000). The kinetic rates have been reported to be independent of pH over the tested range of 4-8 for TCE (Yan and Schwartz 1999, Urynowicz 2000) and 3-10 for PCE (Huang *et al.* 2002).

However, under the varied conditions encountered during in situ oxidation using permanganate, other byproducts can be formed. Oxidation of TCE and PCE by permanganate results in the formation of a cyclic hypomanganate ester, which is rapidly broken down into intermediates (Yan and Schwartz 2000, Huang *et al.* 2002). Yan and Schwartz (2000) reported that for TCE oxidation, this ester broke down via several reaction pathways dependent on system pH. At pH 4, formic acid (HCOOH) is the primary byproduct of the breakdown of the ester, while at pH 6 and 8, the dominant byproducts are oxalic and glyoxalic acids. Huang *et al.* (2002) reported that PCE oxidation followed a similar process. At pH 3, the ester complex was mineralized to CO_2, while at pH 7 and 10, the formation of oxalic acid dominated. For both TCE and PCE, complete dechlorination was observed in both studies, suggesting that chloride ion is a reliable reaction tracer capable of closing a mass balance on TCE and PCE. The organic acids produced by TCE and PCE oxidation can be further oxidized by permanganate to produce CO_2 (Yan and Schwartz 2000). However this further oxidation process is favored at conditions of low pH, and requires excess permanganate to be available to react. Furthermore, the reactions between permanganate and these organic acids are slower than the reaction with aqueous contaminant, and thus the aqueous contaminant will compete for oxidant more effectively than the organic acids. Thus, if complete oxidation does not occur, then it may be possible to form significant concentrations of organic acids (Yan and Schwartz 1999).

2.3.2.2. Oxidation of PCE and TCE with Catalyzed Hydrogen Peroxide. Hydrogen peroxide has been widely used and accepted in the treatment of wastewater (Weber 1972), and due to its ease of application at low concentrations it has been used in the remediation of contaminated soils (e.g., Glaze

and Kang 1988, Watts *et al.* 1990, Watts 1992, Watts *et al.* 1993, Gates and Siegrist 1995,). When H_2O_2 reacts with iron (ferric or ferrous) and organic compounds a variety of competing reactions occur in what is known as the Fenton's process. These possible reactions are as follows:

$$H_2O_2 + Fe^{2+} \Rightarrow Fe^{3+} + OH^- + OH^* \quad (2.10)$$

$$H_2O_2 + Fe^{3+} \Rightarrow Fe^{2+} + H^+ + HO_2^* \quad (2.11)$$

$$RH + OH^* \Rightarrow H_2O + R^* \quad (2.12)$$

$$Fe^{2+} + OH^* \Rightarrow Fe^{3+} + OH^- \quad (2.13)$$

$$R^* + Fe^{3+} \Rightarrow Fe^{2+} + \text{products} \quad (2.14)$$

$$R^* + OH^* \Rightarrow ROH \quad (2.15)$$

$$R^* + H_2O_2 \Rightarrow ROH + OH^* \quad (2.16)$$

$$HO_2^* + Fe^{3+} \Rightarrow O_2 + Fe^{2+} + H^+ \quad (2.17)$$

$$OH^* + H_2O_2 \Rightarrow HO_2^* + H_2O \quad (2.18)$$

In these Equations 'R' denotes the organic compound. The hydroxyl radical (OH*) formed in some of the above reactions is a very powerful and effective nonspecific oxidizing agent (Watts *et al.* 1990), which can react with most organic and many inorganic compounds at rates at or near the diffusion-controlled limit (Greenberg *et al.* 1998, Petigara *et al.* 2002). Reactions between these OH* and organic compounds have been reported as the primary oxidizing reactions of the Fenton's process in situ (at pH below about 6), and have 2nd-order rate constants reported in the range of 10^7-10^{10} L/mol-s (Gates and Siegrist 1995). The application of Fenton's reagent to remediate contaminated soil was initially shown by Watts *et al.* (1990) in batch laboratory-scale experiments, then later in sand-packed column tests by Ravikumar and Gurol (1994). Since then several investigations have shown the effectiveness of Fenton's oxidation in reducing or destroying aqueous solutions and soil systems containing VOCs (Watts *et al.* 1990, 1991, Gurol and Ravikumar 1991, Ravikumar and Gurol 1991, 1994, Leung *et al.* 1992, Hurst *et al.* 1993, Greenberg *et al.* 1998, Kwan and Voelker 2003), with sorbed hexachlorobenzene (Watts *et al.* 1994), and for landfill leachate (Kang and Hwang 2000).

Hydrogen peroxide is most stable in the pH range of 3-4, and its rate of decomposition rapidly increases as pH increases above 5 (Kang and Hwang 2000). This is due to the formation of ferric hydroxo complexes which form at higher pHs and serve to deactivate the ferrous iron catalyzation of H_2O_2 decomposition (Bigda 1995). Research has shown, though, that Fenton's reagent can effectively oxidize pollutants in the pH range of 3 to about 7 (Watts *et al.* 1990, Khan and Watts 1996, Siegrist *et al.* 2001). The catalyzed H_2O_2 reaction can be achieved through either the addition of Fe^{2+} or Fe^{3+} salts, or by the use of existing iron oxides such as goethite, hematite, magnetite, and ferrihydrite (Watts *et al.* 1990, Tyre *et al.* 1991, Khan and Watts 1996, Lin and Gurol 1996, Watts *et al.* 1997, 1999, Kong *et al.* 1998, Valentine and Wang 1998, Chou and Huang 1999).

The simplified stoichiometric reaction for peroxide degradation of TCE is:

$$3H_2O_2 + C_2HCl_3 \Rightarrow 2CO_2 + 2H_2O + 3HCl \quad (2.19)$$

Baciocchi *et al.* (2003) demonstrated that adding iron sulfate to their experimental systems decreased the rate of H_2O_2 consumption by an order of magnitude. Kwan and Voelker (2002) observed the pseudo 1st order k for H_2O_2 decomposition with various organic compounds to be in the range of 0.0082 – 0.084 day^{-1}, and Leung *et al.* (1992) achieved k = 0.206 hr^{-1} +/-0.0360 hr^{-1} for H_2O_2 decomposition when degrading PCE, which had a k of 1.65 hr^{-1} +/- 0.475 hr^{-1}.

2.3.3. ISCO-Enhanced Degradation of DNAPL-Phase PCE and TCE

2.3.3.1 Mass Transfer of DNAPL into an Aqueous Phase. Mass transfer or dissolution of a DNAPL into the aqueous phase is generally modeled based on the well-known stagnant film model (Sherwood *et al.* 1975) utilizing a first-order linear driving force:

$$\frac{dc_\infty}{dt} = -k_{La}(c_\infty - c^*) \tag{2.20}$$

where dc_∞/dt is the rate of change of aqueous concentration per time ($ML^{-3}T^{-1}$), c_∞ is the aqueous solute concentration (ML^{-3}) of the bulk solution, c^* is the aqueous solubility limit of the solute (ML^{-3}), and k_{La} is the DNAPL dissolution rate or lumped mass transfer coefficient (T^{-1}). The origin of this model is Fick's First Law of Diffusion that states mass flux of a substance diffusing across a given cross-sectional area per unit time is proportional to the concentration gradient at the surface:

$$J_a = -D_m \frac{dc}{dz} \tag{2.21}$$

where J_a is the mass flux per unit area ($ML^{-2}T^{-1}$) and dc/dz is the concentration gradient (ML^{-4}). The change in aqueous concentration per time is then the mass flux per unit area (J_a) times the DNAPL-water interfacial area, A_{nw}, (L^2), divided by the porous media volume of interest, V, (L^3). In the stagnant film model (Figure 2.3), the film is assumed to be very thin such that the concentration gradient is linear and can be approximated by the saturated aqueous concentration on the DNAPL side minus the bulk aqueous concentration on the bulk aqueous side, divided by the film thickness, δ, (L). The molecular diffusion coefficient, D_m, divided by the film thickness, δ, then is the intrinsic mass transfer coefficient, k_L, (LT^{-1}). The lumped mass transfer coefficient is the product of the intrinsic mass transfer coefficient, k_L, times the DNAPL-water interfacial area, A_{nw}, divided by the porous media volume of interest, V.

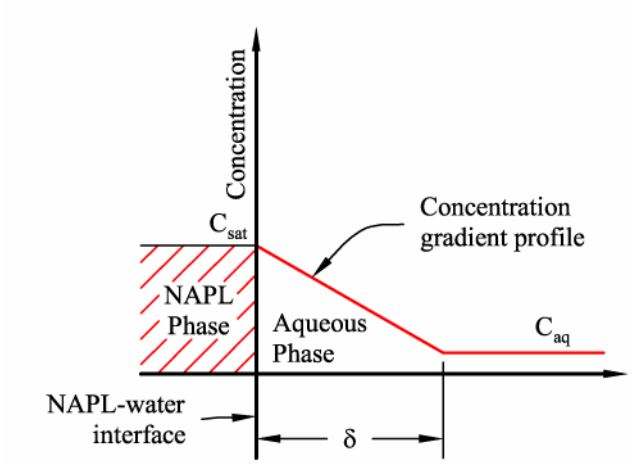

Fig. 2.3. Thin film model for DNAPL dissolution.

The lumped mass transfer coefficient is used because the complex architecture of DNAPL sources makes A_{nw} too difficult to estimate, and the stagnant film thickness is a theoretical construct that can not be measured. Although k_{La} is still a parameter that cannot be measured directly, because it combines parameters that can not be measured, it reduces the unknowns to a single parameter for estimation.

As a result, a considerable amount of research has been devoted to developing methods to estimate k_{La} from measurable system parameters, including pore size and DNAPL saturation which affect the specific interfacial surface area for dissolution (Ewing 1996, Imhoff *et al.* 1994, Miller *et al.* 1990, Nambi 1999, Powers *et al.* 1994a Powers *et al.* 1994b, Saba and Illangasekare 2000). The general approach is to utilize an empirically determined Gilland-Sherwood correlation as given by Welty *et al.* (1976) to estimate the modified Sherwood number (*Sh*) from other dimensionless numbers describing the system (e.g. Reynolds number, *Re*, and Schmidt number, *Sc*), where *a*, *b*, *c*, and *d* are empirically determined constants:

$$Sh = a + b\,\mathrm{Re}^{c}\,Sc^{d} \tag{2.22}$$

The modified Sherwood number relates the mass transport in a system to the diffusive forces, the Reynolds number relates system inertial forces to viscous forces, and the Schmidt number relates viscous forces to diffusive forces. Mathematical equations for these three dimensionless numbers are

$$Sh = \frac{k_{La} d_{50}^{2}}{D_m} \tag{2.23}$$

$$Re = \frac{\rho_w \bar{v} d_{50}}{\mu_w} \tag{2.24}$$

$$Sc = \frac{\mu_w}{\rho_w D_m} \tag{2.25}$$

where ρ_w is the aqueous phase density (ML^3), $\bar{v}$ is the average linear groundwater velocity (LT^{-1}), and μ_w is the aqueous phase dynamic viscosity ($ML^{-1}T^{-1}$). The Sherwood number determined from the empirical correlation is then used in Equation 2.20 to estimate the lumped mass transfer coefficient, k_{La}. Most correlations incorporate volumetric DNAPL content (θ_n) in some form to account for the changing DNAPL-water interfacial area as dissolution proceeds (Miller *et al.* 1990, Powers *et al.* 1994b). Example Gilland-Sherwood relations are shown in Table 2.1.

In the relations shown in Table 2.1, L is the characteristic or dissolution length in the flow direction (L), d_M is the diameter of a "medium" sand grain (defined by U.S. Department of Agriculture as 0.05cm), and x is the distance into the residual DNAPL source in the direction of flow (L). Coefficients of the correlations have typically been found to have 95% confidence intervals of approximately ± 17% for the scaling coefficient at the beginning, ± 12% for the Reynolds number exponent, and ± 13% for the NAPL content exponent (Miller *et al.* 1990, Nambi and Powers 2003, Powers *et al.* 1994b, Saba and Illangasekare 2000, Saenton 2003). Confidence intervals for other coefficients, when present, have not been reported. Differences in empirical coefficients and formulations are at least partly due to differences in experimental conditions. For example Powers *et al.* (1994a) used a 1-D system with spherical dissolving organic media and Powers *et al.* (1994b) used a 1-D homogeneous system, while Saba and Illangasekare (2000) were considering a 2-D system with heterogeneity-induced flow-bypassing. Miller *et al.* (1990) and Imhoff *et al.* (1994) both used 1-D systems. Ewing (1996) and Saba *et al.* (2001) considered a 2-D system with surfactant flushing. Nambi and Powers (2003) further expanded the available choices by looking at 2-D systems with high DNAPL saturations resulting in slower mass transfer characterized by a significantly increased exponent on the DNAPL saturation term. These correlations have been found to be effective for modified Sherwood numbers ranging from 0.01 to over 25.0 (Imhoff *et al.* 1994, Miller *et al.* 1990, Nambi and Powers 2003).

Table 2.1. Gilland-Sherwood mass transfer correlations for NAPL-water systems (Heiderscheidt 2005).

Correlations	Reference
$Sh = 37.15\left(\frac{\theta_n}{n}\right)^{1.24} \mathrm{Re}^{0.61}$ (for $\theta_n/n < 0.35$)	Nambi and Powers (2003)
$Sh = 0.4727\,\mathrm{Re}^{0.2793}\,Sc^{0.33}\left(\frac{\theta_n}{1-\theta_n}\right)^{1.642}\left(\frac{d_{50}}{\tau L}\right)^{0.1457}$	Saba *et al.* (2001)
$Sh = 11.34\,\mathrm{Re}^{0.2767}\,Sc^{0.33}\left(\frac{\theta_n d_{50}}{\tau L}\right)^{1.037}$	Saba and Illangasekare (2000)
$Sh = 4.84\,\mathrm{Re}^{0.219}\,\theta_n^{1.32}$	Ewing (1996)
$Sh = 36.8\,\mathrm{Re}^{0.654}$	Powers *et al.* (1994a)
$Sh = 4.13\,\mathrm{Re}^{0.598}\left(\frac{d_{50}}{d_M}\right)^{0.673} U^{0.369}\left(\frac{\theta_n}{\theta_{n0}}\right)^{\beta}$; $\beta = 0.518 + 0.114\left(\frac{d_{50}}{d_M}\right) + 0.10U$	Powers *et al.* (1994b)
$Sh = 340\theta_n^{0.87}\,\mathrm{Re}^{0.71}\left(\frac{d_{50}}{x}\right)^{0.31}$	Imhoff *et al.* (1994)
$Sh = 12\,\mathrm{Re}^{0.75}\,\theta_n^{0.60} Sc^{0.5}$	Miller *et al.* (1990)

Another useful dimensionless number is the second Damkohler number, *Da(II)*, shown in Equation 2.26, which relates the characteristic time of DNAPL mass transfer or dissolution (τ_m) to the characteristic time of chemical reaction (τ_r). The characteristic time of mass transfer is the inverse of the lumped mass transfer coefficient and the characteristic time of chemical reaction is the inverse of the first-order (or pseudo-first-order) chemical reaction rate. So a working definition of the second Damkohler number is the ratio of chemical reaction rate to mass transfer rate as shown in Equation 2.27.

$$Da(II) = \frac{\tau_m}{\tau_r} \tag{2.26}$$

$$Da(II) = \frac{k_1}{k_{La}} \tag{2.27}$$

This *Da(II)* number has been defined by Belfiore (2003) as shown in Equation 2.28:

$$Da(II) = \frac{k\delta^2}{D_{aq}} \tag{2.28}$$

where, k is the reaction rate, δ is the film thickness and D_{aq} is the aqueous diffusion coefficient of the contaminant in water.

In the context of DNAPL source depletion by chemical oxidation, the magnitude of *Da(II)* provides an indication of whether the rate of mass depletion is rate-limited by either the mass transfer from the DNAPL to aqueous phase or the chemical reaction rate. A *Da(II)*<<1 indicates contaminant mass is transferring into the aqueous phase faster than the chemical reaction can destroy it, while a

Da(II)>>1 suggests that the chemical reaction is faster than the mass transfer. The ideal situation is to adjust system conditions such that the second Damkohler is as near to one as possible.

Similarly, the first Damkohler number, *Da(I)* shown in Equation 2.29 is a dimensionless number relating the characteristic time of fluid motion or hydraulic retention time (τ_f) to the characteristic time of DNAPL mass transfer or dissolution (τ_m). In the hydrology and contaminant transport setting, the retention time is given by Equation 2.30, where L is the characteristic length or length of interest (L) and $\bar{v}$ is the linear pore velocity of the fluid. Equation 2.31 gives the characteristic time for DNAPL mass transfer or dissolution which is just the inverse of the lumped mass transfer coefficient (k_{La}).

$$Da(I) = \frac{\tau_f}{\tau_m} \tag{2.29}$$

$$\tau_f = \frac{L}{\bar{v}} \tag{2.30}$$

$$\tau_m = \frac{1}{k_{La}} \tag{2.31}$$

Combining Equations 2.29 to 2.31 gives a working definition of the first Damkohler number, Equation 2.32, which is a ratio of the dissolution rate to the fluid transport rate.

$$Da(I) = \frac{k_{La} L}{\bar{v}} \tag{2.32}$$

The magnitude of *Da(I)* provides an indication of whether dissolution is occurring at or near equilibrium such that the local equilibrium assumption (LEA) would be valid. Under LEA conditions, estimating mass removal rates from a DNAPL source are simplified and can be accomplished assuming the aqueous phase contacting the DNAPL has a contaminant concentration equal to the contaminant's aqueous solubility. However, deviation from equilibrium dissolution is frequently seen in field situations and is generally a result of rate-limited mass transfer from the DNAPL to aqueous phase, physical heterogeneity, and rate-limited sorption/de-sorption (Brusseau 1992). Generally, Brusseau (1992) found that *Da(I)*>=100 indicates equilibrium, 10=<*Da(I)*<100 indicates near equilibrium, and *Da(I)*<10 indicates rate-limited mass transfer.

Mayer and Miller (1996) performed a series of 2-D simulations and confirmed that moderate heterogeneity can significantly impact mass transfer rates away from LEA conditions. Because the mass transfer rate is dependent upon the water velocity as represented by the Reynolds number (typically to a power other than one) in the correlations, the first Damkohler number may be useful in optimizing the mass transfer of a given system depending on what mass transfer correlation best describes the system (Mayer *et al.* 1999). A caveat from Zhu and Sykes (2000) is that some correlations developed from 1-D column data tend to result in simulation of equilibrium dissolution without changing to rate-limited mass transfer as DNAPL saturation gets low, and so may be ill-suited to large-scale problems.

2.3.3.2. DNAPL Mass Transfer and Depletion in the Subsurface. Numerous lab, modeling and field studies have explored DNAPL mass transfer in the subsurface (Miller *et al.* 1990, Powers *et al.* 1994b, Kennedy and Lennox 1997, Sale and McWhorter 2001, Nambi and Powers 2003, Seagren and Moore 2003, Clement *et al.* 2004). In the field environment, aqueous phase concentrations are frequently less than the aqueous solubility limit (Mercer and Cohen 1990, Soerens *et al.* 1998). This has been attributed to a number of factors, such as non-equilibrium mass transfer due to low NAPL saturations, as well as flow bypassing of NAPL saturated source areas and heterogeneities in the subsurface. As such, studies in one-dimensional relatively homogeneous systems have tended to predict higher mass depletion rates than rates predicted by two and three dimensional tank and field experiments. Oostrom *et al.* (1999b) found that in a 2-D tank, areas of residual saturation were rapidly depleted by flushing with pump

and treat remediation, while DNAPL pools were largely unaffected. The result of depleting the residuals was lower contaminant concentrations across the tank, but a flux of contaminant continued from the pools.

Kennedy and Lennox (1997) studied DNAPL dissolution in a relatively simple system, with water flowing through a single row of glass beads. They evaluated two DNAPL configurations, which were non-wetting spheres, and wetting pendular rings. Spheres were shown to have constant mass transfer rates with time, while pendular rings decreased with time. This was postulated to be due to mass transfer becoming diffusion limited as the rings retreated further into the crevasses away from the main flow through the media. Even in a very simple geometry, considerable scatter occurred in the data, possibly due to localized variations in velocity. Miller *et al.* (1990) studied mass transfer with 1-D column experiments containing DNAPL residuals and evaluated the impact of aqueous phase velocity, NAPL saturation, and particle size. Results indicated that equilibrium between the NAPL and aqueous phases in the column was achieved rapidly for a wide range of velocities and NAPL saturations. The rate of mass transfer was shown to be directly proportional to the velocity and NAPL saturation, while particle size had little effect. However, Powers *et al.* (1994b), in addition to identifying velocity and NAPL saturation as key parameters, also found a significant impact on dissolution by media grain size and grain distribution. This was explained as coarse or graded media entrapped larger and more complex DNAPL blobs, which correspond to smaller specific surface areas for mass transfer to occur across. Powers *et al.* (1994a) postulated that residual DNAPL mass transfer from media with a heterogeneous grain size distribution could be modeled as dissolution from a series of graded spheres of varying radii dependent on measurable media properties. Imhoff *et al.* (1993) also investigated DNAPL residuals in a column study and found that dissolution occurred over a front that lengthened with time, and the mass transfer rate was dependent on the distance into this front.

Seagren and Moore (2003) conducted extensive research looking at mass transfer from a multicomponent NAPL pool as a function of velocity. A wide range of velocities (0.1 to 60 m/d) were tested and showed that while mass transfer was enhanced by increasing velocity, the mass flux from the NAPL pool tapered off and approached a constant for very high velocities (> 10 m/d), suggesting that at very high velocities NAPL dissolution became limited by the kinetics of dissolution. However, below 10 m/day, mass transfer could be modeled using a local equilibrium assumption, where by the bulk aqueous phase adjacent to the DNAPL interphase is at the saturation concentration, and mass transfer is limited by advective transport.

2.3.3.3. Effects of ISCO on DNAPL Mass Transfer and Depletion. A goal of ISCO is to accelerate remediation of a contaminant source zone by inducing increased mass transfer (and subsequent destruction) from a DNAPL source. Based on experimental results, Schnarr *et al.* (1998) suggest that DNAPL dissolution and oxidation are processes that occur in parallel with increased mass transfer during oxidation occurring primarily as a result of an increased aqueous concentration gradient. Figure 2.4, adapted from Schnarr *et al.* (1998), shows how the concentration gradient might be increased by reaction in the aqueous phase. Reaction occurs within the diffusion film layer, which consumes both contaminant and oxidant, causing both concentration gradients to become steeper. This steeper gradient causes an increase in the flux of dissolving contaminant into the aqueous phase and the flux of oxidant towards the interface.

Urynowicz (2000) demonstrated the ability for permanganate to increase dissolution of DNAPL TCE in batch and flow-thru experiments without porous media present; however, the rate decreased as a MnO_2(s) film formed at the DNAPL-water interface. Reitsma and Dai (2001) performed a theoretical study to estimate the maximum expected DNAPL mass transfer enhancement resulting from chemical oxidation. They estimated a maximum five times increase in dispersive mass transport from a PCE DNAPL pool resulting from the increased concentration gradient; however, they predict little enhancement in local-scale mass transfer from DNAPL to aqueous phase suggesting no change in dissolution mass transfer parameters. Further, they suggest that actual enhancement is likely to be less

because permeability reduction and decreased interfacial contact area were not accounted for in the estimate. On the contrary, MacKinnon and Thomson (2002) calculated a ten times initial increase in PCE mass transfer from a DNAPL pool during a 2-D oxidation experiment, with decreasing mass flux over time attributed to MnO_2(s) formation.

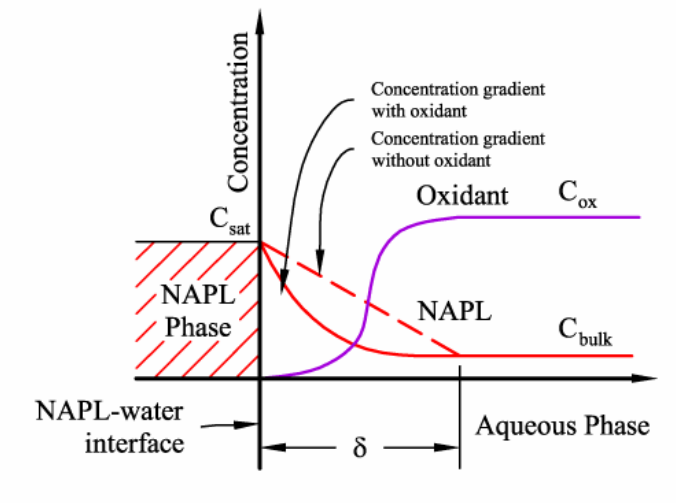

Figure 2.4. Thin film model with chemical oxidation (adapted from Schnarr *et al.* 1998).

Cussler (1997) presented an equation for adjusting the intrinsic mass transfer coefficient, k_L, to account for irreversible, first-order (or pseudo-first-order) homogeneous chemical reaction:

$$k_L^* = (D_m k_1)^{1/2} \coth\left[\left(\frac{k_1}{D_m}\right)^{1/2} \delta\right] \tag{2.32}$$

where k_L^* is the intrinsic mass transfer coefficient with chemical reaction (MT^{-1}), δ is the theoretical thickness of the stagnant film (L), D_m is the molecular diffusion coefficient (L^2T^{-1}), and k_1 is the first-order or pseudo-first-order kinetic reaction rate constant (T^{-1}). Equation 2.29 was presented by Cussler (1997) for diffusion from a well-mixed gas into a liquid that is not well-mixed, across a thin stagnant liquid film at the interface. The equation was developed from a mass balance across the stagnant film with a constant concentration at the well-mixed gas surface and zero concentration at the liquid surface. Urynowicz (2000) found this equation to be applicable to mass transfer from a TCE DNAPL to the aqueous phase for batch systems with no porous media during oxidation using permanganate, before substantial MnO_2(s) formation at the DNAPL surface. In applying this equation to mass transfer from DNAPL to the aqueous phase, it is assumed that the contaminant concentration at the DNAPL surface remains constant and equal to the solubility limit of the contaminant, regardless of DNAPL thickness, until the DNAPL is depleted. This is the same assumption inherent in the common use of the stagnant film model to describe DNAPL mass transfer under natural (non-reaction-enhanced) dissolution conditions.

According to Cussler (1997) adjustment of the mass transfer coefficient is necessary only if the chemical reaction is fast, with half life on the order of minutes. Because δ cannot be measured, it can be replaced with D_m/k_L, where k_L is the intrinsic mass transfer coefficient without chemical reaction (MT^{-1}). Further, k_L is defined as the molecular diffusion coefficient divided by the stagnant film thickness.

Dividing through by k_L gives the change in mass transfer caused by the chemical reaction as given by Cussler (1997):

$$\frac{k_L^*}{k_L} = \left[\frac{D_m k_1}{(k_L)^2}\right]^{1/2} \coth\left[\left(\frac{k_1 D_m}{k_L^2}\right)^{1/2}\right] \tag{2.33}$$

Unfortunately, this requires knowledge of the intrinsic mass transfer coefficient without chemical reaction, k_L, which can not be determined for DNAPL dissolution in porous media because it is not possible to know the DNAPL-water interfacial area needed to obtain k_L from the lumped mass transfer coefficient, k_{La}, which is determined empirically.

2.3.3.4. Mechanisms for ISCO-Enhanced Mass Transfer. As noted above, a number of studies have shown that the rate of mass depletion from the DNAPL phase can be enhanced by reaction in the aqueous phase (Schnarr *et al.* 1998, Urynowicz 2000, Reitsma and Dai 2001). However, there is debate about the mechanism of enhanced mass depletion. This debate relates to how oxidation impacts the concentration gradient across the thin diffusion film boundary layer represented in Figure 2.4. One view is that diffusion of oxidant into the thin film causes a significant amount of reaction to occur within the thin film layer, so the concentration gradient that results is non-linear. If the difference between the linear and non-linear concentration gradients is significant, then the equations used to model DNAPL dissolution would have to be modified to accommodate the non-linear concentration gradient.

However, other studies have found that the kinetic rate of oxidation of TCE and PCE with permanganate is too slow to cause an appreciable amount of reaction to occur within the thin diffusion film boundary layer for most systems. Reitsma and Dai (2001) found that enhanced mass transport resultant of reaction within the thin film layer would only be likely to occur in systems where the distance across which diffusive transport dominated (e.g. the thin film thickness) exceeded several hundred microns. This is likely to be unrealistically large in most systems where significant groundwater advection occurs through the DNAPL source zone itself. Instead they found that mass transfer enhancement occurs primarily due to reaction occurring in the bulk aqueous phase, which will drive down the bulk concentration of contaminant. This results in an increased concentration gradient, which increases the dissolution flux. They specifically expanded on the case of enhancement by reactions occurring in the bulk aqueous phase when advection was present. They used a theoretical model to consider a two dimensional system that evaluated advection and dispersion along a DNAPL pool interface of known area. It was assumed that equilibrium across the thin film interface was achieved rapidly and that the concentration of the bulk aqueous phase adjacent to the interface was at the solubility limit. Significant enhancements were predicted by this mechanism depending on conditions, related by a dimensionless variable M (Equation 2.34):

$$M = \frac{\pi k_2 C_{Ox} x}{4 v_x} \tag{2.34}$$

where M is a dimensionless variable relating reaction rate to contact time, k_2 is the second-order reaction rate coefficient, C_{Ox} is the initial concentration of permanganate before reaction, x is distance along the length of the source zone parallel to the flow field, and v_x is the aqueous phase velocity. Enhancement factors for values of M less than 1 were predicted to see little or no enhancement, and corresponded to slow reaction rates, low permanganate concentrations, short NAPL source zones and high groundwater velocities. For values of M greater than 1, enhancement rose significantly and asymptotically approached a maximum value. It was concluded that maximum mass transfer enhancement factors could range from 5-50 for permanganate and chlorinated ethenes based on advective-dispersive transport with reaction, but without any change in the thin film relationship.

2.3.3.5. Laboratory and Field Studies of DNAPL Degradation by ISCO. Several experimental studies have applied ISCO to DNAPL contamination, with both successful and undesirable results (Schnarr *et al.* 1998, Urynowicz 2000, Schroth *et al.* 2001, Conrad *et al.* 2002, MacKinnon and Thomson 2002, Li and Schwartz 2004b). A number of these studies have explored the mass transfer impacts of DNAPL oxidation, as mechanisms exist that can both enhance and hinder mass transfer. Investigations have also looked at the interaction of ISCO with the subsurface environment, focusing on permeability impacts due to deposition of manganese solids (MnO_2) and gas generation, as well as interactions between the aquifer solids and the oxidant, such as natural oxidant demand (NOD) and metals mobility.

A summary of controlled laboratory studies of oxidation of DNAPLs using permanganate is listed in Table 2.2. The effects observed vary with the type of system in which mass transfer is evaluated. Batch systems allow for the study of numerous experimental conditions, and can be conducted with known NAPL-aqueous phase interfacial areas, which allows direct quantification of the mass transfer rate, as well as investigation of interactions at the interface. However, these mass transfer rates are not wholly relevant in a subsurface environment, where the presence of porous media and an advective flow field impact mass transfer. One-dimensional (1-D) flow studies allow for the inclusion of advective impacts to mass transfer, as well as porous media interactions, but typically investigate fewer conditions than that of batch studies, and also assume a simplified flow field that may not be representative of conditions observed at field scale. Two-dimensional (2-D) and three-dimensional (3-D) studies account for mass transfer in more complex flow fields, and investigate how flow fields change as a result of remediation, but are complex systems limited to very few test conditions, and may require complicated modeling for analysis.

Urynowicz (2000), Jackson (2004) and Kim and Gurol (2004) used batch systems containing NAPL and aqueous phase to study oxidation in a system with no porous media. All three studies found mass transfer to be enhanced with increasing oxidant concentration. Urynowicz (2000) found that this enhancement occurred only for a brief initial time period, followed by a rapid decrease in mass transfer with time, probably due to interfacial resistance caused by the deposition of manganese oxide (MnO_2) solids at the DNAPL-aqueous phase interface. However, the system employed by Kim and Gurol (2004) did not observe the effect of decreasing mass transfer and reported mass transfer enhancements of up to 30 times that of natural dissolution alone.

A number of 1-D flow column studies have also been performed and observed various impacts to mass depletion as well as porous media hydraulic properties. Schnarr *et al.* (1998) found that mass transfer of a PCE DNAPL was enhanced during oxidation and that the resulting chloride could be used to effectively close a mass balance on the DNAPL. Li and Schwartz (2003) observed a high initial rate of mass depletion, which diminished with time. However, contaminant rebound occurred after oxidation indicating the presence of DNAPL although chloride generation during oxidation had effectively ceased. The decrease in mass transfer was attributed to the deposition of MnO_2 solids adjacent to the DNAPL saturated areas, causing localized changes in the advective flow field, reducing mass transfer. In both studies, it was found that nearly complete depletion of the residual DNAPL sources could be achieved.

Table 2.2. Laboratory studies of permanganate oxidation of DNAPLs (Petri 2006)

Study	Type of System	DNAPL Architecture	DNAPL Contaminant	Concentration (mg/L as KMnO4)	Velocities Studied	Mass Transfer and Other Effects Observed
Kim and Gurol 2004	Batch	Known Area	TCE	3000-6000	not applicable	Enhanced with higher oxidant concentrations
Jackson 2004	Batch	Known Area	TCE and PCE	1000-10000	not applicable	Enhanced with higher oxidant concentrations
Urynowicz 2000	Batch	Known Area	TCE	250-25000	not applicable	Enhanced at higher oxidant concentrations, but rapidly decreased with time due to MnO_2 precipitation
	1D Cell, no media	Known Area	TCE	250-2500	1.2-0.12 m/d	No impact due to velocity, Rapidly diminished with at high oxidant concentrations due to MnO_2 Deposition
Li and Schwartz 2003	1D Column	Residual	TCE	1000	2.3 m/d	Rapid initial mass transfer, diminished with time due to MnO_2 deposition
Schnarr et al. 1998	1D Column	Residual	PCE	7500-10000	1.0-1.66 m/d	Significantly enhanced over control systems, complete depletion of residual
Schroth et al. 2001	1D Column	Residual	TCE	800	11.4 m/d	Enhanced mass transfer, gas generation in unbuffered system, pore plugging with MnO_2
Li and Schwartz 2003	2D Tank	natural spill	TCE	200	11.4 m/d	Residuals depleted, pools remained due to flow bypassing, gas generation and formation of MnO_2 rind
Tunnicliffe and Thomson 2004	2D Tank	natural spill	PCE and TCE	1000	fractured, highly variable	Little removal of contaminant mass, significant reduction of advective mass transport due to MnO_2 precipitation
Reitsma and Marshall 2000	2D Tank	pool	PCE and TCE	1000-10000	1.0 m/d	MnO_2 deposition and gas generation resulted in flow bypassing of source, gas mobilized vapor phase contaminant
Mackinnon and Thomson 2002	2D Tank	pool	PCE	10000	0.21 m/d	Initially enhanced, decreased with time due to MnO_2 deposition, 45% mass removal, 75% mass transfer reduction
Conrad et al. 2002	2D Tank	natural spill	TCE	1000	heterogeneous, avg 2.9 m/d	Residuals depleted, pools remainded due to MnO_2 rind formation, permiablilty reduced
Li and Schwartz 2004	2D Tank	natural spill	TCE	200	heterogeneous, avg 7 m/d	Reduced by MnO_2 deposition, cycling organic acid flushes to remove MnO_2 resulted in complete DNAPL removal
Lee et al. 2003	3D Tank	residual	TCE	1660	0.25 m/d	Reaction zone velocity decreases with time, pore plugging by MnO_2 and gas caused flow bypassing, plume margins oxidized

Two-dimensional studies have observed different patterns in mass transfer, due to the more complex flow field. 2-D studies of natural spill patterns consisting of residuals and pools have found that residual DNAPL mass was quickly depleted by the combination of oxidation and flushing, but a rind composed of MnO_2 solids formed around pools, reducing the mass transfer from the pools. This was attributed the MnO_2 rind diverting aqueous flow away from the pools, resulting in limited permanganate delivery by advection (Conrad *et al.* 2002, Li and Schwartz 2003). Because pools have been particularly problematic, some recent research has focused specifically on pools. MacKinnon and Thomson (2002) found that oxidation of a PCE pool which resulted in 43% mass reduction caused a 75% reduction in mass flux from the source. Furthermore, while the mass transfer from the pool during oxidation decreased with time, the overall rate of mass transfer was still enhanced over that of natural dissolution alone. Reducing mass flux within a plume could potentially represent a remediation endpoint, and it has been suggested that reducing contaminant flux from pools by encapsulation with manganese solids may prove a viable way to achieve that endpoint (Thomson *et al.* 2000). However, the long term stability of the manganese coatings is not known. In the experiment conducted by Conrad *et al.* (2002), one of the sand tanks was allowed to sit for several months after the conclusion of the experiment. It was observed after this time had passed, that new fingers of DNAPL had mobilized downward through the MnO_2 rind of one of the encapsulated pools, suggesting that the manganese rind may not be capable of containing DNAPL over the long term. One innovative method that has been proposed to achieve complete removal of DNAPL pools using permanganate is to cycle permanganate and organic acid flushes. Organic acids such as citric and oxalic acid can effectively dissolve MnO_2, and remove the rind so that multiple oxidant flushes are possible (Li and Schwartz 2004a). Using this method, Li and Schwartz (2004b) achieved complete removal of a DNAPL pool in a 2-D flow through tank.

Additional mass transfer considerations need to be made when working in three dimensions. A 3-D study by Lee *et al.* (2003) observed that a 3-D residual source was largely depleted by oxidation, but deposition of MnO_2 and gas in the source over time led to a decrease in the permeability of the source zone. This loss of permeability eventually caused permanganate to bypass both the source and down-gradient plume. In many 2-D studies, where a natural spill DNAPL architecture is used, flow is forced through zones of residual saturation, as the residual zone spans most or all of the flow field. The bypassing of this residual zone indicates that large residuals zones may also be susceptible to flow bypassing similar to pools. Furthermore, blockage of the source zone sheltered the resultant down-gradient plume from direct contact with the oxidant. Transport of permanganate into the plume was likely controlled by vertical and lateral dispersion of permanganate into the plume margins, resulting in oxidation of the sides of the plume, but the core of the plume remained untreated.

Other mass transfer impacts have been noted by studies as well. Because carbon dioxide (CO_2) is one of the primary products of the reaction between permanganate and chloroethenes, gas generation has been noted in several studies (Reitsma and Marshall 2000, Schroth *et al.* 2001, Lee *et al.* 2003, Li and Schwartz 2003). Gas generation has the capability to impact mass transfer both by decreasing the relative saturation of porous media causing a large decrease in the hydraulic conductivity, and also by potentially mobilizing volatile contaminant vapors. Reitsma and Marshall (2000) found that gas generation within a DNAPL pool was so severe that the DNAPL source zone became desaturated, and contaminant vapors in gas bubbles mobilized upward. The bubbles were coated with MnO_2 solids suggesting that vapor phase contaminant had absorbed into the aqueous phase resulting in oxidation of TCE and PCE at the gas-aqueous phase interface. As such, this demonstrates that an additional mass transfer mechanism is possible resulting in enhanced transport and destruction of the contaminant. However, gas generation is generally undesirable due to the large head loss, and difficulty in controlling gas migration in the subsurface. A study by Schroth *et al.* (2001) found that production of the gas could be controlled by buffering the aqueous phase at a high pH, resulting in CO_2 remaining dissolved as bicarbonate, causing less gas formation and less impact to the permeability of the subsurface. At low pH values, carbonate ions are converted to dissolved CO_2 and the solution is more likely to become supersaturated relative to CO_2, resulting in off-gassing (Benjamin 2002).

Pilot and field scale studies have also been used to investigate the effectiveness of ISCO using permanganate on DNAPL sites. Field scale studies do not have as much experimental control as laboratory studies, and typically involve sites with unknown masses and architectures of DNAPL, unknown flow fields, and limited experimental data. However, an understanding of ISCO at the field scale is important so that future remediation designs can be optimized to achieve remediation goals more efficiently. A summary of relevant field studies is given in Table 2.3.

DNAPL field sites vary widely in terms of conditions that impact DNAPL mass transfer, such as the source architecture, the permeability of the subsurface and resulting flow fields and the contaminant type encountered. As such, application of ISCO using permanganate is custom tailored to each particular site. Major design parameters at a given site include the injection technique, the number and placement of injection locations, and the oxidant concentration and injection flow rate used. Among the most common injection regimes are well to well flushing and probe injection. In well to well flushing, oxidant is injected into a well, and surrounding extraction wells provide hydraulic control. This regime is frequently designed to recirculate oxidant and groundwater within the source zone in a closed loop. Typically, such regimes utilize fewer injection wells than extraction wells and are spaced at wide intervals on the order of tens to hundreds of feet. Because this method requires moving large volumes of fluid in the subsurface, sites must have moderate to high permeability to allow fluid movement. Subsurface heterogeneities and source architecture can greatly influence oxidant delivery to the DNAPL source with this method. Probe injection involves pressing an injection lance directly into the ground and then rapidly injecting a volume of oxidant. The probe is then withdrawn and moved to another location for additional injections. With probe injection, a large number of injections can be done in a short time period, allowing for much closer spacing of injection locations, typically on the order of feet to tens of feet. This allows for more control of oxidant delivery to DNAPL, and better delivery into low permeability layers. However, there is no continuous supply of oxidant and treatment ceases when either the oxidant is consumed, or is flushed away by groundwater advection (Siegrist *et al.* 2001).

The field and pilot scale studies of ISCO using permanganate listed in Table 2.3 have had mixed results when applied to DNAPL sites. Several pilot studies conducted in relatively homogenous subsurface systems, and with residual sources, have met with excellent results where over 90% DNAPL mass removal was attained (Schnarr *et al.* 1998, Thomson *et al.* 2000). However, systems with pooled DNAPL, as well as heterogeneities in the subsurface resulted in less removal and contaminant rebound after remediation (Schnarr *et al.* 1998, Huang *et al.* 2000, Moes *et al.* 2000). In many cases, the major limitation in dealing with a DNAPL site is getting sufficient oxidant delivery to the DNAPL so that it can be destroyed. The highly heterogeneous nature of how DNAPL migrates in the subsurface has frequently been implicated as the reason for failure to achieve remediation goals.

Table 2.3. Field studies of permanganate oxidation of DNAPLs (Petri 2006)

Study	Architecture	DNAPL Composition	Concentration (mg/L)	Velocity Range	Field Injection Method	Effects observed
Schnarr et al. 1998	Residual	PCE	10000	~0.05 - 0.1 m/d	Injection / Extraction wells	91% removal, Non-detect post oxidation, mass xfr decrease with time
	natural spill	TCE and PCE	10000	~0.05 - 0.1 m/d	Reciulation	62% removal, heterogeneity led to smaller mass removal
Thomson et al. 2000	Residual	PCE and TCE	8000	0.08 m/d	Injection / Extraction wells	residual destroyed, 99% removal, 95% flux reduced
McKay et al. 1998	Residual	TCE	15000	not reported	multiple well injection, cycled	Attenuation of TCE at one field pilot, inconclusive from other. Noted Chloride Generation, TCE still saturated
McKay et al. 2000	Residual	TCE	15000	not reported	multiple well injection, cycled	Reduction in mass, mass transfer limitations in areas of high concentration (NAPLs) Note, same site as above
Moes et al. 2000	Residual	TCE	50000-60000	not reported	probe injection	Oxidant Delivery limited success, saline system, formation of THMs and mobilized metals, rebound,
Mott-Smith et al. 2000	natural spill	TCE	1000-30000	not reported	probe injection	Significant Mass Reduction, Aqueous Concentrations highly variable, no byproducts, no pore plugging
Nelson et al. 2000	natural spill	PCE	13000-20000	not reported	probe injection	Stacked coellecing treatment zones, density driven advection, micicble salt solution follows similar flow path to DNAPL
Huang et al. 2000	Residual and Pool	TCE	11000	not reported	Injection / Extraction wells	Significant pH drop, rapid oxidation of dissolved phase, rate-limited mass xfr from DNAPL phase, MnO_2 reduced mass xfr from pooled layer

2.4. OXIDANT PERSISTENCE AND STABILITY IN THE SUBSURFACE

2.4.1. Introduction

In addition to reacting with the target organic chemicals such as PCE and TCE, oxidants such as potassium permanganate and catalyzed hydrogen peroxide (CHP) can react with natural components present in the subsurface. These reactions can exert what is referred to as a natural oxidant demand or NOD, which yields a non-productive oxidant depletion and a major effect on oxidant transport away from an injection location into the subsurface region to be treated. Oxidants such as CHP can also degrade by auto-decomposition reactions and persistence under some subsurface conditions can be limited due to these reactions. During this SERDP project, the persistence and stability of permanganate and CHP was evaluated during batch tests and flow-through experiments. The following summary is based on literature reviews completed by CSM team members and presented in M.S. Theses and Ph.D. Dissertations (e.g., Seitz 2004, Heiderscheidt 2005) as well as published papers (e.g., Crimi and Siegrist 2005).

2.4.2. Natural Oxidant Demand for Permanganate

Field soils and aquifer sediments typically contain natural organic matter, reduced metals, and other reductants that can be readily oxidized. These soil constituents are referred to collectively as natural oxidant demand (NOD), or sometimes soil oxidant demand (SOD), and compete with target contaminants for available oxidant. Zhang and Schwartz (2000) proposed that components comprising the NOD have a much faster reaction rate with MnO_4^- than do chlorinated contaminants, in order to explain delayed breakthrough of MnO_4^- in column experiments by Schnarr *et al.* (1998). This conceptual model of NOD oxidation corresponds to an instantaneous sink (Figure 2.5a). Under this concept, all of the NOD must be oxidized before any PCE oxidation occurs; thus, in order to oxidize a given mass of PCE, the mass of MnO_4^- needed will be equal to the NOD plus the demand determined from the reaction stoichiometry. On the other hand, there is evidence that not all NOD components are oxidized faster than the contaminant (Mumford *et al.* 2002, Mumford *et al.* 2005, Siegrist *et al.* 1999, Struse *et al.* 2002, Yan and Schwartz 1999). Because NOD is generally a complex mixture of components whose surface area available for oxidant contact varies, it seems likely that NOD oxidation will be a kinetic process as depicted in Figure 2.5b. This means that oxidation of NOD and PCE or TCE occur simultaneously, with relative rates of oxidation controlling depletion of each.

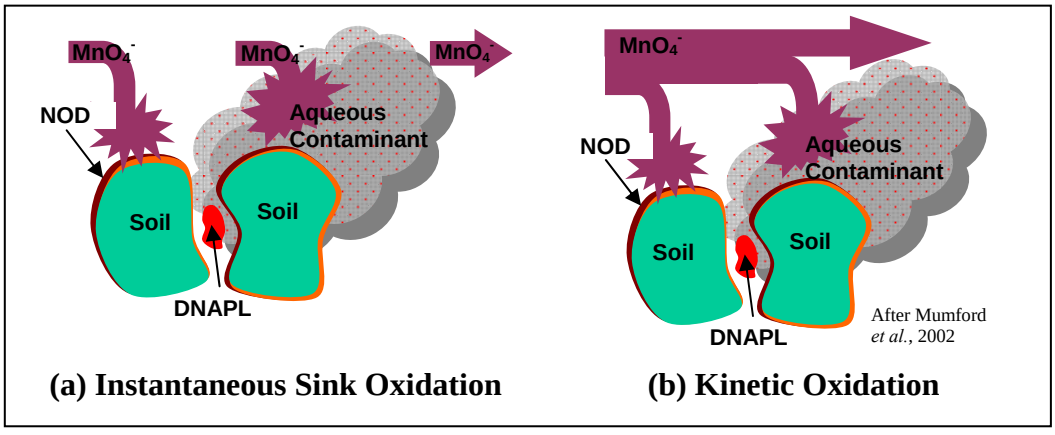

Figure 2.5. Conceptual models for permanganate depletion by NOD (Heiderscheidt 2005).

Further, because NOD results from a mixture of constituents, the kinetic rate for oxidation of NOD can vary widely for different soils. While the kinetic rates for some NOD constituents of a particular soil are often higher than that of the target contaminant, preliminary results related to this research, and that of others, suggests NOD frequently consists of at least two components with markedly different oxidation rates (Crimi and Siegrist 2004, Jackson 2004, Mumford *et al.* 2005). As an example, Chambers *et al.* (2000) found two distinct NOD oxidation rates for each of three different field soils in batch tests. The rate during the first 24 hours was 10 – 20 times faster than the rate during the next 13 days. They also found that the slower rate for the three soils was virtually the same, while the initial fast rate varied by soil type with silt and clay being about twice that of sand.

Mumford *et al.* (2005) considered the possibility that the multiple rates could be a result of organic carbon located within soil grain micropores being more difficult for oxidant to access. They performed batch NOD studies on native coarse sand from the Borden test site (grain size greater than 0.42mm), as well as on coarse Borden sand that had first been crushed (grain size less than 0.074mm). Results from the one week NOD tests showed no significant difference, suggesting that either the proposed geometric configuration is not a rate-limiting factor or that reduced species in micropores are still unavailable even after crushing (Mumford *et al.* 2005).

The research on kinetic rates for NOD oxidation to date has not determined the overall reaction order. The results from the studies already mentioned suggest that it is first-order with respect to NOD, but there has been little study of the effect of MnO_4^- concentration. The work of Crimi and Siegrist (2004) did utilize two MnO_4^- concentrations, and provided some indication that at least the NOD fraction with the slower kinetic rate is also first-order with respect to MnO_4^- (second-order overall), because increasing the oxidant concentration by a factor of four resulted in a doubling of the oxidation rate for the slow fraction of NOD.

Additionally, research is limited on how NOD values determined from batch tests will compare to actual NOD affects in a real-world groundwater system. The results of Huang *et al.* (2000) suggest that batch NOD tests will over-estimate real-world NOD, as represented by NOD determination from a 1-D flow column, by as much as 300 times. However, their batch tests were conducted with unusually high water to solids ratio of 10:1 and their batch tests were vigorously mixed. Crimi and Siegrist (2004) independently varied both water to solids ratio and degree of mixing (static, gentle stirring, completely mixing) to quantify the effects on NOD determination for a field soil. Their results indicate that (for the field soil studied) a water to solids ratio of one or slightly more, combined with static or gently stirred conditions, results in an NOD determination within 10% of that from a 1-D flow column. If the solid to liquid ratio is too high, oxidant is depleted before reaching the actual NOD value. On the other hand, if the solid to liquid ratio is too low, too much oxidant is depleted and oxidant demand is over-estimated because the batch tests typically continue until all or nearly all the oxidant is gone (Crimi and Siegrist 2004). NOD mass fraction estimates determined from batch-scale tests may need to be adjusted or "up-scaled" to be effective in predicting field-scale performance.

Along these lines, Mumford *et al.* (2004) developed an in situ push-pull technique for estimating the NOD mass fraction for a field soil. They injected oxidant and a conservative tracer at three locations of uncontaminated soil within the Borden site, allowed two days for the oxidant to react with aquifer material, and extracted the oxidant and tracer. They also performed batch tests on field soil taken from the site, duplicating conditions of the push-pull tests and found the push-pull tests and the two-day batch tests provided similar results. Mumford *et al.* (2004) concluded that the in situ push-pull technique is viable, with the advantage that it provides a measurement representative of a much larger aquifer volume. Conversely, batch tests can provide NOD estimates representative of actual in situ field performance, provided that the batch tests are not simply carried out as ultimate NOD tests (i.e., run until all oxidizable material is gone) but instead stopped at a representative time. Mumford *et al.* (2004) also found that the variability between replicate batch test results decreased as the soil mass was increased, with least variability when the water to solids ratio was approximately one. Finally, the increased variability for

small batch test soil masses, along with the 30% variation in NOD values estimated from the push-pull tests for the three locations, highlight the variability and site-specific nature of NOD values even for a relatively homogeneous site like Borden (Mumford *et al.* 2004).

2.4.3. Persistence and Stability of Hydrogen Peroxide

When hydrogen peroxide is injected into the subsurface it can react with NOM in a fashion similar to that of potassium permanganate. In addition, it can have complex interactions with components such as organic matter and goethite and other iron-based minerals which in turn, can impact the subsurface reaction chemistry of catalyzed hydrogen peroxide or Fenton's reagent oxidation (Tyre *et al.* 1991, Barcelona and Holm 1991, Watts *et al.* 1993, 1994, Voelker and Sulzberger 1996, Li *et al.* 1997, Lin and Gurol 1998, Valentine and Wang 1998, Watts *et al.* 1999, Petigara *et al.* 2002, Watts *et al.* 2002, Yeh *et al.* 2002, Kwan and Voelker 2003). In general, these studies indicate that organic matter can have complex interactions that will impact oxidation effectiveness and efficiency and that these impacts are dependent on concentrations of NOM and oxidant. They also indicate that the presence of goethite in a peroxide system can significantly facilitate contaminant oxidation via catalysis. Voelker and Sulzberger (1996) and Valentine and Wang (1998) report that the effect of humic acid on oxidation rate and extent depends on its concentration, and that humic acid can act as a free radical scavenger, a radical chain promoter, and a catalytic site inhibitor. These characteristics explain the conflicting information in the literature with respect to the impact of organic matter on oxidation in peroxide systems. Voelker and Sulzberger (1996) indicate that iron-organic matter fulvate complexes can react more rapidly with peroxide than iron-aquo complexes. Voelker and Sulzberger (1996) also report that organic matter can scavenge free radicals forming an organic radical that can lead to peroxide regeneration by reaction with iron(II). Petigara *et al.* (2002) report that higher concentrations of organic matter decrease peroxide decomposition and the amount of free radical generation, but the opposite is true with lower organic matter concentrations due to the different mechanisms of interaction of the organic matter with iron and with peroxide, further emphasizing the findings of Voelker and Sulzberger 1996 and Valentine and Wang 1998. Also, Li *et al.* (1997) noted kinetic differences resulting from the presence of organic matter, consistent with other studies as noted above.

As the NOM content in soils increases, peroxide is degraded faster (Petigara *et al.* 2002). Oxidant also degrades faster when reacting with iron and manganese oxyhydroxides (Kakarla and Watts 1997). While NOM and minerals can exert considerable demand on the oxidant, enhanced desorption of hydrophobic contaminants originally sorbed to NOM has been found effective for PCE (Watts *et al.* 1999a) and chlorophenols (Yeh *et al.* 2002). Furthermore, during oxidation of NOM the free radical degradation pathway dominates, which could aid in assuring that the desired pathway for oxidation of chlorinated compounds is being achieved (Petigara *et al.* 2002). Again, LPM often has higher NOM than permeable media, which results in increased rates of peroxide degradation and reactions with non-target species. However, reactions with NOM could increase enhanced desorption in combination with ensuring that the free radical degradation pathway is being achieved. The combination of desorption of target contaminants and assurance that free radicals are present could allow for CHP to effectively degrade chlorinated compounds during slow transport by diffusion within LPM zones.

Iron and manganese oxyhydroxides are not the only minerals that affect hydrogen peroxide chemistry. Manganese oxides, available manganese, and iron minerals have the ability to catalyze hydrogen peroxide (Watts *et al.* 1999b, Baciocchi *et al.* 2002, Petigara *et al.* 2002). ISCO application to soils high in these minerals could utilize these natural minerals to catalyze the peroxide reaction. It has been reported that naturally occurring iron minerals are actually better catalysts than iron compounds injected into the subsurface (Watts *et al.* 1999b). While an excess of these minerals could increase the rate of hydrogen peroxide degradation, these same minerals found in clays and fine grained silts could supply the catalyst at the LPM contact, which could reduce the hydrogen peroxide degradation prior to entry in the LPM. The same study that found non-target reactions with oxyhydroxides also reports that

particle size fractions are important to peroxide decomposition. High clay or silt content can increase the sorption of hydrophobic contaminants (Watts *et al.* 1999a); however, increases in surface area can catalyze the peroxide reaction also (Baciocchi *et al.* 2002). For ISCO application in LPM, the naturally occurring iron minerals and surface area effects of clay and fine grained soils could act as catalysts for hydrogen peroxide decomposition.

The stabilization of hydrogen peroxide during applications has been studied since its use in wastewater applications (Schumb *et al.* 1955). An entire chapter is devoted to stabilization in Schumb *et al.*'s book Hydrogen Peroxide (1955). The methods employed to stabilize hydrogen peroxide include pH adjustments, removal and understanding of catalysts within the system, the complexation of a catalyst in order to reduce its immediate availability, stabilizing agents, and changing the availability of natural organic matter (Schumb *et al.* 1955, Watts and Dilly 1996, Yeh *et al.* 2002). Businesses that commonly apply Fenton's reagent during ISCO often have a patent on their particular hydrogen peroxide-stabilizer compound or technique (Levin *et al.* 2000 and Nuttall *et al.* 2000); however, most vendors provide information as to the method of stabilization (e.g. a buffer solution or an iron complexing solution).

2.5. ISCO EFFECTS ON SUBSURFACE PERMEABILITY

2.5.1. Introduction

The application of oxidants like potassium permanganate or hydrogen peroxide to a subsurface environment using injection probes or wells can yield permeability changes due to several processes. Permeability losses can occur due to (1) detachment and redeposition of colloids and particulate matter as a result of high rate fluid injection or (2) production of reaction products such as CO_2 (g) or MnO_2(s). Permeability increases can occur in certain formations where the acidity produced by chemical reaction can lower pH and dissolve components such as $CaCO_3$. During this SERDP project, the permeability effects of permanganate and peroxide were evaluated during flow-through experiments. The following summary is based on literature reviews completed by CSM team members and presented in M.S. theses and Ph.D. dissertations (e.g., Seitz 2004, Heiderscheidt 2005, Petri 2006).

2.5.2. Effects of Permanganate on Subsurface Permeability

Research has shown that oxidation of a high DNAPL saturation source using permanganate may result in permeability reductions due to precipitation of manganese oxides thereby reducing the ability for oxidant to be transported to the source (Lee *et al.* 2003, Schroth *et al.* 2001, Siegrist *et al.* 2002). On the other hand, research into permeability effects from permanganate oxidation of DNAPL source zones at lower saturations is a bit more ambiguous. Nelson *et al.* (2001) concluded that the manganese oxides produced during oxidation of a PCE DNAPL present at approximately 4-7% saturation had negligible effect on the permeability, despite the system remaining at a neutral pH due to natural buffering from the carbonate mineral-containing sands. On the contrary, Lee *et al.* (2003) found that permanganate oxidation of a TCE DNAPL source zone at 8% saturation resulted in generation of up to 4900 mg MnO_2(s)/kg porous media, in an unbuffered silica sand system utilizing de-ionized water. Further, they witnessed a six-fold decrease in velocity of the oxidation front over the two-month experiment. They attributed this decrease in oxidation front velocity to decreased oxidation delivery resulting from reductions in permeability.

There are several methods to relate permeability reductions to reductions in porosity resulting from immobile components in porous media pore spaces. These may take the form of power law models as in Equations 2.35 (Wyllie 1962) and 2.36 (Reis and Acock 1994) or capillary-tube models like the Kozeny-Carman equation in Equation 2.37 (Bear 1972):

$$k_{r,w} = \left(\frac{1 - S_n - S_{r,w}}{1 - S_{r,w}} \right)^3 \tag{2.35}$$

$$k_{r,w} = \left(1 - \frac{\phi - \phi_{eff}}{\phi} \right)^b \tag{2.36}$$

$$k_{r,w} = \frac{\phi^3}{K_s (1-\phi)^2} \left(\frac{{d_{50}}^2}{180} \right) \tag{2.37}$$

where $k_{r,w}$ is the relative water permeability, S_n is the saturation of immobile component in the pore space, $S_{r,w}$ is the residual water saturation for the porous media, ϕ is the soil porosity, ϕ_{eff} is the effective soil porosity, b is an empirical exponent related to the type of porous media, K_s is the saturated hydraulic conductivity (LT^{-1}) and d_{50} is the representative (median) grain size (L).

Saenton (2003) found Equation 2.35 to provide good agreement to experimentally derived permeability data (Saba 1999) for DNAPL in silica sands like those that are being used in this research. Additionally, Clement *et al.* (1996) proposed Equation 2.36 (with b = 19/6) for pore-clogging due to microbial growth. However, Reis and Acock (1994) concluded that the various forms of the Kozeny-Carman equation are not generally a good model for the reduction in permeability following chemical precipitation in a porous media because they significantly under-predict permeability reductions. They also pointed out that power law models suffer from under-prediction of permeability reductions, especially at high levels of plugging. This can be seen in the research by Lee *et al.* (2003). Converting the mass of MnO_2(s) generated to a volume, using a MnO_2(s) density of 5040 g/L (CRC 2001) and either Equation 2.35 or Equation 2.36 (with b=3.5, the average value determined from three studies using similar sand, Reis and Acock 1994), the mass of MnO_2(s) generated in the experiment of Lee *et al.* (2003) results in an estimated 1.6% reduction in permeability. However, the CRC (2001) density is for a dry, aged mineral pyrolusite form of MnO_2(s). Li and Schwartz (2004) determined the precipitated MnO_2(s) is a hydrous birnessite-like form expected to have a lower density. Unfortunately, no values for the density of this precipitated form have been determined. Using a lower estimated density (e.g., 1000 g/L) to estimate the volume of MnO_2(s), and Equation 2.35 or 2.36, results in an estimated permeability reduction of 7.5%. However, a much greater reduction would be needed to account for the experimental results, such as would occur if manganese oxides block the pore throats before the entire pore space is filled.

Reitsma and Randhawa (2002) performed 1-D column experiments oxidizing aqueous PCE at approximately 50 mg/L with 2000 mg/L $KMnO_4$ (Darcy velocity of 3.0 m/day) in silica sand. They found that with MnO_2(s) filling as little as 1% of pore space (assuming solid MnO_2(s) with density of 5040 g/L), permeability was reduced by 98%. Even if the density of the precipitated MnO_2(s) is taken as 1000 g/L the predicted permeability reduction (by Equation 2.35 or 2.36) would only be 15%. Reitsma and Randhawa (2000) concluded that the increased permeability reduction must be due to pore-clogging. They also found higher flow rates resulted in slower permeability reduction, possibly because the higher flow rate dislodges some MnO_2(s) particles as they begin to get lodged in pore throats.

Similarly, Schroth *et al.* (2001) performed 1-D column experiments to study the effects of MnO_2(s) formation on permeability. Their study differed from that of Reitsma and Randhawa (2002) in that residual DNAPL TCE was emplaced in 2/3 of the column length, the $KMnO_4$ concentration was 790 mg/L, and the Darcy velocity was 15.8 m/day. They estimated a permeability reduction of 96% in 24 hours. Based on the mass of TCE destroyed, the mass of MnO_2(s) generated can be estimated as 66.2 g. Assuming it was evenly distributed throughout the DNAPL source zone, with a MnO_2(s) density of 5040 mg/L, the estimated permeability reduction (by Equation 2.35 or 2.36) would only be 10%. However, if the MnO_2(s) is considered to be located primarily in the first 25% of the source zone as visually observed by Schroth *et al.* (2001), the estimated permeability reduction becomes 33.6%. Further, if the precipitated

MnO_2(s) density is again taken as 1000 mg/L, and it is considered to be located in the first 25% of the source zone, the estimated permeability reduction (at 95.2%) is quite close to the observed reduction. The column used by Schroth *et al.* (2001) had twice the cross-sectional area and 33 times the length of that used by Reitsma and Randhawa (2002), suggesting that even if throat clogging is occurring at the pore scale, the permeability relations of Equations 2.35 and 2.36 may still be effective at larger scales, as long as an appropriate density is used for the precipitated MnO_2(s).

While permeability reductions in and around the source zone, generated by oxidation using permanganate, are quite possible, they may not be entirely bad. Although flow of additional oxidant through the source zone may be reduced, so would water flow in general. This reduction or blockage of flow through the source zone could act to chemically stabilize a DNAPL source effectively cutting off the flux of dissolved contaminant from the DNAPL (MacKinnon and Thomson 2002). However, Conrad *et al.* (2002) found that, while a MnO_2(s) shell or rind did indeed form around a DNAPL pool during oxidation with permanganate, three months after oxidation the shell failed and DNAPL fingers emerged through it indicating that chemo-stabilization may not be a long term benefit/solution. As alluded to in the previous discussion about the oxidation kinetics, system chemistry impacts the MnO_2(s) generation and subsequent effects on porous media permeability. For example, according to Stewart (1965) and Yan and Schwartz (1999), if the pH drops below 3.5 the kinetics favor production of soluble Mn^{2+} instead of MnO_2(s). Along these lines, in a well-buffered system such as an aquifer of carbonate soils the pH will likely remain more neutral leading to more MnO_2(s) generation. The groundwater flow can also have an effect, such as controlling if and how much MnO_2(s) is transported colloidally instead of being deposited close to the point of generation.

2.6. APPLICATION OF ISCO TO LOW PERMEABILITY ZONES

2.6.1. Introduction

The application of ISCO for remediation of sites contaminated by PCE and TCE DNAPLs may involve subsurface regions that have zones of low permeability media. An attractive feature of chemical oxidants is the potential for them to diffuse into LPM and degrade the PCE and TCE dissolved and sorbed within the LPM matrix. During this SERDP project, Seitz (2004) completed experimental work to examine the application of potassium permanganate and catalyzed hydrogen peroxide for treatment of LPM zones where oxidant transport was by driven by diffusion. This section is excerpted from Seitz (2004) and presents a summary of relevant background concerning application of ISCO to LPM zones.

2.6.2. DNAPL Contamination of Low Permeability Media

Originally, LPM zones were thought to be an effective barrier to downward migration of DNAPLs; however, McKay *et al.* (1993) illustrated the ubiquitous presence of fractures in LPM. Even without the presence of obvious fractures in LPM, numerical models have illustrated that a large mass of DNAPL constituents can diffuse into the lowest displacement pressure areas of LPM at sorbed and dissolved concentrations due to hydraulic gradients and capillary forces (Kueper and McWhorter 1991). While a pool lies on a LPM, migration of DNAPL free phase into fractures coupled with concentration gradient diffusion into the LPM matrix yield a mass sink for the DNAPL (Reynolds and Kueper 2002). Since pool lifetimes for a spill of a few thousand kilograms of dense chlorinated solvents have been numerically modeled to persist for decades to centuries (Johnson and Pankow 1992), there is often sufficient time for the underlying LPM zones or aquitards to become almost saturated with dissolved and sorbed organic contaminants. Imhoff and Miller (1996) found that instabilities in groundwater velocity through DNAPL saturated zones result in nonlaminar flow characteristics. These instabilities found in some DNAPL source zone configurations in 2-D tank studies cause vertical flow components that move contaminant mass via vertical advection further than diffusion alone into the LPM (Wilking 2004).

Even after a pool or overlying DNAPL zone is removed, DNAPL constituents in LPM can still maintain a constant source flux from a LPM zone (Johnson and Pankow 1992). Since higher groundwater flow velocities facilitate dissolution and remediation of groundwater in higher permeability zones, contaminants in these zones are depleted faster than in low velocity LPM. Once the surrounding higher permeability zones are at low concentrations, LPM zones can then be a constant source of contaminant into the higher permeability zones as a result of concentration gradients and back diffusion (Reynolds and Kueper 2002). Even with the majority of the contaminant mass removed, back diffusion from the LPM can result in dissolved plume concentrations above maximum contaminant levels. Left untreated, contaminants diffusing from the LPM into the surrounding matrix can have lifetimes that reach hundreds of years (Parker *et al.* 1994, Siegrist *et al.* 1998). Not only can contaminated zones of LPM become sources of contaminant plumes due to back diffusion, they often have hydraulic properties that make remediation of the contaminant in LPM difficult.

2.6.3. Diffusion in LPM zones

The subsurface environment frequently contains regions of LPM within, or as an aquitard beneath aquifers. Subsequent to contamination within the aquifer, substantial contaminant mass can make its way into the LPM zones by diffusion. For example, in the case of an extremely low permeability clay liner beneath a 5-year old hazardous waste dump containing DNAPLs, Johnson *et al.* (1989) found that organic contaminants (including TCE) had diffused 15-20 cm into the liner in only five years. On the other hand, waste-generated chloride had diffused up to 83 cm in that time. The different distances were attributed to different molecular diffusion rates as well as sorption of the organics retarding diffusion. Similarly, Ball *et al.* (1997) studied a soil core from the aquitard beneath a TCE/PCE plume at Dover Air Force Base (AFB), Delaware. They found that PCE and TCE had diffused approximately 80-100 cm into the aquitard in the estimated 15-20 years since the plume arrived above the core location. In a later field experiment at the Dover AFB site, Liu and Ball (2002) confirmed the validity of their previous diffusion modeling. Their results also appear to provide direct evidence that an underlying confining layer can be contaminated by an overlying plume of aqueous contamination, and the confining layer can subsequently become a source of groundwater contamination through back-diffusion once the primary plume is gone.

On the other hand, LPM may contain fractures large enough to allow DNAPL migration into the LPM fractures. A series of modeling studies have focused on DNAPL migration through such fractures, and the subsequent dissolution and diffusion of contaminant mass into the surrounding matrix. These studies have shown that significant mass of contaminant can end up diffusing into the matrix, in a relatively short time on the order of only a few years (Parker *et al.* 1994, Parker *et al.* 1997, Reynolds and Kueper 2002, Ross and Lu 1999).

As seen by Johnson *et al.* (1989), different solutes diffuse at different rates through porous media. Millington and Quirk (1959, 1961), proposed that the effective diffusion coefficient, D_e, (L^2T^{-1}) of an aqueous solute through a porous media can be estimated from the molecular diffusion coefficient for a bulk solution of the solute (at an infinitely dilute concentration), D_m, (L^2T^{-1}) and the effective porosity, ϕ_{eff}

$$D_e = D_m \phi_{eff}^{4/3} \tag{2.38}$$

In order to account for the reduced effective porosity of a multiphase system, Jury *et al.* (1991) modified the Millington-Quirk relationship, relating it to water content (θ_w) as well as effective porosity.

$$D_e = D_m \frac{\theta_w^{10/3}}{\phi_{eff}^2} \tag{2.39}$$

In the fully water-saturated case, the water content (θ_w) is equal to effective porosity (ϕ_{eff}) and Equation 2.39 simplifies to the Millington-Quirk relation of Equation 2.38.

Tidwell *et al.* (2000) researched the effect of porosity on diffusion of potassium iodide into Culebra dolomite slabs using x-ray absorption imaging at the centimeter-scale. They found that diffusion rates within the slabs indeed varied spatially, and depended on the magnitude of porosity at each location. Conversely, Itakura *et al.* (2003) performed diffusion experiments using three different organic contaminants, including TCE and three soil configurations (reconstituted and intact kaolin clay as well as reconstituted sandy silt), and determined that the relation:

$$D_e = D_m \phi \tag{2.40}$$

inadequately fit a combination of their data (19 points) and that from four other studies (6 points). Subsequently, they concluded "there is little correlation between tortuosity and porosity." However, from the data they present (and excluding only two of the six data points from other studies, keeping 23 of 25 data points), it appears that the Millington-Quirk relation of Equation 2.38 fits reasonably well. Itakura *et al.* (2003) also tested different thicknesses of reconstituted clay, and determined that sample thickness, over the range of 1.25 – 2.97 cm, did not significantly affect the effective diffusion coefficient.

Because different chemicals have different molecular diffusion coefficients, and different sorptive properties, it may be possible to exploit these differences in remediating chlorinated solvent mass located in LPM. Based on the small number of studies reported in the literature, ISCO using permanganate appears promising. Struse *et al.* (2002) studied the transport of permanganate by diffusion through 2.54 cm long, intact cores of low permeability silty clay loam soil. Permanganate diffused through the uncontaminated core in approx. 15 days. When TCE was emplaced in the center of the core, it took twice as long for the permanganate to get all the way through the core; however, nearly all of the TCE was successfully oxidized with none diffusing out of the core despite having only half the distance to travel. These results indicate the permanganate can effectively diffuse into an LPM and oxidize contaminant mass located there. Further, the effective diffusion coefficients correlated well to the porosities, using the Millington-Quirk relation. Similarly, Siegrist *et al.* (1999) tested the ability of permanganate to diffuse into silty clay LPM at a field site in Ohio. The permanganate was emplaced via hydraulic fracturing, and continuous cores were extracted at several times over 15 months. After 10 months, the permanganate had visibly diffused over 15 cm above and below the emplacement, and batch tests showed that this zone still sustained a high degradation potential. However, few additional studies have been reported in the literature and there has been insufficient study of how LPM configuration will impact the effectiveness of chemical oxidation within an aquifer.

2.6.4. ISCO Application to Sites with LPM

Due to the relatively longer stability of the permanganate ion in groundwater, most studies in LPM have been performed with the permanganate ion as the main oxidant. However, several studies of CHP in clay or silty soils have also been reported. Many of the studies focus on the delivery of oxidant into the LPM zone. Most field studies mention the possibility of hydraulic property and soil morphology changes associated with the oxidation, but most studies look primarily at advection systems and not at long contact time diffusion systems. The majority of reported field studies rely on advection of oxidant through LPM zones except one that distinctly focuses on high concentration permanganate diffusing into the clayey soil of the field site (Siegrist *et al.* 1999).

Siegrist *et al.* (2001) outline three major field studies performed with permanganate ISCO in environments with low permeability media. All three performed ISCO in silty-clay low permeability soils through different permanganate delivery methods. The methods included deep soil mixing of $KMnO_4$ solution, direct push injection probes of $KMnO_4$ solution, and hydraulic fracturing coupled with emplacement of $KMnO_4$ solids mixture. The deep soil mixing resulted in an average of 67% removal in mass of contaminant (Siegrist *et al.* 2001). Although it achieved considerable mass destruction, the permanganate solution ponded at the surface of the tight clay soil closer to the surface. Additionally, it was determined that deep soil mixing contaminant destruction is very difficult to assess since observed

VOC increases occurred in some zones after deep soil mixing. This increase was attributed to mixing low contaminant concentration areas with surrounding higher concentration areas. The direct push injection occurred at a clean test site in absence of DNAPL contamination. In a delivery more tailored to diffusive transport, hydraulic fracturing of LPM with emplaced potassium permanganate oxidant solids allowed permanganate ions to diffuse from fracture zones into LPM and oxidize the target contaminant (Siegrist *et al.* 1999). As the permanganate diffused 30 cm above and below the fracture over 10 months, the oxidant achieved an efficiency of greater than 99% degradation closest to the fracture zone (Siegrist *et al.* 1999).

Few laboratory studies have been performed on diffusion of oxidants into low permeable media. In 1999, Struse used laboratory diffusion studies to show the potential for diffusive transport and permanganate oxidation in silty clayey soils. These studies utilized natural soils from an Ohio pilot study site and determined diffusive transport rates of approximately 0.1 cm/d. Both the rate and the effect of non-target oxidizable material are consistent with the observations of emplaced potassium permanganate solids found in the pilot study by Siegrist *et al.* (1999). Struse *et al.* (2002) also reported decreases in the organic carbon content and non-pore clogging deposition of manganese oxides within the treated cores. Aside from Struse *et al.* (2002) and Siegrist *et al.* (1999), most of the studies on permanganate oxidation have focused on advection driven systems.

Similar to permanganate field studies, the majority of the hydrogen peroxide ISCO field studies in LPM focus on delivery methods while laboratory studies focus on natural soil effects on oxidation reactions. Delivery of CHP is often difficult due to extremely fast reactions, potentially elevated temperatures, decreased pH, and off gassing. Some field applications have been able to mitigate adverse effects of the very reactive oxidation with peroxide and produce very high treatment effectiveness. A field study by Vitolins *et al.* (2003) indicated that higher contaminant destruction efficiencies for CHP were achieved in finer grained soils than more coarse material. However, Vitolins *et al.* (2003) assessed effectiveness alone and did not address the mineralogical demand or matrix changes due to oxidation. Subsurface constituents that could quench production of the hydroxyl radicals include transition element minerals, phosphates, carbonates, and catalase enzymes, and these must also be managed for effective CHP oxidation (Watts 1992).

2.7. MATHEMATICAL MODELING AND COMPUTER CODE DEVELOPMENT FOR ISCO

2.7.1. Introduction

During this SERDP CU-1290 project, efforts were made to develop mathematical relationships and computer models to aid understanding of ISCO processes, system design, and performance capabilities. This section presents a summary of background material not previously covered in this Chapter 2 and the information is derived from the M.S. Thesis of Ben Petri (2006) and Ph.D. Dissertation of Jeff Heiderscheidt (2005).

2.7.2. Mathematical Modeling

Modeling the application of ISCO to remediate DNAPL source zones requires mathematical representations of various processes including fluid flow, mass transfer and transport, and chemical reaction.

Mass transfer from one phase to another is theorized to occur in a thin stagnant film layer between the two phases, across which solute from one phase diffuses into the other (Cussler 1997). DNAPL dissolution into water is modeled in this way by Fick's first law of diffusion, where the diffusive flux across an area is proportional to the concentration gradient (Equation 2.41) (Siegrist *et al.* 2001).

$$J = -D_{aq} \frac{dC}{dx} \tag{2.41}$$

where J is the diffusive flux (kg m^{-2} s^{-1}), D is the aqueous phase diffusion coefficient (m^2 s^{-1}) specific to the compound, C is concentration (kg m^{-3}) and x (m) is distance. For DNAPL dissolution into the aqueous phase, the concentration gradient in this thin aqueous film is typically assumed to be linear across the thickness of the film. At the film boundary, the aqueous concentration of the DNAPL compound is assumed to be at the saturation value for water and the expression in Equation 2.41 simplifies to Equation 2.42.

$$J = \frac{D_{aq}}{\delta}(C_{sat} - C_{aq}) \tag{2.42}$$

where, δ is the aqueous phase film thickness (m), C_{sat} is the aqueous solubility limit of the DNAPL compound, and C_{aq} is the contaminant concentration of the bulk aqueous phase. Figure 2.3 illustrates this thin film boundary layer.

Because the film thickness is unknown, the diffusion coefficient and thickness are lumped together as a single mass transfer coefficient k_L.

$$k_L = \frac{D_{aq}}{\delta}$$

Subsurface systems are typically modeled as a series of representative elemental volumes, and as such it is desirable to derive a mass transfer expression for mass exchange on a volumetric basis, which is represented by Equation 2.43 (Saenton 2003).

$$\begin{aligned} J_v &= \frac{1}{V}\frac{dm}{dt} = \frac{A_{nw}}{V}k_L(C_{sat} - C_{aq}) \\ &= a_0 k_L (C_{sat} - C_{aq}) \\ &= k_{La}(C_{sat} - C_{aq}) \end{aligned} \tag{2.43}$$

where J_v is the rate of mass exchange (kg m^{-3} s^{-1}) in a representative volume V (m^3), m is mass (kg), A_{nw} is the area of the NAPL water interface (m^2), and $a_0 = A_{nw}/V$ is the specific surface area of the NAPL. Because no reliable method exists to quantify the area of DNAPL-water interface in the presence of porous media (m^{-1}), the terms k_L and a_0 are lumped together into the value k_{La}, which is the lumped mass transfer coefficient (s^{-1}). Because the k_{La} value is unknown, and must be derived in order to meaningfully model a DNAPL system, numerous correlations have been proposed to estimate k_{La} values based on system specific properties (e.g. Miller *et al.* 1990, Powers *et al.* 1994b, Saba and Illangasekare 2000).

Solving for k_{La} is desirable because k_{La} values can aid in modeling DNAPL dissolution and behavior during ISCO. DNAPL dissolution without oxidation in a one-dimensional flow field can be modeled using the 1-D advection-dispersion-reaction equation given by Equation 2.44 (Saenton 2003).

$$R\frac{\partial C_{aq}}{\partial t} = D\frac{\partial^2 C_{aq}}{\partial x^2} - v_x\frac{\partial C_{aq}}{\partial x} + k_{La}(C_{sat} - C_{aq}) \tag{2.44}$$

where R is the retardation factor (unitless), caused by sorption in the system, t is time (s), D is the longitudinal dispersion coefficient specific to the system (m^2 s^{-1}), v_x is the longitudinal pore velocity (m s^{-1}), and x is distance along the domain (m). If the system is at steady state, and diffusive transport is small relative to advective transport, then a simplified solution to Equation 2.44 for k_{La} can be developed, presented by Equation 2.45 (adapted from Saenton 2003).

$$k_{La,avg} = -\frac{v}{L}\left(1 - \frac{C_{sat}}{C_{ss}}\right)^{-1} \quad (2.45)$$

where $k_{La, avg}$ is the average k_{La} at steady state (s^{-1}), v is the Darcy velocity (m s^{-1}), L is the length of the DNAPL source area (m), and C_{ss} is the steady state aqueous contaminant concentration.

Second-order reaction, such as oxidation of PCE and TCE with permanganate can be added to Equation 2.44 to yield Equation 2.46.

$$R\frac{\partial C_{aq}}{\partial t} = D\frac{\partial^2 C_{aq}}{\partial x^2} - v_x\frac{\partial C_{aq}}{\partial x} + k_{La}(C_{sat} - C_{aq}) - k_2 C_{ox} C_{aq} \quad (2.46)$$

where k_2 is the second-order rate constant (m^3 $mole^{-1}$ s^{-1}) and C_{ox} is the concentration of oxidant within the unit volume (kg m^{-3}). However, because second-order reaction kinetics require an additional mass balance equation for the oxidant, and are mathematically difficult to solve, kinetics of oxidation are typically simplified by assuming pseudo first-order reaction kinetics given by Equation 2.47.

$$k_{ox} = k_2 C_{ox} \quad (2.47)$$

where k_{ox} is the pseudo first-order reaction rate coefficient (s^{-1}), and C_{ox} is the concentration of oxidant across a representative volume. Under the pseudo steady-state assumption, C_{ox} is assumed to be well in excess of the chemical reaction demands, and thus does not change significantly. In this study, there is no sorption, so R = 1 and is neglected. The above simplification yields equation 2.48.

$$\frac{\partial C_{aq}}{\partial t} = D\frac{\partial^2 C_{aq}}{\partial x^2} - v_x\frac{\partial C_{aq}}{\partial x} + k_{La}(C_{sat} - C_{aq}) - k_{ox} C_{aq} \quad (2.48)$$

Numerous analytical solutions for differential equations have been derived and reported by van Genuchten and Alves (1982) for various sets of assumptions and boundary conditions. Inverse modeling for solving Equations 2.44 and 2.48 may allow for estimation of k_{La} from experimental data.

2.7.3. Numerical Modeling of ISCO

Site conditions such as NAPL architecture, soil heterogeneity, oxidant delivery, and soil natural oxidant demand are critical factors affecting ISCO implementation. In order to implement ISCO effectively, it is important to consider the interaction of these factors under realistic conditions. Field-scale investigations provide realistic conditions, but do not allow for complete control of experimental conditions. Additionally, they generally allow only limited monitoring, preventing a full understanding of how site and source conditions are affecting the chemical oxidation. For example, even at the Canadian Forces Base Borden, Ontario, Canada (with extensive monitoring and site characterization), researchers were not able to fully characterize the DNAPL source distribution before or after oxidation (Nelson *et al.* 2000, Nelson *et al.* 2001). Large tanks designed to simulate a subsurface soil and ground water system provide an alternative and enable more complete control. Unfortunately, large-scale tank experiments are costly, time-consuming, and difficult to set up, so only a limited number can be performed. Because of these challenges posed by large-tank lab and field-scale experiments, a computer model code is needed for simulating chemical oxidation and related processes under a wide range of hydrogeologic and source conditions. Such a model would aid understanding of ISCO processes and performance as well as provide a tool for decision-making during technology selection and system design. Such a model code should incorporate the processes listed in Table 2.4.

Table 2.4. Processes important to capture during numerical modeling of ISCO.

Process	Examples relevant to ISCO applied to DNAPLs
Advection	2nd Order Contaminant Oxidation
Dispersion	Kinetic NOD oxidation
Sorption	Multiple NOD components
Diffusion	Permeability decrease due to MnO_2(s) formation
DNAPL Dissolution	Permeability Increase due to DNAPL Dissolution

To date, there have been few efforts to develop a computer model code to simulate ISCO and those efforts that have been reported were for ISCO using permanganate (Hood 2000, Hood and Thomson 2000, Zhang and Schwartz 2000). While previous efforts incorporated some of the important processes (second order oxidation, rate-limited or kinetic sorption, and Gilland-Sherwood type DNAPL dissolution mass transfer correlations), they are not in the public domain, nor are they readily available for use or modification. Additionally, although reported to incorporate kinetic NOD oxidation, published simulations have treated NOD as an instantaneous sink. In essence, this means oxidant within a model cell is not available for destroying contaminant until all NOD within that cell has been oxidized. Further, it is important to note that these previous efforts made no attempt to simulate MnO_2(s) generation or incorporate changing permeability as a result; however they each pointed to this as an area for further research. Finally, they did not attempt to capture diffusion as an important transport process in the application of ISCO using permanganate.

There are three main applications for a new numerical model code for simulating ISCO using permanganate. The first is as a tool to investigate the interaction of site and source conditions with different transport and reactive processes, providing insight into how these factors affect oxidation effectiveness. Similarly, the second is as a decision tool that can be used to assess whether ISCO using permanganate is a feasible technology for further consideration at a specific site based on site and source conditions. For example, the model code might be used to assess whether oxidation appears feasible for a site suspected of having a large mass of DNAPL present in a long thick pool where the overlying aquifer is moderately heterogeneous with a high NOD content. The third is as a design tool to assist in determining the optimal oxidant delivery scheme (what oxidant concentration at what flow rate and in what locations?) for a site based on site and source conditions. Although there is typically a large degree of uncertainty in site characterization, the new modeling code will be useful for comparing different scenarios. Further, by performing simulations using the expected upper and lower limits for site parameters, the effect of the uncertainty can be examined; this may provide insight into additional site characterization to perform.

2.8. COUPLING ISCO WITH OTHER REMEDIATION METHODS

2.8.1. Coupling ISCO with Bioremediation

2.8.1.1. Introduction. In this SERDP project, research was completed to assess the effects of ISCO on subsurface conditions that would facilitate or impede the application of engineered bioremediation or natural bioattenuation as a post-ISCO remedy. Sahl (2005) completed a literature review in support of his M.S. Thesis research and this is highlighted below and presented in a recent review paper (Sahl and Munakata-Marr 2006).

2.8.1.2. Effects of Chemical Oxidants on Subsurface Conditions and Microbial Processes. The addition of oxidants to the subsurface can have potentially dramatic effects on subsurface environmental conditions and microbial populations and processes. For example, during ISCO using permanganate, the generation of free protons may result in a pH drop as the permanganate ion reacts with the contaminant as well as natural organic matter. Catalyzed hydrogen peroxide is often introduced at acidic pH (Watts and Dilly 1996) to promote solubility of the reaction catalyst (typically iron Fe^{2+}) when a chelator for the catalyst (Pignatello and Baehr 1994) is not employed. These pH effects are important because low pH can significantly reduce microbial growth rates, possibly altering the diversity of the microbes that repopulate sites of oxidant application (Landa *et al.* 1994).

The E_h of a system can also change following the addition of a chemical oxidant. Redox conditions in the subsurface have been reported to be among the most important factors influencing natural attenuation processes via bioremediation, especially reductive processes (Ter Meer *et al.* 2001). For example, at one site the redox potential increased from 100 mV to 800 mV following permanganate application (Klens *et al.* 2001). Additionally, the autodecomposition of CHP can result in the generation of oxygen which could disrupt anaerobic redox conditions. Changes in the availability of terminal electron acceptors could have a serious impact on the composition and diversity of subsurface microbial communities following oxidant application.

ISCO has also been shown to enhance microbial activity by increasing substrate availability or reactivity. Pre-oxidation of recalcitrant compounds using CHP, $KMnO_4$, and O_3 to enhance biodegradation by oxidizing complex organic molecules into bio-available substrates has been used for years in the treatment of wastewater and contaminated soils (Kao and Wu 2000, Larking *et al.* 1999, Lee and Hosomi 2001, Martens and Frankenberger 1995, Nadarajah *et al.* 2002, Nam and Kukor 2000, Nam *et al.* 2001, Piskonen and Itavaara 2004, Zeng *et al.* 2000). A comprehensive literature review of pre-oxidation processes has been compiled (Scott and Ollis 1995). Of the forty-three studies in the literature review and ten additional studies reviewed concerning pre-oxidation, all of them showed an increase in contaminant treatment effectiveness when implementing pre-oxidation, although 15% of these studies also showed adverse affects from oxidant pre-treatment when experimental parameters were modified. Most of these studies involved the sequential application of chemical and biological processes to enhance biodegradation of recalcitrant compounds with limited exposure of the cultures to direct oxidation.

In field applications of ISCO, treating contaminated soil with a chemical oxidant may produce substrates that are more biodegradable by direct oxidation of contaminants (Huang *et al.* 2002, Yan and Schwartz 1999) or by oxidation of humic and fulvic acids found in naturally occurring organic matter (Almendros *et al.* 1989, Griffith and Schnitzer 1975, Ortiz De Serra and Schnitzer 1973). Many of these oxidation by-products have been found to be easily biodegradable in anaerobic wastewater systems (Dinsdale *et al.* 2000) as well as in marine and freshwater environments (Kieber *et al.* 1989, Moran and Zepp 1997, Tranvik and Bertilisson 2001), and could potentially be utilized in terrestrial systems. The bioremediation activity of microbes living down-gradient from oxidant application and reaction may be enhanced due to the presence of bioavailable oxidation by-products carried by up-gradient groundwater.

2.8.1.3. Direct Effects of Oxidants on Microbes. The direct effects of chemical oxidants on microbes have been explored at the cellular level. Potassium permanganate has been shown to be effective at oxidizing pyrimidine bases in cellular DNA (Bui and Cotton 2002, Freeman *et al.* 1975, Rubin and Schmid 1980), resulting in decomposition of the DNA structure. The hydroxyl radical generated in Fenton's reactions has been shown to contribute to mutagenesis, cell death (Imlay and Linn 1988), DNA destruction (Imlay *et al.* 1988), protein and lipid membrane damage (Izawa *et al.* 1996) and has even been shown to be toxic to peroxide-acclimated microbes (Büyüksönmez *et al.* 1998). However, many microbes have developed mechanisms to defend against the toxic effects of some oxidants. In times of stress, microbes have been shown to produce antioxidative enzymes such as catalase and superoxide dismutase, defenses against reactive compounds such as H_2O_2 and OH• (Fridovich 1978, Izawa *et al.* 1996). Schlegel found that catalase protected one microbial culture from a high concentration

of H_2O_2 [34 g/L], while a lower H_2O_2 concentration [0.34 g/L] completely inhibited a culture lacking catalase expression (Schlegel 1977). Many aerobic and facultative anaerobic microbes found in soil and groundwater communities are catalase-positive (Pardieck *et al.* 1992), potentially protecting them from exposure to CHP oxidation.

2.8.1.4. ISCO Effects on Subsurface Bioprocesses. Few studies have analyzed the feasibility of coupling CHP and aerobic bioremediation processes in the treatment of contaminated soil. Chemical and biological processes have been shown to coexist in laboratory studies in the aerobic mineralization of PCE with no observable adverse effects of oxidant addition to microbial biomass or bioremediation ability (Howsawkeng *et al.* 2001). Stokley *et al.* (1997) reported a rebound of cell numbers following ISCO using medium concentrations of CHP, while a high concentration resulted in cell numbers that were too small to measure. The authors did not report the toxic CHP concentration, whether a rebound would be possible once oxidation processes were concluded, or whether catalase was being expressed by the culture. Others have observed a decline in cell numbers at H_2O_2 concentrations greater than 77 mg/L, indicating a possible negative effect of CHP on microbial biomass (Büyüksönmez *et al.* 1999).

Other work has found a potentially synergistic relationship between CHP oxidation and microbial biomass. For example, Allen and Reardon (2000) observed an initial decrease in microbial populations following CHP oxidation in a laboratory study, but a rebound was observed with population values surpassing the original microbial biomass after two weeks. Miller *et al.* (1996) reported a decrease in microbial diversity following CHP oxidation with an increase in microbes capable of bioremediation, suggesting that ISCO can be effectively coupled with in situ bioremediation (ISB).

Studies have also been conducted to investigate the effects of CHP oxidation on subsurface microbial bioremediation in field experiments. Kastner *et al.* (2000) examined the effect of CHP oxidation on aerobic trichloroethene biodegradation rates at a field site contaminated with PCE and TCE. The authors found that low pH resulting from CHP application appeared to inhibit microbial TCE degradation in some sampling wells, but that viable aerobic, co-metabolic processes existed post-treatment in wells with a higher pH. Their results suggest that following oxidation, the slow increase in groundwater pH due to inflow of up-gradient groundwater should allow for the re-establishment of microbial populations.

The effect of permanganate oxidation on microbial activity has primarily been explored in field experiments, but recent laboratory studies have been conducted to better understand the effects of permanganate oxidation on bioremediation processes in anaerobic systems. Hrapovic *et al.* (2005) investigated the effect of permanganate oxidation on reductive dechlorination processes in laboratory column studies. After feeding columns containing field soil undergoing natural attenuation unamended distilled water, the authors observed no dechlorination activity following potassium permanganate oxidation. Subsequent bioaugmentation of some columns with a culture capable of reductive dechlorination followed by ethanol amendment resulted in an eventual resumption of bioremediation activity. One column that was not bioaugmented eventually did show by-products of reductive dechlorination processes, but in low concentrations. The pre-oxidation level of dechlorination activity was not determined in this column and therefore the relative impact of oxidation on the dechlorination activity of the original culture cannot be established.

Field studies have also been conducted to understand the effects of permanganate oxidation on subsurface microbial populations. Many of the field studies conducted have focused on microbial biomass following oxidation and not on post-oxidation bioremediation activity. Klens *et al.* (2001) observed a rebound in subsurface microbial populations following oxidation using a 0.7 percent solution of $KMnO_4$. Six months following oxidation, results from standard plate count analysis showed viable populations of anaerobic heterotrophs, nitrate reducers, and sulfate reducers. The redox potential changed considerably following the addition of permanganate, but initial conditions were re-established six months post-treatment. Hazen *et al.* (2000) used a variety of molecular techniques to analyze microbial

activity and biomass following permanganate application at the Cape Canaveral Air Station in Florida. Their results indicated that both aerobic and anaerobic microbial communities were adversely affected one month post-treatment. However, six months post-oxidation, a strong rebound of viable aerobic and anaerobic microbes was observed. Gardner *et al.* (1996) investigated the effect of permanganate oxidation on microbial biomass as measured by plate counts for aerobic microbes and growth in an anaerobic media for anaerobic microbes. They observed no adverse impacts of permanganate oxidation on microbial biomass immediately following oxidant application. Azadpour-Keeley *et al.* (2004) found that permanganate application stimulated microbial abundance based on an observed increase in microbial biomass. The authors suggest that sulfate-reducing bacteria were stimulated by the oxidation of lignin and humics, releasing bio-available carbon for microbial metabolism. The authors did not, however, determine how this stimulation in biomass may translate into rates of contaminant bioremediation. Macbeth *et al.* (2005) investigated the effect of ISCO using potassium permanganate on microbial biomass and diversity in a PCE-contaminated aquifer. The authors determined that injecting high concentrations of permanganate resulted in decreased microbial biomass as well as diversity, but a rebound of the microbial community occurred following oxidation. Although all of these studies showed a rebound of microbial biomass following chemical oxidation, none of them specifically examined the goal of coupling permanganate oxidation with bioremediation processes.

An additional field study has shown a positive interaction between chemical oxidation and microbial remediation activity. Droste *et al.* (2002) implemented a technology utilizing sodium persulfate and permanganate at a field site contaminated primarily with TCE. They observed enhanced reductive dechlorination of TCE in and down-gradient of the injection area during post-injection monitoring at the site. They concluded that the persulfate stimulated sulfate-reducing bacteria, enhancing post-oxidation biodegradation of TCE at this site.

2.8.1.5. Feasibility of Coupling ISCO with Bioremediation. All experiments compiled in this literature review related to the effects of ISCO on microbiological processes are summarized in Table 2.5. Under certain conditions, every study either showed a rebound of biological biomass/activity or no observable adverse effects (NOE) following ISCO. However, two studies showed a rebound of cell numbers (Stokley *et al.* 1997) or NOE to mineralization rates (Büyüksönmez *et al.* 1999) after treatment with a lower concentration of CHP, while a higher concentration was shown to be toxic to biological processes.

The reported rebound of biomass/bioremediation presented in Table 2.5 suggests that biological processes may be adversely affected in the short-term, but a rebound of biological activity can be expected following ISCO. A rebound of microbial activity or biomass following exposure to a chemical oxidant may be attributed to attenuated concentrations of contaminants (Chapelle *et al.* 2005), repopulation of oxidized areas by up-gradient groundwater, the generation of bio-available substrates (Azadpour-Keeley *et al.* 2004), or a rebound of indigenous microbes once conditions revert to pre-oxidation conditions (Klens *et al.* 2001).

In some studies, enhanced biological growth and/or bioremediation activity was observed following oxidant application (Allen and Reardon 2000, Azadpour-Keeley *et al.* 2004, Droste *et al.* 2002, Kastner *et al.* 2000). Although increases in microbial biomass following oxidation have been attributed to the availability of bioavailable oxidation by-products (Azadpour-Keeley *et al.* 2004, Scott and Ollis 1995), no study has yet conclusively determined the mechanism for increased post-oxidation microbial biomass. Additionally, anecdotal evidence suggests that by-products of permanganate-oxidized porous media can enhance rates of contaminant bioremediation (Sahl 2005), suggesting that the generation of bioavailable substrates may enhance the efficiency of coupling ISCO with ISB.

A decrease in microbial community diversity has been observed following oxidant application (Macbeth *et al.* 2005, Miller *et al.* 1996) and there is evidence that selection for cultures capable of bioremediation may occur following ISCO (Miller *et al.* 1996). A decrease in microbial diversity has

been observed in the presence of a strong unidirectional factor (e.g. chemical oxidation) which can cause microbial specialization and subsequent domination by relatively few species (Atlas and Bartha 1987). If selection for bioremediation processes following oxidation does occur, competition for substrates may be diminished, increasing the effectiveness of bioremediation processes. For example, the reductive dechlorination of chloroethenes by dehalorespiring organisms can occur with hydrogen as the electron donor. In a mixed culture, other microbes (e.g. methanogens) also use hydrogen as an electron donor, creating competition for a limited resource. Evidence suggests that methanogenic organisms may be more sensitive to chemical oxidation than other anaerobic organisms (Klens *et al.* 2001), potentially reducing community diversity as well as substrate competition within mixed cultures.

2.8.2. Coupling of ISCO with Surfactant Enhanced Aquifer Restoration

2.8.2.1. Introduction. Within the last decade, surfactant-enhanced aquifer remediation (SEAR), has been developed for in situ remediation of DNAPL contamination in the subsurface. Numerous laboratory and field applications of SEAR have been directed at aggressive DNAPL remediation (e.g., Palmer and Fish 1992, Abriola *et al.* 1993, Annable *et al.* 1998, Pennell *et al.* 1993 1994, 1996, Shiau *et al.* 1994, 1996, 2000, Sabatini *et al.* 1995, 1997, 1998, 2000, Pope *et al.* 1995). Despite these efforts, complete DNAPL removal has proven to be difficult using SEAR and high concentrations of contaminants remain (DNAPLs in the residual, dissolved and sorbed phases (U.S. EPA 2003). An emerging remediation strategy involves combining compatible technologies in a concurrent or sequential manner to increase the overall treatment effectiveness and achieve performance objections. Given the functional attributes of SEAR and ISCO as highlighted below it is reasonable that with proper engineering and design, coupling of these two technologies may be a effective strategy for remediation of DNAPL-contaminated sites. In this SERDP project, research was completed to assess the potential for coupling ISCO with SEAR. Dugan (2006) completed a literature review in support of her Ph.D. research and this is presented in the following sections.

2.8.2.2. Surfactant Enhanced Aquifer Remediation. SEAR involves flushing a region of contaminated groundwater with a surfactant solution. Surfactants are surface-active agents that can be particularly useful for DNAPL remediation because they alter organic-water interfaces. They are amphilic compounds possessing both hydrophobic (non-polar) and hydrophilic (polar) functional groups. The hydrophilic "head" often includes an anion or cation such as sodium, or chloride. The hydrophobic "tail" is composed of a long hydrocarbon chain. When surfactant concentrations exceed the critical micelle concentration (CMC) the surfactant molecules (monomers) self-aggregate into spherical structures known as micelles. Typically micelles contain 50 to 100 surfactant monomers. Below the CMC there is minimal effect between the organic-water interface.

In a micellar structure, the hydrophobic tails cluster together forming a non-polar cavity, while the hydrophilic heads remain in the water. The polar exterior makes micelles highly soluble in water, while the non-polar interior provides a hydrophobic sink for organic compounds, thereby increasing the apparent solubility of the organic contaminant. When properly designed, SEAR can promote DNAPL solubilization and/or mobilization by incorporating NAPL molecules into micellar structures in the aqueous phase, or by reducing the interfacial tension (IFT) between the NAPL and the aqueous phase (Fountain *et al.* 1991 and 1996, Pope *et al.* 1994). Cosolvents or salinity modifications are often required to bring about significant lowering of IFT. Prior to application of SEAR in field operations, surfactant phase behavior experiments are conducted to identify adverse phase behavior such as gel formation or crystalline precipitation that can result in pore plugging (Dwarakanath *et al.* 1998). Surfactant phase behavior is commonly represented by volumetric fraction and ternary diagrams. When NAPL constituents are solubilized at the center of a micelle, a transparent solution termed a Winsor Type I system is formed. The increase in the "apparent" aqueous solubility of organic compounds at supra-CMC surfactant concentrations is referred to as micellar solubilization, where as the surfactant concentration increases, additional micelles are formed with resulting increases in contaminant solubility.

Table 2.5. Summary of research concerning the effects of ISCO on subsurface bioprocesses (Sahl and Munakata-Marr 2006)

Study	Oxidant	Oxidant Concentration	Experiment Type	COC	Culture Type	Rebound?	Time to Rebound	Type of Rebound
Miller *et al.* 1996	CHP	30000-72000 mg/L	lab	pendimethalin	aerobic	yes	~60 hours	increased biomass, decreased diversity
Stokley *et al.* 1997	CHP	NR	lab	PAHs	NR	yes	1 week	slight decrease in bacteria biomass following oxidation
Büyüksönmez *et al.* 1999	CHP	77-200 mg/L	lab	PCE	aerobic	NOE	NA	mineralization decreased when $[H_2O_2]$>77 mg/L
Kastner *et al.* 2000	CHP	50000 mg/L	field	TCE	aerobic	yes	10 months	Rebound in microbial biomass/activity
Allen and Reardon 2000	CHP	10000-20000 mg/L	lab	PAHs, PCP	aerobic	yes	6 days	Rebound of cell concentrations
Nam *et al.* 2001	CHP	300000 mg/L	lab	PAHs	aerobic	NOE	NA	successful coupling observed
Gardener *et al.* 1996	$KMnO_4$	40000 mg/L	field	TCE	anaerobic, aerobic	NOE	NA	no observed negative effects to microbial activity
Hazen *et al.* 2000	$KMnO_4$	14000-20000 mg/L	field	TCE	anaerobic, aerobic	yes	6 months	rebound of aerobic, anaerobic biomass
Klens *et al.* 2001	$KMnO_4$	7000 mg/L	field	TCE	anaerobic, aerobic	yes	6 months	rebound of aerobic, anaerobic biomass
Droste *et al.* 2002	$KMnO_4$ $Na_2S_2O_8$	5000-10000 mg/L 2000 mg/L	field	TCE	anaerobic	yes	immediate	enhanced reductive dechlorination
Azadpour-Keeley *et al.* 2004	$KMnO_4$	NR	field	TCE	anaerobic, aerobic	yes	immediate	short-term increased biomass
Hrapovic *et al.* 2005	$KMnO_4$	2500 mg/L	lab	TCE	anaerobic	yes	6-7 months	slight rebound of TCE dechlorination
Macbeth *et al.* 2005	$KMnO_4$	NR	field	PCE	anaerobic	yes	1 year	increased biomass, decreased diversity

acroynyms

COC	contaminant(s) of concern
NR	not reported
NOE	no observed effect
NA	not applicable

PCE	tetrachloroethene
TCE	trichloroethene
PAHs	polycyclic aromatic hydrocarbons
PCP	pentachlorophenol

Winsor Type II surfactants are oil soluble and will form reverse micelles where the surfactant partitions into the oil phase. Reverse micelles have hydrophilic interiors and hydrophobic exteriors; the resulting phenomenon is analogous to dispersed water drops in the oil phase and an undesirable system for NAPL remediation. Surfactant systems that are intermediate between Winsor Type I systems and Winsor Type II systems result in a third phase with properties (e.g., density) between oil and water. This third phase is referred to as a middle phase microemulsion (Winsor Type III system) and is known to coincide with ultra-low interfacial tensions. In these systems mobilization is the dominant NAPL removal mechanism with bulk extraction of organics from residual saturation.

Microemulsions are a special class of a Winsor Type I system with NAPL-in-water droplets, which form spontaneously without mixing (i.e., thermodynamically stable), and are referred to as single-phase micro-emulsions. These microemulsions consist of organic liquid droplets of 0.01 to 0.1 µm in diameter, which are optically transparent, and low viscosity. A properly designed microemulsion system is transported through porous media by miscible displacement. This is in contrast to Winsor Type III middle-phase microemulsions, which tend to form cloudy solutions and depend on mobilization to transport the NAPL phase as an immiscible displacement process. Shiau *et al.* (1994) demonstrated that middle-phase micro emulsions could accommodate organic concentrations several orders of magnitude greater than surfactant systems geared toward solubilization; however, middle-phase micro emulsion systems may also result in extremely low IFTs (e.g., 10^{-3} to 10^{-4} dyn/cm). Field results indicate that mobilization has the potential to be significantly more effective than solubilization (e.g., Falta *et al.* 1999, Annable *et al.* 1998); however, proper engineering and design must be taken into account to mitigate the risk of uncontrolled downward DNAPL vertical migration into previously uncontaminated areas (Pankow and Cherry 1996).

Cosolvents are water-miscible alcohols (e.g., tert-butanol, methanol, isopropanol) that are often combined with a surfactant flush to enhance surfactant performance. The addition of a cosolvent to the surfactant solution will produce stable microemulsions. Cosolvents are similar to surfactants in that they can alter the properties of organic-water interfaces bringing about both an increase in aqueous DNAPL solubility and lowering of DNAPL-water IFT.

Table 2.6 below provides examples of recent field applications of cosolvent and surfactant/cosolvent flushing and provides information regarding the flushing solution and dominant NAPL removal mechanism, the approximate number of pore volumes flushed through the NAPL test area, as well as the overall % mass removal.

2.8.2.3. Coupling ISCO with SEAR. The coupling of in situ flushing remedial agents may be accomplished in two ways: (1) co-injection of remedial fluids, or (2) sequential application of SEAR followed by ISCO. With appropriate design and engineering both SEAR and ISCO alone are capable of achieving high remediation efficiencies at some sites. Table 2.7 provides examples of laboratory, pilot, and full-scale operations, where SEAR, ISCO, or coupling of SEAR with ISCO was implemented for remediation of COCs.

To date there have not been any studies reported in the literature involving the co-injection of surfactant with oxidant. However, there are several recent laboratory and field studies involving sequential application of SEAR followed by ISCO (e.g., Conrad *et al.* 2002, Shiau 2003). Conrad *et al.* (2002) conducted a 2-D tank experiment for removal of TCE DNAPL with a sequential surfactant/permanganate flush using the surfactant polyoxyethylene (20) sorbitan monooleate (Tween 80). In this study the authors reveal difficulties with significant loss of permeability due to precipitation of MnO_2 solids. Results from batch screening experiments conducted as part of these studies indicated that for concentrations ranging from 1-5-wt% Tween 80 was extremely incompatible when coupled with permanganate due to excessive nonproductive oxidant consumption and significant generation of MnO_2 solids. Shiau (2003) conducted column and pilot-scale studies using sequential surfactant and oxidant

flushing for NAPL remediation. Results from the sequential application of surfactants and Fenton's reagent indicate a 99.6% and 99% removal of TPHs in the column and field studies respectively, with a 99.9% removal of TCE in column tests after coupling surfactant flushing with potassium permanganate.

The question as to whether permanganate is capable of oxidizing contaminant while the contaminant has partitioned inside the hydrophobic cavity of the micelle was recently evaluated in batch studies by looking at reaction rates of MnO_4^- degradation of TCE DNAPL in the presence and absence of surfactant (Li 2004). Li (2004) found that in the absence of surfactant, the observed pseudo-first-order rate constant (k_{obs}) was 0.08–0.19 min^{-1} and the half-life was 4–9 min for MnO_4^-. When the surfactant concentration was less than the CMC, the k_{obs} values increased to 0.42–0.46 min^{-1} and the half-life was reduced to 1.5–1.7 min for MnO_4^-. As the surfactant concentration was increased (i.e., above the CMC), the k_{obs} values increased to 0.56–0.58 min^{-1} and the half-life was reduced to 1.2–1.3 min.

PCE DNAPL dissolution and desorption is generally slow, in view of the low aqueous solubility of most chlorinated hydrocarbons, with published PCE aqueous solubility values ranging from 150-to-250 mg/L (Broholm *et al.* 1992, Montgomery and Welkom 1989, Ladaa *et al*. 2001, Schwarzenbach 2001). Therefore, coupling treatments that enhance mass transfer (i.e., SEAR) and destroy COCs in situ (i.e., ISCO), presents an appealing remedial approach for DNAPL-contaminated sites.

Table 2.6. Examples of field experiences with use of SEAR to remediate NAPL sites (Dugan 2006).

Site	Flushing solution	Removal mechanism	P.V.s	COC	% Mass removal	Reference
Dover AFB, DE	Surfactant/cosolvent/electrolyte 3.3% AMA-80I + 3.3% IPA+ 0.4% $CaCl_2$	Solubilization, mobilization	10	PCE	68	Childs *et al.* 2006
Bachman Road, MI	Surfactant 1%Tween 80	Solubilization	1.5	PCE	>94%	Abriola *et al.* 2005
Sages Dry cleaners, FL	Cosolvent 95% ethanol + 5% water	Solubilization, mobilization	2	PCE	62	Jawitz *et al.* 2000
Camp Lejeune, NC	Surfactant/cosolvent/electrolyte 4% AMA-80I + IPA + NaCl	Solubilization, mobilization	5	PCE	>99	INTERA 1998
Hill AFB, UT	Cosolvent 80% tert-butanol, 15% n-hexanol	Mobilization	4	PCE Jet Fuel		Falta *et al.* 1999
Hill AFB, UT	Surfactant/cosolvent Winsor Type I surfactant/cosolvent	Solubilization	10	LNAPL Mix	90-95	Jawitz *et al.* 1998
Thouin Sand Pit, Quebec	Surfactant/cosolvent/polymer Hostapur SAS 60+n-butanol	Solubilization	1	Solvent DNAPL Mix	~86	Martel *et al.* 1998
Hill AFB, UT	Cosolvent 70% ethanol, 12% pentanol, 28% water	Solubilization	9	PCE Jet Fuel	75	Rao *et al.* 1997; Sillan *et al.* 1998
Borden, ON, Canada	Surfactant 2% solution of nonylphenol ethyoxilate (NPEO) and NPEO phosphate	Solubilization	14	PCE	80	Fountain *et al.* 1992

Table 2.7. Examples of recent field applications of SEAR and ISCO.

Remedial technology	Location, date, flushing agent	Pilot/full-scale or lab study; Media	Contaminant	Performance results	Volume treated/ cost
SEAR	Hill AFB OU2[a], Ogden, UT; 8-wt% AMA-80I + 4%- wt% Isopropanol + 0.12-wt% NaCl	Pilot/ground water	PCE	98% reduction	352 m^3 $1,200,000
	Bachman Road Site[b]; Oscada, MI; 6-wt% Tween 80	Full /ground water	PCE	Aqueous VOC 4000 μg/L ⇒650 μg/L	212 m^3 $850,000
	Alameda Naval Air Station[a], Alameda, CA; 2-wt% AMA-80I + 5-wt% Dowfax 8390 + 3-wt% NaCl	Pilot/ground water	Solvent mixture	97% reduction	198 m^3 $ 658,000
ISCO	LC 34 Cape Canaveral[b], FL; 0.1–3.0% $KMnO_4$	Pilot/ground water/soil	TCE	Ground water 1,100 mg/L ⇒ 89-95% reduction Soil 82% ↓	3,186 m^3 $1,013,947
	Portsmouth Gaseous Diffusion Plant[b], Piketon, OH 1.5 – 2.5% $KMnO_4$	Full /ground water	TCE	8000 mg/L ⇒ below detection 54 – 302 mg/kg ⇒ below detection	3,370 m^3 $562,000
	Canadian Forces Base Borden[c], Ontario, CN 1996; 8 g/L $KMnO_4$	Pilot/ground water	TCE PCE	1200 mg/kg ⇒ 99% reduction 6700 mg/kg ⇒ 99% reduction	10,000 m^3 $45,000
SEAR+ ISCO coupling	SEAR then $KMnO_4$[d]	Lab with site ground water and soil	TCE	99.6% reduction	NA

References: [a]ITRC (2003); [b]GeoSyntec Consultants (2004); [c]USEPA (1998); [d]Shiau, B-J. (2003)

2.9. PARTITIONING TRACERS FOR PERFORMANCE ASSESSMENT AT ISCO SITES

2.9.1. Introduction

This section describes background and previous research findings concerning the use of partitioning tracers for characterizing the volume and spatial distribution of DNAPL in the subsurface and the viability of using partitioning tracers for performance assessment at DNAPL sites treated using ISCO. The information provided below was prepared in support of the Ph.D. dissertation of Pamela Dugan (2006).

2.9.2. Application of Partitioning Tracers at ISCO Sites

2.9.2.1. Approaches to Characterization and Assessment at DNAPL Sites. Nonaqueous phase liquid (NAPL) contamination has proven to be an extremely recalcitrant and enduring form of subsurface contamination. Detecting and quantifying the volume and spatial distribution of NAPL contamination is difficult to accomplish with traditional point-sampling methods (e.g., soil coring, ground water sampling,

and soil gas surveys). These methods are labor and cost intensive and sample a relatively small volume of the subsurface. Porous media heterogeneities and spatial variability in the NAPL distribution limit the efficacy of these characterization techniques in that they can only provide data at discrete points making accurate characterization of large systems problematic. With the representative elementary volume (REV) for NAPL in soil ranging from 10^{-2}-10^{4} cm^3 (Mayer and Miller 1992), and the volume of a typical soil sample between 30-10^{2} cm^3, Meinardus *et al.* (2002) estimated that soils suspected of containing NAPLs must be sampled on the order of every 10 cm vertically and 100 cm aerially to ensure accurate representative results. Although concentration data are useful, the inherent small-scale variations in contaminant concentrations within a NAPL source zone suggests there are serious deficiencies to using core-scale data (with the requisite interpolation between sampling points) as the sole metric for site-scale characterization and post-remediation performance assessment. There are numerous metrics for measuring performance; however, each has certain advantages and limitations. To compensate for the limitations and uncertainties associated with relying upon a single measure of success, if possible several lines of evidence should be used.

2.9.2.2. Overview of the Partitioning Interwell Tracer Test. The partitioning interwell tracer test (PITT) is a method of site characterization that allows for the direct measurement of the amount and spatial distribution of NAPL over a relatively large volume of the subsurface. PITTs, whether conducted in the saturated or unsaturated zone, may be used to (1) detect and estimate the initial volume of NAPL for preliminary site characterization; and (2) as a performance assessment tool after in situ NAPL remediation treatments have been implemented. The PITT involves the pulse injection (and subsequent extraction) of a suite of nonpartitioning and partitioning tracers at one or more locations in a NAPL-contaminated zone. The nonpartitioning (i.e., conservative) tracers travel in the mobile phase. In saturated-zone and unsaturated-zone PITTs, the mobile phases are water and air respectively. Under ideal conditions, the nonpartitioning tracer travels through the subsurface without adsorbing to soil particles or partitioning into NAPL, therefore its concentration signal at the recovery well should be indicative of the dispersion caused by the porous media. The partitioning tracers (at equilibrium) reversibly partition to varying degrees between the mobile phase and immobile NAPL-phase resulting in delayed arrival of the tracer signals at the extraction well. A properly engineered PITT can be particularly beneficial for pre-remedial design and post-remediation assessment by permitting direct quantification of NAPL volume, essentially eliminating data interpolation errors. Use of the PITT for NAPL site characterization at the field scale, in combination with soil and ground water quality sampling, has the potential advantage of representing subsurface NAPL volume at both the micro- and macro- scale.

Throughout the last decade, the PITT has been conducted in over 40 field studies to estimate the average pore space NAPL saturation (S_N) in saturated conditions (e.g., Pope *et al.* 1994, Jin *et al.* 1995, Falta *et al.* 1999, Rao *et al.* 1997, Annable *et al.* 1998a,b, Jawitz *et al.* 2003, Nelson and Brusseau 1999, Young et. al 1999, Cain *et al.* 2000, Meinardus *et al.* 2002, and Divine *et al.* 2004). While PITTs have most commonly been applied in the saturated zone, the general technique has also been used with gas tracers for NAPL detection and volume estimation in the vadose zone (Simon *et al.* 1998, Deeds *et al.* 1999a,b, Mariner *et al.* 1999, Brusseau *et al.* 2003), and has been proposed for simultaneously estimating NAPL and trapped air saturation below the water table (e.g., Divine *et al.* 2003).

Successful and cost-effective implementation of the PITT requires careful consideration of a number of design components, including; quantitative and qualitative hydrogeologic interpretation, tracer selection and target tracer sweep zone dimensions, numerical flow and transport modeling, uncertainty analysis, batch and bench-scale studies, injection/extraction system hydraulics, test duration, sampling frequencies, and treatment of extraction fluids. Furthermore, these criteria must also meet practical constraints, including project cost and time budgets. In that S_N values are unknown prior to conducting the PITT, it is generally beneficial for the tracer suite to include tracers that provide a relatively large range of NAPL-water-or air partition coefficients, (K_{NW}), particularly if the preliminary S_N estimate is highly uncertain. Choosing tracers with higher K_{NW} values ensures sufficient separation between breakthrough

curves (BTCs) while tracers with smaller K_{NW} values allow tests to be completed in a reasonable time period (Jin *et al.* 1995, Jawitz *et al.* 2000). As a general rule, tracers with larger K_{NW} values are used after remediation when the NAPL saturation is reduced. Dwarakanath *et al.* (1999) indicates that when a retardation factor (R_f) is less than 1.2, the error in the saturation estimate is high and is largely dependent in the error in the retardation factor. Alternatively, for higher values of retardation factors, the error in the saturation estimate is largely dependent on the partition coefficient while using tracers with relatively higher retardation coefficients may result in PITTs of undesirably long duration. To minimize the error in the saturation estimates, and maintain desirable test durations, a target range of retardation factors is: $1.2 < R_f < 4$ (Dwarakanath *et al.* 1999).

A particularly important design component is the selection of the tracer suite. An ideal partitioning tracer should possess the following properties: (1) non-hazardous and non-toxic, (2) reasonable cost and availability, (3) partition into NAPL in a known and predictable manner, (4) low volatility, (5) somewhat hydrophobic yet water soluble, (6) recalcitrant to degradation, (7) exhibit minimal sorption to native aquifer materials, (8), offer good analytical detection limits, (9) partition coefficients in desired range for NAPL conditions anticipated and, (10) insensitive to small variations in NAPL composition (Pope *et al.* 1994, Young *et al.* 1999).

NAPL partitioning tracers that have been utilized in either the lab or field under saturated or unsaturated zone conditions include; aliphatic alcohols (e.g., 2,3-dimethyl-2-butanol, Jin *et al.* 1995), noble gases (e.g., helium, Divine *et al.* 2004), synthetic inert gases (e.g., sulfur hexafluoride, Wilson and Mackay 1993), perfluorocarbons (e.g., perfluoro-1,3-dimethylcyclohexane, Deeds 2000), Rn^{222} (e.g., Hunkeler *et al.* 1997), short half-life radioisotopes (e.g., 7-bromo-1-heptanol, Jayanti 2000), fluorescent dyes (e.g., rhodamine WT (Ghanem 2003)), and interfacial tracers (i.e., surface-active agents, sodium dodecylbenzene sulfonate (Saripelli *et al.* 1997, Annable *et al.* 1998b)).

To accurately determine the initial and final NAPL volume using data obtained from a PITT, it is necessary that the physical and chemical properties of the tracers remain unaffected by the remedial activity. In saturated zone PITTs, alcohols have traditionally been used as the partitioning tracer; however, given alcohol's susceptibility to oxidation by permanganate (e.g., Carey 2003, Stewart 1964) due to the reactivity of the hydroxyl group, and the possibility of residual oxidant in the source zone following treatment, they are potentially unsuitable for use during the post-PITT. For example, at a site where 2-wt% $KMnO_4$ was implemented for NAPL remediation, residual permanganate (i.e., 93 mg/L) was detected more than three years after the pilot test had concluded (AIMTech 2001). In addition to the potential for tracer mass loss due to oxidation, tracer partitioning could be inhibited by ISCO reaction products (e.g., the presence of entrapped CO_2 gas or MnO_2(s) deposits). Both of these factors have potential to influence partitioning tracer transport, which could lead to inaccurate estimates of the post-remediation S_N and performance assessment after ISCO.

2.9.2.3. Theoretical Basis for Interpreting Partitioning Tracer Behavior at DNAPL Sites. Jin *et al.* (1995) present in detail the theoretical and experimental basis for the use of partitioning tracers and method of moments for quantification of NAPL saturation and volume using the 0^{th}, 1^{st}, and 2^{nd} moments of the tracer BTC. The 0^{th} moment, M_0, is the integral of the breakthrough curve (BTC), and provides the total recovered mass of tracer:

$$M_0 = m = \int C dt = \sum_{k=0}^{n} \frac{C_k + C_{k-1}}{2} \times \left(t_k - t_{k-1}\right) \tag{2.49}$$

where m is the mass of tracer, C_k is the aqueous concentration of tracer at time k, and t is time. The 1^{st} moment (M_1) provides the mean residence time t_r of the center of mass of the tracer slug, and is used to estimate the residual NAPL saturation, tracer swept pore volume, and the NAPL volume:

$$M_1 = t_r = \int Ctdt = \sum_{k=0}^{n} \frac{C_k + C_{k-1}}{2} \times \left(t_k - t_{k-1}\right) \times \left(\frac{t_k + t_{k-1}}{2}\right) \tag{2.50}$$

The 2nd temporal moment (M_2) is used to calculate dispersivity when the tracer test is conducted without the presence of NAPL:

$$M_2 = \int Ct^2 dt = \sum_{k=0}^{n} \frac{C_k + C_{k-1}}{2} \times \left(t_k - t_{k-1}\right) \times \left(\frac{t_k + t_{k-1}}{2}\right)^2 \tag{2.51}$$

PITT theory is based on the well-characterized tracer partitioning relationships between the NAPL and aqueous (or gaseous) phases as described by the laboratory-measured NAPL-water partition coefficient:

$$K_{NW} = \frac{C_N}{C_W} \tag{2.52}$$

where C_N and C_W are the equilibrium tracer concentrations in the immobile NAPL-phase and mobile fluid phase. This relation requires the assumption that tracer partitioning follows a linear, reversible isotherm. The retardation factor (R_f) is determined from PITT tracer travel times and defined as the ratio of the mean arrival times (i.e., first normalized temporal moments) of the partitioning tracer ($\overline{t_p}$) and the nonpartitioning tracer ($\overline{t_{np}}$), both corrected for the solute pulse injection duration ($\overline{t_0}$):

$$R_f = \frac{\overline{t_p - \frac{t_0}{2}}}{t_{np} - \frac{t_0}{2}} \tag{2.53}$$

This relationship assumes sorption onto aquifer materials is insignificant. The average NAPL saturation is a function of K_{NW} and R_f as given by Equation 2.54 (Pope *et al.* 1994a, Jin *et al.* 1995).

$$S_N = \frac{R_f - 1}{R_f + K_{NW} - 1} \tag{2.54}$$

Data collected from fully screened extraction wells enables calculation of the S_N value that represents an average of the fraction of pore space occupied by the NAPL over the entire flow domain swept by the tracers. Use of Equation 2.54 requires a nonpartitioning tracer; however, S_N can be also determined from the transport of two partitioning tracers (*1* and *2*) by:

$$S_N = \frac{\overline{t_1} - \overline{t_2}}{\overline{t_2}(K_{NW1} - 1) - \overline{t_1}(K_{NW2} - 1)} \tag{2.55}$$

where $\overline{t_1}$ and $\overline{t_2}$ are the mean travel times for each tracer and $K_{NW,1}$ and $K_{NW,2}$ are the NAPL-water partition coefficients for each partitioning tracer.

The effective pore volume for an extraction well (V_{PV}) is determined using the average travel time of a nonpartitioning tracer as given by:

$$V_{PV} = Qt_{np} \tag{2.56}$$

where Q is the extraction well pumping rate. The total NAPL volume (V_N) in the tracer swept zone of each extraction well is given by:

$$V_N = \frac{\overline{S_N} - \overline{V_{PV}}}{1 - S_N} \tag{2.57}$$

The application of the above equations are subject to the following critical assumptions as outlined by Annable *et al.* (1998): (1) The observed tracer retardation is solely due to NAPL partitioning, (2) the values of the NAPL water partition coefficient must not vary with tracer or NAPL concentration and partitioning must be governed by equilibrium, and (3) the injected tracer must effectively contact all the NAPL in the medium. Reliable S_N estimates from tracer data require good resolution of tracer BTCs. During the final stages of the PITT, low tracer concentrations, at or below detection limits (i.e., 1 ppm) can result in truncated BTCs producing moment analyses that will underestimate the NAPL present. Exponential extrapolation of tracer BTC tails is used to minimize the errors associated with early truncation of these curves (Jin *et al.* 1995, Annable *et al.* 1998). The resulting spatial integration of the NAPL is free from the problems associated with extrapolating a point measurement such as a core, to a larger area (Annable *et al.* 1998).

2.10. REFERENCES

Abriola, L.M., T.J. Dekker, and K.D. Pennell (1993). Surfactant-Enhanced Solubilization of Residual Dodecane in Soil Columns: 2. Mathematical Modeling. *Environmental Science and Technology,* 27: 2341–2351.

Abriola, L.M., C.D. Drummond, E.J. Hahn, K.F. Hayes, T.C.G. Kibbey, L.D. Lemke, K.D. Pennell, E.A. Petrovskis, C.A. Ramsburg, and K.M. Rathfelder (2005). Pilot-Scale Demonstration of Surfactant-Enhanced PCE Solubilization at the Bachman Site. 1. Site Characterization and Test Design. *Environmental Science and Technology,* 39(6):1778-1790.

Allen, S.A., and K.F. Reardon (2000). Remediation of Contaminated Soils by Combined Chemical and Biological Treatments. Physical and thermal technologies: Remediation of Chlorinated and Recalcitrant Compounds, G.B. Wickamanayake and A.R. Gavaskar (eds.), Battelle Press, Columbus, Ohio.

Almendros, G., F.J. Gonzalez-Vila, and F. Martin (1989). Room Temperature Alkaline Permanganate Oxidation of Representative Humic Acids. *Soil Biology and Biochemistry*, 21(4):481-486.

Annable, M.A., P.S.C. Rao, K. Hatfield, W. Graham, A.L. Wood, and C.G. Enfield (1998a). Partitioning Tracers for Measuring Residual DNAPL: Field-Scale Test Results. *J. Environ. Eng.*, 124 (6), 498-503.

Annable, M.A., J.W. Jawitz, P.S.C. Rao, D. Dai, H. Kim, and A.L. Wood (1998b). Field Evaluation of Interfacial and Partitioning Tracers for Characterization of Effective NAPL-Water Contact Areas. *Ground Water,* 36(4):495-502.

Atlas, R.M., and R. Bartha (1987). Microbial Ecology, Benjamin/Cummings Publishing Company, Menlo Park, California.

Azadpour-Keeley, A., L.A. Wood, T.R. Lee, and S.C. Mravik (2004). Microbial Responses to In Situ Chemical Oxidation, Six-Phase Heating, and Steam Injection Remediation Technologies in Groundwater. *Remediation Journal*, 14(4):5-17.

Baciocchi, R., M.R. Boni, and L. D'Aprile (2003). Hydrogen Peroxide Lifetime as an Indicator of the Efficiency for 3-Chlorophenol Fenton's and Fenton-Like Oxidation in Soils. *Journal of Hazardous Materials*, B96, pg. 305-329.

Barcelona, M.J., and T.R. Holm (1991). Oxidation-Reduction Capacities of Aquifer Solids. *Environmental Science and Technology*, 259:1565–1572.

Bear, J. (1972). Dynamics of Fluids in Porous Media. American Elsevier Publishing Company, Dover, NY, 764 pp.

Belfiore, L.A. (2003). Transport Phenomena for Chemical Reactor Design. Hoboken, New Jersey, John Wiley and Sons.

Benjamin, M.M. (2002). Water Chemistry. New York, McGraw-Hill.

Bigda, R.J. (1995). Consider Fenton's Chemistry for Wastewater Treatment. *Chemical Engineering Progress*, 91:62-66.

Broholm, K.S., and S. Feenstra (1995). Laboratory Measurements of the Aqueous Solubility of Mixtures of Chlorinated Solvents. *Environmental Toxicology and Chemistry*, 14(1):9-15.

Brusseau, M.L. (1992). Rate-Limited Mass Transfer and Transport of Organic Solutes in Porous Media that Contain Immobile Immiscible Organic Liquid. *Water Resources Research*, 28(1):33-45.

Bui, C.T., and R.G.H. Cotton (2002). Comparative Study of Permanganate Oxidation Reactions of Nucleotide Bases by Spectroscopy. *Bioorg. Chem.*, 30:133-137.

Büyüksönmez, F., T.F. Hess, R.L. Crawford, A. Paszczynski, and R.J. Watts (1999). Optimization of Simultaneous Chemical and Biological Mineralization of Perchloroethylene. *Applied Environmental Microbiology*, 65(6):2784-2788.

Büyüksönmez, F., T.F. Hess, R.L. Crawford, and R.J. Watts (1998). Toxic Effects of Modified Fenton Reactions on *Xanthobacter flavus* FB71. *Applied Environmental Microbiology*, 64(10):3759-3764.

Cain, R.B., G.R. Johnson, J.E. McCray, W.J. Blanford, and M.L. Brusseau (2000). Partitioning Tracer Tests for Evaluating Remediation Performance. *Ground Water*, 38(5):752-761.

Chambers, J., A. Leavitt, C. Waiti, C.G. Schreier, J. Melby, and L. Goldstein (2000). In Situ Destruction of Chlorinated Solvents with $KMnO_4$ Oxidizes Chromium. In: Wickramanayake, G.B., Gavaskar, A.R., Chen, A.S.C. (eds.), Chemical Oxidation and Reactive Barriers. Battelle Press, Columbus, OH, pp. 49-55.

Chapelle, F.H., P.M. Bradley, and C.C. Casey (2005). Behavior of a Chlorinated Ethene Plume Following Source-Area Treatment with Fenton's Reagent. *Ground Water Monitoring and Remediation,* 25(2): 131-141.

Childs, J., E. Acosta, M. Annable, M. Brooks, C. Enfield, J.H. Harwell, M. Hasegawa, R.C. Knox, P.S.C. Rao, and D.A. Sabatini (2006). Field Demonstration of Surfactant-Enhanced Solubilization of DNAPL at Dover Air Force Base, Delaware. *Journal of Contaminant Hydrology*, 82(1-2):1-22.

Chou, S. and C. Huang (1999). Application of a Supported Iron Oxyhydroxide Catalyst in Oxidation of Benzoic Acid by Hydrogen Peroxide. *Chemosphere*, 38(12):2719-2731.

Clement, T.P., Y.-C. Kim, T.R. Gautam and K.-K. Lee (2004). Experimental and Numerical Investigation of DNAPL Dissolution Processes in a Laboratory Aquifer Model. *Ground Water Monitoring and Remediation*, 24(4):88-96.

Cline, S.R., O.R. West, N.E. Korte, F.G. Gardner, R.L. Siegrist, and J.L. Baker (1997). $KMnO_4$ Chemical Oxidation and Deep Soil Mixing for Soil Treatment. *GeoTech. News*, 15 (5): 25-28.

Conrad, S.H., J.L. Wilson, W.R. Mason and W. J. Peplinski (1992). Visualization of Residual Organic Liquid Trapped in Aquifers. *Water Resources Research*, 28(2):467-478.

Conrad, S.H., R.J. Glass, and W.J. Peplinski (2002). Bench-Scale Visualization of DNAPL Remediation Processes in Analog Heterogeneous Aquifers: Surfactant Floods and In Situ Oxidation Using Permanganate. *Journal of Contaminant Hydrology*, 58(1-2):13-49.

CRC (2001). CRC Handbook of Chemistry and Physics, 82nd Ed. CRC Press, Cleveland, OH. 2664 pp.

Crimi, M.L. (2002). Particle Genesis and Effects on Metals in the Subsurface During In Situ Chemical Oxidation using Permanganate. Ph.D. dissertation, Colorado School of Mines, Golden, CO. April.

Crimi, M.L., and R.L. Siegrist (2004). Experimental Evaluation of In Situ Chemical Oxidation Activities at the Naval Training Center (NTC) Site, Orlando, Florida. Naval Facilities Engineering Command, Port Hueneme CA. 64 pp.

Crimi, M.L., and R.L. Siegrist (2005). Factors Affecting Effectiveness and Efficiency of DNAPL Destruction Using Potassium Permanganate and Catalyzed Hydrogen Peroxide. *Journal of Environmental Engineering*, 131(12):1724-1732.

Cussler, E.L. (1997). Diffusion: Mass Transfer in Fluid Systems. Cambridge, UK, Cambridge University Press.

Deeds, N.E., D.C. McKinney, and G.A. Pope (1999a). Vadose Zone Characterization at a Contaminated Field Site Using Partitioning Interwell Tracer Technology. *Environmental Science and Technology*, 33(16):2745-2751.

Deeds, N.E., D.C. McKinney, G.A. Pope, and G.A. Whitley (1999b). Difluoromethane as Partitioning Tracer to Estimate Water Saturations. *Environmental Science and Technology,* 32:630-633.

Deeds, N.E., D.C. McKinney, and G.A. Pope (2000). Laboratory Characterization of Non-Aqueous Phase Liquid/Tracer Interaction in Support of a Vadose Zone Partitioning Interwell Tracer Test. *Journal of Contaminant Hydrology,* 41:193-204.

Dekker, T.J., and L.M. Abriola (2000a). The Influence of Field-Scale Heterogeneity on the Infiltration and Entrapment of Dense Non-Aqueous Phase Liquids in Saturated Formations. *Journal of Contaminant Hydrology*, 42(2):187-218.

Dinsdale, R.M., F.R. Hawkes, and D.L. Hawkes (2000). Anaerobic Digestion of Short Chain Organic Acids in an Expanded Granular Sludge Bed Reactor. *Water Research*, 34(9):2433-2438.

Divine, C.E., W.E. Sanford, and J.E. McCray (2003). Helium and Neon Groundwater Tracers to Measure Residual DNAPL: Laboratory Investigation. *Vadose Zone Journal*, 2:382-388.

Divine, C.E., J.E. McCray, L.M. Wolf-Martin, W.J. Blanford, D.J. Blitzer, M.L. Brusseau, and T.B. Boving (2004). Partitioning Tracer Tests as a Remediation Metric: Case study at Naval Amphibious Base Little Creek, Virginia Beach, Virginia. *Remediation Journal*, 14(2):7-31.

Droste, E.X., M.C. Marley, J.M. Parikh, and A.M. Lee (2002). Observed Enhanced Reductive Dechlorination after In Situ Chemical Oxidation Pilot Test. In: Remediation of Chlorinated and Recalcitrant compounds; Gavaskar, A.R. and A.S.C. Chen (eds.); Proceedings of the 3rd Intern. Conf. on Remediation of Chlorinated and Recalcitrant Compounds; Battelle Press: Columbus, OH.

Dugan, P.J., J.E. McCray, and G.D. Thyne (2003). Influence of a Solubility-Enhancing Agent (Cyclodextrin) on NAPL-Water Partition Coefficients, with Implications for Partitioning Tracer Tests. *Water Resources Research*, 39(5):1.1-1.7.

Dugan, P. (2006). Coupling In Situ Technologies for DNAPL Remediation and Viability of the PITT for Post-Remediation Performance Assessment. Ph.D. dissertation, Environmental Science and Engineering Division, Colorado School of Mines, Golden, CO. December 2006.

Dwarakanath, V., and G.A. Pope (1998). A New Approach for Estimating Alcohol Partition Coefficients between Nonaqueous Phase Liquids and Water. *Environmental Science and Technology*, 32(11):1662-1666.

Dwarakanath, V., K. Kostarelos, G.A. Pope, D. Schotts, and K.H. Wade (1999). Anionic Surfactant Remediation of Soil Columns Contaminated by Nonaqueous Liquids. *Journal of Contaminant Hydrology*, 38(4):465–488.

Ewing, J.E. (1996). Effects of Dimensionality and Heterogeneity on Surfactant-Enhanced Solubilization of Non-Aqueous Phase Liquids in Porous Media. M.S. Thesis, University of Colorado at Boulder, 152 pp.

Falta, R.W., C.M. Lee, S.E. Brame, E. Roeder, J.T. Coates, C. Wright, A.L. Wood, and C.G. Enfield. (1999). Field Test of High Molecular Weight Alcohol Flushing for Subsurface Nonaqueous Phase Liquid Remediation. *Water Resources Research,* 35(7):2095-2108.

Feenstra, S., and J.A. Cherry (1996). Diagnosis and Assessment of DNAPL Sites. In: J.F. Pankow and J.A. Cherry (eds.) Dense Chlorinated Solvents and Other DNAPLs In Groundwater: History, Behavior, and Remediation. Waterloo Press, Portland, OR. pp. 395-473.

Fountain, J.C. (1992). Field Tests of Surfactant Flooding: Mobility Control of Dense Nonaqueous Phase Liquids. In: Transport and Remediation of Subsurface Contaminants, D. A. Sabatini and R. C. Knox, (eds.), American Chemical Society, Washington, D.C., 182-191.

Fountain, J.C., R.C. Starr, T. Middleton, M. Beikirch, C. Taylor, and D. Hodge (1996). A Controlled Field Test of Surfactant-Enhanced Aquifer Remediation. *Ground Water*, 34(5):910-916.

Fountain, J.C., A. Klimek, M.G. Beikirch, and T.M. Middleton (1991). The Use of Surfactants for In Situ Extraction of Organic Pollutants from a Contaminated Aquifer. *Journal of Hazardous Materials*, 28:295-311.

Freeman, F., C.O. Fuselier, and E.M. Karchefski (1975). Permanganate Ion Oxidation of Thymine: Spectrophotometric Detection of a Stable Organomanganese Intermediate. *Tetrahedron Lett.*, 25:2133-2136.

Freeze, R.A., and D.B. McWhorter (1997). A Framework for Assessing Risk Reduction Due to DNAPL Mass Removal from Low-Permeability Soils. *Ground Water*, 35(1):111-123.

Fridovich, I. (1978). The biology of oxygen radicals. *Science*, 201, 875-880.

Gardner, F.G., N. Korte, J. Strong-Gunderson, R.L. Siegrist, O.R. West, S.R. Cline, and J.L. Baker (1996). Implementation of Deep Soil Mixing at the Kansas City Plant. ORNL/TM-13552, Oak Ridge National Laboratory, TN.

Gates-Anderson, D.D., R.L. Siegrist, and S.R. Cline (2001). Comparison of Potassium Permanganate and Hydrogen Peroxide as Chemical Oxidants for Organically Contaminated Soils. *Journal of Environmental Engineering*, 127(4):337-347.

Gates, D.D., and R.L. Siegrist (1995). In-Situ Chemical Oxidation of Trichloroethylene Using Hydrogen Peroxide. *Journal of Environmental Engineering*, 121(9):639-644.

GeoSyntec (2004). Assessing the Feasibility of DNAPL Source Zone Remediation: Review of Case Studies. *Contract Report CR-04-002-ENV*, Guelph, Ontario, Canada.

Glaze, W.H., and J.W. Kang (1988). Advanced Oxidation Processes for Treating Groundwater Contaminated with TCE and PCE: Laboratory Studies. *Journal American Water Works Association,* 88(5):57-63.

Greenberg, R., T. Andrews, P.K.C. Kakarla, and R.J. Watts (1998). In-Situ Fenton-Like Oxidation of VOCs: Laboratory, Pilot, and Full-Scale Demonstration. *Remediation Journal*, Spring, pp. 29-42.

Griffith, S.M., and M. Schnitzer (1975). Oxidative Degradation of Humic and Fulvic Acids Extracted from Tropical Volcanic Soils. *Canadian Journal of Soil Science*, 55:251-267.

Gurol, M.D., and J.X. Ravikumar (1991). Chemical Oxidation of Hazardous Compounds in Soil. Proc. Nat. Res. and Dev. Conf. on the Control of Hazardous Material.

Hazen, T.C., G. Sewell, and A.R. Gavaskar (2000). The Effect of Source Remediation Methods on the Presence and Activity of Indigenous Subsurface Bacteria at Launch Complex 34, Cape Canaveral Air Station, Florida. Evaluation Work Plan, Battelle Press.

Heiderscheidt, J.L. (2005). DNAPL Source Zone Depletion During In Situ Chemical Oxidation (ISCO): Experimental and Modeling Studies. Ph.D. dissertation, Environmental Science and Engineering Division, Colorado School of Mines, Golden, CO. August 2005.

Held, R.J., and T.H. Illangasekare (1995a). Fingering of Dense Non-Aqueous Phase Liquids in Porous Media: 1. Experimental Investigation. *Water Resources Research*, 31(5):1213-1222.

Held, R.J., and T.H. Illangasekare (1995b). Fingering of Dense Non-Aqueous Phase Liquids in Porous Media: 2. Analysis and Classification. *Water Resources Research*, 31(5):1223-1231.

Hood, E. (2000). Permanganate Flushing of DNAPL Source Zones: Experimental and Numerical Investigation. Ph.D. dissertation, University of Waterloo, Waterloo, ON. 243 pp.

Hood, E., and N.R. Thomson (2000). Numerical Simulation of In Situ Chemical Oxidation. In: Chemical Oxidation and Reactive Barriers, Wickramanayake, G.B., Gavaskar, A.R., Chen, A.S.C. (eds.). Battelle Press, Columbus, OH, pp. 83-90.

Hood, E., N.R. Thomson, D. Grossi, and G.J. Farquhar (2000). Experimental Determination of the Kinetic Rate Law for the Oxidation of Perchloroethylene by Potassium Permanganate. *Chemosphere* 40:1383-1388.

Howsawkeng, J., R.J. Watts, D.L. Washington, A.L. Teel, T.F. Hess, and R.L. Crawford (2001). Evidence for Simultaneous Abiotic-Biotic Oxidations in a Microbial-Fenton's System. *Environmental Science and Technology*, 35:2961-2966.

Hrapovic, L., B.E. Sleep, D.J. Major, and E. Hood (2005). Laboratory Study of Treatment of Trichloroethene by Chemical Oxidation Followed by Bioremediation. *Environmental Science and Technology*, 39:2888-2897.

Huang, K., G.E. Hoag, P. Chheda, B.A. Woody, and G.M. Dobbs (1999). Kinetic Study of Oxidation of Trichloroethylene by Potassium Permanganate. *Environmental Engineering Science*, 16(4):265-274.

Huang, K.C., G.E. Hoag, and P. Chheda (2000). Soil Oxidant Demand During Chemical Oxidation of Trichloroethylene by Permanganate in Soil Media. Proc., 32nd Mid-Atlantic Industrial and Hazardous Waste Conference, Technomic Publishing Co. pp. 617-626.

Huang, K., G.E. Hoag, P. Chheda, B.A. Woody, and G.M. Dobbs (2001). Oxidation of Chlorinated Ethenes by Potassium Permanganate: A Kinetics Study. *Journal of Hazardous Materials*, 87(1-3):155-169.

Huang, K.-C., P. Chheda, G.E. Hoag, B.A. Woody, and G.M. Dobbs (2000). Pilot-Scale Study of In-Situ Chemical Oxidation of Trichloroethene with Sodium Permanganate. The 2nd Intern. Conf. on Remediation of Chlorinated and Recalcitrant Compounds, Monterey, California, Battelle Press.

Huang, K.C., G.E. Hoag, P. Chheda, B.A. Woody and G.M. Dobbs (2002). Kinetics and Mechanism of Oxidation of Tetrachloroethylene with Permanganate. *Chemosphere,* 46:815-825.

Hurst, D.A., K.G. Robinson, and R.L. Siegrist (1993). Hydrogen Peroxide Treatment of TCE Contaminated Soils. Proc. 3rd Int. Symp. on Chemical Oxidation, Lancaster, PA: Technomic Pub. Inc.

Ibaraki, M., and F.W. Schwartz (2001). Influence of Natural Heterogeneity on the Efficiency of Chemical Floods in Source Zones. *Ground Water*, 39(5):660-666.

Illangasekare, T.H., E.J. Armbruster, III, and D.N. Yates (1995a). Non-Aqueous-Phase Fluids in Heterogeneous Aquifer - Experimental Study. *Journal of Environmental Engineering*, 121(8):571-579.

Illangasekare, T.H., J.L. Ramsey, K.H. Jensen, and M. Butts (1995b). Experimental Study of Movement and Distribution of Dense Organic Contaminants in Heterogeneous Aquifers: An Experimental Study. *Journal of Contaminant Hydrology*, 20(1-2):1-25.

Imhoff, P.T., P.R. Jaffé, and G.F. Pinder (1993). An Experimental Study of Complete Dissolution of a Nonaqueous Phase Liquid in Saturated Porous Media. *Water Resources Research,* 30(2):307-320.

Imlay, J.A., S.M. Chin, and S. Linn (1988). Toxic DNA damage by hydrogen peroxide through the Fenton reaction in vivo and in vitro. *Science*, 240:640-642.

Itakura, T., D.W. Airey, and C.J. Leo (2003). The Diffusion and Sorption of Volatile Organic Compounds through Kaolinitic Clayey Soils. *Journal Contaminant Hydrology*, 65(3-4):219-243.

Izawa, S., Y. Inoue, and A. Kimura (1996). Importance of Catalase in the Adaptive Response to Hydrogen Peroxide: Analysis of Acatalasaemic *Saccharomyces cerevisiae*. *Biochemistry Journal*, 320:61-67.

INTERA (1998). Final Report on the Demonstration of Surfactant Enhanced Aquifer Remediation of Chlorinated Solvent DNAPL at Operable Unit 2, Hill AFB, UT. Prepared for AFCEE Technology Transfer Division Brooks AFB, San Antonio, TX.

ITRC (2002). Regulatory Overview--DNAPL Source Reduction: Facing the Challenge. Interstate Technology and Regulatory Cooperation Work Group (ITRC), Dense Non-aqueous Phase Liquids Team, Washington D.C. Apr 2002, 42 pp. http://www.itrcweb.org/user/DNAPL-2.pdf.

ITRC (2003). Technology and Regulatory Guidance for Surfactant/Cosolvent Flushing of DNAPL Source Zones. Interstate Technology Regulatory Council. http://www.itrcweb.org.

Jackson, S.F. (2004). Comparative Evaluation of Potassium Permanganate and Catalyzed Hydrogen Peroxide During In Situ Chemical Oxidation of DNAPLs. M.S. thesis, Environmental Science and Engineering Division, Colorado School of Mines, Golden, CO. January 2004.

Jafvert, C. (1996). Surfactants/ Cosolvents (Technology Evaluation Report). Ground-Water Remediation Technologies Analysis Center. TE-96-02. December.

Jawitz, J.W., R.K. Sillian, M.D. Annable, P.S.C. Rao, and K. Warner (2000). In-Situ Alcohol Flushing of a DNAPL Source Zone at a Dry Cleaner Site. *Environmental Science and Technology*, 32(4):523-530.

Jawitz, J.W., M.D. Annable, G.G. Demmy, and P.S. C. Rao (2003). Estimating Nonaqueous Phase Liquid Spatial Variability Using Partitioning Tracer Higher Temporal Moments. *Water Resources Research,* 39(7):1-19.

Jayanti, S. (2000). Evaluation of New Surfactants and Tracers. M.S.E. thesis, Univ. of Tex. at Austin, Austin, Tex.

Jin, M., M. Delshad, V. Dwarakanath, D.C. McKinney, G.A. Pope, K. Sepehrnooro, C.E. Tillberg, and R.E. Jackson (1995). Partitioning Tracer Test for Detection, Estimation, and Remediation Performance assessment of subsurface nonaqueous phase liquids. *Water Resources Research*, 31:1201-1211.

Johnson, R.L., and J.F. Pankow (1992). Dissolution of Dense Chlorinated Solvents into Groundwater. 2. Source Functions for Pools of Solvent. *Environmental Science and Technology*, 26(5):896-901.

Johnson, R.L., J.A. Cherry, and J.F. Pankow (1989). Diffusive Contaminant Transport in Natural Clay: A Field Example and Implications for Clay-Lined Waste Disposal Sites. *Environmental Science and Technology*, 23(3):340-349.

Jury, W.A., W.R. Gardner, and W.H. Gardner (1991). Soil Physics, 5th Ed. John Wiley & Sons, New York, NY, 328 pp.

Kakarla, P.K.C., and R.J. Watts (1997). Depth of Fenton-Like Oxidation in Remediation of Surface Soil. *Journal of Environmental Engineering*, Jan-97.

Kang, Y.W., and K.Y. Hwang (2000). Effects of Reaction Conditions on the Oxidation Efficiency in the Fenton's Process. *Water Research*, 34(10):2786-2790.

Kao, C.M., and M.J. Wu (2000). Enhanced TCDD Degradation by Fenton's Reagent Preoxidation. *Journal of Hazardous Materials*, 74:197-211.

Kastner, J.R., J.S. Domingo, M. Denham, M. Molina, and R. Brigmon (2000). Effect of Chemical Oxidation on Subsurface Microbiology and Trichloroethene Biodegradation. *Bioremediation Journal*, 4(3):219-236.

Kennedy, C.A., and W.C. Lennox (1997). A Pore-Scale Investigation of Mass Transport from Dissolving DNAPL Droplets. *Journal of Contaminant Hydrology,* 24:221-246.

Khan, A.J., and R.J. Watts (1996). Mineral-Catalyzed Peroxidation of Tetrachloroethylene. *Water, Air, Soil Pollution*, 88:247-260.

Kieber, D.J., J. McDaniel, and K. Mopper (1989). Photochemical Source of Biological Substrates in Sea Water: Implications for Carbon Cycling. *Nature*, 637-639.

Kim, K., and M.D. Gurol (2004). Nonaqueous-Phase TCE Degradation in the Presence of Permanganate in Batch System. The 4th Intern. Conf. on the Remediation of Chlorinated and Recalcitrant Compounds, Monterey, California, Battelle Press.

Klens, J., S. Scarborough, and D. Graves (2001). The Effects of Permanganate Oxidation on Subsurface Microbial Populations. In: Natural Attenuation of Environmental Contaminants; A. Leeson, M. E. Kelley, H. S. Rifai, and V. S. Magar (eds.); Battelle Press: Columbus, Ohio; Vol. 6, pp 253-259.

Kong, S.H., R.J. Watts, and J.H. Choi (1998). Treatment of Petroleum-Contaminated Soils Using Iron Mineral Catalyzed Hydrogen Peroxide. *Chemosphere*, 37(8):1473-1482.

Kueper, B.H., and E.O. Frind (1991a). Two-Phase Flow in Heterogeneous Porous Media, 1. Model Development. *Water Resources Research*, 27(6):1049-1057.

Kueper, B.H., and E.O. Frind (1991b). Two-Phase Flow in Heterogeneous Porous Media, 2. Model Application. *Water Resources Research*, 27(6):1059-1070.

Kueper, B.H., G.P. Wealthall, J.W.N. Smith, S.A. Leharne, and D.N. Lerner (2003). An Illustrated Handbook of DNAPL Transport and Fate in the Subsurface. Environment Agency R&D Publication 133, Environmental Agency, Almondsbury, Bristol, U.K. 67 pp.

Kwan, W.P., and B.M. Voelker (2002). Decomposition of Hydrogen Peroxide and Organic Compounds in the Presence of Dissolved Iron and Ferrihydrite. *Environmental Science and Technology*, 36:1467-1476.

Kwan, W.P., and B.M. Voelker (2003). Rates of Hydroxyl Radical Generation and Organic Compound Oxidation in Mineral-Catalyzed Fenton-Like Systems. *Environmental Science and Technology*, 37:1150-1158.

Ladaa, T.I., C.M. Coates, and R.W. Falta (2001). Cosolvent Effects of Alcohols on the Henry's Law Constant and Aqueous Solubility of Tetrachloroethylene (PCE). *Chemosphere*, 44(5):1137-1143.

Landa, A.S., E.M. Sipkema, J. Weijma, A.A. Beenackers, J. Dolfing, and D.B. Janssen (1994). Cometabolic Degradation of Trichloroethylene by *Pseudomonas cepacia* G4 in a Chemostat with Toluene as the Primary Substrate. *Applied Environmental Microbiology*, 60:3368-3374.

Larking, D.M., R.L. Crawford, G. Christie, and G. Lonegran (1999). Enhanced Degradation of Polyvinyl Alcohol by *Pycnoporus cinnabarinus* after Pretreatment with Fenton's Reagent. *Applied Environmental Microbiology*, 65:1798-1800.

Lee, K.Y., and C.V. Chrysikopoulos (1998). NAPL Pool Dissolution in Stratified and Anisotropic Porous Formations. *Journal of Environmental Engineering*, 124(9):851-862.

Lee, B. D., and M. Hosomi (2001). A Hybrid Fenton Oxidation-Microbial Treatment for Soil Highly Contaminated with Benz(a)anthracene. *Chemosphere*, 43:1127-1132.

Lee, E.S., Y. Seol, Y.C. Fang, and F.W. Schwartz (2003). Destruction Efficiencies and Dynamics of Reaction Fronts Associated with the Permanganate Oxidation of Trichloroethylene. *Environmental Science and Technology,* 37:2540-2546.

Leung, S.W., R.J. Watts, and G.C. Miller (1992). Degradation of Perchloroethylene by Fenton's Reagent: Speciation and Pathway. *Journal of Environmental Quality*, 21:377-381.

Levin, R., E. Kellar, J. Wilson, L. Ware, J. Findley, and J. Baehr (2000). Full-Scale Soil Remediation of Chlorinated Solvents by In Situ Chemical Oxidation. In: Proceeding from the 2nd Intern. Conf. on Remediation of Chlorinated and Recalcitrant Compounds, Monterey, CA, May 22-25, 2000.

Li, Z.M., P.J. Shea, and S.D. Comfort (1997). Fenton Oxidation of 1,4,6-Trinitrotoluene in Contaminated Soil Slurries. *Environmental Engineering Science*, 141:55-66.

Li, X.D., and F.W. Schwartz (2000). Efficiency Problems Related to Permanganate Oxidation Schemes. In: Wickramanayake, G.B., Gavaskar, A.R., Chen, A.S.C. (eds.), Chemical Oxidation and Reactive Barriers. Battelle Press, Columbus, OH, pp. 41-48.

Li, X.D., and F.W. Schwartz (2003). Permanganate Oxidation Schemes for the Remediation of Source Zone DNAPLs and Dissolved Contaminant Plumes. Chlorinated Solvent and DNAPL Remediation. S.M. Henry and S.D. Warner. Washington, DC, American Chemical Society**:** 73-85.

Li, Z. (2004). Surfactant-Enhanced Oxidation of Trichloroethylene by Permanganate: Proof of Concept-Short Communication. *Chemosphere*, 54(3):419–423.

Li, X.D., and F.W. Schwartz (2004a). DNAPL Remediation with In Situ Chemical Oxidation Using Potassium Permanganate. I. Mineralogy of Mn Oxide and its Dissolution in Organic Acids. *Journal of Contaminant Hydrology,* 68:39-53.

Li, X.D., and F.W. Schwartz (2004b). DNAPL Remediation with In Situ Chemical Oxidation Using Potassium Permanganate. II. Increasing Removal Efficiency by Dissolving Mn Oxide Precipitates. *Journal of Contaminant Hydrology,* 68:269-287.

Lin, S.S., and M.D. Gurol (1996). Heterogeneous Catalytic Oxidation of Organic Compounds by Hydrogen Peroxide. *Water Science and Technol*ogy, 34(9):57-64.

Lin, S., and M.D. Gurol (1998). Catalytic Decomposition of Hydrogen Peroxide on Iron Oxide: Kinetics, Mechanism, and Implications. *Environmental Science and Technology*, 32(10):1417–1423.

Liu, C., and W.P. Ball (2002). Back Diffusion of Chlorinated Solvent Contaminants from a Natural Aquitard to a Remediated Aquifer Under Well-Controlled Field Conditions: Predictions and Measurements. *Ground Water*, 40(2):175-184.

Lowe, K.S., F.G. Gardner, and R.L. Siegrist (2002). Field Evaluation of In Situ Chemical Oxidation through Vertical Well-to-Well Recirculation of $NaMnO_4$. *Ground Water Monitoring and Remediation*, 22(1):106-115.

Macbeth, T.W., L.N. Peterson, R.C. Starr, K.S. Sorenson, R. Goehlert, and K.S. Moor (2005). ISCO Impacts on Indigenous Microbes in a PCE-DNAPL Contaminated Aquifer. In Situ and On-Site Bioremediation Symposium, Baltimore, Maryland.

Mackay, D.M., B.L. Roberts, and J.A. Cherry (1985). Transport of Organic Chemicals in Groundwater – Distribution and Fate of Chemicals in Sand and Gravel Aquifers. *Environmental Science and Technology*, 19(5):384-392.

Mackay, D.M., and J.A. Cherry (1989). Groundwater Contamination: Pump-and-Treat Remediation. *Environmental Science and Technology*, 23(6):630-636.

MacKinnon, L.K., and N.R. Thomson (2002). Laboratory-Scale In Situ Chemical Oxidation of a Perchloroethylene Pool Using Permanganate. *Journal of Contaminant Hydrology,* 56:49-74.

McKay, D.J., J.A. Stark, B.L. Young, J.W. Govoni, C.M. Berini, T.J. Cronan, and A.D. Hewitt (2000). A Field Demonstration of Trichloroethylene Oxidation Using Potassium Permanganate. The 2nd Intern. Conf. on Remediation of Chlorinated and Recalcitrant Compounds, Monterey, California, Battelle Press.

Mariner, P.E., M. Jin, J.E. Studer, and G.A. Pope (1999). The First Vadose Zone Partitioning Tracer Test for Nonaqueous Phase Liquid and Water Residual. *Environmental Science and Technology*, 33:2825-2828.

Martel, R., P.J. Gelinas, and L. Saumure (1998a). Aquifer Washing by Micellar Solutions: 3 Field Test at the Thouin Sand Pit (L'Assomption, Quebec, Canada). *Journal of Contaminant Hydrology*, 30(1-2):33-48.

Martens, D.A., and W.T. Frankenberger (1995). Enhanced Degradation of Polycyclic Aromatic Hydrocarbons in Soil Treated with an Advanced Oxidative Process - Fenton's Reagent. *Journal of Soil Contamination*, 4(2):175-190.

Marvin, B.K., J. Chambers, A. Leavitt, and C.G. Schreier (2002). Chemical and Engineering Challenges to In Situ Permanganate Remediation. Proc., 3rd Int. Conf. on Remediation of Chlorinated and Recalcitrant Compounds, Monterey CA, May 2002. Battelle Press, Columbus, OH. 2C-04 (8pp.).

Mayer, A.S., and C.T. Miller (1992). The Influence of Porous Medium Characteristics and Measurement Scale on Pore-Scale Distributions of Residual Nonaqueous Phase Liquids. *Journal of Contaminant Hydrology*, 11(3&4):189-213.

Mayer, A.S., and C.T. Miller (1996). The Influence of Mass Transfer Characteristics and Porous Media Heterogeneity on Non-Aqueous Phase Dissolution. *Water Resources Research*, 32(6):1551-1567.

Mayer, A.S., L. Zhong, and G.A. Pope (1999). Measurement of Mass-Transfer Rates and Surfactant-Enhanced Solubilization of Non-Aqueous Phase Liquids. *Environmental Science and Technology*, 33(17):2965-2972.

Meinardus, H.W., V. Dwarakanath, J. Ewing, G.J. Hirasaki, R.E. Jackson, M. Jin, J.S. Ginn, J.T. Londergan, C.A. Miller, and G.A. Pope (2002). Performance Assessment of NAPL Remediation in Heterogeneous Alluvium. *Journal of Contaminant Hydrology*, 54:173-193.

Mercer, J.W., and R.M. Cohen (1990). A Review of Immiscible Fluids in the Subsurface: Properties, Models, Characterization and Remediation. *Journal of Contaminant Hydrology,* 6:107-163.

Miller, C.T., M.M. Poirier-McNeill, and A.S. Mayer (1990). Dissolution of Trapped Nonaqueous Phase Liquids: Mass Transfer Characteristics. *Water Resources Research,* 26(11):2783-2796.

Miller, C.M., R.L. Valentine, M.E. Roehl, and P. Alvarez (1996). Chemical and Microbiological Assessment of Pendimethalin-Contaminated Soil after Treatment with Fenton's Reagent. *Water Research*, 30(11):2579-2586.

Millington, R.J., and J.P. Quirk (1959). Permeability of Porous Media. *Nature*, 183:387-388.

Millington, R.J., and J.P. Quirk (1961). Permeability of Porous Solids. *Trans. Faraday Society*, 57:1200-1207.

Moes, M., C. Peabody, R.L. Siegrist, and M.A. Urynowicz (2000). Permanganate Injection for Source Zone Treatment of TCE DNAPL. The 2nd Intern. Conf. for Remediation of Chlorinated and Recalcitrant Compounds, Monterey, California, Battelle Press.

Montgomery, J., and L. Welkom (1989). Ground Water Chemicals Desk Reference, Lewis Publishers, Chelsea, MI.

Moran, M.A., and R.G. Zepp (1997). Role of Photoreactions in the Formation of Biologically Labile Compounds from Dissolved Organic Matter. *Limnology and Oceanography*, 6:1307-1316.

Mott-Smith, E., W.C. Leonard, R. Lewis, W.S. Clayton, J. Ramirez, and R. Brown (2000). In Situ Oxidation of DNAPL Using Permanganate: IDC Cape Canaveral Demonstration. The 2nd Intern. Conf. on the Remediation of Chlorinated and Recalcitrant Compounds, Monterey, California, Battelle Press.

Mumford, K.G., C.S. Lamarche, and N.R. Thomson (2004). Natural Oxidant Demand of Aquifer Materials Using the Push-Pull Technique. *Journal of Environmental Engineering*, 130(10):1139-1146.

Mumford, K.G., N.R. Thomson, and R.M. Allen-King (2005). Bench-Scale Investigation of Permanganate Natural Oxidant Demand Kinetics. *Environmental Science and Technology*, 39(8):2835-2840.

Nadarajah, N., J. Van Hamme, J. Pannu, J. Singh, and O. Ward (2002). Enhanced Transformation of Polycyclic Aromatic Hydrocarbons Using a Combined Fenton's Reagent, Microbial Treatment and Surfactants. *Applied Microbiology and Biotechnology*, 59:540-544.

Nam, K., and J.J. Kukor (2000). Combined Ozonation and Biodegradation for Remediation of Mixtures of Polycyclic Aromatic Hydrocarbons in Soil. *Biodegradation*, 11(1):1-9.

Nam, K., W. Rodriguez, and J.J. Kukor (2001). Enhanced Degradation of Polycyclic Aromatic Hydrocarbons by Biodegradation Combined with a Modified Fenton Reaction. *Chemosphere*, 45:11-20.

Nambi, I.M., and S.E. Powers (2003). Mass Transfer Correlations for Nonaqueous Phase Liquid Dissolution from Regions with High Initial Saturations. *Water Resources Research,* 39(2).

Nelson, N.T., and M.L. Brusseau (1996). Field Study of the Partitioning Tracer Method for Detection of Dense Nonaqueous Phase Liquid in a Trichloroethene Contaminated Aquifer. *Environmental Science and Technology*, 30(10):2895-2863.

Nelson, M.D., B.L. Parker, T.A. Al, J.A. Cherry, and D. Loomer (2001). Geochemical Reactions Resulting from In Situ Oxidation of PCE-DNAPL by $KMnO_4$ in a Sandy Aquifer. *Environmental Science and Technology*, 35(6):1266-1275.

Nuttall, H.E., V. Rao, S.R. Doppatapudi, and W. Lundy (2000). Chemical Oxidation of PCE at a Dry Cleaner Site. In Proceeding from the 2nd Intern. Conf. on Remediation of Chlorinated and Recalcitrant Compounds, Monterey, CA, May 22-25, 2000.

Oostrom, M., C. Hofstee, R.C. Walker, and J.H. Dane (1999a). Movement and Remediation of Trichloroethylene in a Saturated, Heterogeneous Porous Medium 1. Spill Behavior and Initial Dissolution. *Journal of Contaminant Hydrology,* 37:159-178.

Oostrom, M., C. Hofstee, R.C. Walker, and J.H. Dane (1999b). Movement and Remediation of Trichloroethylene in a Saturated, Heterogeneous Porous Medium 2. Pump-and-Treat and Surfactant Flushing. *Journal of Contaminant Hydrology,* 37:179-197.

Ortiz De Serra, M.I., and M. Schnitzer (1973). The Chemistry of Humic and Fulvic Acids Extracted from Argentine Soils-II. Permanganate Oxidation of Methylated Humic and Fulvic Acids. *Soil Biology and Biochemistry*, 5:287-296.

Palmer, C.D., and W. Fish (1992). Chemical Enhancements to Pump and Treat Remediation. USEPA, EPA/540/S-92/001, 20 pp.

Pankow, J.F., and J.A. Cherry (eds.). (1996). Dense Chlorinated Solvents and Other DNAPLs in Groundwater: History, Behavior, and Remediation. Waterloo Press, Portland, OR, 525 pp.

Pardieck, D.L., E.J. Bouwer, and A.T. Stone (1992). Hydrogen Peroxide Use to Increase Oxidant Capacity for In Situ Bioremediation of Contaminated Soils and Aquifers: A Review. *Journal of Contaminant Hydrology*, 9:221-242.

Parker, B.L., R.W. Gillham, and J.A. Cherry (1994). Diffusive Disappearance of Immiscible-Phase Organic Liquids in Fractured Geologic Media. *Ground Water*, 32(5):805-820.

Parker, B.L., D.B. McWhorter, and J.A. Cherry (1997). Diffusive Loss of Non-Aqueous Phase Organic Solvents from Idealized Fracture Networks in Geologic Media. *Ground Water*, 35(6):1077-1087.

Parker, B.L., J.A. Cherry, S.W. Chapman, and M.A. Guilbeault (2003). Review and Analysis of Chlorinated Solvent Dense Non-Aqueous Phase Liquid Distributions in Five Sandy Aquifers. *Vadose Zone Journal*, 2 (2):116-137.

Pennell, K.D., L.M. Abriola, and W.J. Weber Jr. (1993). Surfactant-Enhanced Solubilization of Residual Dodecane in Soil Columns: 1. Experimental Investigation. *Environmental Science and Technology,* 27(12):2332-2340.

Pennell, K.D., M. Jin, L.M. Abriola, and G.A. Pope (1994). Surfactant Enhanced Remediation of Soil Columns Contaminated by Residual Tetrachloroethylene. *Journal of Contaminant Hydrology,* 16(1):35-53.

Pennell, K.D., G.A. Pope, and L.M. Abriola (1996). Influence of Viscous and Buoyancy Forces on the Mobilization of Residual Tetrachloroethylene During Surfactant Flushing. *Environmental Science and Technology,* 30(4):1328-1335.

Petigara, B.R., N.V. Blough, and A.C. Mignerey (2002). Mechanisms of Hydrogen Peroxide Decomposition in Soils. *Environmental Science and Technology*, 36:639-645.

Petri, B.G. (2006). Impacts of Subsurface Permanganate Delivery Parameters on Dense Nonaqueous Phase Liquid Mass Depletion Rates. M.S. thesis, Environmental Science and Engineering Division, Colorado School of Mines, Golden, CO. January 2006.

Pignatello, J.J., and K. Baehr (1994). Ferric Complexes as Catalysts for "Fenton" Degradation of 2,4-D and Metolachlor in Soil. *Journal of Environmental Quality*, 23:365-370.

Piskonen, R., and M. Itavaara (2004). Evaluation of Chemical Pretreatment of Contaminated Soil for Improved PAH Bioremediation. *Applied Microbiology and Biotechnology*, 65:627-634.

Polak, A., A.S. Grader, R. Wallach, and R. Nativ (2003). Chemical Diffusion Between a Fracture and the Surrounding Matrix: Measurement by Computed Tomography and Modeling. *Water Resources Research*, 39 (4):1106, doi:10.1029/2001WR000813.

Pope, G.A., K. Sepehrnoori, M. Delshad, B.A. Rouse, V. Dwarakanath, and M. Jin (1994). NAPL Partitioning Interwell Tracer Test in OU1 Test Cell at Hill Air Force Base, Utah. Final EPA Rep. Prepared for Mantech. Environmental Research Services Corp., PO No. 94RC0251, GL No. 2000-602-4600.

Pope, G.A., and W.H. Wade (1995). Lessons from Enhanced Oil Recovery Research for Surfactant-Enhanced Aquifer Remediation. In: Surfactant-Enhanced Subsurface Remediation Emerging Technologies; Sabatini, D. A., Knox, R. C., Harwell, J. H. (eds.); ACS Symposium Series 594; American Chemical Society: 142-160. Washington, DC.

Poulsen, M.M., and B.H. Kueper (1992). A Field Experiment to Study the Behavior of Tetrachloroethylene in Unsaturated Porous Media. *Environmental Science and Technology*, 26(5):889-895.

Powers, S.E., I.M. Nambi, and G.W. Curry, Jr. (1998). NAPL Dissolution in Heterogeneous Systems: Mechanisms and a Local Equilibrium Modeling Approach. *Water Resources Research*, 34(12):3293-3302.

Powers, S.E., L.M. Abriola, J.S. Dunkin, and W.J. Weber, Jr. (1994a). Phenomenological Models for Transient NAPL-Water Mass-Transfer Processes. *Journal of Contaminant Hydrology,* 16:1-33.

Powers, S.E., L.M. Abriola, and W.J. Weber, Jr. (1994b). An Experimental Investigation of Nonaqueous Phase Liquid Dissolution in Saturated Subsurface Systems: Transient Mass Transfer Rates. *Journal of Contaminant Hydrology,* 30(2):321-332.

Rao, P.S.C., M.D. Annable, R.K. Sillan, D. Dai, D. Hatfield, W.D. Graham, A.L. Wood, and C.G. Enfield (1997). Field-Scale Evaluation of In Situ Cosolvent Flushing for Enhanced Aquifer Remediation. *Water Resources Research,* 33(12):2674-2686.

Ravikumar, J.X., and M.D. Gurol (1994). Chemical Oxidation of Chlorinated Organics by Hydrogen Peroxide in the Presence of Sand. *Environmental Science and Technology*, 28:394-400.

Ravikumar, J.X., and M.D. Gurol (1991). Effectiveness of Chemical Oxidation to Enhance the Biodegradation of Pentachlorophenol in Soil: A Laboratory Study. Proc. 23rd Mid-Atlantic Ind. Waste Conf., Lancaster, PA: Technomic Pub. Inc.

Reis, J.C., and A.M. Acock (1994). Permeability Reduction Models for the Precipitation of Inorganic Solids in Berea Sandstone. *In Situ*, 18(3):347-368.

Reitsma, S., and Q.L. Dai (2001). Reaction-Enhanced Mass Transfer and Transport from Non-Aqueous Phase Liquid Source Zones. *Journal of Contaminant Hydrology,* 49:49-66.

Reitsma, S., and M. Marshall (2000). Experimental Study of Oxidation of Pooled NAPL. The 2nd Intern. Conf. on Remediation of Chlorinated and Recalcitrant Compounds, Monterey, California, Battelle Press.

Reitsma, S., and J. Randhawa (2002). Experimental Investigation of Manganese Dioxide Plugging in Porous Media. In: Gavaskar, A.R. and Chen, A.S.C. (eds.), Proc., 3rd Int. Conf. on Remediation of Chlorinated and Recalcitrant Compounds, Monterey CA, May 2002. Battelle Press, Columbus, OH. 2C-39 (8pp.).

Reynolds, D.A., and B.H. Kueper (2002). Numerical Examination of the Factors Controlling DNAPL Migration through a Single Fracture. *Ground Water*, 40(4):368-377.

Rivett, M.O., S. Feenstra, and J. A. Cherry (2001). A Controlled Field Experiment on Groundwater Contamination by a Multicomponent DNAPL: Creation of the Emplaced-Source and Overview of Dissolved Plume Development. *Journal of Contaminant Hydrology,* 49:111-149.

Ross, B., and N. Lu (1999). Dynamics of DNAPL Penetration into Fractured Porous Media. *Ground Water*, 37(1):140-147.

Rouse, J.D., D.A. Sabatini, and J.H. Harwell (1993). Minimizing Surfactant Losses Using Twin-Head Anionic Surfactants in Subsurface Remediation. *Environmental Science and Technology,* 27(10):2072–2078.

Rubin, C.M., and C.W. Schmid (1980). Pyrimidine-Specific Chemical Reactions Useful for DNA Sequencing. *Nucleic Acids Res.*, 20(8):4613-4619.

Saba, T.A., and T.H. Illangasekare (2000). Effect of Groundwater Flow Dimensionality on Mass Transfer from Entrapped Nonaqueous Phase Liquid Contaminants. *Journal of Contaminant Hydrology,* 51(1-2):63-82.

Saba, T.A. (1999). Upscaling of Mass Transfer from Entrapped NAPLs Under Natural and Enhanced Conditions. Ph.D. Dissertation, University of Colorado, Boulder CO. 204 pp.

Saba, T.A., T.H. Illangasekare, and J.E. Ewing (2001). Investigation of Surfactant-Enhanced Dissolution of Entrapped Non-Aqueous Phase Liquid Chemicals in a Two Dimensional Groundwater Flow Field. *Journal of Contaminant Hydrology*, 51:63-82.

Sabatini, D.A., R.C. Knox, and J.H. Harwell (eds.) (1995). Surfactant-Enhanced Subsurface Remediation. ACS Symp. Series, vol. 594. American Chemical Society, Washington, DC, p. 300.

Sabatini, D.A., R.C. Knox, J.H. Harwell, T.S. Soerens, L. Chen, R.E. Brown, and C. West (1997). Design of a Surfactant Remediation Field Demonstration Based on Laboratory and Modeling Studies. *Ground Water,* 35(6):954-963.

Sabatini, D.A., J.H. Harwell, M. Hasegawa, and R.C. Knox (1998). Membrane Processes and Surfactant-Enhanced Subsurface Remediation: Results of a Field Demonstration. *Journal of Membrane Science,* 151(1):89-100.

Sabatini, D.A., R.C. Knox, and J.H. Harwell (2000). Integrated Design of Surfactant Enhanced DNAPL Remediation: Efficient Supersolubilization and Gradient Systems. *Journal of Contaminant Hydrology,* 45:99-121.

Saenton, S. (2003). Prediction of Mass Flux from DNAPL Source Zone with Complex Entrapment Architecture: Model Development, Experimental Validation, and Up-Scaling. Ph.D. dissertation, Colorado School of Mines, Golden, Colorado. 246 pp.

Saenton, S., T.H. Illangesekare, K. Soga, and T.A. Saba (2002). Effects of Source Zone Heterogeneity on Surfactant-Enhanced NAPL Dissolution and Resulting Remediation End-Points. *Journal of Contaminant Hydrology*, 59:27-44.

Sahl, J. (2005). Coupling In Situ Chemical Oxidation (ISCO) with Bioremediation Processes in the Treatment of Dense Non-aqueous Phase Liquids (DNAPLs). M.S. thesis, Environmental Science and Engineering Division, Colorado School of Mines, Golden, CO. April 2005.

Sahl, J., and J. Munakata-Marr (2006). The Effects of In Situ Chemical Oxidation on Microbial Processes: A Review. *Remediation Journal*, 16(3):57-70.
Sale, T.C., and D.B. McWhorter (2001). Steady State Mass Transfer from Single-Component Dense Nonaqueous Phase Liquids in Uniform Flow Fields. *Water Resources Research,* 37(2):393-404.
Sanford, W.E., R.G. Shropshire, and D.K. Solomon (1996). Dissolved Gas Tracers in Groundwater: Simplified Injection, Sampling and Analysis. *Water Resources Research*, 32:1635-1642.
Saripalli, K.M., H. Kim, P.S.C. Rao, and M.D. Annable (1997). Measurement of Specific Fluid-Fluid Interfacial Areas of Immiscible Fluids in Porous Media. *Environmental Science and Technology,* 31(3): 932-936.
Schlegel, G. (1977). Aeration Without Air: Oxygen Supply by Hydrogen Peroxide. *Biotechnology and Bioengineering*, 19:413-424.
Schnarr, M., C. Truax, G. Farquhar, E. Hood, T. Gonullu, and B. Stickney (1998). Laboratory and Controlled Field Experiments Using Potassium Permanganate to Remediate Trichloroethylene and Perchloroethylene DNAPLs in Porous Media. *Journal of Contaminant Hydrology,* 29:205-224.
Schroth, M.H., M. Oostrom, T.W. Wietsma, and J.D. Istok (2001). In-Situ Oxidation of Trichloroethene by Permanganate: Effects on Porous Medium Hydraulic Properties. *Journal of Contaminant Hydrology,* 50:79-98.
Schumb, W.C., C.N. Satterfield, and R.L. Wentworth (1955). Hydrogen Peroxide. Reinhold Publishing Corp., New York.
Schwarzenbach, R.P., P.M. Gschwend, and D.M. Imboden (1993). Environmental Organic Chemistry. John Wiley & Sons, Inc. New York.
Schwille, F. (1988). Dense Chlorinated Solvents in Porous and Fractured Media. Lewis Publishers, Chelsea, MI. Translated by J.F. Pankow, 146 pp.
Scott, J.P., and D.F. Ollis (1995). Integration of Chemical and Biological Oxidation Processes for Water Treatment: Review and Recommendations. *Environmental Progress*, 14(2):88-103.
Seagren, E.A., and T.O. Moore, II (2003). Nonaqueous Phase Liquid Pool Dissolution as a Function of Average Pore Water Velocity. *Journal of Environmental Engineering,* 129(9):786-799.
Seitz, S.J. (2004). Experimental Evaluation of Mass Transfer and Matrix Interactions During In Situ Chemical Oxidation Relying on Diffusive Transport. M.S. thesis, Environmental Science and Engineering Division, Colorado School of Mines, Golden, CO. December 2004.
Seol, Y., H. Zhang, and F.W. Schwartz (2003). A Review of In Situ Chemical Oxidation and Heterogeneity. *Environmental and Engineering Geosciences*, 9(1):37-49.
Sherwood, T.K., R.L. Pigford, and C.R. Wilke (1975). Mass Transfer. McGraw-Hill, New York, NY. 677 pp.
Shiau, B.J. (2003). In-Situ Surfactant and Chemical Oxidant Flushing for Complete Remediation of Contaminants and Methods of Using Same. U.S. Patent Application Publication No. 2003/0175081.
Shiau, B.J., D.A. Sabatini, and J.H. Harwell (1994). Solubilization and Mobilization of DNAPLs Using Direct Food Additive (Edible) Surfactants. *Ground Water* 32(4):561-569.
Siegrist, R.L., and Lowe, K.S. (eds.). (1996). In Situ Remediation of DNAPL Compounds in Low Permeability Media: Fate/Transport, In Situ Control Technologies, and Risk Reduction. Oak Ridge National Laboratory Rep. No. ORNL/TM-13305 for the DOE Office of Science and Technology.
Siegrist, R.L., K.S. Lowe, L.D. Murdoch, W.W. Slack, and T.C. Houk (1998). X-231A Demonstration of In Situ Remediation of DNAPL Compounds in Low Permeability Media by Soil Fracturing with Thermally Enhanced Mass Recovery or Reactive Barrier Destruction. Oak Ridge National Laboratory Report. ORNL/TM-13534. Oak Ridge, TN.
Siegrist, R.L., K.S. Lowe, L.C. Murdoch, T.L. Case, and D.A. Pickering (1999). In Situ Oxidation by Fracture Emplaced Reactive Solids. *Journal of Environmental Engineering*, 125(5):429-440.
Siegrist, R.L., M.A. Urynowicz, O.R. West, M.L. Crimi, and K.S. Lowe (2001). Principles and Practices of In Situ Chemical Oxidation Using Permanganate. Columbus. Ohio, Battelle Press.

Siegrist, R.L., M.A. Urynowicz, M.L. Crimi, and K.S. Lowe (2002). Genesis and Effects of Particles Produced During In Situ Chemical Oxidation Using Permanganate. *Journal of Environmental Engineering*, 128(11):1068-1079.

Sillan, R.K., P.S.C. Rao, M.D. Annable, D. Dai, K.G. Hatfield, A.L. Wood, and C.G. Enfield (1998). Evaluation of In-Situ Cosolvent Flushing Dynamics Using a Network of Spatially Distributed Multilevel Samplers. *Water Resources Research*, 34(9):2191-2202.

Simon, M., M.L. Brusseau, R. Golding, and P.J. Cagnetta (1998). Organic and Aqueous Partitioning Gas Tracer Field Experiment. Proc. Conf. Remediation of Chlorinated and Recalcitrant Compounds. Monterey, CA. May 8–21, Battelle, Columbus, OH.

Soerens, T.S., D.A. Sabatini, and J.H. Harwell (1998). Effects of Flow Bypassing and Nonuniform NAPL Distribution on the Mass Transfer Characteristics of NAPL Dissolution. *Water Resources Research,* 34(7):1657-1673.

Stewart, R. (1965). Oxidation by Permanganate. In: Wiberg, K.B. (ed.), Oxidation in Organic Chemistry, Part A, Chap. 1. Academic Press, New York, NY. pp. 1-68.

Stokley, K.E., E.N. Drake, and R.C. Prince (1997). The Role of Fenton's Reagent in Soil Bioremediation. Fourth International In Situ and On-Site Bioremediation Symposium, New Orleans, LA, 487-492.

Stroo, H.F., M. Unger, C.H. Ward, M.C. Kavanaugh, C. Vogel, A. Leeson, J.A. Marqusee, and B.P. Smith (2003). Remediating Chlorinated Solvent Source Zones. *Environmental Science and Technology*, 37(11):224A-230A.

Struse, A.M. (1999). Mass Transport of Potassium Permanganate in Low Permeability Media and Matrix Interactions. M.S. thesis, Colorado School of Mines, Golden. 86 pp.

Struse, A.M., R.L. Siegrist, H.E. Dawson, and M.A. Urynowicz (2002). Diffusive Transport of Permanganate During In Situ Oxidation. *Journal of Environmental Engineering*, 128(4):327-334.

Taylor, T.P., K.D. Pennell, L.M. Abriola, and J.H. Dane (2001). Surfactant Enhanced Recovery of Tetrachloroethylene from a Porous Medium Containing Low Permeability Lenses: 1. Experimental Studies. *Journal of Contaminant Hydrology*, 48(3-4):325-350.

Ter Meer, J., M.V. Eekert, J. Gerritse, and Rijnaarts (2001). Hydrogen as Indicator of Redox Conditions and Dechlorination. In: Natural Attenuation of Environmental Contaminants, Battelle Press, Columbus, Ohio.

Thomson, N.R., E. Hood, and L.K. MacKinnon (2000). Source Zone Mass Removal Using Permanganate: Expectations and Potential Limitations. The 2nd Intern. Conf. on Remediation of Chlorinated and Recalcitrant Compounds, Monterey, California, Battelle Press.

Tidwell, V.C., L.C. Meigs, T. Christian-Frear, and C.M. Boney (2000). Effects of Spatially Heterogeneous Porosity on Matrix Diffusion as Investigated by X-ray Absorption Imaging. *Journal of Contaminant Hydrology*, 42(2):285-302.

Tranvik, L.J., and S. Bertilisson (2001). Contrasting Effects of Solar UV Radiation of Dissolved Organic Sources for Bacterial Growth. *Ecology Letters*, 4(5):458-463.

Tyre, B.W., R.J. Watts, and G.C. Miller (1991). Treatment of Four Biorefractory Contaminants in Soils Using Catalyzed Hydrogen Peroxide. *Journal of Environmental Quality*, 20(4):832-838.

Urynowicz, M.A. (2000). Dense Nonaqueous Phase Trichloroethene Degradation with Permanganate Ion. Doctor of Philosophy, Colorado School of Mines, Golden. 149 pp.

USEPA (1992). Dense Non-Aqueous Phase Liquids—A Workshop Summary. U.S. EPA Rep. No. EPA/600/R-92/030, Office of Research and Development, Washington D.C., 78 pp.

USEPA (1993). Evaluation of the Likelihood of DNAPL Presence at NPL Sites. U.S. EPA Rep. No. EPA/540/R-93/073, Office of Solid Waste and Emergency Response, Washington D.C. 114 pp., http://www.epa.gov/superfund/resources/remedy/pdf/540r-93073-s.pdf.

USEPA (1998). In Situ Remediation Technology: In Situ Chemical Oxidation. EPA/542/R96/005, Office of Solid Waste and Emergency Response, Washington D.C. 39 pp.

USEPA (1998). Field Applications of In Situ Remediation Technologies: Chemical Oxidation. EPA 542-R-98-008. Office of Solid Waste and Emergency Response, USEPA, Washington, D.C.

USEPA (2003). The DNAPL Remediation Challenge: Is there a Case for Source Depletion? U.S. EPA Rep. No. EPA/600/R-03/143, Office of Research and Development, Washington D.C., 129 pp., http://www.epa.gov/ada/download/reports/600R03143/600R03143-fm.pdf.

USEPA (2004a). Contaminant Focus-Trichloroethylene. U.S. EPA, Technology Innovation Program, Washington D.C. http://www.clu-in.org/contaminantfocus/default.focus/sec/Trichloroethylene_(TCE)/cat/Overview/.

USEPA (2004b). Discussion paper--Cleanup Goals Appropriate for DNAPL Source Zones. U.S. EPA, Office of Solid Waste and Emergency Response, Washington D.C., 16 pp., http://gwtf.cluin.org/docs/options/dnapl_goals_paper.pdf.

Valentine, R.L., and H.C. Wang (1998). Iron Oxide Surface Catalyzed Oxidation of Quinoline by Hydrogen Peroxide. *Journal of Environmental Engineering,* 124(31):34-38.

van Genuchten, M.T., and W.J. Alves (1982). Analytical Solutions of the One-Dimensional Convective-Dispersive Solute Transport Equation. USDA, Agricultural Research Service. Technical Bulletin Number 1661**:** 151.

Vella, P.A., and B. Veronda (1994). Oxidation of Trichloroethylene: A Comparison of Potassium Permanganate and Fenton's Reagent. Proc., 3rd Intl. Symposium, Chemical Oxidation: Technologies for the Nineties, Vol. 3. Vanderbilt University, Nashville, TN, Feb 1993. Technomic Publishing, Lancaster, PA. pp. 62-73.

Voelker, B.M., and B. Sulzberger (1996). Effects of Fulvic Acid on Fe(II) Oxidation by Hydrogen Peroxide. *Environmental Science and Technology*, 30:1106-1114.

Vitolins, A.R., B.R. Nelson, and S.A. Underhill (2003). Fenton's Reagent-Based In Situ Chemical Oxidation Treatment of Saturated and Unsaturated Soils at a Historic Railroad Site. *Soil and Sediment Contamination*, 12(1):139-150.

Watts, R.J., P.A. Rausch, S.W. Leung, and M.D. Udell (1990). Treatment of Pentachlorophenol-Contaminated Soils Using Fenton's Reagent. *Journal of Hazardous Waste and Hazardous Materials*, 7:335-345.

Watts, R.J. (1992). Hydrogen Peroxide for Physicochemically Degrading Petroleum – Contaminated Soils. *Remediation Journal*, Autumn 1992, pp. 413-425.

Watts, R.J., M.D. Udell, and R.M. Monson (1993). Use of Iron Minerals in Optimizing the Peroxide Treatment of Contaminated Soils. *Water Environment Research*, 65, 832–838.

Watts, R.J., S. Kong, M. Dippre, and W.T. Barnes (1994). Oxidation of Sorbed Hexachlorobenzene in Soils Using Catalyzed Hydrogen Peroxide. *Journal of Hazardous Materials*, 39:33-47.

Watts, R.J., and S.E. Dilley (1996). Evaluation of Iron Catalysts for the Fenton-Like Remediation of Diesel Contaminated Soils. *Journal of Hazardous Materials,* 51:209-224.

Watts, R.J., A.P. Jones, P.H. Chen, and A. Kenny (1997). *Water Environment Research*, 69:269-275.

Watts, R.J., M.D. Udell, S.H. Kong, and S.W. Leung (1999). *Environmental Engineering Science,* 16:93-103.

Watts, R.J., B.C. Bottenburg, T.F. Hess, M.D. Jensen, A.L. Teel (1999a). Role of Reductants in the Enhanced Desorption and Transformation of Chloroaliphatic Compounds by Modified Fenton's Reactions. *Environmental Science and Technology*, 33(19):3432-3437.

Watts, R.J., M.K. Foget, S. Kong, A.L. Teel (1999b). Hydrogen Peroxide Decomposition in Model Subsurface System. *Journal of Hazardous Materials*, 69:229-243.

Watts, R.J., P.C. Stanton, J. Howsawkeng, and A.L. Teel (2002). Mineralization of a Sorbed Polycyclic Aromatic Hydrocarbon in Two Soils using Catalyzed Hydrogen Peroxide. *Water Research*, 36(17):4283–4292.

Weber Jr., W.J. (1972). Physicochemical Processes for Water Quality Control. New York, N.Y.: Wiley-Interscience.

Wilking, B. (2004) Factors Controlling Matrix Storage During DNAPL Mass Depletion in Heterogeneous Porous Media. M.S. thesis, Colorado School of Mines, Golden, CO. 183 pp.

Wilson, R.D., and D.M. Mackay (1995). Direct Detection of Residual Nonaqueous Phase Liquid in the Saturated Zone using SF_6 as a Partitioning Tracer. *Environmental Science and Technology*, 29:1255-1258.

Wyllie, M.R.J. (1962). Relative Permeability. In: Petroleum Production Handbook, Reservoir Engineering, Vol. II, Frick, T.C. (ed.). McGraw-Hill, New York, NY.

Xie, G., and M.J. Barcelona (2003). Sequential Chemical Oxidation and Aerobic Biodegradation of Equivalent Carbon Number-based Hydrocarbon Fractions in Jet Fuel. *Environmental Science and Technology,* 37(20):4751-4760.

Yan, Y.E., and F.W. Schwartz (1999). Oxidative Degradation and Kinetics of Chlorinated Ethylenes by Potassium Permanganate. *Journal of Contaminant Hydrology,* 37:343-365.

Yan, E.Y., and F.W. Schwartz (2000). Kinetics and Mechanisms for TCE Oxidation by Permanganate. *Environmental Science and Technology*, 34(12):2535-2541.

Yeh, C.K., Y. Kao, and C. Cheng (2002). Oxidation of Chlorophenols in Soil at Natural pH by Catalyzed Hydrogen Peroxide: The Effect of Soil Organic Matter. *Chemosphere*, 46:67-73.

Young, C.M., R.E. Jackson, M. Jin, J.T. Londergan, P.E. Mainer, G.A. Pope, F.J. Anderson, and T. Houk (2001). Characterization of a TCE DNAPL Zone in Alluvium by Partitioning Tracers. *Ground Water Monitoring and Remediation*, 19(1):84-94.

Zeng, Y., P.K. Hong, and D. Wavrek (2000). Integrated Chemical-Biological Treatment of Benzo[a]pyrene. *Environmental Science and Technology*, 34:854-862.

Zhang, H., and F.W. Schwartz (2000). Simulating the In Situ Oxidative Treatment of Chlorinated Ethylenes by Potassium Permanganate. *Water Resources Research*, 36(10):3031-3042.

Zhu, J., and J.F. Sykes (2000). The Influence of NAPL Dissolution Characteristics on Field-Scale Contaminant Transport in Subsurface. *Journal of Contaminant Hydrology*, 41:133-154.

CHAPTER 3

MATERIALS AND METHODS

3.1. SPECIFIC EXPERIMENTAL OBJECTIVES AND APPROACHES

To accomplish the goals outlined in Chapter 1, controlled experimentation was carried out using different experimental approaches and apparatus. A summary of the specific objectives of each series of experiments follows.

3.1.1. Bench-Scale Kinetic and DNAPL Degradation Studies

Bench-scale studies involving aqueous phase vial reactors (VRs) were used to determine how dissolved phase reaction kinetics for TCE and PCE are affected by the composition of the bulk aqueous phase. Conditions that were investigated include the presence or absence of natural organic mater (NOM), the impact of porous media, buffered versus unbuffered aqueous phases, and the concentration and type of oxidants used. Additional studies conducted in multiphase vial reactors (MVRs), investigated the impact of ISCO on TCE and PCE DNAPL mass transfer rates as a function of aqueous phase compositions. The phase compositions investigated in MVRs included the presence or absence of NOM, two varied compositions of NOM, and the oxidant type and loading to the system. A series of response variables, described in Section 3.2.5, were developed that evaluate the efficiency and effectiveness of ISCO under the varied phase compositions investigated in the VRs and MVRs.

3.1.2. Bench-Scale Studies of Porous Media Effects on Oxidation Reactions

Bench-scale studies involving slurry reactors and diffusion cells were used to determine the effects of porous media of varying properties on oxidant transport and the degradation of DNAPLs. These were conducted under contrasting transport regimes of either completely mixed systems or static, diffusion-controlled systems. Zero-headspace reactors (ZHRs) were utilized to investigate the impact of differing contaminant types, masses of contaminants, the presence and composition of NOM, oxidant type and oxidant load on the efficiency and effectiveness of ISCO within well-mixed soil slurry systems. Steady-state diffusion tests were performed to determine the viability of diffusive transport of oxidants potassium permanganate and catalyzed hydrogen peroxide for contaminant destruction in low permeability media, as well as calculating diffusion coefficients for both oxidants. Impacts to porous media properties due to of oxidation were also determined. As part of the investigation into diffusive transport of oxidants, it was necessary to evaluate natural oxidant demand (NOD) for the porous media under investigation, and to determine if CHP could be stabilized to promote diffusive transport.

3.1.3. Upscaling Reactive Transport During ISCO: Experimental and Modeling Studies

Bench and intermediate scale studies were used to evaluate the reaction and transport processes that occur at the pilot-scale, including the effects of ISCO systems of varied designs on different DNAPL mass and entrapment architectures. Bench scale 1-D flow-through tube reactor studies (FTRs) were utilized, focusing on permanganate, to investigate the impact of varied oxidant delivery velocities and concentrations on mass depletion rates and treatment efficiencies in systems with varied DNAPL types and entrapment architectures. Further experimentation was conducted in 2-D flow-cell systems, which investigated varied oxidant types and delivery techniques on an experimental system with a more complex source architecture and flow field. Finally, several intermediate-scale and large-scale 2-D tank systems were used to investigate complex DNAPL entrapment architectures and complex heterogeneous flow fields to determine impacts to DNAPL mass depletion and mass flux resultant of ISCO using permanganate, with particular emphasis on the reduction in permeability due to manganese oxide

precipitation. In addition to providing a thorough investigation of the impacts to DNAPL mass depletion and mass transfer by ISCO within flowing systems, these experiments assisted with testing of a model, which was developed as part of this project, as well as in cooperation with SERDP project CU-1294: Mass Transfer from Entrapped DNAPL Sources Undergoing Remediation: Characterization Methods and Prediction Tools. This new model, CORT3D, based on the RT3D modeling code, was developed to account for interactions between permanganate, multiple rate-limited natural oxidant demand fractions, DNAPL mass transfer, and changes in porous media flow properties resulting from permanganate oxidation.

3.1.4. Experimental Evaluation of Coupling ISCO

Extensive experimentation was performed to evaluate the viability and effectiveness of coupling other remediation technologies with ISCO systems of varying designs. Studies were conducted to investigate the feasibility and design considerations of coupling ISCO with both anaerobic and aerobic bioremediation technologies, utilizing batch microcosm studies and 1-D column experiments. Experimentation also investigated coupling ISCO with surfactant and cosolvent remediation. Batch screening studies were conducted to determine which surfactants and cosolvents were most compatible with the oxidants in this study, and follow up experimentation was conducted within a 2-D flow cell to determine the effectiveness of various coupling regimes.

3.1.5. Evaluation of Partitioning Tracer Test (PTT) Methods for ISCO Site Characterization and Performance Monitoring

Experimentation was conducted to evaluate whether or not partitioning tracer test methods provide a viable way to measure DNAPL mass removals after ISCO has been applied to a DNAPL site. Experiments were conducted to determine how residual oxidant, as well as MnO_2 deposition at the NAPL-water interface, might impact alcohol and ketone tracers and their respective NAPL-water partitioning coefficients. Effective tracers were then applied in 2-D flow cell systems to determine how effective they are at measuring performance at ISCO treated sites.

3.2. MATERIALS AND METHODS COMMON TO MULTIPLE EXPERIMENTAL STUDIES

A wide variety of materials and methods were employed to investigate application of oxidants to DNAPL contamination to meet the objectives of this project. However, whenever practical, common materials, experimental apparatus, reagents or analytical methods were employed to facilitate the comparison of results from one project component to another. Furthermore, materials were utilized that have been well characterized by previous CSM research (e.g. Struse 1999, Van Cuyk *et al.* 2001) to reduce characterization needs and to minimize uncertainty about their performance in experimental systems. This section presents a summary of common materials and methods that were used for the primary experimental efforts completed during the course of SERDP project CU-1290.

3.2.1. Conceptual Model Used for Experimental Design

A conceptual model for conditions in the subsurface during the injection of oxidant into the subsurface at a DNAPL site is presented in Figure 3.1. The oxidant concentration and groundwater velocity profile at an ISCO site may vary greatly depending on selected design parameters and site conditions such as the injection method selected, the injection flow rate, the concentration of oxidant, the DNAPL architecture and the type of the DNAPL. In this conceptual model, in areas adjacent to the injection well or probe (condition 1), the velocity is high because of the fluid addition. However, as distance from the well increases (conditions 2 and 3), the velocity decreases due to the radial flow pattern away from the well. Oxidant concentration is also highest next to the well at the point of injection

(condition 1). However, oxidant concentrations also decrease as distance to the well increases both due to consumption of the oxidant by contaminant and aquifer materials, as well as by dilution with surrounding groundwater (conditions 2 and 3).

As Figure 3.1 suggests, a complex distribution of varying oxidant concentrations and varying velocities in the subsurface can result, even in relatively simple homogeneous systems. The addition of heterogeneity such as layering in the subsurface would likely add to this complexity. The goal of the experimental approach selected for this study was to test a wide range of velocities and oxidant concentrations that may represent site conditions at particular points within the conceptual model, such as at condition 1 or condition 2.

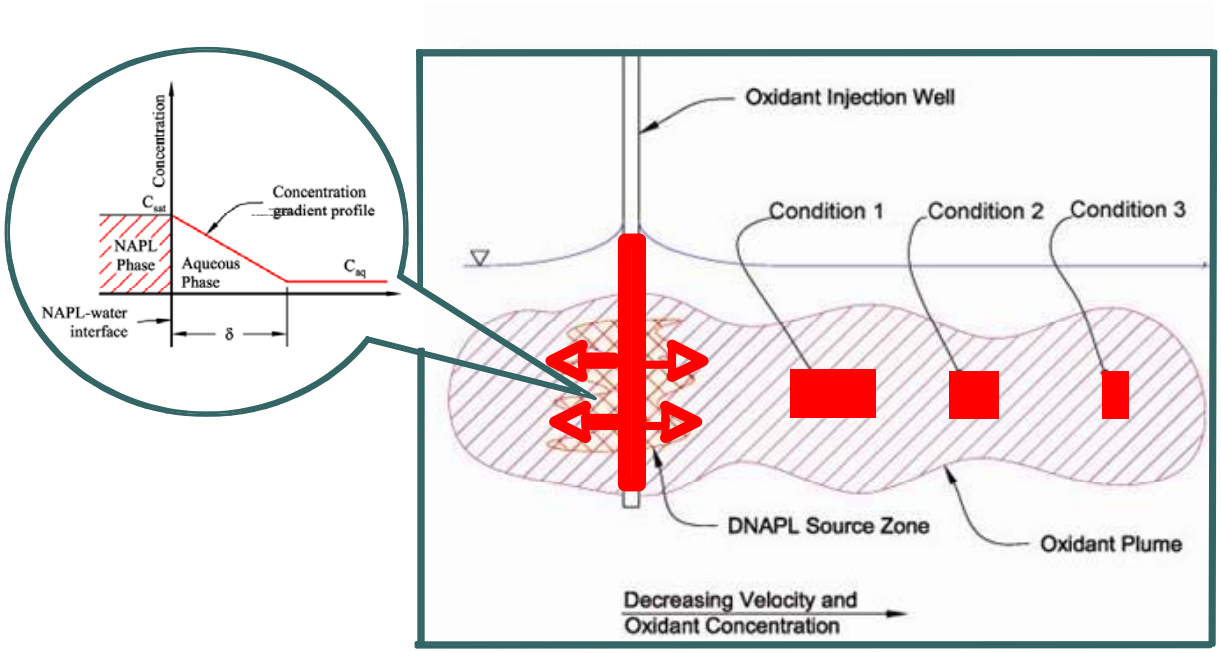

Figure 3.1. Conceptual model for design of experiments to evaluate ISCO applied to DNAPL sites.

3.2.2. Porous Media Types Used in Investigations

Several different porous media types were utilized in these investigations. These include a laboratory base sand, a field soil from the Colorado School of Mines Wastewater Reclamation Field Test Site in Golden, CO (Mines Park), a field soil from the Naval Training Center in Orlando, FL (NTC soil), and 7 commercially available silica sands supplied by the Unimin, Wedron, U.S. Silica and Manley Brothers corporations. These media types were selected to represent a wide range of media properties, including varied hydraulic conductivities, total organic carbon (TOC) contents, and particle size distributions. The properties of these media types are summarized in Table 3.1.

Table 3.1. Properties of porous media utilized in this study.

Properties	Base sand	Mines Park (MP)	NTC field soil	#8 sand (Unimin)	#16 sand (Unimin)	#30 sand (Unimin)	#50 sand (Wedron)	#70 sand (Unimin)	#110 sand (U.S. Silica)	#140 sand (Manley Bros.)
Soil type	Silica sand	Sandy loam	Silica sand	Silica sand	Silica sand	Silica sand	Silica sand	Silica sand	Silica sand	Silica sand
Soil pH	6.8[a]	6.24[b]	6.7[c]	7.39[b]	7.39[b]	7.39[b]	7.39[b]	7.39[b]	7.39[b]	7.39[b]
TOC content (dry wt. %)	0.017%[a]	1.37%[b]	0.38%[c]	0.019%[b]	0.019%[b]	0.019%[b]	0.019%[b]	0.019%[b]	0.019%[b]	0.019%[b]
d_{10} / d_{60} or d_{50}, (U)[h]	0.22 / 0.60[a]	0.079 / 0.32[b]	0.141 / 0.263[c]	0.125 (1.56)[d]	0.088 (1.72)[d]	0.049 (1.50)[d]	0.030 (1.94)[d]	0.019 (1.86)[d]	0.010 (2.00)[d]	0.025 / 0.079[b]
Particle density (g/cm^3)	2.65	2.44[b]	-	2.65[e]	2.65[e]	2.65[e]	2.65[e]	2.65[e]	2.65[e]	2.65[b]
Dry bulk density (g/cm^3)	1.70[g]	1.52[b]	1.83[e]	1.6[e]	1.6[e]	1.6[e]	1.8[e]	1.6[e]	1.8[e]	1.6[e]
Saturated hydraulic conductivity (cm/min)	1.92[a]	0.029[b]	-	101.3[d]	37.5[d]	11.8[d]	2.267[d]	1.458[d]	0.383[d]	0.126[f]

References: [a](Van Cuyk *et al.* 2001), [b](Seitz 2004), [c](Crimi and Siegrist 2004), [d](Saenton, 2001), [e](Heiderscheidt 2005), [f](Wilking 2004), [g](Sahl 2005), [h]Uniformity coefficient

3.2.3. Ground Water Types Used in Investigations

In addition to utilizing different porous media types, the effects of ISCO were evaluated in several different ground water types. These included a simulated ground water, prepared in the lab from deionized water and reagent grade salts, a ground water from the CSM Wastewater Reclamation Field Test Site in Golden, CO, a ground water from the Naval Training Center (NTC) in Orlando, FL, and tap water from the City of Golden, CO municipal water supply. The simulated ground water allowed for investigation of ISCO interactions in a ground water matrix that is representative of subsurface conditions, while retaining control over the composition of that ground water. The two field ground waters allowed for the investigation of ISCO in more complex ground water matrices, particularly due to the introduction of significant dissolved organic carbon (DOC) content. Finally, tap water was utilized in the large tank experiments, as the large volume of water required for these experiments made it impractical to use any other water source. The properties of these water sources are summarized in Table 3.2.

3.2.4. Properties of Key Reagents Used in this Study

This study focused on two DNAPL types, trichloroethene (TCE) and tetrachloroethene (PCE), as well as two ISCO agents, potassium permanganate ($KMnO_4$) and catalyzed hydrogen peroxide (CHP). 5 mM ferrous sulfate has been used in published literature to activate CHP (e.g. Watts and Dilly 1996, Watts and Stanton 1999) and was used in many of the experiments as an activation method. In several experimental systems, humic acid was used as a surrogate for natural organic matter and goethite as a surrogate for natural iron bearing minerals. Information about the main reagents used for this study is presented in Table 3.3.

Table 3.2. Properties of ground water sources used in this study.

Property	Simulated groundwater[a]	Mines park groundwater (MP)[b]	NTC groundwater[c]	Tap water[d]
pH	7.0[a]	7.71	5.7[b]	7.4
Conductivity (μmhos)	277[a]	467	165[b]	348
Alkalinity (mg/L as $CaCO_3$)	40[a]	147	43.5[b]	35.2
DOC (mg/L)	0.3[e]	1.27	2.09[b]	1.14 (TOC)
Fluoride (mg/L)	BDL	0.53	1.86	1.5
Chloride (mg/L)	52.5	18.9	1.35	25
Bromide (mg/L)	BDL	n/a	n/a	BDL
Nitrate (mg/L)	0.73	2.09	BDL	0.89
Phosphate (mg/L)	BDL	0.09	BDL	BDL
Sulfate (mg/L)	98.8	37.59	18.06	75.3
Total solids (mg/L)	n/a	n/a	135	200
TDS (mg/L)	211.9	n/a	170	185
Calcium (mg/L)	41.2	37.8	18.3	27.4
Magnesium (mg/L)	17.5	27.3	3.3	7.85
Sodium (mg/L)	0.27	22.3	15.6	25.4
Potassium (mg/L)	0.44	4.99	2.03	5.66
Iron (mg/L)	0.44	0.33	0.07	0.04
Manganese (mg/L)	0.00	n/a	0.03	0.02

References: [a](Struse 1999), [b](Seitz 2004), [c](Crimi and Siegrist 2004), [d](Heiderscheidt 2005), [e](Sahl 2005)
BDL = Below detection limit

Table 3.3. Sources and properties of main reagents used in this study.

Reagent	Trichloroethene	Tetrachloroethene	Potassium permanganate	Hydrogen peroxide	Ferrous sulfate heptahydrate	Humic acid	Goethite [$Fe^{3+}O(OH)$]
Manufacturer	Mallinckrodt	Mallinckrodt	Carus Chemical	Mallinckrodt	Mallinckrodt	Fluka	Alfa Aesar
Grade	Analytical	Analytical	Cairox USP	Analytical	Analytical	Technical	Analytical
Concentration	100%	99%	99%	30%	100%	N/A	100%
Solubility (mg/L)	1447[a]	206[a]	64000[b]	miscible[b]	soluble[b]	insoluble	insoluble
Density	1.462[b]	1.623[b]	2.703[b]	1.407[b]	1.898	N/A	3.3-3.9
Molecular weight	131.4	165.8	158.03	34.01	278.0	N/A	88.85

[a] In simulated ground water at 25°C measured by Petri (2006), [b](Chemfinder.com 2006)

3.2.5. Quantitative Analytical Methods

A variety of analytical methods were employed throughout the SERPD project to measure concentrations of contaminants, oxidants, byproducts and geochemical effects. In some cases, multiple methods were used to measure concentrations of the same compounds, due to sampling method needs. Table 3.4 summarizes these methods.

Table 3.4. Analytical method summaries.

Method	Sample type	Equipment used	Detectable analytes
Gas chromatography with electron capture detection (GC-ECD)	Hexane phase from aqueous extraction	HP 6890 GC with ECD, 7683 autosampler, HP-624 0.53mm column	PCE, TCE and cis-DCE
Gas chromatography with flame ionization detection (GC-FID)	Aqueous	HP 6890 GC with FID, 7683 autosampler, HP-624 0.53mm column	PCE, TCE, phenol, methanol, partitioning tracers
Gas chromatography with flame ionization detection (GC-FID)	Headspace	HP 6890 GC with FID, manual injection, HP-624 0.53mm column	PCE, TCE, cis-DCE, VC, ethene,
Ion chromatography with organic acid analysis (IC-ORGAC)	Aqueous	Dionex DX-600 system with AS11-HC column, 12mM NaOH eluent	Chloride, bromide, nitrate, sulfate, acetate, formate, oxalate, monochloroacetate, dichloroacetate
Ion chromatography with standard anion analysis (IC-6ANION)	Aqueous	Dionex DX-600 system with AS14 column, 1 mM $NaHCO_3$, 8mM Na_2CO_3 eluent	Chloride, bromide, nitrate, sulfate, phosphate, fluoride
Permanganate absorbance at 525 nm (HACH-525)	Aqueous, 0.2 micron filtered	Hach DR 4000 spectrophotometer	Permanganate ion
Hydrogen peroxide idometric titration	Aqueous	Hach HYP-1 hydrogen peroxide test kit	Hydrogen peroxide
Phenol photometric method (Standard Method 5530)	Aqueous	Hach DR 4000 spectrophotometer	Phenol
Chemical oxygen demand (COD) test	Aqueous	Hach COD TNTplus low and high range test kits, Hach DR4000 spectrophotometer	COD in water
Dissolved organic carbon (DOC) absorbance at 254 nm (HACH-254)	Aqueous	Hach DR 4000 spectrophotometer	DOC in water
Dissolved organic carbon (DOC) by catalyst aided combustion	Aqueous	Shimadzu 400 TOC analyzer for water	DOC in water
Total organic carbon (TOC) in soil	Soil solids	Coulometrics TOC analyzer for solids	TOC in soil
Inductively coupled plasma – atomic emission spectrometry (ICP-AES)	Aqueous, acidified	Perkin-Elmer Optima 3000 ICP-AES	Major metal cations in water, (typically iron and manganese)
Exchangeable cations	Soil solids	Adapted from method 19.2 for exchangeable cations by BaCl, analysis by ICP-AES	Exchangeable cations in porous media
Alkalinity titration	Aqueous	Hach Alkalinity titration kit	Alkalinity
Particle distribution in porous media	Soil solids	Hydrometer and ASTM E11 sieve analysis	Particle size distribution and uniformity index

3.2.6. Common Data Analysis Techniques

Over the course of this project, several different experimental systems in different apparatuses yielded data that could be analyzed in similar fashion. Thus, several common variables were developed allowing for evaluation of system efficiency and effectiveness, which could be compared from one system to another. These performance indicators were particularly useful in comparing various batch scale systems, but are applicable to some flowing systems as well. The description of these performance indicators follows.

K_{ox}	=	Pseudo first-order effective rate constant for oxidant consumption, based on permanganate concentration versus time data. Lower values indicate a more efficient system with better oxidant persistence and lower oxidant demand. (Units of $time^{-1}$)
K_{DNAPL}	=	Pseudo first-order effective rate constant for DNAPL destruction, based on contaminant concentration versus time data. Indicates effectiveness of remediation, as faster DNAPL destruction may yield larger mass removals as well as faster cleanup times. (Units of $time^{-1}$)
RTE	=	K_{ox} / K_{DNAPL}, the relative treatment efficiency, which indicates efficiency of oxidant use, with a lower value being more desirable (unitless). A value less than 1 indicates that DNAPL is being destroyed faster than oxidant is being consumed, and thus a more efficient system. Values higher than 1 indicate that oxidant is being consumed faster than the DNAPL, indicating inefficient conditions.
Oxidant Demand	=	(initial mol oxidant – final mol oxidant) / (Initial mol DNAPL – final mol DNAPL), indicates the amount of oxidant needed to degrade a given amount of DNAPL under the conditions tested. A lower value is more efficient. (Units of $mol_{oxidant}$ / mol_{DNAPL})
Media Demand	=	(initial oxidant mass – final oxidant mass) / (mass of media), which indicates the amount of oxidant consumed by contaminated media. Note that this includes oxidant demand due to DNAPL degradation if DNAPL is present in the system. Lower values are more efficient. (Units of $mg_{oxidant}$ / kg_{media})
% DNAPL Destroyed	=	100 x (initial DNAPL mass – final DNAPL mass) / initial DNAPL mass, which indicates remediation effectiveness. (Unitless)

3.3. BENCH-SCALE KINETIC AND DNAPL DEGRADATION STUDIES

Two series of experiments were conducted under this portion of the project, which included aqueous phase vial reactors and multiphase vial reactors. Additional method information for experimental work using both VRs and MVRs is available in Jackson (2004).

3.3.1. Aqueous Phase Vial Reactor Studies

Aqueous phase vial reactor experiments were conducted in 20mL amber glass vials with Teflon lined caps. Experiments were conducted using simulated ground water as an aqueous phase, and base sand as a porous media. A large number of conditions were tested in a fractional factorial experiment design, with oxidant type ($KMnO_4$ vs. CHP), oxidant concentration (2x vs. 10x stoichiometric demands), media (10 wt.% vs. none), and natural organic mater (0.2 wt.% vs. none) as primary factors, giving a 2^4

design, or 16 runs. Secondary factors as part of the design included pH buffering (buffered vs. unbuffered) and contaminant type (aqueous TCE vs. aqueous PCE). Several additional conditions outside the factorial design evaluated the impact of aqueous mixtures of TCE and PCE. The conditions tested are included in Table 3.5.

Table 3.5. Experimental conditions tested in VRs.

Run[a] #	NOM	Oxidant concentration	Media	pH	Contaminant type
1, 9	0.2 wt.%	10x	10 wt.%	buffered	PCE
2, 10	none	10x	10 wt.%	unbuffered	PCE
3, 11	0.2 wt.%	2x	10 wt.%	unbuffered	TCE
4, 12	none	2x	10 wt.%	buffered	TCE
5, 13	0.2 wt.%	10x	none	buffered	TCE
6, 14	none	10x	none	unbuffered	TCE
7, 15	0.2 wt.%	2x	none	unbuffered	PCE
8, 16	none	2x	none	buffered	PCE
17, 19	none	10x	none	buffered	PCE & TCE
18, 20	0.2 wt.%	2x	10 wt.%	buffered	PCE & TCE

[a]Runs 1-8, 17, 18 are with $KMnO_4$, 9-16, 19, 20 are with CHP

Humic acid was used as a surrogate for NOM. For permanganate runs, pH was phosphate buffered to pH 7, and adjusted to pH 3 with sulfuric acid for CHP runs. All CHP runs included a 5mM ferrous sulfate solution to catalyze the oxidation reaction. Sacrificial vials were prepared according to the conditions above for sampling at 0, 1, 3, 10, 30 and 100 minute time points, and all vials were run in duplicate. Aqueous phase PCE and TCE contamination in simulated ground water was emplaced through septa to achieve concentrations at 1/5 saturation, and the VRs were shaken for 1 hour to equilibrate. Oxidant was added through the septa at time 0. Vials were sacrificed at each time point and sampled for TCE and PCE, MnO_4^-, H_2O_2, COD, chloride, DOC, metals, pH, temperature, and solid phase TOC in systems with media. Data were analyzed with the factorial design using Minitab, statistical analysis program, with respect to the common performance indicators K_{ox}, K_{DNAPL}, RTE, oxidant demand, media demand, and % DNAPL destroyed. For K_{DNAPL}, no DNAPL is present, but instead represents the pseudo first-order degradation of aqueous phase contaminant. Additionally, observations on system chemistry effects were made.

3.3.2. Multiphase Vial Reactor Studies

Experiments using MVRs were conducted in 40mL amber glass vials with a Teflon coupon of known area at the bottom of the vial, and Teflon-silicon septa caps, using an apparatus design first employed by Urynowicz (2000). The vials contain equal amounts of unbuffered simulated ground water as the aqueous phase, and a hexane phase on top of the aqueous phase. 3μL of DNAPL is placed onto the coupon so that dissolution over a known surface area can be monitored, and the hexane phase provides a continuous concentration gradient so that dissolution occurs continuously. MVRs are unmixed so that the different phases remain separate. Four factors were tested in MVRs in a full factorial design. Factors included oxidant type ($KMnO_4$ vs. CHP), oxidant load (low vs. high), three levels of NOM presence and DNAPL type (TCE vs. PCE). This gives a 2x2x2x3 factorial design, or 24 runs. The three levels of NOM included no NOM, 0.2 wt.% humic acid, and 0.2 wt.% humic acid with 0.2 wt.% goethite. For oxidant loading, permanganate concentrations were 0.1 wt. % for “low” and 1.0 wt. % for “high”, and CHP concentrations were 1.0 wt. % for “low” and 10 wt. % for “high”. Controls were run simultaneously. Conditions tested are presented in Table 3.6.

Table 3.6. Experimental conditions tested in MVRs.

Run[a] #	Oxidant load	NOM	DNAPL type
1, 13	low	none	TCE
2, 14	low	none	PCE
3, 15	low	0.2% humic Acid	TCE
4, 16	low	0.2% humic Acid	PCE
5, 17	low	0.2% humic acid, 0.2% goethite	TCE
6, 18	low	0.2% humic acid, 0.2% goethite	PCE
7, 19	high	none	TCE
8, 20	high	none	PCE
9, 21	high	0.2% humic acid	TCE
10, 22	high	0.2% humic acid	PCE
11, 23	high	0.2% humic acid, 0.2% goethite	TCE
12, 24	high	0.2% humic acid, 0.2% goethite	PCE

[a]Runs 1-12 are with permanganate, runs 13-24 are with CHP

Similar to the VR systems, MVR systems were run with duplicate sacrificial vials with sampling time points at 0, 0.3, 1, 3 10 and 30 hours. Samples were taken from the aqueous phase for TCE, PCE, chloride, $KMnO_4$, hydrogen peroxide, metals, and DOC at each time point. In addition, samples were taken from the hexane phase for TCE and PCE at each time point, and a final shake extraction of the vials was conducted after 30 hours of reaction with additional sampling of the hexane phase to close a mass balance. Data from the full factorial experiment were analyzed using Minitab, using the common performance indicators K_{ox}, K_{DNAPL}, RTE, oxidant demand and % DNAPL destroyed. System chemistry observations were also made. Because the MVR systems contain DNAPL phase contaminant placed on a coupon of known surface area, interface mass transfer coefficients, the mass flux rate, and the second order reaction rate coefficient could be directly calculated as well. For the method of calculation, see Jackson (2004).

3.4. BENCH-SCALE STUDIES OF POROUS MEDIA EFFECTS ON OXIDATION REACTIONS

Investigation of interactions between porous media included studies of interactions between oxidants, DNAPLs and soils in zero headspace reactor slurry systems, in 1-D diffusive transport cells, and batch investigations of hydrogen peroxide stability and permanganate NOD. For additional description of ZHR methods, see Crimi and Siegrist (2005). Methods for 1-D diffusive transport cells and batch studies of hydrogen peroxide stability and permanganate NOD are described in Seitz (2004).

3.4.1. Zero Headspace Reactor Studies

Experiments were conducted in 160 mL stainless steel zero-headspace reactors, which maintain positive pressure within the reactor to prevent gas infiltration or loss during sampling (see Figure 3.2). Base sand was used as a porous media and simulated ground water as the aqueous phase. ZHRs were continuously tumbled 360º on an end-over-end mixer throughout the experiment. A fractional factorial design was utilized to investigate ISCO application to DNAPL contaminated media with varying properties and mass distributions. Five factors were evaluated in the experiment design, including oxidant type, oxidant loading, media composition, DNAPL contaminant type, and DNAPL contaminant mass distribution. Contaminant distribution was designed using a fugacity based partitioning model by Dawson (1997) to determine the amount of DNAPL needed to achieve 0.2x, 2x, and 3x the total capacity

of media and ground water for the contaminant (sorbed and aqueous phases). All ZHR systems were run in duplicate. Table 3.7 presents the conditions tested in the ZHRs.

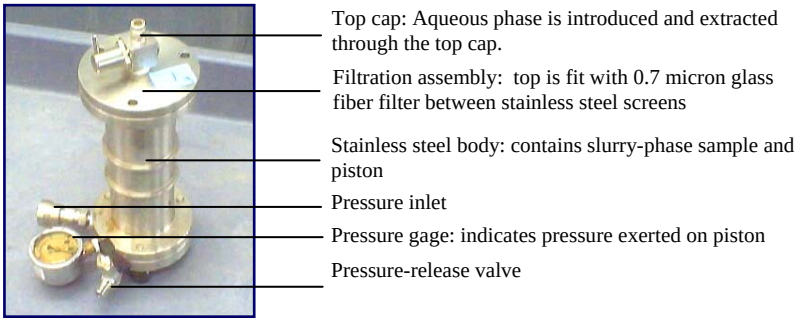

Figure 3.2. ZHR experimental apparatus.

Table 3.7. ZHR study conditions.

Run #	Oxidant	Media composition[a]	Oxidant concentration wt. % (load)[b]	DNAPL amount (μL) and (capacity)[c]	DNAPL type	Design contaminant distribution (aqueous/solids/DNAPL)
1	$KMnO_4$	Sand+HA	0.025 (1)	2.21 (0.2)	PCE	PCE: 44/56/00
2	$KMnO_4$	Sand+HA	0.5 (2)	13.9 (0.2)	TCE	TCE: 85/15/00
3	$KMnO_4$	Sand	5 (2)	121 (2)	TCE	TCE: 49/01/50
4	$KMnO_4$	Sand	0.25 (1)	11.6 (2)	PCE	PCE: 42/08/50
5	$KMnO_4$	Sand+HA	0.25 (1)	13.9/2.21 (0.2)	TCE/PCE	TCE: 85/15/00 PCE: 44/56/00
6	$KMnO_4$	Sand	2.5 (1)	121/11.6 (2)	TCE/PCE	TCE: 49/01/50 PCE: 42/08/50
7	$KMnO_4$	Sand	5 (2)	181 (3)	TCE	TCE: 32/01/67
8	$KMnO_4$	Sand	0.5 (1)	17.4 (3)	PCE	PCE: 28/05/67
9	$KMnO_4$	Sand+HA+Fe	0.025 (1)	2.21 (0.2)	PCE	PCE: 44/56/00
10	$KMnO_4$	Sand+HA+Fe	0.5 (2)	13.9 (0.2)	TCE	TCE: 85/15/00
11	H_2O_2	Sand	0.05 (1)	12.1 (0.2)	TCE	TCE: 97/03/00
12	H_2O_2	Sand+HA	0.1 (2)	22.2 (2)	PCE	PCE: 22/28/50
13	H_2O_2	Sand+HA	0.5 (1)	139 (2)	TCE	TCE: 42/08/50
14	H_2O_2	Sand	0.008 (2)	1.16 (0.2)	PCE	PCE = 84/16/0
15	H_2O_2	Sand+HA	1 (2)	139/22.2 (2)	TCE/PCE	TCE: 42/08/50 PCE: 22/28/50
16	H_2O_2	Sand	0.1 (2)	12.1/1.16 (0.2)	TCE/PCE	TCE: 97/03/00 PCE: 84/16/00
17	H_2O_2	Sand+HA	0.2 (2)	33.2 (3)	PCE	PCE: 15/19/66
18	H_2O_2	Sand+HA	1 (1)	208 (3)	TCE	TCE: 28/05/67
19	H_2O_2	Sand+HA+Fe	0.1 (2)	22.2 (2)	PCE	PCE: 22/28/50
20	H_2O_2	Sand+HA+Fe	0.5 (1)	139 (2)	TCE	TCE: 42/08/50

[a] HA indicates 0.2 wt. % humic acid addition to base sand, Fe indicates 0.2 wt. % goethite addition to base sand.
[b] Load indicates oxidant loading a 1x or 2x the stoichiometric demand of the DNAPL.
[c] Capacity indicates target mass loading to achieve 0.2x, 2x, and 3x the total capacity of soil and ground water based on partitioning model.

The media, aqueous phase and DNAPL were added to the ZHRs in such a way as to avoid any volatilization loss of contaminant from the system. Following contaminant addition, ZHRs were tumbled for 24 hours to equilibrate. Sampling for a 0 time point occurred after this 24-hour period, and then oxidant was added to the ZHRs. Samples were withdrawn at 2, 8 and 24 hour time points, and analyzed for concentrations of TCE, PCE, $KMnO_4$ and hydrogen peroxide. Following the 24-hour sample time, hexane was injected into each ZHR and tumbled to extract any remaining DNAPL. Evaluation of results was performed focusing on impacts to the performance indicators K_{ox}, K_{DNAPL}, RTE, oxidant demand, media demand, and % DNAPL destroyed, and were analyzed within the fractional factorial design using the software program Minitab 13.0.

3.4.2. Natural Oxidant Demand Studies for Diffusion Cell Core Design

In order to select an appropriate experimental scale to conduct the diffusion cell studies, the kinetic rates of oxidant consumption by low permeability media (LPM) had to be determined from natural oxidant demand batch tests. NOD has been shown to exhibit a least two differing rates of reaction, with a relatively rapid initial rate of reaction as oxidant targets readily oxidized soil compounds, and a slower final rate of reaction as easily oxidized compounds are depleted and only oxidation resistant compounds remain. To quantify the rates of reaction, NOD studies were conducted in 15 mL amber glass vials, using Mines Park ground water as the aqueous phase, and either Mines Park soil or #140 sand as porous media. These media types were selected as they were used during the diffusion cell tests (Section 3.4.4). Vials were equilibrated for 12 hours, and were agitated on a rotary mixer throughout the experiment. After equilibration, permanganate at varied concentrations (5, 3, 1, 0.5 0.25, 0.125 wt.%) was added at time 0, and permanganate concentrations were measured at times 0, 1, 4, 6, and 24 hours, then periodically for 14-18 days. From this concentration vs. time data, first order degradation rate constants were calculated.

3.4.3. Catalyzed Hydrogen Peroxide Stabilization Studies

Hydrogen peroxide stabilization batch tests were performed to determine which conditions might be most favorable for diffusive transport of hydrogen peroxide into porous media. Because hydrogen peroxide reaction and decomposition rates are much more rapid that permanganate reactions, maintaining elevated concentrations suitable for diffusive transport is difficult. Thus stabilization is necessary to slow the reactions down. Stabilization tests were conducted in 20mL amber glass vials containing Mines Park ground water, and either Mines Park soil or #140 sand as media, as well as no media controls. These systems evaluated hydrogen peroxide alone (1.0 wt.%), as well as in the presence of different amendments. These amendments include 20 mM and 40 mM phosphate buffers, pH adjustment to pH 2 and pH 3, use of iron (II) sulfate and iron (III) sulfate as catalysts, and evaluation of 10mM citric acid as an iron complexing agent both with and without amended iron (II) sulfate. Duplicate systems were run for 21 days after oxidant addition, agitated on a rotary mixer, with sampling for peroxide concentration and pH changes at 0.5, 1, 2, 3, 4, 5, 6, and 7 days. After 7 days sampling frequency decreased. Determination of oxidant stability was based on analysis of the oxidant mass remaining versus time.

3.4.4. Diffusion Cell Studies

To determine the ability of oxidants to diffuse into low permeability media, as well as the impacts of oxidation on LPM, experiments were conducted in 1-D diffusion cells (see Figure 3.3). These cells consist of a small circular soil core (2.5 cm long x 3.81 cm diameter) in horizontal position, located between two large acrylic chambers. Acrylic may be used when contaminants are not present in a NAPL phase. One of the chambers is an influent chamber where concentrated solutes may be delivered, and the other is the effluent chamber on the other side of the soil core. The chambers are very large relative to the soil core (100x), which allows steady state diffusion to occur. The two chambers are well mixed using recessed stir bars in a configuration that avoids scouring at the surface of the soil core. Ports allow for

sampling of the bulk aqueous phases in the influent and effluent chambers, as well as samples in close proximity to the surface of the soil core, but no sampling ports are located within the core.

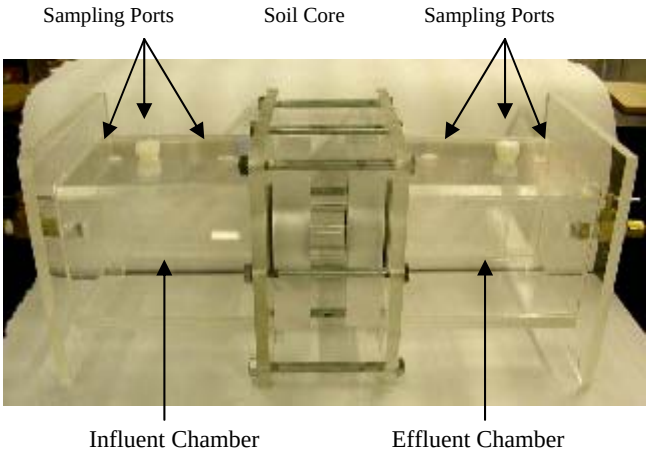

Figure 3.3. 1-D diffusion cell apparatus.

Bromide was used as a conservative tracer to determine the impact of diffusive oxidant transport on porous media. To determine diffusive interactions between the oxidant and the bromide tracer, 3 preliminary experiments were run in the diffusion cells using 0.32 mm acrylic beads as a non-reactive, uncontaminated media, and a 3.5 cm long core to increase tortuosity for the larger media grain size. Experiments were conducted using 1 wt.% $KMnO_4$, 1 wt.% H_2O_2, and 1 wt.% H_2O_2 + 20mM KH_2PO_4 buffer (pH 6) as influent chamber solutions, in addition to 100 mg/L bromide as a tracer. First, bromide was added to the cell influent chamber to establish steady state diffusion, followed by oxidant addition at the concentrations specified. Cells operated for 6 hours at steady state diffusion for bromide, and then 6 hours for steady state oxidant diffusion. Sampling for concentrations of oxidants, bromide, pH and conductivity were measured every hour in both influent and effluent chambers, to yield data for calculation of diffusion parameters. Based on the data from these preliminary experiments, a length of 2.5 cm for the LPM soil core in the diffusion studies was selected based on diffusion modeling using the Millington-Quirk relation, which predicted that permanganate could diffuse 2.5cm within one month (see Seitz (2004) for modeling approach). It was also predicted from preliminary experiments that it was possible to maintain hydrogen peroxide concentrations in the influent chambers and to proceed with experimentation on LPM with CHP.

A total of four diffusion cells were run with low permeability media, the conditions of which are listed in Table 3.8. Diffusion cells were run with soil cores contaminated with sorbed and aqueous phase TCE and PCE.

Table 3.8. Experimental conditions for 1-D oxidant diffusion cell studies.

Experimental run	Oxidant type and concentration	Media type	Contaminant load [A] (mg/kg LPM)
A	1 wt.% $KMnO_4$	Mines Park sandy loam	972 mg-TCE/kg; 332 mg-PCE/kg
B	1 wt.% $KMnO_4$	#140 Sand	131 mg-TCE/kg; 19 mg-PCE/kg
C	1 wt.% H_2O_2	#140 Sand	208 mg-TCE/kg; 26 mg-PCE/kg
D	1 wt.% H_2O_2	Mines Park sandy loam	842 mg-TCE/kg; 320 mg-PCE/kg

[A]Load was based on a fugacity-based modeling estimate to yield ~50% of the LPM's capacity before DNAPL phase was present.

The soil cores were carefully wet packed using degassed ground water to avoid air entrapment and were packed to achieve duplicate homogeneous packings for comparison between experiments. Once the core was emplaced in the diffusion cell, an initial bromide tracer (100 mg/L in the influent chamber) test was performed over 30 days, with sampling for bromide, metals, pH and conductivity every 2 days to determine the initial diffusion properties of the core. After this initial tracer test, the cores were contaminated by injecting pure phase TCE and PCE into the cores through a needle sized hole in the apparatus, and then the hole was immediately sealed. The contaminant load was 50% of the total capacity for contaminant of the aqueous and sorbed phases as predicted by using a fugacity based model by Dawson (1997), to allow for complete dissolution of DNAPL into the soil cores. The cells equilibrated for 7-8 days, to allow for DNAPL dissolution, and were monitored for TCE and PCE concentrations, in addition to bromide, metals, pH and conductivity. After this time period, oxidant was added, with care exercised to maintain the same fluid levels in the influent and effluent chambers. After oxidant addition, permanganate cells were run for 113-115 days, and peroxide cells were run for 50 days. Samples from the well mixed influent and effluent chambers were taken every 2-3 days and analyzed for oxidant, contaminant, bromide, dissolved organic carbon (DOC) and metals concentrations, as well as pH and conductivity. After the completion of the run, the chamber contents were tested for total solids, total suspended solids and total dissolved solids. The soil core was immediately dissected into five 0.5 cm sections along its length, and each section is sub-sectioned for analysis of TCE and PCE, solid phase total organic carbon (TOC), residual oxidant, water content, exchangeable cations, and environmental scanning electron microscopy (ESEM). Concentration versus time data in the influent and effluent chambers was used to calculate diffusive transport parameters using equations proposed by Cussler (1997), based on Fick's First Law of Diffusion.

3.5. UPSCALING REACTIVE TRANSPORT DURING ISCO: EXPERIMENTAL AND MODELING STUDIES

To understand the impacts of varied ISCO application techniques and site specific conditions on DNAPL mass transfer and depletion rates, as well as the applicability of observations from bench scale experimentation to pilot scale implementation of ISCO, experiments were conducted to investigate chemical oxidation in flowing porous media systems of varied scales and degrees of heterogeneity. Experimental methods for 1-D flow through tube reactors are presented in detail in Petri (2006). Additional details for the 2-D flow cell experimental methods are presented in detail in Appendix A. Detailed information about the 2-D intermediate scale tank experiments and CORT3D model development are available in Heiderscheidt (2005) as well as in the final project report for SERDP Project CU-1294.

3.5.1. One-Dimensional Flow-Through Tube Reactor Experiments

Experimentation was conducted in 1-D horizontal flow-through tube reactors (FTRs) to determine how conditions in the subsurface during ISCO injection, such as varied ground water velocities, oxidant concentrations, DNAPL types and DNAPL entrapment architectures impact contaminant mass transport and the efficiency of ISCO application. FTRs are 46-cm long, 1.3-cm diameter glass tubes, which are homogeneously packed with fine glass beads and saturated with simulated ground water (see Figure 3.4). FTRs simulate subsurface conditions without media interactions such as sorption or NOD. A coarse bead DNAPL source zone is packed into the center of reactor, and surrounded by finer beads, using the change in capillary entry pressures to create a controlled DNAPL source configuration that could be replicated. DNAPL residuals geometries with large surface area to mass ratios were created by saturating the coarse bead source zone with DNAPL, and then withdrawing DNAPL, leaving behind DNAPL residuals. Additional experimentation also evaluated large DNAPL ganglia systems, using injection of a fixed volume of DNAPL into this zone, resulting in one large interconnected DNAPL ganglion. DNAPLs were dyed with Sudan IV to assist with injection and

observation. The FTRs have ground water delivered by peristaltic and syringe pumps, and sample ports in the reactor allow for sampling of concentrations up-gradient (A), shortly down-gradient (B), and farther down-gradient (C) of the DNAPL source zone. Experimentation focused on permanganate, as gas generation by CHP precluded the ability to investigate peroxide delivery within this apparatus.

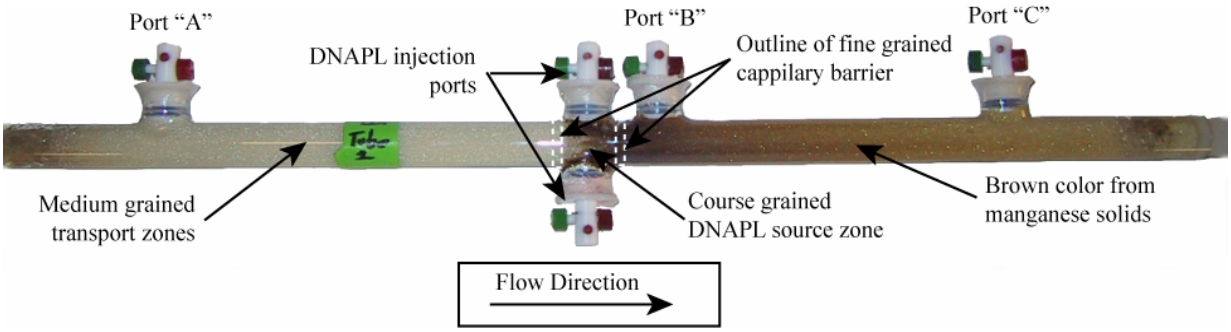

Figure 3.4. FTR apparatus.

A full factorial experiment design was used to evaluate the impacts of ground water velocity, oxidant concentration, and DNAPL type on DNAPL mass depletion rates from residual source zones. Additional experimental work, outside this factorial design investigated the impact of contaminant entrapment architecture, by comparing residual and large ganglia geometries. It was not practical to run duplicates of all FTRs, so only select duplicates were run. The conditions of all FTR experimental trials conducted are presented in Table 3.9.

Each FTR trial consisted of three experimental phases. An initial pre-oxidation phase commenced upon introduction of DNAPL into each FTR and the start of ground water flow, which established baseline DNAPL dissolution conditions. A second, oxidation phase then began, with the introduction of permanganate at the specified concentration into the FTR. Then a final post-oxidation phase began, during which oxidant flushing ceased and ground water flow resumed, enabling observation of changes to the system from initial conditions, resulting from oxidant flushing. The lengths of the experiments varied with the velocity and DNAPL type under investigation, but high velocity TCE systems were run for 1-2 days, low velocity systems for 2-3 weeks, and all others for 7-8 days. Velocities remained constant throughout the experiment. Sampling occurs throughout each FTR experiment for TCE, PCE, chloride and pH, with sampling for permanganate during the oxidation and post-oxidation phases. Metals were monitored in the effluent.

The collection of data yielded contaminant mass balance data, which allowed for calculation of the DNAPL mass depletion rates within each individual FTR, for all three phases of the experiment. These depletion rates can then be compared between different phases of each FTR trial to evaluate how ISCO has impacted DNAPL mass depletion and mass transfer, as well as determine which conditions are more effective or efficient. Also, several efficiency terms were calculated for the FTR systems, which differ from those described in Section 3.2.5. These include the molar treatment efficiency (MTE), which indicates the efficiency of oxidant use, and the volumetric depletion efficiency (VDE), which indicates the efficiency of the fluid flushing regime.

Table 3.9. FTR experimental conditions.

Trial	Velocity range	Actual avg. pore velocity (m/day)	Concentration (mg/L as $KMnO_4$)	DNAPL identity	Architecture	DNAPL mass (g)	DNAPL source zone saturation
FTR1	High	16.6	100	TCE	residual	0.365	16.5%
FTR2	High	18.0	1000	TCE	residual	0.435	19.6%
FTR3	High	pump malfunction	10000	TCE	residual	0.531	24.0%
FTR4	High	15.9	1000	TCE	large ganglia	0.231	10.4%
FTR5	High	14.9	10000	TCE	large ganglia	0.221	10.0%
FTR6	High	16.6	10000	PCE	residual	0.443	18.2%
FTR7	High	15.4	1000	PCE	large ganglia	0.326	13.3%
FTR8	High	14.6	1000	PCE	residual	0.348	14.3%
FTR9	High	14.5	10000	PCE	large ganglia	0.399	16.3%
FTR10	High	15.1	100	PCE	residual	0.404	16.5%
FTR11	Medium	1.17	100	TCE	residual	0.353	15.9%
FTR12	Medium	1.42	1000	TCE	residual	0.381	17.2%
FTR13	Medium	1.31	10000	TCE	residual	0.313	14.1%
FTR14	Medium	1.04	1000	PCE	residual	0.705	21.6%
FTR15	Medium	1.28	100	PCE	residual	0.952	38.5%
FTR16	Low	0.156	100	TCE	residual	0.347	15.7%
FTR17	Low	0.156	1000	TCE	residual	0.453	20.5%
FTR18	Low	0.156	10000	TCE	residual	0.385	17.4%
FTR19	Medium	1.10	1000	TCE	residual	0.325	14.7%
FTR20	Medium	1.06	10000	PCE	residual	0.521	21.4%
FTR21	Low	0.156	100	PCE	residual	0.482	19.8%
FTR22	Low	0.156	1000	PCE	residual	0.515	21.2%
FTR23	Low	0.156	10000	PCE	residual	0.475	19.5%
FTR24	Low	0.156	10000	TCE	residual	0.387	17.5%
FTR25	High	17.2	10000	TCE	residual	0.374	16.9%
FTR26	Low	0.156	0	TCE	residual	0.329	14.9%
FTR27	Low	0.156	0	PCE	residual	0.449	18.4%
FTR28	Medium	1.05	0	PCE	residual	0.395	16.2%
FTR29	Medium	0.98	0	TCE	residual	0.599	22.0%
FTR30	Medium	1.05	0	TCE	residual	0.395	17.9%
FTR31	High	14.8	0	TCE	residual	0.321	14.5%
FTR32	High	17.2	0	PCE	residual	0.614	25.2%

3.5.2. Two-Dimensional Flow Cell Studies

To determine how ISCO applications of varying oxidant types and techniques in a complex flow field impact remediation efficiency and effectiveness, experimentation was conducted in 2-D flow cells. The 2-D flow cell is a 30x30x2.5 cm Delrin box, with an array of 100 sampling ports on the back face of the box, and a glass window on the front to enable observation of experimentation (see Figure 3.5). The box contains influent and effluent ports on the ends of the box, influent flow is provided by a peristaltic pump, and a constant head device controls effluent. The box was wet packed with #140 sand and simulated ground water, and a base sand DNAPL source zone lens was emplaced near the center of the 2-D flow cell. DNAPL phase PCE dyed with Sudan IV was directly injected into this source zone to create DNAPL pools and residuals. Two stainless steel screens at the influent and effluent ends of the box distributed flow uniformly to the cell, and a bentonite layer packed at the top of the cell resulted in confined aquifer flow conditions.

Similar to the FTR experiments, the 2-D flow cell experiments employed a three phase experimental approach with a 3 day pre-oxidation phase to establish baseline DNAPL dissolution, a 12-24 hour oxidation phase for oxidant delivery, and a 7 day post-oxidation phase for performance assessment. The 2-D flow cells evaluated the conditions of varied oxidant types, varied delivery rates, varied oxidant concentrations, and in the case of CHP, varied oxidant activation methods, with the goal of optimizing oxidant delivery and treatment. The conditions tested by the 2-D flow cell experiments are summarized in Table 3.10.

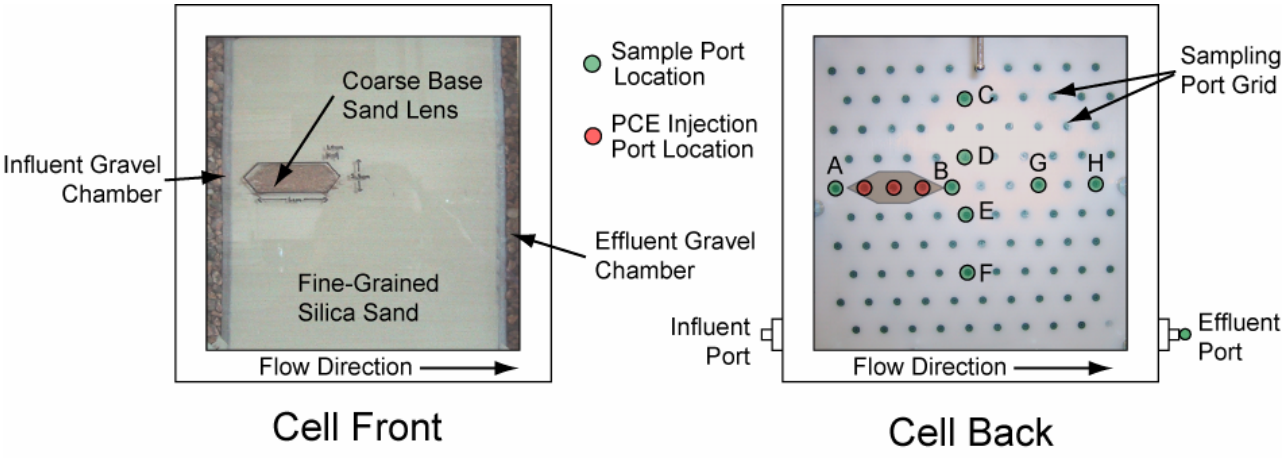

Figure 3.5. 2-D cell apparatus.

Table 3.10. 2-D flow cell experimental conditions.

Cell ID	Oxidant	Oxidant concentration	Oxidant activation method	Oxidant delivery rate
1	Catalyzed hydrogen peroxide	3 wt.%	5 mM $FeSO_4$, pH 3	Pressurized
2	Catalyzed hydrogen peroxide	10 wt.%	5 mM $FeSO_4$ pH 3	Pressurized
3	Catalyzed hydrogen peroxide	3 wt.%	Natural Iron in media pH 3	Gravity feed
4	Catalyzed hydrogen peroxide	3 wt.%	Natural iron in media Citric acid chelating flush	Gravity feed
5	Potassium permanganate	1 wt.%	None	Pressurized
6	Potassium permanganate	1 wt.%	None	Gravity feed
7	None – control	None	None	Pressurized
8	None – control	None	None	Gravity feed

Gravity feed delivery rates simulate subsurface oxidant delivery from gravity feed wells, and pressurized delivery indicates active oxidant injection under pressure, resulting in increased subsurface velocity during ISCO. For delivery rate, velocity was 12 cm/day in the cell throughout all phases for the "gravity feed" systems. For "pressurized" systems, velocity was 45 cm/day during the oxidation phase and 12 cm/day for the pre-oxidation and post-oxidation phases. Samples were collected from the 2-D flow cells through an array of sample ports at the back of the cell, and at the cell effluent. The sampling array at the back of the cell included sample ports aligned in both a vertical and horizontal transect, the vertical consisting of 4 sample ports located shortly down-gradient of the DNAPL source zone (C, D, E, and F). The horizontal transect also included 4 sample ports, one located up-gradient of the source zone (A), and three located down-gradient (B, G, and H). Samples were taken from all 8 transect ports every 12-24 hours during experimentation, with increased frequency sampling during the oxidation phase, and analyzed for TCE, PCE, chloride, pH and oxidant concentrations, as well as metals in the effluent. After experiment shutdown, five soil cores were taken from the 2-D flow cell, progressing down-gradient, with the first three in the source zone, and two in the down-gradient plume zone, and were analyzed for exchangeable cations. Data from the 2-D flow cells were used to analyze the effectiveness of oxidant delivery, the impact of ISCO on contaminant mass distribution, and system geochemistry. In addition, the 6 efficiency and effectiveness terms described in Section 3.2.6 were calculated for the 2-D flow cells.

3.5.3. Two-Dimensional Intermediate-Scale Tank Studies

To study the impacts of permanganate application in more complex DNAPL sources and in more complex ground water flow fields, with particular emphasis on the impact of manganese solids on flow fields, experimentation was conducted in large 2-D tanks. An acrylic tank (L x W x H = 243.5 x 8 x 45.5 cm) was constructed and equipped with numerous sampling ports on the back face of the tank (see figure 3.6). Three preliminary tank experiments were run utilizing a single rectangular PCE DNAPL source. The first experiment involved dissolution of a small PCE DNAPL residual zone overlying a DNAPL pool. The second experiment duplicated the DNAPL source configuration, but added a low permeability media (LPM) layer beneath the source to look at diffusion of aqueous PCE into the LPM. The third experiment involved flushing the tank from the second experiment with permanganate after residual PCE DNAPL was depleted. The purpose of these experiments was to examine interaction of PCE dissolution, aqueous PCE diffusion, permanganate diffusion, and oxidation by systematically adding each process to a

previously studied system. These experiments served to refine cell assembly and sampling protocols, as well as pointing out the value of using a larger, complex, DNAPL source zone for this research.

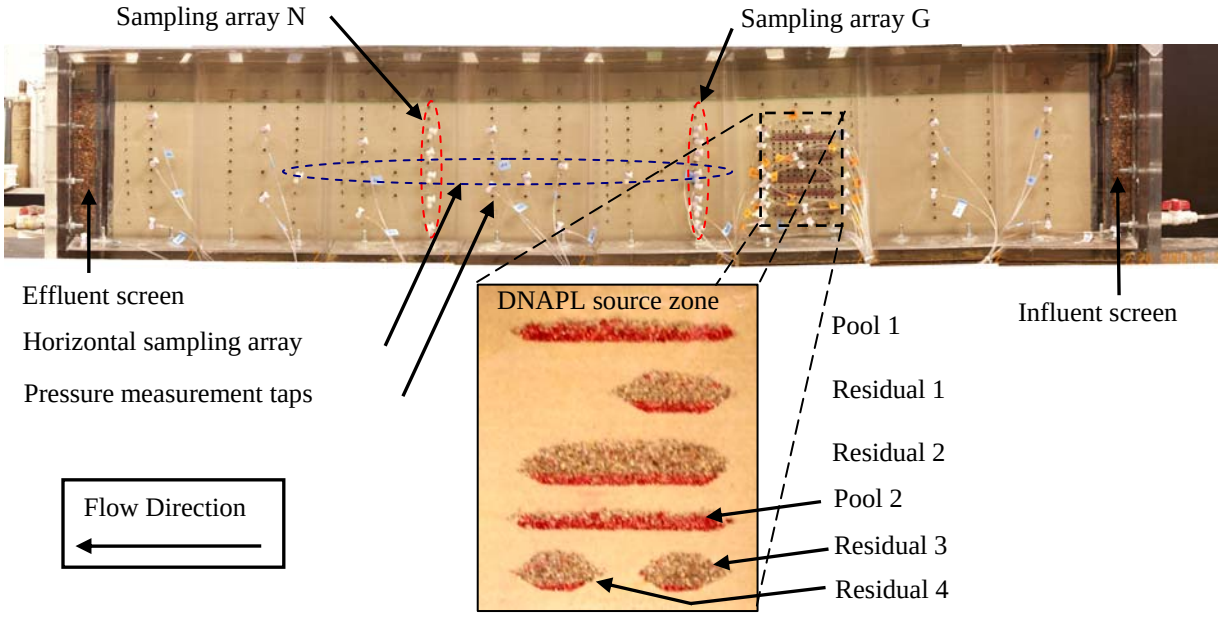

Figure 3.6. 2-D Intermediate-scale tank apparatus.

These preliminary experiments culminated in a final primary experiment. For this final experiment, the tank was wet packed using #70 silica sand and degassed tap water, and #8 silica sand to emplace 6 discrete coarse grained DNAPL source zones, including 4 residual DNAPL sources, and 2 pooled sources (Figure 3.6). These include residual 1 and pool 1, which were emplaced in such a configuration that it was expected they would have little influence on each other, residual 2 and pool 2 which were emplaced to simulate a residual smear zone above a DNAPL pool, and residuals 3 and 4 which were emplaced in series to investigate interactions when oxidant flowed through successive residual sources. Stainless steel screens and gravel packs were used to distribute influent and effluent to the tank. An impermeable bentonite clay layer sealed the top of the tank and allowed the tank to be run as a confined aquifer. Degassed, filtered tap water was used as the flow medium, a peristaltic pump provided constant flow, and a constant head device was used at the effluent. The tank had an average pore velocity of 1.88 m/day throughout the experiment.

The experiment procedure consisted of tank packing, followed by a 5 day water flush for equilibration, and a dye test to ensure uniform flow. After 5 days, a PCE DNAPL dyed with Sudan IV was injected into the source lenses, with injection only for the pool sources, and injection and withdrawal for the residual sources. At total mass of 143.33 g of PCE was injected between all lenses. An 8 day natural dissolution phase then followed, with a conservative bromide tracer test (200 mg/L) performed on the second day. Then an oxidation phase began with permanganate delivered in tap water at 2800 mg/L (as $KMnO_4$) for a total of 59 hours. The total mass of permanganate delivered to the tank, 110.4g, was insufficient to completely destroy the DNAPL, ensuring that PCE would remain after the experiment. Following the oxidation phase, an 11 day post-oxidation phase allowed for monitoring of changes in contaminant flux resultant from ISCO treatment.

The 2-D intermediate-scale tank required extensive sampling. An automated hydraulic head monitoring and data acquisition system provided for measurement of hydraulic pressures at 48 locations throughout the tank, taking measurements at 10 locations each minute. Aqueous phase samples were taken at 14 locations throughout the tank, located in two vertical transects down gradient of the source zone, a horizontal transect along the tank centerline, and the tank effluent. Samples were analyzed for aqueous PCE, chloride, bromide, permanganate, pH and metals concentrations. After experiment shutdown, a total of 168 cores were taken from the source zone areas, and 44 from the rest of the tank. These cores were extracted with hexane for PCE quantification, and then extracted for MnO_2 solids using hydroxylamine hydrochloride. Data from this experiment were compared to a model developed as part of this project (CORT3D, see Section 3.5.5).

3.5.4. Two-Dimensional Large-Scale Tank Experiments

Two large tank (LxWxH 480 x 5.0 x 120 cm) experiments were run to investigate the impact of subsurface heterogeneity on permanganate delivery to a PCE spill source zone. The first experiment investigated a high degree of heterogeneity by utilizing 5 different silica sands of varied hydraulic conductivity (#16, #30, #50, #70, #110), and the second investigated a low degree of heterogeneity using three different silica sands (#30, #50, #70). These tank studies were conducted in cooperation with another CSM SERDP project: "Mass Transfer from Entrapped DNAPL Sources Undergoing Remediation: Characterization Methods and Prediction Tools" (SERDP Project CU-1294).

As part of this cooperative effort, a number of phases to each experiment were performed, including natural dissolution, surfactant enhanced remediation, partitioning tracer test (PTT) evaluation and chemical oxidation. A diagram of the 2-D large-scale tank apparatus is available in Figure 3.7. Before and after each phase, a partitioning tracer test (PTT) was performed and the DNAPL source zone was scanned with a dual-energy gamma attenuation system to determine the mass distribution of the DNAPL in the tanks. The initial surfactant flush was performed with Tween-80, at 50 g/L. Chemical oxidation was performed as the final experiment in each tank, and the tanks were flushed for several weeks prior to the chemical oxidation phase to remove residual surfactant. For more detailed information regarding this set of experiments, the reader is referred to the final report for SERDP Project CU-1294.

The tank experiments were conducted using tap water as the flow medium, and a natural PCE spill was used to create a source zone containing residuals and pools. A homogeneous #16 sand influent zone was located at the influent end of the tank for flow distribution. Constant head devices were located at the influent and effluent ends of the tank, providing a constant overall hydraulic gradient through the tanks. A total of 8 vertical arrays of sampling or injection ports were located 62.5 cm apart across the tank. The first array was used to deliver permanganate directly into the homogeneous influent zone to allow for mixing of the oxidant with the tap water for uniform distribution into the tank. The second array was used for injection of PCE dyed with Sudan IV into the source zone and not used for sampling. Samples were taken from selected locations within the 6 sets of sampling arrays down gradient of the source and from the tank effluent. Important conditions for each tank are presented in Table 3.11.

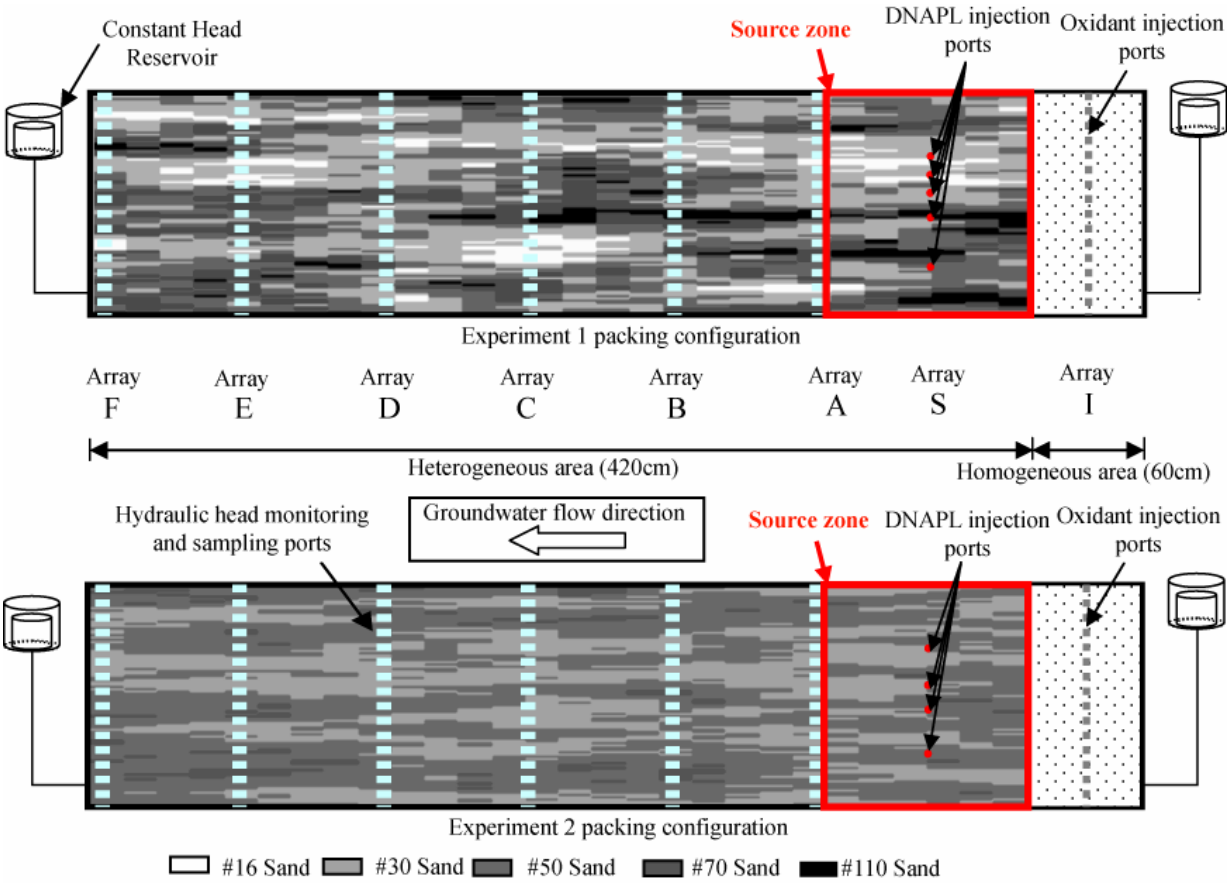

Figure 3.7. 2-D Large-scale tank experimental apparatus at CSM.

Table 3.11. Conditions of the large-scale tank ISCO investigation.

Property	Tank experiment 1	Tank experiment 2
Initial mass of PCE emplaced (g)	952.5	461.1
Approximate PCE mass remaining at start of chemical oxidation (g)	509.2	273.3
Theoretical average (log) hydraulic conductivity (m/d)	4.18	4.18
Theoretical variance (log) hydraulic conductivity (m/d)	1.22	0.25
Permanganate injection concentration (mg/L)	8000	5000
Oxidant injection duration (hrs)	48.5	24.5
Oxidant injection rate (mL/min)	8.0	8.0
Maximum PCE oxidation possible according to stoichiometry (g)	146.6	46.3

3.5.5. Development of a Model for DNAPL Remediation Using Permanganate

A new model, Chemical Oxidation Reactive Transport in 3D (CORT3D) was developed as a part of this project, based on existing code from Reactive Transport 3D version 2.5 (Clement 1997, Clement 2002). This model included processes that have been incorporated into other models of ISCO using permanganate, among these: advection, dispersion, sorption, diffusion, DNAPL dissolution, 2^{nd} order contaminant oxidation, and permeability increases due to DNAPL dissolution. However, this model is unique because it has been expanded to include several additional phenomena unique to ISCO with permanganate, including: multiple natural oxidant demand components, kinetic rate-limited NOD oxidation, and permeability reductions resultant of deposition of MnO_2 solids generation. The widely accepted ground water flow code MODFLOW-2000 was used to generate the underlying spatial and temporal variation in ground water head distribution. For more specific information on the formulation of the CORT3D model, see Heiderscheidt (2005).

After the model was formulated, it was verified by comparison to analytical solutions. The verification was performed stepwise to compare specific processes of the model to other analytical solutions, as no analytical solution exists that can compare all processes in the model. Comparison was made to a number of analytical solutions derived by others. These include: (1) Hood (2000) for permanganate oxidation (without NOD) and product (chloride) formation under no flow conditions, (2) first order reaction kinetics for NOD oxidation kinetics, (3) van Genuchten and Alves (1982) for 1-D advection, dispersion and first-order reaction, and (4) Wexler (1992) for 2-D dispersion, advection and first-order reaction. For analytical solutions including transport, the model had to be compared using pseudo first-order assumptions because no known analytical solution exists for second-order reactive transport. As a final verification step, the CORT3D model was compared to the original RT3D model code, for both diffusion only and advective diffusive-dispersive conditions. All comparisons to analytical and numerical solutions confirmed that CORT3D was properly calculating system equations.

The next step in model testing was to apply the model to a series of 1-D experiment systems, and compare the simulation results to experimental data from those systems, with the goal of demonstrating whether or not the model captured specific ISCO-related processes and effects. It was not intended to universally validate the model code against all conditions. The model code was first tested against a data set collected by Schroth *et al.* (2001) in a series of 1-D column experiments oxidizing a TCE DNAPL. This allowed comparison of permeability effects between the model and pressure data collected from the experiment, as well as contaminant concentration and mass depletion data. A second experimental data set by Schnaar *et al.* (1998) included oxidation of a PCE DNAPL in 1-D columns using two concentrations of oxidant and two different velocities. This second series of simulations were conducted to determine if CORT3D could capture a number of effects. These include: increases in DNAPL mass transfer during oxidation, effects of NOD of varied kinetic rates (fast vs. slow) on PCE oxidation and permanganate breakthrough, simultaneous existence of PCE and oxidant in the effluent, contaminant rebound after the conclusion of oxidant flushing, and generation of chloride as PCE is oxidized. However, only limited NOD data were available from this study. Thus, as a follow-up study, a final series of test simulations was performed against data from 1-D column studies of NOD by Crimi and Siegrist (2004), with the goal of determining if the model could effectively capture the oxidation of NOD.

A final application of the CORT3D model was to investigate how to optimize permanganate delivery at the Naval Training Center site in Orlando Florida, where a field soil presented significant oxidant delivery challenges partially due to NOD. The Groundwater Modeling System 5.0 was used for pre and post processing of simulations, and a MODFLOW-2000 model provided by the Navy (Tetra Tech NUS 2002) was used to input a ground water flow solution. The NTC site model was set up with a 1600ft x 1200ft grid, with three layers including 5ft thick top layer, a 20ft middle layer, and a 40ft bottom layer. The model included recharge from the top and leakage from the bottom. A general head boundary defined the east boundary condition, a lake to the west, and zero flow to the north and south. The goal of the simulations was to study oxidant delivery optimization, rather than contaminant destruction efficiency

and effectiveness. Thus, as contamination at a site with very high NOD is not anticipated to significantly impact oxidant delivery relative to NOD impacts, the model simulations were run without including contaminant. A total of 19 simulations were run with varied parameters including permanganate injection concentration and well flow rates to determine optimal ISCO design, as well as NOD amount and the rate of NOD oxidation to determine how much impact NOD had on oxidant delivery. The conditions of these simulations are presented in Table 3.12.

Table 3.12. NTC field site CORT3D simulation conditions.

Oxidant concentration (mg/L)	Fast NOD fraction (mg/mg)		Slow NOD fraction (mg/mg)		Fast NOD Rate (1/sec)	Slow NOD Rate (1/sec)	Total flow rate of all oxidant injection wells (gpm)
	Layers 1 & 2	Layer 3	Layers 1 & 2	Layer 3			
250	0	0	0	0	5.56E-05	0	8
250	0.00717	0.01	0	0	5.56E-05	0	5
250	0.00717	0.01	0	0	5.56E-05	0	8
250	0.00717	0.01	0	0	5.56E-05	0	10
250	0.00717	0.01	0	0	5.56E-05	0	15
1000	0.00717	0.01	0	0	5.56E-05	0	5
1000	0.00717	0.01	0	0	5.56E-05	0	8
1000	0.00717	0.01	0	0	5.56E-05	0	10
1000	0.00717	0.01	0	0	5.56E-05	0	15
1000	0.00717	0.01	0	0	5.56E-05	0	48
4000	0.00717	0.01	0	0	5.56E-05	0	5
4000	0.00717	0.01	0	0	5.56E-05	0	8
4000	0.00717	0.01	0	0	5.56E-05	0	10
4000	0.00717	0.01	0	0	5.56E-05	0	15
4000	0.00717	0.01	0	0	5.56E-05	0	48
250	0.00717	0.01	0	0	5.56E-05	0	8
250	0	0	0.00717	0.01	0	2.78E-05	8
250	0.010755	0.015	0	0	5.56E-05	0	8
250	0.003585	0.005	0	0	5.56E-05	0	8

3.6. EXPERIMENTAL EVALUATION OF COUPLING ISCO WITH OTHER REMEDIATION TECHNOLOGIES

As part of meeting the objective of determining whether or not ISCO can be applied before, after or simultaneously with other remediation technologies, controlled laboratory experimentation was conducted to elucidate screening, characterization, treatability and design information to consider when evaluating coupling. Specific remediation technologies considered for coupling include surfactant and cosolvent enhanced recovery and bioremediation. The research concerned with coupling of ISCO with surfactant/cosolvent flushing was performed as part of a doctoral dissertation, which should be finalized in December 2006 (Dugan 2006). The research that was focused on coupling of ISCO with bioremediation was performed as part of a master's thesis project (Sahl 2005).

3.6.1. Screening Tests for Coupling Surfactants and Cosolvents with ISCO

Batch screening tests were conducted to determine the compatibility of oxidants potassium permanganate and catalyzed hydrogen peroxide with selected surfactants and cosolvents. A total of 72 surfactants and 8 cosolvents were investigated in the screening study. The batch tests were conducted in 40 mL glass vials with Teflon septa, with 30 mL of aqueous solution, and 10 mL of headspace in the event of gas or foam generation. Two cases of conditions were investigated. The first case tested high concentrations of surfactant in the presence of moderate to high concentrations of oxidants, which could represent conditions of oxidant injection shortly after surfactant injection, or potentially co-injection of oxidant and surfactant at the same time. The second case tested low concentrations of surfactant in the presence of oxidant, which represents conditions that may occur if oxidant is injected at a site where surfactant/cosolvent flushing had been previously applied and residual surfactant is still present. For permanganate screening studies, high concentrations of surfactant ranged from 1.0 to 5.0 wt.% and low concentration ranged from 0.01 to 0.1 wt.%. Oxidant concentrations of 5000 and 500 mg/L were used for screening surfactants with respect to permanganate. For CHP screening studies, surfactant concentrations ranged from 1.0 to 3.5 wt.%, and oxidant concentrations ranged between 3 to 30 wt.%. Hydrogen peroxide was activated with 5 mM $FeSO_4$. Batch tests were run for 24 hours, with sampling for oxidant concentrations at 3 and 24 hours. Qualitative observations of gas generation, foaming, temperature increase and in the case of permanganate, color change, were made at each time point. These data were used to determine the stability of the oxidant in the presence of surfactant, indicating compatibility.

3.6.2. Upscaling Experimental Evaluation of Coupling ISCO with Surfactant/Cosolvent Flushing in 2-D Flow Cell Experiments

Prior to upscaling surfactant/cosolvent flushing to 2-D flow cell experiments, it was necessary to determine PCE solubilization by selected surfactants and cosolvents. Batch 20 mL vial studies were performed in triplicate utilizing concentrations of two ISCO-compatible surfactant/cosolvent solutions. For these studies, Dowfax 8390 was used alone at concentrations ranging from 0 to 10 wt.%, or at 3.5 wt.% with 2.5 wt.% tert-butanol (TBA). PCE was added to the vials containing surfactant or surfactant/cosolvent solution. The vials were agitated for 24 hours, after which time they were centrifuged and sampled to determine PCE solubilization. This was done to determine the proper surfactant/cosolvent dose for the 2-D flow cell experiments.

Coupling of ISCO with surfactant and cosolvent flushing was evaluated in a 2-D flow cell to determine the viability of DNAPL remediation involving either sequential or co-injection applications of surfactant and oxidant. The 2-D flow cell, identical to the one described in Section 3.5.2, was a 30x30x2.5 cm Delrin box, with sampling ports on the back and a glass front to enable visual observations (see Figure 3.5). The cell was wet packed with #140 sand and a base sand DNAPL source zone lens using degassed simulated ground water. The cell was capped with a bentonite layer resulting in confined aquifer conditions. Stainless steel screens and gravel packs provided uniform flow distribution. A piston pump provided flow and a constant head effluent device provided hydraulic control. A dye test was performed prior to each experiment to ensure uniform flow distribution through the cell. Average pore ground water velocity in the cell was approximately 43 cm/day.

PCE dyed with Sudan IV was injected into the source lens at experiment commencement, attaining an 11% saturation of the source lens. After DNAPL injection, a natural dissolution phase began, with a pre-oxidation phase partitioning tracer test (PTT). This was followed by either co-injection of surfactant, permanganate, and cosolvent, or sequential application of surfactant/cosolvent, followed by a water flush, and then a permanganate flush. A post-oxidation phase then followed, which included monitoring for DNAPL dissolution as well as performing a post-oxidation PTT. Samples were taken from 8 sample ports in a horizontal and vertical transect and the cell effluent, similar to the sampling

procedure described in Section 4.5.2. After experiment shutdown, the cell was dissected with source zone extractions for quantification of PCE.

3.6.3. Microbial Culture Preparation for Evaluation of Coupling ISCO with Bioremediation

In order to evaluate coupling of ISCO with bioremediation, two chlorinated contaminant degrading cultures, one anaerobic and one aerobic, were obtained and utilized in the investigation of coupling bioremediation with chemical oxidation. The anaerobic mixed culture KB-1was obtained from Dr. Elizabeth Edwards and researchers as the University of Toronto and has been used frequently for bioaugmentation (Major *et al.* 2002). This culture has the ability to completely dechlorinate PCE to ethene due to the presence of relatives of *Dehalococcoides ethenogenes* (Duhamel *et al.* 2002), can utilize multiple electron donors in dehalorespiration, and is easy to grow and maintain. The aerobic cometabolic culture used was *Burkholderia cepacia* G4 (G4), which was originally isolated from an industrial waste treatment facility in Pensacola, Florida (Nelson *et al.* 1986). This aerobic culture degrades TCE by cometabolism in the presence of an aromatic substrate such as toluene or phenol.

The anaerobic mixed culture KB-1 was grown in anaerobic growth medium (AGM), which contains a phosphate buffer, salt solutions, trace minerals, magnesium chloride or magnesium sulfate, sodium bicarbonate, vitamins, resazurin, and amorphous ferrous sulfide solution. For the precise composition of AGM, see Sahl (2005). Resazurin is a colorimetric indicator compound that turns pink if anaerobic conditions are not maintained. The culture, which was stored in an anaerobic glove box, was regularly fed a PCE-methanol mixture and periodically fresh AGM was added to maintain the culture. Headspace samples were taken regularly to verify that PCE was being completely dechlorinated to ethene.

The aerobic G4 culture was removed from frozen storage and grown on agar plates at room temperature containing standard mineral base (SMB) (Cohen-Bazire *et al.* 1957) and 30 mg/L phenol. SMB contains important buffering, nutrient, salt, metals and organic compounds to maintain the culture (see Sahl (2005) for composition). Single colonies were harvested into 50mL centrifuge tubes containing SMB and phenol, placed on a shaker table and tested for phenol degradation. Once phenol degradation was confirmed, indicating that the microbes were actively growing, the culture was placed in a 1L glass bottle on a stir plate, and topped with a foam stopper to allow for oxygen transfer. The culture was routinely sampled for phenol to ensure active degradation, and fresh phenol and SMB were added periodically to maintain the culture. A preliminary batch microcosm screening study was then performed to confirm whether or not the G4 culture could cometabolically degrade TCE. Once aerobic degradation of TCE was confirmed, the G4 culture was used in 1-D column studies (Section 3.6.4).

3.6.4. Evaluation of Permanganate Oxidation Impacts on Contaminant Degrading Cultures using 1-D Column Studies

Two series of column studies were performed to evaluate the impacts of potassium permanganate on the ability of the KB-1 and G4 cultures to degrade DNAPL contaminants under aerobic and anaerobic conditions. The first series of column experiments investigated the ability of aerobic G4 culture to degrade TCE after the exposure of the microbes to oxidant. Two columns (30cm long, 2.5cm diameter) were used for the investigations, an inoculated column, and an uninoculated control. The columns were wet packed with base sand using the G4 SMB liquid culture in the inoculated column, and simulated ground water in the control. Flow was provided with a syringe pump at an average pore velocity of 5.5 cm/day, and samples were taken from the effluent. Phenol (8 mg/L) was delivered to both columns for a total of approximately 2 pore volumes until phenol degradation could be observed in the inoculated column. Then potassium permanganate was delivered at 1000 mg/L for 2 pore volumes at an increased average pore velocity of 33 cm/day, to simulate a pressurized oxidant flush. Following oxidation, the columns were fed a solution containing phenol at 30 mg/L and TCE at 8 mg/L to determine if the G4

culture could still actively degrade TCE. The phenol concentration was increased over the initial concentration to enhance the ability to detect phenol degradation. After the experiment, a solution containing m-trifluoromethylphenol (TFMP) was pumped through the columns. To cometabolically degrade TCE, *B. cepacia* must express the enzyme toluene ortho mono-oxygenase (TOM), and if TOM is actively expressed, the bacteria will degrade TFMP to a non-metabolizable molecule TFHA. TFHA is a bright yellow color and allows for visual observation of whether or not the enzyme TOM is being expressed, and thus whether or not the culture is capable of degrading TCE.

The second series of column studies were conducted to determine how permanganate impacts the ability of the KB-1 culture to anaerobically degrade TCE. The conditions evaluated were conceptualized as conditions that may result from a hypothetical oxidant injection well in a subsurface. Condition 1 lies in an area in close proximity to the well, where concentrations of oxidant and fluid velocity are high. Condition 2 is located further down-gradient, where velocities are reduced due to radial flow patterns projecting away from the well, and concentrations of oxidant are partially diminished due to contaminant and NOD oxidation. Condition 3 is located much father down-gradient where velocities are indicative of native ground water flow outside the influence of the well, and oxidant concentration are low, but still detectable.

The anaerobic column studies were conducted using the same columns as in the aerobic column studies, but special care was taken to avoid any oxygen intrusion into the experimental apparatus. The columns were wet packed in an anaerobic glove box, using deoxygenated #70 sand, with a 2.5-cm thick base sand lens at the bottom of each column; uninoculated AGM was used for a flow medium. The porosity of the column was then determined with a tracer test or from bulk media addition. The base sand lens allowed for emplacement of a PCE DNAPL source zone at the bottom of the column (approximately 1.62g). Methanol (25mM) in AGM was pumped through the columns to provide a carbon and energy source, followed by 2 pore volumes of the KB-1 culture in all inoculated columns. Flow was delivered at a Darcy velocity of 2 to 4 cm/day during both the initial pre-oxidation and post-oxidation phases of the experiment in which reductive dechlorination was monitored. After reductive dechlorination was established in the columns in the pre-oxidation phase, oxidant was then delivered at a specified concentration and velocity; insufficient oxidant was applied to completely deplete the DNAPL. A total of eight columns were run, the conditions of which are listed in Table 3.13. Samples taken periodically from the effluent periodically were analyzed for PCE, and anaerobic degradation products TCE, *cis*-DCE, VC and ethene.

Table 3.13. Anaerobic column study conditions.

Column label*	Permanganate concentration (mg/L)	Oxidant injection velocity (Darcy) (cm/day)	Total oxidant dose (mL)	Inoculation condition
LL	100	8	1250	Inoculated
LL-2	100	8	1250	Inoculated
MM	1000	12	205	Inoculated
MM-C	1000	12	205	Uninoculated
LH	100	120	2050	Inoculated
LH-C	100	120	2050	Uninoculated
HH	10000	120	51.2	Inoculated
NOOX-C	0		None	Inoculated

*Column label corresponds to (oxidant concentration, velocity), e.g. LH=low concentration, high velocity. "C" represents control.

3.6.5. Anaerobic Batch Microcosm Studies

Batch microcosm studies were performed to determine how byproducts of oxidation of porous media and ground water impact rates of anaerobic reductive dechlorination behavior. The study investigated the impacts of oxidant type ($KMnO_4$, CHP) on three different soil and ground water environments (simulated ground water, Mines Park (MP), Naval Training Center (NTC)). A total of six different ground waters types were investigated in the batch microcosms. Unoxidized Mine Park and NTC ground water were termed pre-oxidation ground waters. For permanganate oxidized systems, post-oxidation MP and NTC ground waters were generated from columns packed with uncontaminated MP or NTC soil and ground water, oxidized with permanganate (4000 mg/L), and the ground water effluent from the columns was collected prior to permanganate breakthrough. From the MP soil and ground water system, post-oxidation ground water was also generated from CHP (3% H_2O_2, 5mM $FeSO_4$, pH 2.7) oxidation as well, but it had to be generated using a batch reactor because of excessive gas production in a column system.

A simulated ground water system was also investigated to determine how a low dissolved organic carbon (DOC) water source would impact reductive dechlorination. Batch microcosms consisted of 30mL sealed serum bottles, containing a 1:12 electron equivalent PCE-methanol mixture (85mg/L PCE, 13.3 mg/L methanol), with the varied ground water types previously described, as well as varied KB-1 doses, the conditions of which are indicated in Table 3.14. Batch microcosms were run for 90-170 hours, with routine headspace sampling for PCE and degradation products TCE, *cis*-DCE, VC and ethene for determination of reductive dechlorination rates. The batch studies were conducted in three separate runs, with uninoculated controls for each run. Two KB-1 controls were used to determine baseline KB-1 degradation rates, and a pre-oxidation control was run to determine if any microbes capable of reductive dechlorination were present in the site ground water.

Table 3.14. Conditions of anaerobic batch microcosm studies.

Run number	System description	KB-1 dose (mL)	Ground water type
1	Control 1	0	none
2	Control 2	0	none
3	Control 3	0	none
4	KB-1 control	4	none
5	KB-1 control	15	none
6	pre-oxidation control	0	MP pre-ox
7	pre-oxidation	4	NTC pre-ox
8	pre-oxidation	4	MP pre-ox
9	pre-oxidation	15	MP pre-ox
10	post-oxidation	4	NTC $KMnO_4$ post-ox
11	post-oxidation	4	MP $KMnO_4$ post-ox
12	post-oxidation	15	MP CHP post-ox
13	simulated ground water	4	Simulated ground water

3.7. Experimental Investigation of Partitioning Tracer Test (PTT) Methods for Performance Evaluation at ISCO Treated Sites

Batch and 2-D flow cell studies were performed to determine how ISCO may interact with partitioning tracer test (PTT) methods, in order to assess the viability of using PTT at DNAPL sites as a performance indicator where ISCO has been applied. Specific objectives of this portion of the project were to evaluate tracer mass loss due to oxidation with permanganate, evaluate the impacts of oxidant as well as MnO_2 film formation on the TCE and PCE NAPL-water partition coefficient (K_{NW}), and implement the PTT in 1-D and 2-D flowing systems to upscale application of PTT methods under conditions representative of the subsurface both before and after ISCO. This experimental work was performed as part of a doctoral dissertation that should be finalized in December 2006 (Dugan 2006).

This dissertation (and subsequent publications) will detail the complete set of methods used and results obtained during this work.

3.7.1. Batch Studies of Interactions Between Oxidants and Partitioning Tracers

A total of 28 partitioning tracers broken into five groups were evaluated for mass loss due to oxidation and impacts to their respective NAPL-water partition coefficients in the presence of oxidant. The groupings of tracers included a range of linear alcohols (Groups 1 and 2), diol alcohols (Group 3), tertiary alcohols (Group 4), and ketones (Group 5), which were grouped so as to avoid any interference between tracers with gas chromatography detection methods. Tracer Groups 1 and 2 were chosen because they have a wide range of K_{NW} values and have been used in previous lab and field PTT studies (Divine *et al.* 2004, Dugan *et al.* 2003, Dwarakanath and Pope 1998). The tracers in Groups 3-5 were investigated because their chemical structures potentially make them more resistant to oxidation by permanganate. The identities and groupings of tracers investigated are listed in Table 3.15.

For measurement of the K_{NW} values, stock solutions of each tracer group were prepared in ultra-purified water at concentrations of 1000 mg/L, except for one primary alcohol (2E1H), the diols (1,2BUT-doil, 1,7HEP-diol), and two ketones (5M2HEX-one and 2OCT-one), which were prepared at 400, 325, and 225 mg/L respectively. This reduction was necessary due to the lower solubility limit of these compounds. Serial dilutions of the stock solutions were made to create 8 concentration levels varying from 2-1000 mg/L. Three series of batch tests were conducted, first to elucidate the initial K_{NW} value without oxidant, followed by a study to determine K_{NW} with permanganate present, and finally a study to determine K_{NW} with manganese oxide solids precipitated on the surface of the DNAPL. All batch tests were run in triplicate. The initial set of batch tests were performed in 5mL glass vials with Teflon septa where TCE or PCE DNAPL was emplaced in the vials with tracer solution. The vials were agitated on an orbital mixer for 24 hours to ensure equilibrium, and then aqueous phase concentrations of tracers were measured with GC-FID to determine K_{NW} values. The second series of batch tests, similar to the first, were conducted in 20mL vials with TCE or PCE DNAPL and deionized water, equilibrated for 24 hours, then subsequent addition of tracer solution and 500 mg/L permanganate, with another 24 hours of equilibration. The vials are then sampled for TCE, PCE and tracers to calculate K_{NW}. The final series of batch tests used 20 mL vials with DNAPL phase TCE, PCE or 50:50 TCE/PCE mix with 40000 mg/L of permanganate, which was allowed to react for 48 hours with slow agitation so that the permanganate could react to completion. Excess DNAPL remained allowing manganese oxides to establish a film over the DNAPL. Then tracer solution was added with very gentile agitation, and subsequent sampling 24 hours later to determine the K_{NW}.

One additional set of batch experiments was performed to determine tracer mass losses due to oxidation with permanganate. These tests were performed in 2mL GC vials with tracer stock solution, and three concentration levels of permanganate: 5, 50 and 500 mg/L. Vials were reacted for 24 hours, after which the reaction was stopped with the quenching reagent sodium bisulfite. The vials were immediately analyzed for tracer concentrations to determine tracer mass depletion.

3.7.2. Up-scaling PTT Application to 1-D and 2-D Systems

As part of a Ph.D. dissertation (Dugan 2006), experimental plans involved 2-D porous media systems to evaluate the viability of PTT methods when applied in the subsurface after ISCO with permanganate had been implemented. The experimental procedure used for this portion of the research followed that described in Section 3.6.2 and refinements made specific to this work. The complete experimental methods employed will be described in detail in a forthcoming dissertation (Dugan 2006).

Table 3.15. Tracers evaluated during batch studies.

Group 1	Group 2	Group 4	Group 5
2-methyl-1-butanol (2M1B)	1-propanol (isopropanol)(IPA)	Tert-butanol (TBA)	Acetone (Zemel)
2-ethyl-1-butanol (2E1B)	2-methyl-1-pentanol (2M1P)	2-methyl-2-butanol (2M2B)	3-methyl-2-butanone (3M2BUT-one)
4-methyl-2-pentanol (4M2P)	2,2-dimethyl-3-pentanol (22DM3P)	2-methyl-2-hexanol (2M2Hex)	3,3-dimethyl-2-butanone (33DM2BUT-one)
2,4-dimethyl-3-pentanol (24DM3P)	4,4-dimethyl-2-pentanol (44DM2P)	2-methyl-2-pentanol (2M2P)	2-methyl-3-pentanone (2M3PENT-one)
2-ethyl-1-hexanol (2E1Hex)	6-methyl-2-heptanol (6M2Hep)	3-methyl-3-pentanol (3M3P)	2,4-dimethyl-3-pentanone (24DM3PENT-one)
	Group 3	3-ethyl-3-pentanol (3E3P)	5-methyl-2-hexanone (5M2HEX-one)
	1,2-butanediol (1,2BUT-diol)		2,6-dimethyl-4-pentanone (26DM4PENT-one)
	1,7-heptanediol (1,7HEP-diol)		2-octanone (2OCT-one)

3.8. REFERENCES

Chemfinder.com. (2006). Chemfinder.com: Database and Internet Searching. CambridgeSoft Corporation, Cambridge, MA.

Clement, T.P. (1997). A Modular Computer Code for Simulating Reactive Multi-Species Transport in 3D Groundwater Systems. *PNNL-11720,* Pacific Northwest National Laboratory, Richland WA.

Clement, T. P. (2002). What's New in RT3D Version 2.5. Pacific Northwest National Laboratory, Richland WA.

Cohen-Bazire, G., W.R. Sistrom, and R.Y. Stanier (1957). Kinetic Studies of Pigment Synthesis by Non-Sulfer Purple Bacteria. *Journal of Cellular and Comparative Physiology*, 49:25-68.

Crimi, M.L., and R.L. Siegrist (2004). Experimental Evaluation of In Situ Chemical Oxidation Activities at the Naval Training Center (NTC) Site, Orlando, Florida, Colorado School of Mines, Golden.

Crimi, M.L., and R.L. Siegrist (2005). Factors Affecting Effectiveness and Efficiency of DNAPL Destruction Using Potassium Permanganate and Catalyzed Hydrogen Peroxide. *Journal of Environmental Engineering*, 131(12):1724-1732.

Cussler, E.L. (1997). Diffusion: Mass Transfer in Fluid Systems, Cambridge University Press, Cambridge, UK.

Dawson, H.E. (1997). Screening Level Tools for Modeling Fate and Transport of NAPLs and Trace Organic Chemicals in Soil and Groundwater: SOILMOD, TRANS ID, and NAPLMOB. Office of Special Programs and Continuing Education, Colorado School of Mines, Golden, Colorado.

Divine, C.E., J.E. McCray, L.M. Wolf Martin, W.J. Blanford, D.J. Blitzer, M.L. Brusseau, and T.B. Boving (2004). Partitioning tracer tests as a remediation metric: Case study at Naval Amphibious Base Little Creek (NABLC), Virginia Beach. *Remediation Journal*, 14(2):7-31.

Dugan, P.J., J.E. McCray, and G.D. Thyne (2003). Influence of a Solubility-Enhancing Agent (Cyclodextrin) on NAPL-Water Partitioning Coefficients, with Implications for Partitioning Tracer Tests. *Water Resources Research*, 39(5):1123.

Duhamel, M., S.D. Wehr, L. Yu, H. Rizvi, D. Seepersad, S.M. Dworatzek, E.E. Cox, and E.A. Edwards (2002). Comparison of Anaerobic Dechlorinating Enrichment Cultures Maintained on Tetrachloroethene, Trichloroethene, *cis*-Dichloroethene, and Vinyl Chloride. *Water Research*, 36:4193-4202.

Dwarakanath, V., and G.A. Pope (1998). A New Approach for Estimating Alcohol Partition Coefficients Between Nonaqueous Phase Liquids and Water. *Environmental Science and Technology*, 32(11):1662-1666.

Heiderscheidt, J.L. (2005). DNAPL Source Zone Depletion During In Situ Chemical Oxidation (ISCO): Experimental and Modeling Studies. Ph.D. dissertation, Colorado School of Mines, Golden, CO.

Hood, E. (2000). Permanganate Flushing of DNAPL Source Zones: Experimental and Numerical Investigation. Ph.D. dissertation, University of Waterloo, Waterloo, ON.

Jackson, S.F. (2004). Comparative Evaluation of Potassium Permanganate and Catalyzed Hydrogen Peroxide During In Situ Chemical Oxidation of DNAPLs. M.S. thesis, Colorado School of Mines, Golden.

Major, D.W., M.L. McMaster, E.A. Edwards, S.M. Dworatzek, E.R. Hendrickson, M.G. Starr, J.A. Payne, and L.W. Buonamici (2002). Field Demonstration of Successful Bioaugmentation to Achieve Dechlorination of Tetrachloroethene to Ethene. *Environmental Science and Technology*, 36:5106-5116.

Nelson, M.J.K., S.O. Montgomery, E.J. O'Neill, and P.H. Pritchard (1986). Aerobic Metabolism of Trichloroethylene by a Bacterial Isolate. *Applied Environmental Microbiology*, 52(2):383-384.

Petri, B.G. (2006). Impacts of Subsurface Permanganate Delivery Parameters on Dense Nonaqueous Phase Liquid Mass Depletion Rates. M.S. thesis, Colorado School of Mines, Golden, CO.

Sahl, J. (2005). Coupling In Situ Chemical Oxidation (ISCO) with Bioremediation Processes in the Treatment of Dense Non-Aqueous Phase Liquids (DNAPLs). M.S. thesis, Colorado School of Mines, Golden, CO.

Schnarr, M., C. Truax, G. Farquhar, E. Hood, T. Gonullu, and B. Stickney (1998). Laboratory and Controlled Field Experiments Using Potassium Permanganate to Remediate Trichloroethylene and Perchloroethylene DNAPLs in Porous Media. *Journal of Contaminant Hydrology*, 29(3):205.

Schroth, M.H., M. Oostrom, T.W. Wietsma, and J.D. Istok (2001). In-Situ Oxidation of Trichloroethene by Permanganate: Effects on Porous Medium Hydraulic Properties. *Journal of Contaminant Hydrology*, 50(1-2):79.

Seitz, S.J. (2004). Experimental Evaluation of Mass Transfer and Matrix Interactions During In Situ Chemical Oxidation Relying on Diffusive Transport. M.S. thesis, Colorado School of Mines, Golden, Colorado, CO.

Struse, A.M. (1999). Mass Transport of Potassium Permanganate in Low Permeability Media and Matrix Interactions. M.S. thesis, Colorado School of Mines, Golden, CO.

TetraTech NUS. (2002). Remedial Design Report for the In Situ Chemical Oxidation System, NTC, Orlando, Florida. Pittsburgh PA.

Urynowicz, M.A. (2000). Dense Nonaqueous Phase Trichloroethene Degradation with Permanganate Ion. Ph.D. dissertation, Colorado School of Mines, Golden, CO.

Van Cuyk, S., R.L. Siegrist, A. Logan, S. Masson, E. Fischer, and L. Figueroa (2001). Hydraulic and Purification Behaviors and Their Interactions During Wastewater Treatment in Soil Infiltration Systems. *Water Research*, 35(4):953-964.

van Genuchten, M.T., and W.J. Alves (1982). Analytical Solutions of the One-Dimensional Convective-Dispersive Solute Transport Equation. USDA Agricultural Research Service, 151.

Watts, R.J., and S.E. Dilly (1996). Evaluation of Iron Catalysts for the Fenton-like Remediation of Diesel-Contaminated Soils. *Journal of Hazardous Materials*, 51:209-224.

Watts, R.J., and P.C. Stanton (1999). Mineralization of Sorbed and NAPL-Phase Hexadecane by Catalyzed Hydrogen Peroxide. *Water Research*, 33(6):1405-1414.

Wexler, E. (1992). Analytical Solutions for One-, Two-, and Three-Dimensional Solute Transport in Ground-water Systems with Uniform Flow. U.S. Geological Survey Techniques of Water Resources Investigations, U.S. Geological Survey, Denver CO, 198.
Wilking, B. (2004). Factors Controlling Matrix Storage during Mass Depletion in Heterogeneous Porous Media. M.S. thesis, Colorado School of Mines, Golden, CO.

CHAPTER 4

RESULTS AND DISCUSSION

4.1. INTRODUCTION

The results and discussion are divided into sections, based on project objectives and tasks. Data and major findings are presented for each set of experiments that were conducted under each project component. The components are: bench scale kinetic and DNAPL degradation studies, bench scale studies of porous media effects on oxidation reactions, up-scaling reactive transport during ISCO, experimental evaluation of coupling ISCO with other remediation technologies, and experimental investigation of partitioning tracer test methods for performance evaluation at ISCO treated sites.

4.2. BENCH SCALE KINETIC AND DNAPL DEGRADATION STUDIES

Bench scale kinetic and DNAPL degradation studies were conducted to determine the impacts to DNAPL mass transfer rates and degradation for two oxidants (catalyzed hydrogen peroxide and permanganate) as a function of oxidant concentration, porous media types, and subsurface environmental properties. This work included the aqueous phase vial reactor experiments and the multiphase vial reactor experiments, which were completed as part of a M.S. thesis and are documented in detail in Jackson (2004).

4.2.1. Aqueous Phase Vial Reactor Experiments

The aqueous phase vial reactor experiments, run in accordance with the conditions described by Table 3.5, were analyzed with regard to the six efficiency and effectiveness responses described in Section 3.2.5, which include k_{ox}, k_{DNAPL}, RTE, media demand, oxidant demand, and % DNAPL destroyed. In addition, the system's natural oxidant demand was calculated from control systems run without contaminant present. Table 4.1 presents the mean values obtained from these experiments, which were run as duplicates. The efficiency and effectiveness data were analyzed within a fractional factorial design using the statistical analysis software program, Minitab v10. Data from the contaminant mixture systems (runs 17-20) present results for both TCE and PCE, and were not included in the factorial analysis. Due to the fractional factorial design, several factors confounded each other, requiring several additional trials to be run outside of the experimental design to determine the nature of their interaction. The results of these extra interaction studies are discussed in Jackson (2004).

Table 4.2 summarizes the analysis of variance with regard to the 6 efficiency and effectiveness variables presented in Table 4.1 for permanganate ($KMnO_4$) VR systems. The analysis of variance information includes main effects, which indicate the mean response of a factor independent of other factors, as well as interactions, which indicate the differences in mean response dependent on other factors. The statistical significance of each main effect and interaction was also determined, as well as the relative influence of each factor on the response. In Table 4.2, only main effects that were statistically significant at a 95% confidence interval ($\alpha \leq 0.05$) are presented. In parentheses below each factor for the main effects, are the "low" and "high" conditions for each variable. The trend noted under each response indicates the trend as the factor is increased from its "low" to "high" condition. For example, increasing the oxidant concentration from 2x to 10x the stoichiometric demand increased k_{DNAPL} (the rate of contaminant destruction). In parentheses preceding the trend is a number, which ranks the top three factors or interactions that most impact the response. For example, k_{DNAPL} was most impacted by DNAPL type, followed by oxidant concentration and then media addition. For interactions, a comment on the trend of the interaction is made, denoted as either "additive" or "subtractive". For interactions, the baseline condition is always taken to be the "low" condition of both interacting factors. If a trend is

"additive", then the response at the "high" condition of both variables is much higher than would be predicted based on the individual main effects of both factors. If a trend is "subtractive" then the response at both factors "high" condition is much lower than would be expected based on the main effects of the two factors. Please note that for RTE values, a lower value is more advantageous. With regard to this, the trend is noted as "improved" if the RTE value decreased, and "worsened" if the RTE increased.

Table 4.1. Efficiency and effectiveness terms from VR experiments.

	Efficiency terms					Effectiveness terms	
Run #	Media demand (mg oxidant / kg soil)	Natural oxidant demand (mg oxidant / kg soil)	Oxidant demand (mol oxidant / mol contaminant)	k_{ox} (min^{-1})	RTE (k_{ox} / k_{DNAPL})	k_{DNAPL} (min^{-1})	% DNAPL degraded
1	2523	1600	11.6	0.0323	0.15	0.2163	100.0%
2	5525	400	63.1	0.0028	1.25	0.0023	25.3%
3	5407	1825	12.2	0.1391	4.64	0.036	15.5%
4	3400	125	2.48	0.0398	0.07	0.5775	100.0%
5	-	-	6.93	0.0347	0.013	2.735	98.0%
6	-	-	3.11	0.1271	0.056	2.275	100.0%
7	-	-	2.17	0.0023	0.474	0.0049	39.4%
8	-	-	9.43	0.0073	1.2	0.0061	50.8%
9	300	300	1.76	0.203	2.61	0.0777	89.0%
10	345	270	0.918	0.2905	0.209	1.387	90.4%
11	3300	3000	1.66	0.016	0.006	2.628	97.5%
12	2550	2400	2.41	0.0146	0.006	2.614	95.4%
13	-	-	16.9	0.0208	0.008	2.566	97.6%
14	-	-	9.03	0.0214	0.008	2.842	97.3%
15	-	-	1.06	0.1099	0.307	0.3749	42.4%
16	-	-	2.25	1.498	3.48	0.4386	46.0%
17-TCE	-	-	13.1	0.11	0.053	2.1	95.6%
17-PCE			45.6		0.661	0.223	100.0%
18-TCE	4800	1975	7.9	0.098	0.492	0.206	92.2%
18-PCE			31.7		5.34	0.017	83.7%
19-TCE	-	-	12	0.021	0.008	2.69	96.7%
19-PCE			203		-	-	100.0%
20-TCE	2625	2850	1.6	0.012	0.005	2.65	96.7%
20-PCE			203		-	-	100.0%

A number of main effects were observed to occur between the various factors in the permanganate VR systems. The oxidant demand decreased with the addition of NOM, possibly due to sorption of contaminant compounds to the NOM, causing the contaminant to become less available to the oxidant. This increased oxidant persistence resulted in a better relative treatment efficiency. Increasing oxidant concentration increased the rate of contaminant destruction, resulting in a larger amount of contaminant destruction, and also improved the RTE and increased the demand for the oxidant. The addition of porous media to the system increased oxidant demand, reduced contaminant destruction rates, and worsened the RTE, presumably because the media introduced natural oxidant demand to the system, which competes with the contaminant for oxidant. The absence or presence of a pH buffer did not impact the efficiency or effectiveness variables in the aqueous phase VR systems. However, the DNAPL type impacted the efficiency, as PCE resulted in slower oxidant depletion, slower contaminant oxidation, a

decreased amount of contaminant destruction and a less favorable RTE, than corresponding TCE systems. This is probably due to the slower kinetics of PCE oxidation, in addition to the lower concentrations of PCE associated with a lower solubility limit.

Interestingly, the role of NOM in permanganate oxidation was found to be complicated by nine statistically significant interactions with response variables, all of which involved NOM. NOM interacted most with oxidant concentration, where the rate of oxidant depletion, oxidant demand, and media demand had significantly smaller values at high oxidant concentration with NOM present, than would have been predicted based on the main effects of oxidant concentration and NOM. The RTE was improved due to better oxidant persistence, and the amount of DNAPL degraded increased, again more than the amount predicted based on main effects, possibly due to enhanced sorption and desorption. Another series of interactions were found with respect to NOM and the DNAPL type. PCE systems with NOM present saw increased contaminant destruction, and reduced oxidant demand over TCE systems with NOM. An improved RTE also resulted. One final interaction identified was between NOM and media presence, where the rate of oxidant depletion was much higher in systems with both NOM and base sand media present, than would be predicted based on only NOM or base sand systems alone.

Table 4.2. Statistically significant findings from permanganate VR studies.[a]

Factor (Low / high)	k_{ox}	k_{DNAPL}	RTE (k_{ox}/k_{DNAPL})	media demand	oxidant demand	% DNAPL degraded
~ Main effects ~						
NOM content (none / humic acid)	-	-	improved	-	decreased	-
Oxidant concentration (2x / 10x)	-	(2) increased	(1) improved	-	(1) increased	(3) increased
Media addition (none / base sand)	-	(3) decreased	worsened	-	increased	-
pH buffering (unbuffered / buffered)	-	-	-	-	-	-
DNAPL type (TCE / PCE)	(1) decreased	(1) decreased	(2) worsened	-	(2) increased	decreased
~ Interactions ~						
NOM-oxidant concentration	(2) subtractive	-	subtractive	(1) subtractive	subtractive	(1) additive
NOM-DNAPL type	-	-	(3) subtractive	-	(3) subtractive	(2) additive
NOM-media	additive	-	-	-	-	-

[a] Significant trends are given and in parentheses preceding the trend is a number, which ranks the top three factors or interactions that most impact the response. Interactions are denoted as either "additive" or "subtractive". For interactions, the baseline condition is always taken to be the "low" condition of both interacting factors. If a trend is "additive", then the response at the "high" condition of both variables is much higher than would be predicted based on the individual main effects of both factors. If a trend is "subtractive" then the response at both factors "high" condition is much lower than would be expected based on the main effects of the two factors. For RTE values, a lower value is more advantageous and so the trend is noted as "improved" if the RTE value decreased, and "worsened" if the RTE increased.

Similar to Table 4.2, Table 4.3 presents the analysis of variance output for the CHP VR studies. Again, only trends that were statistically significant at a 95% confidence level are presented.

Table 4.3. Statistically significant findings from CHP VR studies.[a]

Factor (low / high)	k_{ox}	k_{DNAPL}	RTE (k_{ox}/k_{DNAPL})	media demand	oxidant demand	% DNAPL degraded
~ Main effects ~						
NOM (none / humic acid)	(2) decreased	-	-	-	-	-
Oxidant concentration (2x / 10x)	decreased	-	-	(1) decreased	(3) increased	(2) increased
Media addition (none / base sand)	decreased	-	-	-	(1) decreased	(3) increased
pH buffering (unbuffered / adjusted to pH 3)	increased	-	(2) worsened	-	-	-
DNAPL type (TCE / PCE)	(1) increased	(1) decreased	(1) worsened	-	(2) decreased	(1) decreased
~ Interactions ~						
NOM-oxidant concentration	-	-	-	-	-	-
NOM-DNAPL type	(3) subtractive	-	-	-	-	-
NOM-media	additive	-	(3) additive	-	-	-

[a] Significant trends are given and in parentheses preceding the trend is a number, which ranks the top three factors or interactions that most impact the response. Interactions are denoted as either "additive" or "subtractive". For interactions, the baseline condition is always taken to be the "low" condition of both interacting factors. If a trend is "additive", then the response at the "high" condition of both variables is much higher than would be predicted based on the individual main effects of both factors. If a trend is "subtractive" then the response at both factors "high" condition is much lower than would be expected based on the main effects of the two factors. For RTE values, a lower value is more advantageous and so the trend is noted as "improved" if the RTE value decreased, and "worsened" if the RTE increased.

A number of statistically significant main effects occurred with respect to oxidation by catalyzed hydrogen peroxide and the factors included in the VR studies. The addition of NOM decreased the rate of oxidant depletion, possibly due to chelation of iron with humic acid, resulting in moderation of hydroxyl radical formation. Increasing the oxidant concentration increased the oxidant demand and the amount of contaminant destroyed. However, increasing CHP concentration also decreased the rate of oxidant depletion and decreased the media demand as well, which was not anticipated. The addition of media also had unanticipated effects, as it increased the amount of contaminant destroyed, and decreased both the oxidant demand and the rate of oxidant depletion. The adjustment of pH to 3 increased the rate of oxidant depletion, but the decreased longevity of the oxidant at low pH resulted in a less favorable RTE. DNAPL type had a number of effects on the efficiency and effectiveness variables, as PCE resulted in an

increased rate of oxidant depletion, a reduced rate and extent of contaminant destruction, and a less favorable RTE. However, the oxidant demand was reduced.

The VR systems were also analyzed for system chemistry effects, which are presented in Table 4.4. System chemistry data of interest include chemical oxygen demand, DOC, pH, temperature, the reduction in dissolved manganese in permanganate systems and reduction in dissolved iron in catalyzed hydrogen peroxide systems, and chloride generation due to destruction of the DNAPL compounds. Average laboratory temperature was 22.7 ºC. COD measures the amount of oxygen needed to thoroughly oxidize all organic matter, but cannot differentiate between degradable and inert organics, or reduced inorganic species (Tchobanoglous and Schroeder 1987). Total organic carbon (TOC) on dry solids was analyzed in systems with base sand media present. TOC and COD data were taken because they have the potential to be used to estimate natural oxidant demand. Permanganate ion interferes with the COD and DOC tests; however, a calibration was performed to correct for these interferences. From the COD data, it also appears that hydrogen peroxide may also interfere with COD, but no correction could be made. The reduction of COD and DOC after 100 minutes of oxidation reaction is also presented expressed as percentage of the initial mass. The measured chloride generation is compared the amount of chloride generation expected based on a mass balance on the aqueous phase contaminant. Complete data sets are available in Jackson (2004).

All systems observed a reduction in pH during oxidation, with unbuffered permanganate and CHP systems resulting in the largest pH changes. The presence or absence of a buffer and the reduction in pH did not have any statistically significant effects on the efficiency and effectiveness of oxidation of TCE or PCE in the permanganate systems. However, some response to system pH was still observed. The oxidant depletion rate was higher in the unbuffered systems, potentially indicating that autocatalytic decomposition of oxidant was more pronounced at the low pH encountered in these systems. Below pH 3, MnO_4^- ion is reduced to Mn^{2+}, but with excess permanganate available, the Mn^{2+} species can be oxidized by permanganate to MnO_2. Buffering pH to 7 prevents this from occurring and the media demand, k_{ox} and oxidant demand, as well as NOD in control systems without contaminant present, were all lower under buffered conditions, indicating a more efficient system. In the CHP systems, the influence of pH was more complex. In the CHP systems adjusted to pH 3, the oxidant depletion rates were much higher, presumably due to the higher rate of hydroxyl radical (OH^-) generation. This did not result in a faster rate of contaminant destruction, but did result in a greater extent of contaminant degradation. For both permanganate and CHP, TCE systems resulted in a larger pH drop, likely due to the higher molar concentration of TCE present initially due to the higher solubility limit, and larger number of protons released during oxidation of TCE.

Some interesting effects were noted with respect to dissolved metals concentrations. Because CHP oxidation requires dissolved iron to catalyze production of OH^-, iron availability may be a controlling factor in CHP oxidation systems. Dissolved iron concentrations decreased in the systems adjusted to pH 3, which was likely due to precipitation of iron complexes. In TCE systems as well, the dissolved iron concentrations dropped more, possibly due to the larger pH change associated with TCE oxidation. When NOM was added to the system, dissolved iron concentrations decreased, probably due to the complexation of iron with humic acid in a filterable state. In the permanganate systems, dissolved manganese concentrations tended to mirror effects witnessed with permanganate concentrations measured by the photometric method, indicating that permanganate oxidation generally resulted in production of insoluble MnO_2, and that appreciable concentrations of Mn^{2+} were not present.

Table 4.4. System chemistry data for aqueous phase VR experiments.

Run #	Initial COD (mg/L)	% COD red.	TOC (wt.%)	Initial DOC (mg/L)	% DOC red.	Initial pH [a]	pH drop	Temp. rise (°C)	Diss. Mn loss (mg/L)	Diss. Fe loss (mg/L)	Cl^- generated (mg/L)	Expected Cl^- generation (mg/L)
1	110	97%	0.0155	70.6	4.0%	7 (b)	0.44	1.3	109	-	54.5	18.7
2	125	18%	ND [b]	61.8	5.7%	5 (u)	1.66	1.6	15	-	102.4	7.5
3	74	100%	0.0319	46.3	69.1%	5 (u)	1.3	1.7	199	-	123.3	36.7
4	85	84%	ND	45.2	11.7%	7 (b)	0.78	1.4	130	-	52.1	110.6
5	83	100%	-	178	7.3%	7 (b)	0.7	1.2	302	-	47.8	99.2
6	119	100%	-	173	20.2%	5 (u)	2.32	1.9	92	-	97.0	232.2
7	43	70%	-	11.4	36.8%	5 (u)	1.5	1.5	44	-	97.3	11.0
8	49	8%	-	13.5	20.7%	7 (b)	0.47	1.6	13	-	36.2	9.5
9	25	20%	0.00753	137	45.3%	3 (b)	0.35	2.8	-	206	-	14.7
10	26	27%	ND	146	47.3%	5 (u)	2.41	0.8	-	150	70.8	32.2
11	131	76%	0.0211	164	30.5%	5 (u)	2.53	0.7	-	56	-	161.3
12	152	80%	ND	179	7.8%	3 (b)	0.47	3	-	136	280.8	86.5
13	646	89%	-	175	5.7%	3 (b)	0.44	3	-	90	83.7	83.7
14	689	88%	-	178	33.7%	5 (u)	2.48	1	-	21	122.8	150.8
15	53	34%	-	36.3	63.4%	5 (u)	2.03	1.1	-	34	61.3	13.8
16	48	8%	-	38.1	39.4%	3 (b)	0.16	3	-	28	70.3	8.1
17	1646	1%	-	161	0.4%	7 (b)	0.6	0.4	53	-	-	-
18	374	20%	0.0070	46.6	0.9%	7 (b)	0.53	0.4	36	-	-	-
19	688	86%	-	173	30.6%	3 (b)	0.46	1.2	-	18	-	-
20	119	76%	0.0052	164	34.8%	3 (b)	0.36	1.2	-	72	-	-

[a] (b) = buffered and (u) = unbuffered.
[b] ND = None detectable based on the methods employed.

Chloride generation was observed in all contaminant oxidation systems. However, a mass balance on chloride, within the VR experimental system, tended to over-predict the mass of contaminant oxidized, when compared to the aqueous phase contaminant mass balance. Schnarr *et al.* (1998) also observed this effect. This excess chloride may potentially be due to oxidant impurities, media-associated addition and interactions with the oxidant, or possibly oxidation of humic acid.

All experimental runs resulted in a decrease in system DOC. During oxidation, DOC concentrations can potentially increase, as oxidation of organic matter in soil can potentially liberate low molecular weight dissolved organic species (Goldstone *et al.* 2002). However, this was not observed in the VR studies. Interestingly, in permanganate systems DOC removal increased when NOM was added, indicating that NOM was competing with the contaminant for oxidant; however, in CHP systems, the

addition of NOM resulted in decreased removal of DOC, potentially indicating production of low molecular weight dissolved organics. DOC removal increased for both oxidants as oxidant concentration was increased.

Figure 4.1 plots TOC as well as COD data vs. oxidant and media demand, for both permanganate and CHP systems, to determine if there was any quantifiable relationship. TOC in soil data has been used in the past to estimate NOD, but lab studies have shown this is not very accurate (Siegrist *et al.* 2001). The results from the VR studies mirror this as no linear trends with respect to TOC and oxidant or media demand are observed in the data, for either permanganate or CHP (Figures 4.1a, 4.1b, 4.1e and 4.1f). However, the COD data potentially indicate that a linear relationship may exist between media demand and COD for both permanganate and CHP (Figures 4.1c and 4.1g), and oxidant demand and COD for permanganate systems (Figure 4.1d). Thus, if a correlation between COD and permanganate or CHP natural oxidant demand can be established, then the COD test may represent a simple and effective way for predicting NOD in field soils. However, further research would be necessary to elucidate the nature of the relationship between COD and NOD for both oxidants.

4.2.2. Multiphase Vial Reactor Experiments

The multiphase vial reactor experiments, conducted under the conditions outlined in Section 3.3.2, were analyzed with regard to five efficiency and effectiveness response variables. These include k_{ox}, k_{DNAPL}, RTE, oxidant demand, and percent DNAPL destroyed. In addition, the interface mass transfer coefficient, the DNAPL dissolution mass flux rate, and the second order degradation rate constant for each MVR system were calculated. Table 4.5 presents these data from the multiphase vial reactors.

Because the MVR experiments contain a DNAPL phase, an aqueous phase, and a hexane phase, the systems had to remain quiescent during the experimental runs to keep the phases separate. Because oxidant is added to the quiescent system at time 0, with the multiple phases already present, no mechanical mixing may occur during oxidant addition. In the permanganate systems, the density difference between the oxidant and the aqueous phase resulted in considerable stratification, and thus permanganate concentrations varied with depth. Because of this, permanganate concentration data, as well as resulting chloride concentration data were inconclusive. In the CHP systems, gas generation resultant of oxidation mixed the aqueous phase, allowing for use of the oxidant and chloride concentration data from these systems.

The efficiency and effectiveness data from Table 4.5 were analyzed using Minitab (version 10xtra), in a similar fashion as described in Section 4.2.1. For the analysis of the MVR factorial design, two separate blocks were analyzed, the first "presence of NOM" block comparing systems with humic acid only to systems with no humic acid, and the "solid phase content" block comparing systems with humic acid only to systems with humic acid and goethite. Trends are noted for responses that are statistically significant at a 95% confidence interval as factors change from the "low" to "high" condition. Interactions are "additive" if the response is much higher for the two interacting factors at their respective "high" conditions, than would be based on main effects alone, or subtractive if the response is much lower. Table 4.6 presents the findings from permanganate systems and Table 4.7 from CHP systems.

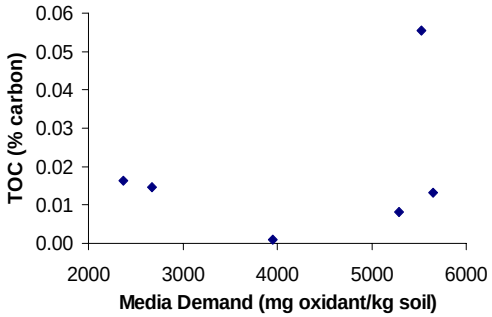

Figure 4.1a

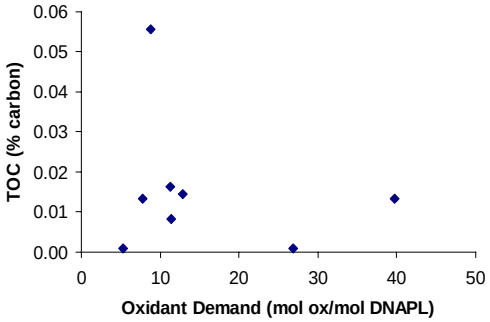

Figure 4.1b

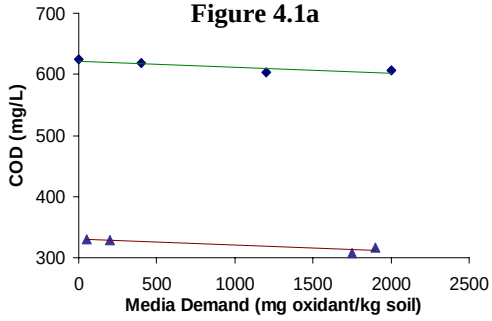

Figure 4.1c

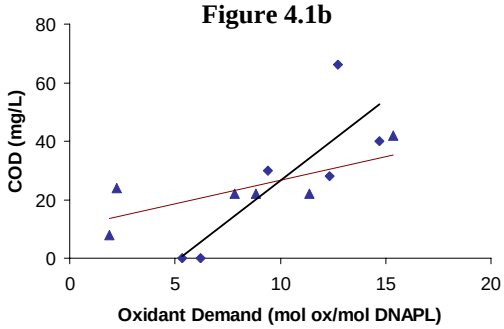

Figure 4.1d

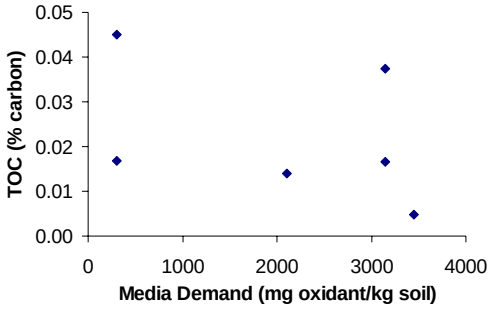

Figure 4.1e

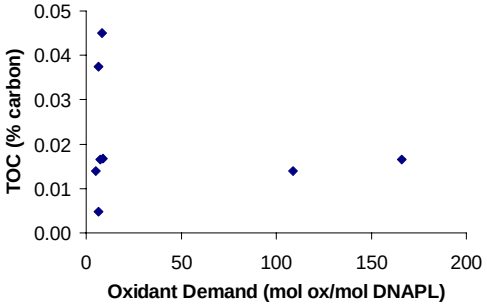

Figure 4.1f

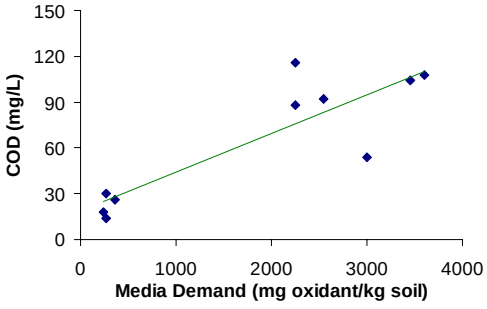

Figure 4.1g

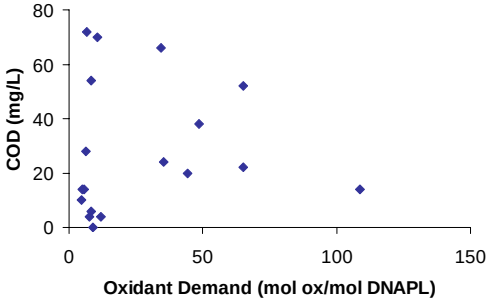

Figure 4.1h

Figure 4.1. Relationships between TOC and COD with oxidant and media demand: TOC vs. media demand for permanganate systems (Fig. 4.1a), TOC vs. oxidant demand for permanganate systems (Fig. 4.1b), COD vs. media demand for permanganate systems, split by oxidant concentration (Fig. 4.1c), COD vs. oxidant demand for TCE permanganate systems (Fig. 4.1d), TOC vs. media demand for CHP systems (Fig. 4.1e), TOC vs. oxidant demand for CHP systems (Fig. 4.1f), COD vs. media demand for CHP systems (Fig. 4.1g), COD vs. oxidant demand for CHP systems (Fig. 4.1h).

Table 4.5. Efficiency and effectiveness results from the MVR experiments.

Run #	Oxidant Demand (mol_{ox} / mol_{DNAPL})	k_{ox} (min^{-1})	RTE (k_{ox} / k_{DNAPL})	k_{DNAPL} (min^{-1})	% DNAPL degraded	Interphase mass transfer rate (cm/s)	Mass flux rate (g/m^2-hr)	k_2 (L/mol-s)
1	6.7	0.002	0.42	0.006	51.9%	3.1E-05	1.10	1.1E-02
2	4.4	0.000	0.61	0.001	76.3%	1.1E-05	0.37	1.0E-03
3	24.6	0.002	0.41	0.006	21.8%	3.2E-05	3.13	1.2E-02
4	58.2	0.001	0.63	0.001	15.3%	1.2E-05	0.71	2.0E-03
5	7.4	0.004	0.66	0.006	62.3%	3.2E-05	2.17	1.2E-02
6	4.8	0.001	0.72	0.002	88.6%	1.7E-05	0.40	3.0E-03
7	83.9	0.006	0.54	0.013	56.7%	4.4E-05	2.08	2.0E-03
8	205	0.001	0.64	0.002	22.0%	1.8E-05	0.45	3.9E-04
9	80.8	0.002	0.44	0.006	58.4%	3.1E-05	2.98	1.0E-03
10	74.6	0.002	0.57	0.003	64.7%	2.2E-05	0.79	5.9E-04
11	66.8	0.002	0.60	0.003	61.7%	2.1E-05	3.66	5.0E-04
12	85.5	0.001	0.68	0.002	60.3%	1.8E-05	0.56	3.8E-04
13	904	0.006	1.95	0.003	22.6%	2.4E-05	3.52	2.5E-04
14	459	0.006	2.42	0.003	43.6%	2.2E-05	1.15	2.3E-04
15	358	0.006	0.95	0.007	49.1%	3.4E-05	4.13	3.1E-04
16	430	0.007	1.01	0.007	46.3%	3.3E-05	0.99	2.8E-04
17	518	0.006	1.88	0.004	46.4%	2.6E-05	4.07	2.7E-04
18	500	0.006	0.38	0.017	41.6%	5.4E-05	0.46	3.8E-04
19	28150	0.010	0.12	0.080	3.1%	1.2E-04	4.33	-
20	12813	0.010	1.43	0.007	21.1%	3.4E-05	0.70	4.0E-05
21	4016	0.010	0.50	0.022	44.0%	6.0E-05	4.43	6.1E-05
22	8588	0.010	0.10	0.101	11.7%	1.3E-04	1.22	7.4E-05
23	4401	0.009	1.60	0.007	40.2%	3.3E-05	5.03	4.9E-05
24	11975	0.010	0.30	0.033	16.8%	7.5E-05	1.20	5.0E-05

Table 4.6. Statistically significant findings from permanganate MVR studies.[a]

Factor (low / high)	k_{ox}	k_{DNAPL}	RTE (k_{ox}/k_{DNAPL})	Oxidant demand	% DNAPL degraded	k_2
~ Block one: presence of NOM ~						
~ Main effects ~						
Oxidant concentration (0.1% / 1.0%)	(2) increased	-	-	(1) increased	-	(2) decreased
NOM (none / humic acid present)	-	-	-	-	-	-
DNAPL Type (TCE / PCE)	(1) decreased	(1) decreased	(1) worsened	increased	-	(1) decreased
~ Interactions ~						
Oxidant conc. x DNAPL type	-	-	-	-	-	additive
Oxidant conc. x NOM	-	-	-	(2) subtractive	(1) additive	-
~ Block two: solid phase content ~						
~ Main effects ~						
Oxidant concentration (0.1% / 1.0%)	decreased	-	-	(1) increased	-	(1) decreased
NOM (humic acid / humic acid + goethite)	-	-	(1) worsened	-	(2) increased	-
DNAPL Type (TCE / PCE)	(1) decreased	(1) decreased	(2) worsened	-	-	(2) decreased
~ Interactions ~						
Oxidant conc. x DNAPL type	(2) additive	(2) additive	-	-	-	additive
Oxidant conc. x NOM	subtractive	-	-	-	(1) subtractive	-

[a] Significant trends are given and in parentheses preceding the trend is a number, which ranks the top three factors or interactions that most impact the response. Interactions are denoted as either "additive" or "subtractive". For interactions, the baseline condition is always taken to be the "low" condition of both interacting factors. If a trend is "additive", then the response at the "high" condition of both variables is much higher than would be predicted based on the individual main effects of both factors. If a trend is "subtractive" then the response at both factors "high" condition is much lower than would be expected based on the main effects of the two factors. For RTE values, a lower value is more advantageous and so the trend is noted as "improved" if the RTE value decreased, and "worsened" if the RTE increased.

A number of interesting effects were observed with respect to the permanganate ($KMnO_4$) MVR systems. Increasing oxidant concentration had the result of increasing the rate of oxidant consumption, and the oxidant demand, which has been observed by others (MacKinnon and Thomson 2002, Siegrist *et al.* 2002, Siegrist *et al.* 2001), but the calculated second order reaction rate decreased. Increases in the rate and extent of DNAPL degradation as well as increases in the interface mass transfer rate were seen at

higher oxidant concentrations, but these changes were not statistically significant at the 95% level. The increase in oxidant depletion rates, coupled with the relatively insignificant increase in the DNAPL destruction rate might be attributable to decomposition of permanganate in the presence of MnO_2 solids, resulting from oxidation of the DNAPL. Another interesting observation is that using a similar experimental apparatus, Urynowicz (2000) found that DNAPL mass transfer rates decrease due to deposition MnO_2 at the DNAPL interface over time; however this effect was not observed under the conditions of this study. The addition of humic acid to the permanganate MVR systems, when compared to no NOM controls, did not result in any statistically significant main effects, in contrast to the VR experimental systems. There were however, two significant interactions with oxidant concentration, with a subtractive interaction observed with oxidant demand and an additive interaction with the % DNAPL degraded. Interestingly, these same interactions were discovered in the VR systems. Apparently, higher concentrations of oxidant coupled with NOM result in better destruction of the DNAPL, possibly due to enhanced sorption and desorption, but without substantially increasing oxidant demand. The DNAPL type also had impacts on efficiency and effectiveness. TCE had higher rates of destruction, oxidant depletion, mass transfer, a faster calculated second order reaction rate, less oxidant demand, and a better RTE than PCE. These changes can be attributed to the faster rate of reaction for TCE coupled with the higher solubility limit of TCE. However, an interaction occurred between the DNAPL type and the oxidant concentration, where PCE systems with high oxidant concentrations saw larger rates of oxidant depletion and DNAPL degradation than would be predicted based on the main effects observed.

The addition of goethite to permanganate systems also had impacts on the efficiency and effectiveness of contaminant destruction. The trends of the main effects mainly remained the same, with the exception that the rate of oxidant depletion actually decreased slightly with increasing oxidant concentration, and two new main effects were seen resulting from NOM content type. Humic acid systems with goethite present increased the amount of DNAPL destroyed, but the RTE was less efficient. Two subtractive interactions were witnessed between NOM content and oxidant concentration, where humic acid systems with goethite present and higher concentrations of oxidant had lower oxidant depletion rates and lower % DNAPL degraded than would be expected based on main effects. An additive interaction found between oxidant concentration and DNAPL type with respect to the calculated second order reaction rate was also observed in the other experimental block. However two additional additive interactions were seen in the solid phase contact block where PCE systems with high oxidant concentrations resulted in higher oxidant depletion and DNAPL destruction rates than predicted by main effects.

DNAPL dissolution was found to be enhanced by the addition of permanganate, as the mass flux rates were found to increase over control systems. TCE DNAPLs had higher mass flux rates, due to the higher solubility limit of TCE. Higher permanganate concentrations were found to enhance the DNAPL mass flux more than lower concentrations. Also, several interesting observations were made with respect to the mass flux rates and the addition of humic acid. The addition of humic acid enhanced DNAPL mass flux, possibly due to enhanced sorption and desorption. However, the addition of goethite in the presence of humic acid decreased this effect.

Table 4.7 presents the statistical analysis of response variables for the MVR systems utilizing CHP. Again, two experimental blocks were used, a presence of NOM block which compares systems with humic acid to systems with no NOM, and a solid phase content block which compares humic acid systems with and without goethite present.

Table 4.7. Statistically significant findings from CHP MVR studies.[a]

Factor (low / high)	k_{ox}	k_{DNAPL}	RTE (k_{ox}/k_{DNAPL})	oxidant demand	% DNAPL degraded	k_2
~ Block one: presence of NOM ~						
~ Main effects ~						
Oxidant concentration (1% / 10%)	-	(1) increased	decreased	increased	-	decreased
NOM (none / humic acid present)	-	(3) increased	-	-	-	-
DNAPL Type (TCE / PCE)	(1) increased	decreased	-	-	-	-
~ Interactions ~						
Oxidant conc. x DNAPL type	(2) subtractive	subtractive	-	-	-	-
Oxidant conc. x NOM	-	additive	-	-	-	-
NOM x DNAPL type	-	(2) additive	-	-	-	-
~ Block two: solid phase content ~						
~ Main effects ~						
Oxidant concentration (1% / 10%)	increased	(1) increased	-	(1) increased	-	decreased
NOM (Humic acid / humic acid + goethite)	-	decreased	-	increased	-	-
DNAPL Type (TCE / PCE)	increased	(2) increased	-	(2) increased	-	-
~ Interactions ~						
Oxidant conc. x DNAPL type	-	additive	-	(3) additive	-	-
Oxidant conc. x NOM	-	(3) subtractive	-	additive	-	-
NOM x DNAPL type	-	subtractive	-	additive	-	-

[a] Significant trends are given and in parentheses preceding the trend is a number, which ranks the top three factors or interactions that most impact the response. Interactions are denoted as either "additive" or "subtractive". For interactions, the baseline condition is always taken to be the "low" condition of both interacting factors. If a trend is "additive", then the response at the "high" condition of both variables is much higher than would be predicted based on the individual main effects of both factors. If a trend is "subtractive" then the response at both factors "high" condition is much lower than would be expected based on the main effects of the two factors. For RTE values, a lower value is more advantageous and so the trend is noted as "improved" if the RTE value decreased, and "worsened" if the RTE increased.

From Table 4.7, it is interesting to note that for CHP oxidation, every factor as well as three factor interactions impacted k_{DNAPL} in both experimental blocks, indicating that the rate of DNAPL destruction is highly dependent on the factors that were studied. Evaluating the first block, increasing oxidant concentrations from 1% to 10% increased the rate of DNAPL destruction and increased the oxidant demand as expected, with the result of improving the RTE. The addition of humic acid to the system also increased the rate of DNAPL destruction, possibly indicating enhanced sorption and desorption due to oxidation. The contaminant destruction rate decreased in PCE systems, probably due the lower solubility of PCE, while the rate of oxidant depletion increased. Three interactions were also found to impact the rate of contaminant destruction. Two subtractive interactions between DNAPL type and oxidant concentration resulted, where higher CHP concentrations with PCE were observed to result in a much lower contaminant destruction rate and lower oxidant depletion rate that anticipated based on main effects. Additive interactions were discovered between NOM and both oxidant concentration and DNAPL type, where humic acid presence increased the rates of contaminant destruction in systems with higher oxidant concentrations and systems containing PCE.

The analysis of the solid phase content block also generated interesting results. The "presence of NOM" block resulted in a total of 7 significant main effects and 4 interactions, while the "solid phase content" block resulted in 9 significant main effects and 6 interactions. Four of the main effects trends observed were consistent with both blocks, while all interactions were different. Also, oxidant demand had significant main effects and interactions in every category, unlike the presence of NOM block, indicating that it was highly dependent on the solid phase content. The presence of goethite in the humic acid systems resulted in an increased oxidant demand, while decreasing the rate of contaminant destruction. Two interactions, between NOM and both oxidant concentration and DNAPL type, were both additive for oxidant demand, and subtractive for the rate of contaminant destruction. In these interactions, the presence of goethite with PCE or high oxidant concentrations resulting in reduced performance. Also interesting is that the interaction between oxidant concentration and DNAPL type reversed its trend relative to the "presence of NOM" block, as PCE systems with high concentrations witnessed increased DNAPL destruction rates and higher oxidant demands.

The DNAPL mass flux and dissolution rates were found to be enhanced with CHP, similar to the permanganate systems. Again, the mass flux rates were higher for TCE systems and with higher oxidant concentrations. Interestingly, the same trend found in the permanganate system with respect to NOM content was also observed, in that the addition of humic acid caused an increase in the DNAPL mass flux, due to possible sorption and desorption, but the addition of goethite reduced this effect.

4.3. BENCH-SCALE STUDIES OF POROUS MEDIA EFFECTS ON OXIDATION REACTIONS

Bench-scale studies with porous media were conducted to determine the impact of porous media types and properties on DNAPL degradation and mass transfer during ISCO, as well as determine their effects on oxidant transport. Below are presented major findings from the zero headspace reactor and diffusion cell studies.

4.3.1. Zero Headspace Reactor Studies

The zero headspace reactor studies were conducted according the methods described in Section 3.4.1, and the results have been published in Crimi and Siegrist (2005). Below is a summary of results from these studies. The ZHR studies were analyzed with respect to 6 efficiency and effectiveness variables described in Section 3.2.5, which includes k_{ox}, k_{DNAPL}, RTE, media demand, oxidant demand, and %DNAPL destroyed. The data are presented in the publication and were analyzed within a fractional factorial design, which considered the impacts of oxidant type ($KMnO_4$ vs. CHP), media type (sand, sand + humic acid, sand + humic acid + goethite), oxidant load (1× vs. 2× stoichiometric demand), DNAPL load (0.2×, 2×, 3× soil and ground water capacity), and DNAPL type (TCE, PCE, TCE + PCE).

The ZHR experiments determined that the efficiency and effectiveness of oxidation treatment are largely dictated by environmental conditions. Under optimized conditions, DNAPL oxidation can be achieved efficiently and effectively, using either permanganate or CHP. Of the factors investigated, the oxidant type was most influential on the efficiency and effectiveness, and the oxidant load exerted the least impact. The media demand was the most sensitive response and the percent DNAPL destroyed was the least sensitive to the factors investigated.

It was found that under certain conditions, oxidation of DNAPL phase contamination could be more effective and efficient than that of sorbed phase contaminant, with faster mass destruction rates and higher percentages of contaminant destroyed. DNAPL systems observed more efficient kinetics than sorbed systems; however, oxidant demand and media demand were higher when DNAPL was present. In DNAPL systems, the percent contaminant destruction, oxidant depletion rate, and RTE were less sensitive to changes in other system factors, while the rate of contaminant destruction, oxidant demand and media demand were more sensitive to interaction with other environmental factors.

Another major finding of the ZHR studies was that permanganate was generally more effective at contaminant destruction, while CHP was more efficient. Permanganate systems were less impacted by other factors with respect to percent DNAPL destroyed, but the efficiency responses were more sensitive to changes in environmental factors. CHP efficiency was more stable as media demand, oxidant and contaminant degradation rates, and RTE were less impacted by conditions. However, the percent destroyed was more sensitive with CHP, and the oxidant demand was highly variable. With both oxidants, increasing oxidant load was found not to increase the rate and extent of contaminant destruction, but did increase oxidant demand and media demand.

Media composition was also important to oxidation efficiency and effectiveness. Generally, a simple sand media is assumed to be the most efficient and effective to remediate compared to more complex media containing natural organic matter, silt and clay fractions, or reduced minerals. However, it was found from the ZHR studies that complex medias, which may exert a higher NOD, can be more effective and efficient under some conditions. The presence of humic acid was found to increase the percent contaminant destroyed, despite a lower rate of contaminant destruction, possibly indicating that humic acid enhanced the dissolution or desorption of contaminant. Several interesting impacts to efficiency and effectiveness were also noted with respect to the presence of the iron-bearing mineral goethite. In permanganate systems, the addition of goethite in the presence of humic acid appeared to enhance the efficiency and effectiveness of PCE oxidation, but not TCE oxidation, and did not impart significant oxidant demand or media demand. In CHP systems, the addition of goethite improved PCE oxidation efficiency, but the overall effectiveness was reduced.

The findings from these studies indicate that the environmental factors that interact during oxidation of DNAPLs in porous media have a complex impact to remediation efficiency and effectiveness.

4.3.2. Diffusion Cell Studies

The diffusion cell studies included several components, including natural oxidant demand studies for permanganate and the porous media used in the diffusion experimentation, described in Section 3.4.2, catalyzed hydrogen peroxide stabilization studies described in Section 3.4.3, and diffusion cell studies, described in Section 3.4.4. This work was completed as part of a master's thesis project, and is presented in detail in Seitz (2004).

4.3.2.1. Natural Oxidant Demand Studies. Evaluation of NOD is important to modeling of diffusive transport of oxidants, requiring NOD studies. Preliminary diffusion modeling was conducted in order to select an appropriate experimental scale, such that steady state oxidant diffusion could occur within a reasonable period of time. Concentration vs. time data for the varied permanganate

concentrations tested in the NOD studies for the sandy loam low permeability media, are presented in Figure 4.2. In addition, data comparing the total NOD after the 14-18 day reaction period for both sandy loam and silica sand LPM are presented for the varied permanganate concentrations in Figure 4.3.

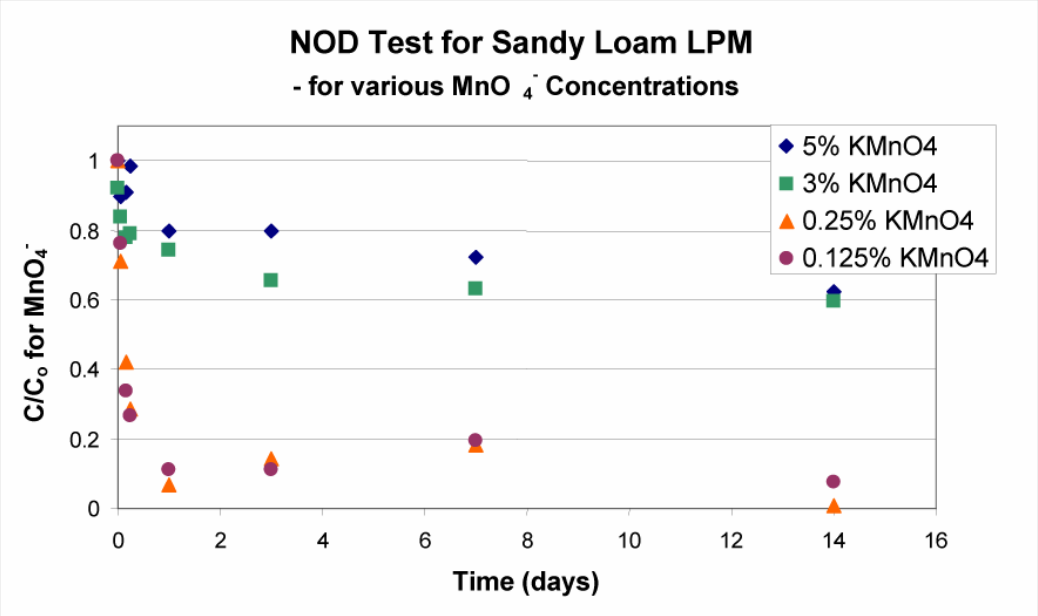

Figure 4.2. Permanganate concentrations vs. time for sandy loam LPM.

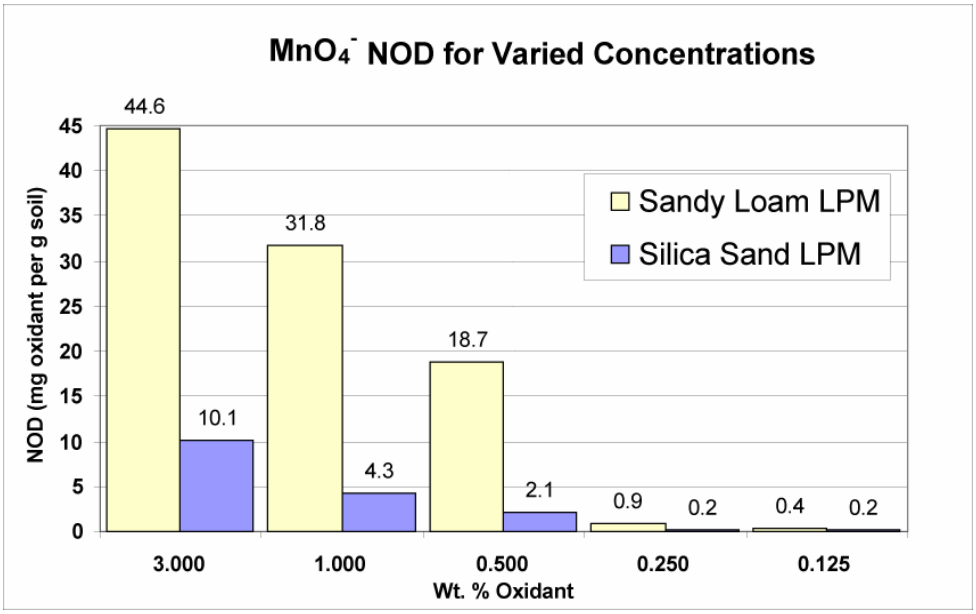

Figure 4.3. Comparison of NOD for different LPM and oxidant concentrations.

Three primary conclusions were found from the NOD studies. First, increasing permanganate concentration also increased the non-productive oxidant demand, a finding which is consistent with other studies (Siegrist *et al.* 2001, Struse 1999, Urynowicz 2000), and was evidenced by the increasing total demand with increasing oxidant dose in Figure 4.3. A second major finding was that the sandy loam LPM had a much higher NOD than the silica sand LPM at all concentrations tested. This was expected as medias with higher TOC contents, a higher clay fraction with a resulting higher surface area, and more reduced mineral content, are anticipated to increase NOD (Siegrist *et al.* 2001, Struse 1999). The third major conclusion was that rate of oxidant consumption by NOD decreases with time, and on the basis of data from the sandy loam LPM, could be approximated by two different rates. Figure 4.2 demonstrates that the initial 24 hours of reaction result in a very steep slope in the concentration vs. time plot for all oxidant concentrations, indicating that there is an initial "fast" reaction rate that consumes oxidant. However, this rate rapidly declines with time, and from 24 hours to 14-18 days, the concentrations decline at a much lower rate, indicating that there is a "slow" NOD fraction. These two varied rates have important implications for oxidant delivery in the subsurface as "slow" NOD may impact oxidant delivery even after the "fast" NOD has been depleted, resulting in oxidant delivery challenges. This is especially true when diffusive transport is relied on for oxidant delivery, due to the extended contact time with the media. This slowing of the rate of NOD may in part be due to reaction by TOC components that are more resistant to oxidation, after easily oxidized components have been depleted, as well as potential coating of reactive surfaces with MnO_2 precipitants that build up as the reaction proceeds with time (Siegrist *et al.* 2001, Struse 1999).

The results from the NOD studies were used in a modeling study to determine the proper length of soil core to use that would result in a reasonable experimental run time for the permanganate diffusion cell studies (see Seitz (2004) for modeling approach). The completely mixed NOD studies were chosen to represent the NOD exerted during diffusive transport of permanganate as during a completely mixed NOD test, all reactive sides of each soil particle are assumed to have contacted oxidant. During diffusive transport, oxidant can diffusive into pore spaces where no advective flow may occur, and thus oxidant may be more uniformly delivered to the media, despite the system not being mixed. However, it is important to recognize that NOD results measured in lab studies may only be applicable to field application when the study conditions represent the field delivery mechanisms.

4.3.2.2. Catalyzed Hydrogen Peroxide Stabilization Studies. The catalyzed hydrogen peroxide stabilization studies investigated the persistence of concentrations of hydrogen peroxide in the presence of the porous media types used in the diffusion cell investigations and various amendments to reduce the decomposition rate of hydrogen peroxide versus time. Figure 4.4 presents the concentration of hydrogen peroxide versus time for the various systems described in Section 3.4.3.

The goal of CHP stabilization was to determine the system with the slowest degradation of oxidant over an 18-21 hour period, which was to be selected to promote diffusive transport in the diffusion cell experiments. The study evaluated 1 wt.% H_2O_2 in a non-amended control, pH 2 and pH 3 adjusted ground water, a low (20mM) and high (40mM) phosphate buffer, ferrous (Fe^{2+}) and ferric (Fe^{3+}) iron catalyst amended ground waters, citric acid in ground water, and citric acid with ferrous (Fe^{2+}) iron amended ground water. The rates of H_2O_2 decomposition are much faster than for permanganate during the NOD tests. Figure 4.4 shows the concentration of hydrogen peroxide, relative to the initial concentration, versus time for the CHP stabilization studies using the sandy loam LPM.

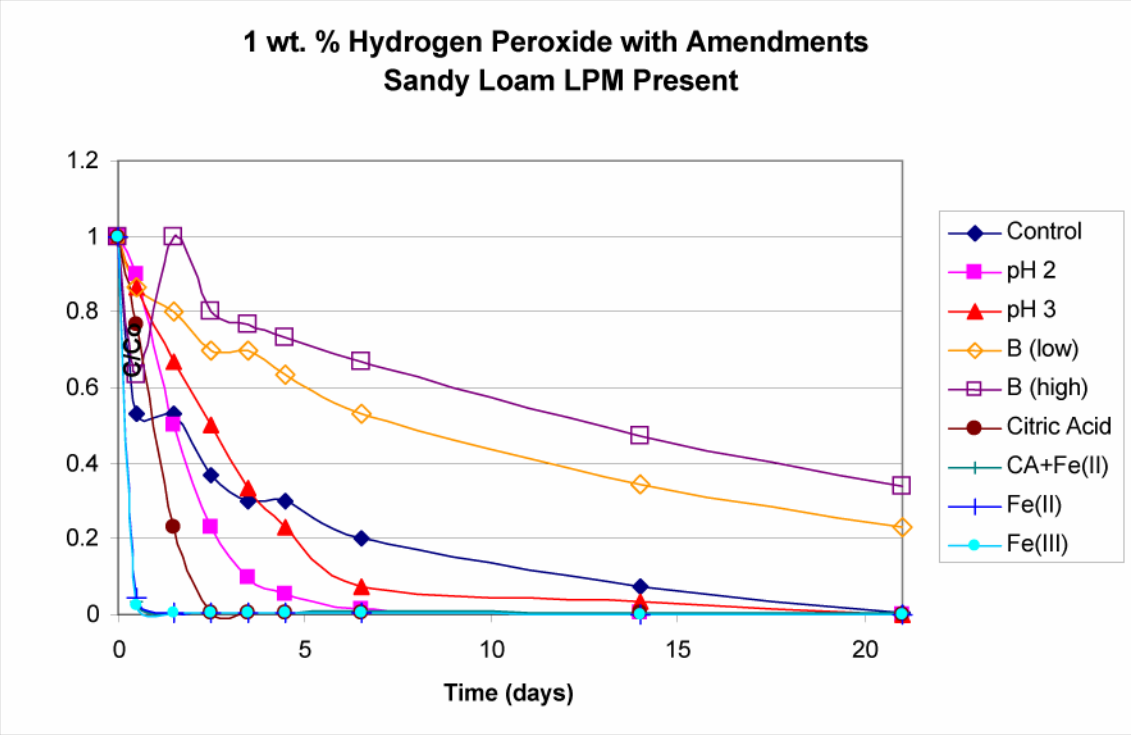

Figure 4.4. Sandy loam CHP stabilization results.

Figure 4.4 illustrates that substantial depletion of oxidant occurred in the presence of sandy loam LPM after 21 days under all conditions studied. The two phosphate buffered systems fared best, with the higher buffer reducing the oxidant depletion rate the most. The control system with no amendment resulted in the next lower oxidant depletion rate, followed by the pH 3 system, the pH 2 system and the citric acid only system. The addition of any iron, whether ferrous or ferric, resulted in a dramatic depletion of the oxidant, with essentially no oxidant remaining after 1 day. In control systems with no media, the persistence was longer than in the presence of media, but the overall oxidant persistence followed the same trends as in the systems with sandy loam LPM.

Based on the hydrogen peroxide stabilization study results, it was decided to use hydrogen peroxide with no amendments in the diffusion cell studies. The hydrogen peroxide only systems had the third most favorable performance, after the two phosphate buffered systems, but based on degradation rates, it was predicted that a hydrogen peroxide only system would maintain about 50% of the initial concentration of oxidant after 2 days. For experimental purposes in the diffusion cells, every 2 days fresh peroxide would be added to the diffusion cell influent chamber to maintain a stable oxidant concentration. However, during experimentation, it was found that hydrogen peroxide concentrations in the influent chamber declined much more rapidly with time than anticipated, and within 24 hours were non-detectable. Oxidant addition still occurred every 2 days, with fluid removal to maintain a zero hydraulic gradient in the diffusion cell system. Maintaining a constant hydrogen peroxide influent concentration remained an issue throughout the diffusion cell studies.

4.3.2.3. Diffusion Cell Studies. Four primary diffusion cell experiments were run, according to the conditions outlined in Table 3.8. Figure 4.5 shows the bromide concentrations in the effluent chambers of these diffusion cells versus time, with separate linear trend lines fit to the data for both pre-oxidation and oxidation times. Both permanganate cells achieved steady-state diffusion. Contrary to the preliminary experiments using permanganate, the bromide flux changed only slightly after oxidant addition in oxidation cells A and B. Struse (1999) found that the bromide flux increased by a factor of 15-16 using similar apparatus in a system with a core length to average pore size ratio of 600, in comparison to this system which has a ratio of 1100. The increased tortuosity in this system may be large enough to overcome this co-diffusion effect. Also of note in Figure 4.5, is that the effluent bromide concentrations from CHP diffusion cell D are much more variable. This is likely due to shifting concentrations of bromide in the influent. Fresh oxidant was added every two days, and a corresponding volume of fluid was removed to maintain a zero hydraulic gradient across the core. Small amounts of bromide were added to compensate for this loss, but the influent concentration was inevitably more variable. Cell C developed a leak after contaminant addition, which resulted in de-saturation of the soil core, and could not be repeated due to time limitations. Due to the difficulties maintaining oxidant concentrations in cell D, and the cell C leak, neither hydrogen peroxide cell achieved steady-state diffusion. From the bromide data, effective diffusion coefficients were calculated for diffusion cells A and B, which are presented in Table 4.8. For more information on how these values were calculated, see Seitz (2004).

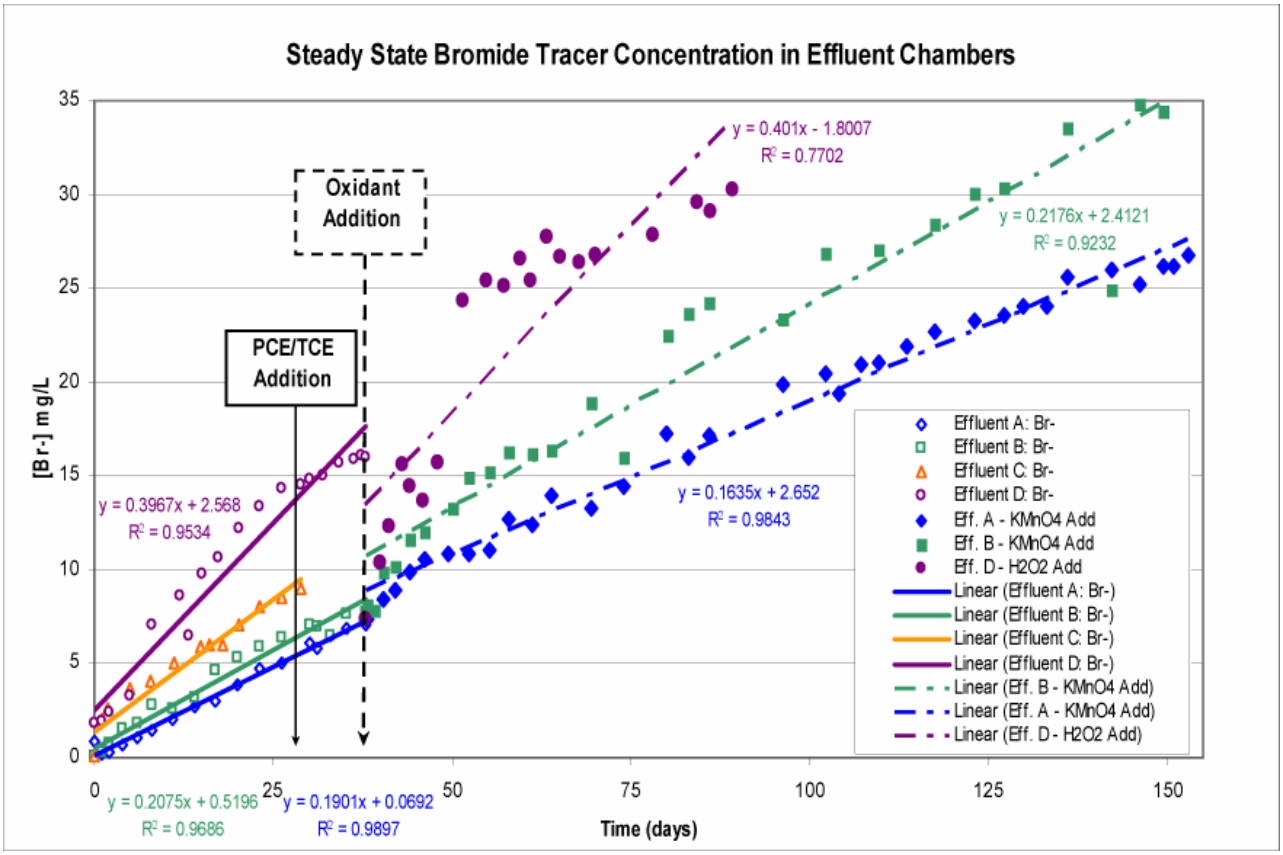

Figure 4.5. Effluent chamber bromide concentrations from 1-D diffusion cell runs.

Table 4.8. Bromide diffusion rate in LPM diffusion cells.

Diffusion cell	Pre-oxidation bromide flux (mg / cm^2-s)	Oxidation bromide flux (mg / cm^2-s)	Ratio $J_{pre\text{-}ox}$ / J_{ox}	Pre-oxidation apparent tortuosity (τ_a)	Oxidation apparent tortuosity (τ_a)	Oxidant effective diffusion coefficient (cm^2/s)
A	2.10E-07	1.74E-07	1.21	0.73	0.97	$1.295x10^{-5}$
B	2.29E-07	2.32E-07	0.984	0.78	1.35	$1.305x10^{-5}$
C	2.29E-07	N/A	N/A	0.80	N/A	N/A
D	4.37E-07	4.32E-07	1.012	1.92	N/A	N/A

Of interest, the effective diffusion coefficients for permanganate in both the silica sand and the sandy loam were very similar. However, the breakthrough concentration profiles between the two soil types were very different. Figure 4.6 reveals this by showing cell A and cell B at the same time points throughout the experiment. The silica sand demonstrated a much more rapid breakthrough with detectable oxidant concentrations in the effluent chamber 24 hours after oxidant addition, while the sandy loam did not observe breakthrough until 80 days into experimentation. This difference is likely due to the fact that the silica sand has little sorption or NOD to limit permanganate diffusion or reaction with contaminant, while the sandy loam is more complex with higher surface area, organic content and NOD. Also of note are the angled permanganate breakthrough fronts, which is a density-driven effect due to the higher density of 1 wt.% $KMnO_4$ solution with respect to the simulated ground water in the effluent chamber. This vertical migration suggested that density-driven permanganate flow may be advantageous to delivery of oxidant into LPM.

The increase in tortuosity noted in Table 4.8 from the pre-oxidation to the oxidation stage is interesting as well, as an increase in tortuosity usually indicates an increase in permeability. Such a permeability increase is possible if depletion of NOM or reduced minerals results in an increase in porosity. This could also be an artifact if co-diffusion is occurring within the LPM core. However, this increase does indicate that it is unlikely that either manganese oxide solids (MnO_2) deposition in the core or CO_2 gas generation from oxidation of organics are occurring at a significant enough magnitude to reduce permeability.

The pre-oxidation value for tortuosity for cell D is unreasonably high, as values for tortuosity in excess of 1.0 are frequently due to advective influences. Due to the inability of cell D to achieve steady state diffusion, diffusive transport characteristics could not be calculated for cell D. However, the cell D core was dissected to determine if any changes in the porous media indicated whether the oxidant had any effect on the core.

Conductivity data, available in Seitz (2004), concluded that no sharp solute fronts were observed in either permanganate cell effluent chamber, but rather a gradual increase in conductivity. The influent chamber conductivities gradually decreased as the experiments progressed. No significant change in temperature was witnessed to occur in any of the diffusion cells. In cell A, pH gradually increased in the effluent chamber after oxidant was added; however, in cell B, pH increased in the effluent chamber, but then decreased after permanganate breakthrough, indicating that H^+ generation was occurring, possibly from contaminant oxidation.

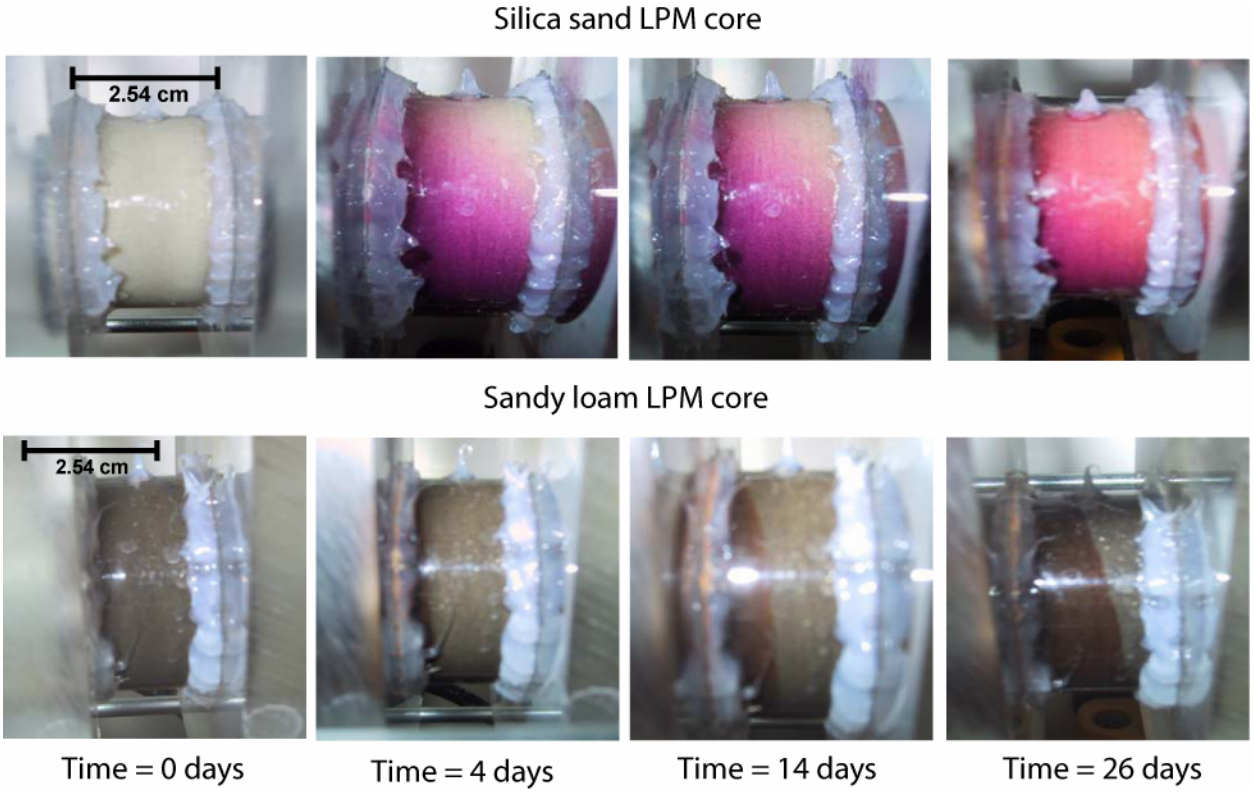

Figure 4.6. Observation of permanganate breakthrough in cores A and B.

After experiment shutdown, the soil cores from cells A, B, and D were dissected to determine how diffusive transport of oxidants impacted soil properties and contaminant destruction. Extractions were preformed on five discrete subsections of each core progressing along the length of the core to determine oxidant, TOC, TCE and PCE, exchangeable cation, and manganese concentrations, as well as pore water content. Oxidant, TOC and pore water data from these extractions are presented in Table 4.9. Use Figure 4.7 as a reference diagram subsection location.

In the two permanganate cells, the permanganate pore water concentrations increased from the influent chamber to the effluent chamber, while remaining TOC concentrations are highest near the effluent end of the core and decrease moving toward the influent. This indicates that permanganate consumed TOC as part of natural oxidant demand. Interestingly, although no CHP was ever detected in the effluent chamber, and would decompose typically within 24 hours in the influent chamber, the TOC in the cell D soil core decreases from the effluent to the influent, as in the permanganate system. This pattern in the TOC data indicate that perhaps some peroxide was able to diffuse into the core and react with TOC, despite the difficulties in maintaining oxidant concentration in this cell.

Table 4.9. Oxidant and TOC results from diffusion cell soil core analysis.

Diffusion cell	Subsection	Distance from influent (cm)	Water content (dry wt.%)	TOC (mg TOC / g dry soil)	TOC consumed (mg TOC / g dry soil	Oxidant (mg/L)
Cell A – $KMnO_4$ in sandy loam LPM	a	0-0.5	28.8%	0.15	1.23	2145.3
	b	0.5-1.0	32.5%	0.23	1.15	1188.9
	c	1.0-1.5	30.7%	0.27	1.11	1005
	d	1.5-2.0	30.5%	0.43	0.95	182.9
	e	2.0-2.5	30.7%	0.69	0.69	31.6
Cell B – $KMnO_4$ in silica sand LPM	a	0-0.5	18.6%	0.014	0.0055	4592
	b	0.5-1.0	18.2%	0.015	0.0039	3441.8
	c	1.0-1.5	18.5%	0.018	0.0015	2988.3
	d	1.5-2.0	18.3%	0.02	-0.0005	2693.2
	e	2.0-2.5	17.3%	0.02	-0.0005	2481.4
Cell D – H_2O_2 in sandy loam LPM	a	0-0.5	25.8%	0.93	0.45	ND [a]
	b	0.5-1.0	26.8%	0.98	0.40	ND
	c	1.0-1.5	24.1%	1.03	0.35	ND
	d	1.5-2.0	22.6%	1.09	0.29	ND
	e	2.0-2.5	25.8%	1.21	0.17	ND

[a] ND = Non-detectable, detection limit approximately 17 mg/L H_2O_2.

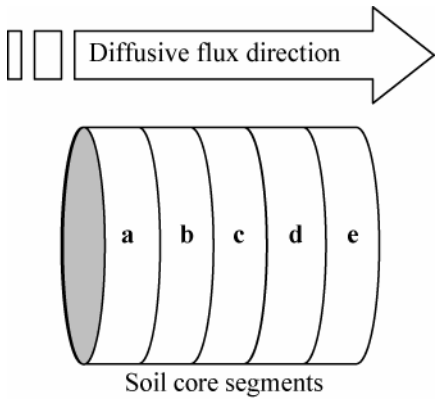

Figure 4.7. Soil core dissection diagram.

TCE and PCE concentrations in the soil cores from cells A and B were non-detectable at the time of extraction (analytical detection limit <64 ppb TCE and <23 ppb PCE). In the cell D core, some removal of TCE and PCE was observed, with estimated 32.2% TCE and 19.5% PCE mass reductions. Exchangeable cation data in cell A indicated that an ionic sweep may have occurred within the soil core. Due to the high concentration of potassium ions in solution, calcium and magnesium ions sorbed to the soil may have been displaced, as potassium concentrations were very high at the influent end, while calcium and magnesium concentrations were elevated above background levels near the effluent end. Also of interest is that manganese deposition in the soil core was minimal. Manganese extraction data revealed that only 0.008 mg of Mn in cell A, and 6.07 mg of mg in cell B had accumulated in the core during oxidation. This corresponds to less than 0.07% reduction in porosity (assuming the density of dry MnO_2 solids), which is negligible. The soil cores were further analyzed using Environmental scanning

electron microscopy (ESEM) to determine the nature of the pore scale changes. For the silica sand LPM, sand grains in the oxidized media were slightly more angular and appear more porous than a control sample of media. Furthermore, several manganese particles were observed, whose composition was confirmed by an X-ray detector, and were observed to form in plate like discrete particles. However, the LPM samples must be dried for ESEM analysis, and it is unknown if drying the LPM may have caused the MnO_2 solids to agglomerate into particles. ESEM analysis of the sandy loam was less conclusive. Due to the presence of clay and natural organic matter, the sandy loam LPM was visually more complex, and discrete manganese solids could not be identified by the X-ray detector. Visually, the oxidized media appeared to have less stringy and less angular material than observed in the sandy loam control.

4.4. UP-SCALING REACTION AND TRANSPORT DURING ISCO: EXPERIMENTAL AND MODELING STUDIES

The following section presents selected data, results, and discussion from the reaction and transport experiments that were completed to evaluate DNAPL mass transfer and transport in flowing porous media systems undergoing oxidation. Experiments were conducted in 1-D flow-through tube reactors, 2-D flow-through cells, 2-D intermediate-scale tanks, 2-D large-scale tanks. Mathematical modeling was also completed to simulate ISCO processes using permanganate.

4.4.1. Flow-Through Tube Reactor Studies

The flow-through tube reactor experiments consisted of a total of 32 trials at varied permanganate concentrations and delivery velocities, varied DNAPL types and DNAPL source architectures to study the impacts of permanganate flushing velocities on contaminant mass depletion rates. This work was completed as part of an M.S. thesis project and is presented in detail in Petri (2006).

A large amount of concentration vs. time data was generated from the FTR experiments, which were used to calculate response variables that indicate impacts to contaminant mass transfer. Table 4.10 presents a summary of these response variables for each FTR. Contained in Table 4.10, are β values for each phase of each FTR trial, which are quantitative indicators of the rate of DNAPL mass depletion in each FTR system. A separate β value was calculated for each phase of each FTR trial, and is similar to a degradation rate constant with units of 1/time. The ratio of β values from one experimental phase to another was termed the slope ratio (SR), which indicates the relative change in the mass depletion rate resultant from oxidation. These include SR_{max}, which indicates the relative magnitude of mass transfer enhancement due to oxidation, and $SR_{post\text{-}ox}$, which indicates the relative magnitude of contaminant rebound after oxidation. In addition, two efficiency variables were developed. The molar treatment efficiency (MTE) is an indicator of how efficiently the oxidant was used in the system, with a higher value indicating better oxidant use. The volumetric depletion efficiency (VDE) indicates the effectiveness of the flushing regime, with a higher value indicating that fewer pore volumes of oxidant solution will be needed to deplete the DNAPL. Also reported in Table 4.10 is the total mass fraction of DNAPL depleted from each FTR at the conclusion of the experiment, as well as a qualitative observation of the trend in mass transfer at the conclusion of the experiment. If the DNAPL appeared to be completely depleted and plume concentrations were low or non-detectable, then a "depleted" trend was entered. If contaminant concentration rebound was observed, it was entered as "rebound," or if concentrations were approaching zero, then a "tailing" effect was noted. For more information on how these values were calculated from the data, see Petri (2006).

Table 4.10. Summary data from the FTR trials.

Trial	$\beta_{pre\text{-}ox}$ (min^{-1})	$\beta_{ox\ max}$ (min^{-1})	$\beta_{post\text{-}ox}$ (min^{-1})	SR_{max} (-)	SR_{postox} (-)	MTE (-)	$VDE_{pre\text{-}ox}$ (-)	VDE_{ox} (-)	Mass fraction removed	Mass transfer trend	Gas generation observed?
FTR1	2.4607	2.1165	0.0139	0.86	0.01	0.325	0.717	0.236	0.722	Depleted	No
FTR2	1.5190	2.1638	0.0038	1.40	0.00	0.375	0.506	0.404	0.790	Depleted	No
FTR3	No data	No data	No data	No data	No data	No data	No data	No data	No data	No data	Yes
FTR4	0.8939	3.1006	0.0386	3.55	0.05	0.460	0.174	0.288	0.849	Depleted	No
FTR5	1.3206	0.7680	0.0062	0.57	0.00	0.030	0.255	0.067	0.345	Depleted	No
FTR6	0.1348	0.0620	0.0076	0.46	0.05	0.005	0.347	0.117	0.485	Depleted	No
FTR7	0.2207	0.2138	0.0188	0.97	0.09	0.010	0.444	0.172	0.798	Depleted	No
FTR8	0.1617	0.3126	0.0026	1.92	0.02	0.008	0.390	0.298	0.737	Depleted	No
FTR9	0.1173	0.1888	0.1812	1.73	1.62	0.006	0.283	0.496	1.022	Tailing	No
FTR10	0.1559	0.3140	0.0010	2.01	0.01	0.013	0.397	0.251	0.620	Depleted	No
FTR11	0.1996	0.1810	0.0561	0.90	0.28	0.833	0.821	0.471	0.911	Tailing	No
FTR12	0.2414	0.3847	0.0036	1.59	0.01	0.621	0.645	0.355	0.698	Depleted	No
FTR13	0.2132	2.1434	0.0010	9.79	0.00	0.221	0.696	0.756	1.192	Depleted	No
FTR14	0.0144	0.0195	0.0142	1.36	0.99	0.181	0.925	1.118	0.114	Rebound	No
FTR15	0.0091	0.0081	0.0062	0.89	0.68	0.086	0.680	0.557	0.058	Rebound	No
FTR16	0.0272	0.0296	0.0293	1.09	1.08	1.753	0.795	0.765	0.522	Rebound	No
FTR17	0.0208	0.0286	0.0237	1.37	1.14	0.909	0.800	1.017	0.441	Rebound	No
FTR18	0.0241	0.1006	0.0028	4.13	0.11	0.530	0.743	1.447	0.442	Tailing	Yes
FTR19	0.2170	0.1793	0.0013	0.82	0.01	0.784	0.870	0.483	0.748	Depleted	No
FTR20	0.0230	0.0871	0.0215	3.76	0.93	0.117	1.034	3.759	0.331	Rebound	Yes
FTR21	0.0033	0.0041	0.0036	1.24	1.10	1.309	0.963	1.232	0.052	Rebound	No
FTR22	0.0031	0.0129	0.0041	4.14	1.30	1.268	1.015	3.772	0.092	Rebound	No
FTR23	0.0035	0.0540	0.0032	15.61	0.93	0.507	0.999	12.596	0.281	Rebound	Yes
FTR24	0.0245	0.1898	0.0226	7.70	0.92	1.267	0.843	4.818	0.947	Tailing	Yes
FTR25	2.5333	12.1161	0.0353	4.79	0.01	0.521	0.741	1.176	0.799	Depleted	Yes
FTR26	0.0285	0.0284	0.0277	1.00	0.97	N/R	0.738	0.753	0.299	Rebound	No
FTR27	0.0035	0.0032	0.0033	0.92	0.95	N/R	0.781	0.826	0.034	Rebound	No
FTR28	0.0244	0.0289	0.0254	1.19	1.04	N/R	0.901	0.951	0.160	Rebound	No
FTR29	0.0938	0.1116	0.0753	1.20	0.81	N/R	0.784	0.756	0.553	Rebound	No
FTR30	No data	No data	No data	No data	No data	N/R	No data	No data	No data	No data	No
FTR31	1.5781	1.3427	0.3896	0.85	0.25	N/R	0.469	0.334	0.748	Tailing	No
FTR32	0.2553	0.2620	0.2590	1.03	1.02	N/R	0.857	0.878	0.386	Rebound	No

The data values in Table 4.10 were analyzed within a factorial design using Minitab 14, a statistical analysis program, to determine the trends in the data and statistical confidence of effects observed. A 95% confidence interval was used to determine statistical significance. The following is a summary of major findings from this analysis.

The DNAPL type was observed to impact DNAPL mass depletion rates in the FTR systems. TCE resulted in faster mass depletion rates than PCE, which was anticipated due to the higher solubility limit of TCE. However, the initial magnitude of mass depletion rate enhancement due to oxidation was not found to differ significantly between TCE and PCE. One possible explanation for this is that the order of magnitude increase in kinetic reaction rate between PCE and TCE is offset by the order of magnitude increase in solubility limit, resulting in similar magnitudes of mass depletion rate enhancement. This is interesting as other DNAPL compounds may perform differently depending on relative reaction rates and solubility limits.

Impacts to the mass depletion rates were also noted with respect to the DNAPL entrapment architecture. Several preliminary experiments evaluated large DNAPL ganglia, whereas the factorial design evaluated DNAPL residuals. These large ganglia experiments could still be evaluated in a fractional factorial yielding information about interactions with other factors. All of the large ganglia experiments were evaluated at high velocities, and the large ganglia were located in the bottom half of the FTR. The residuals were found to have faster mass depletion rates than the large ganglia, which could be due to the smaller interfacial areas of large ganglia for dissolution to occur across, possible non-equilibrium mass transfer due to the high velocity of the system, and flow bypassing of the ganglia in the upper half of the reactor. However, the impacts to mass depletion rates during oxidation were interesting. A significant interaction between oxidant concentration and the architecture was observed, where medium concentrations of oxidant (1000 mg/L $KMnO_4$) saw similar mass transfer enhancements for both residuals and large ganglia. However, high oxidant concentration systems observed larger mass depletion rate enhancements in the residual systems, while mass depletion rates decreased in large ganglia systems, possibly indicating that manganese solids (MnO_2) deposition was limiting mass transfer from the large ganglia.

The oxidant concentration was observed to impact mass depletion rates and remediation efficiency in several ways. The addition of oxidant had the result of increasing the DNAPL mass depletion rate, and higher concentrations resulted in faster mass depletion rates. Thus mass transfer was enhanced by oxidant flushing, due to bulk aqueous phase reaction, as well as possibly changes in theoretical mass transfer relationships resulting from the presence of oxidant. The magnitude of the this enhancement, when compared to pre-oxidation phase mass depletion rates, increased with increasing concentration, but was highly dependent on the ground water flushing velocity of the system. Increasing velocity increased DNAPL mass depletion rates, as expected and correlates with a number of other studies of DNAPL mass transfer (Imhoff *et al.* 1993, Miller *et al.* 1990, Powers *et al.* 1994). However, the magnitude of the mass transfer enhancement due to oxidant flushing decreased with increasing velocity. Thus a significant interaction between oxidant concentration and oxidant flushing velocity was discovered with respect to DNAPL mass depletion rates. When either oxidant delivery velocity or oxidant concentration is increased, the DNAPL mass depletion rate increases, but if both are done simultaneously, the increase is much smaller than doing one or the other alone. However, the overall magnitude of the mass depletion rate increase is much larger for a proportional increase in velocity, than for a proportional increase in oxidant concentration.

A hypothesis for the mechanism that controls the magnitude of mass depletion rate enhancement was proposed, in which two competing kinetic rates control the magnitude of enhancement. These kinetic rates include the rate of DNAPL mass transfer, and the rate of oxidation reaction. This is conceptualized by considering two cases. In case one (see Figure 4.8), the rate of DNAPL mass transfer is much faster than the rate of reaction, owing to higher velocities that increase the mass transfer rate, or lower oxidant concentrations which reduce the reaction rate. The result is that the reaction is unable to appreciably

impact bulk aqueous contaminant concentrations within the source zone and thus is unable to cause a large mass transfer enhancement. Thus reaction occurs both within the source zone, as well as in a "reaction cloud" down-gradient of the source zone until sufficient contact time has occurred to deplete either the aqueous contaminant or the oxidant in its entirety. While this case does not cause as much mass transfer enhancement due to oxidation reaction, it has the advantage of a much higher mass depletion rate owing to the high mass transfer rate, and also the resulting MnO_2 solids are deposited over a larger volume of aquifer materials, potentially reducing permeability changes. In the second case (see Figure 4.8), the rate of oxidation reaction is much faster than the mass transfer rate, which could result from lower velocities or higher oxidant concentrations. This results in appreciable reduction of contaminant concentrations in the source zone allowing for much more mass transfer enhancement. Due to the lower velocities of these systems, sufficient contact time is available for complete oxidant consumption, even in high concentration systems, resulting in all MnO_2 solids depositing within the source zone, and potentially causing pore clogging. Little or no reaction occurs down gradient of the source.

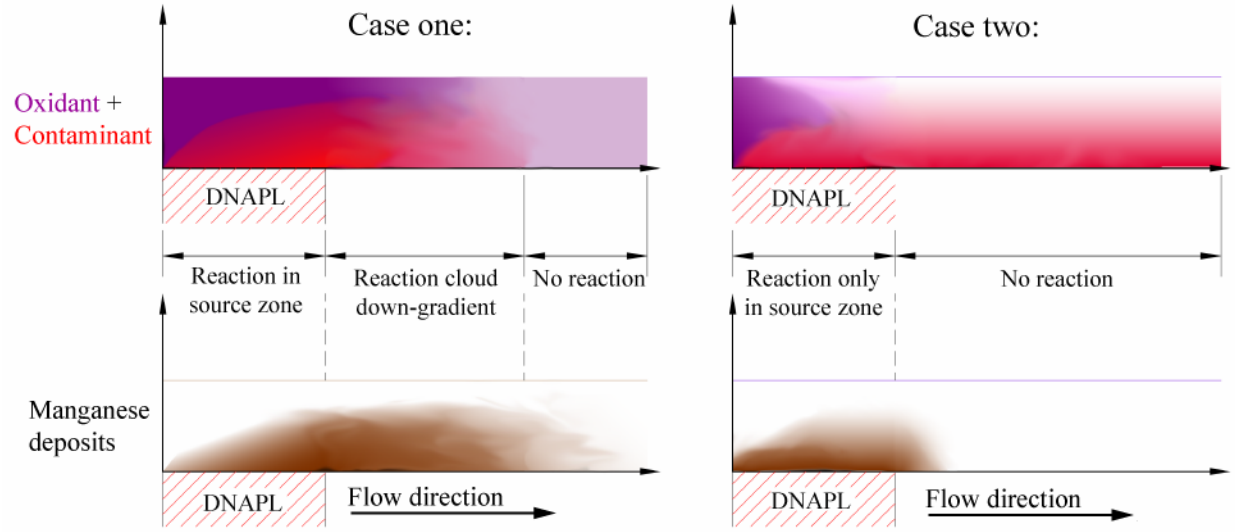

Figure 4.8. Conceptualization of mass transfer enhancement mechanism (Petri 2006).

Several other interesting observations were made with respect to the impacts to mass transfer after oxidant flushing had ceased. $SR_{post\text{-}ox}$, which indicates the magnitude of contaminant rebound after oxidation, was found to be highly dependent on the total mass of DNAPL depleted, and the trend in mass transfer noted in Table 4.10 at experiment shutdown. If $SR_{post\text{-}ox}$ is near 1, then it indicates that the contaminant mass depletion rate rebounded to a level essentially identical to the pre-oxidation rate, indicating that the contaminant plume flux was not reduced by oxidant treatment. If $SR_{post\text{-}ox}$ is near 0, then rebound did not occur. Figure 4.9 is a plot of $SR_{post\text{-}ox}$ vs. the fraction of DNAPL mass depleted.

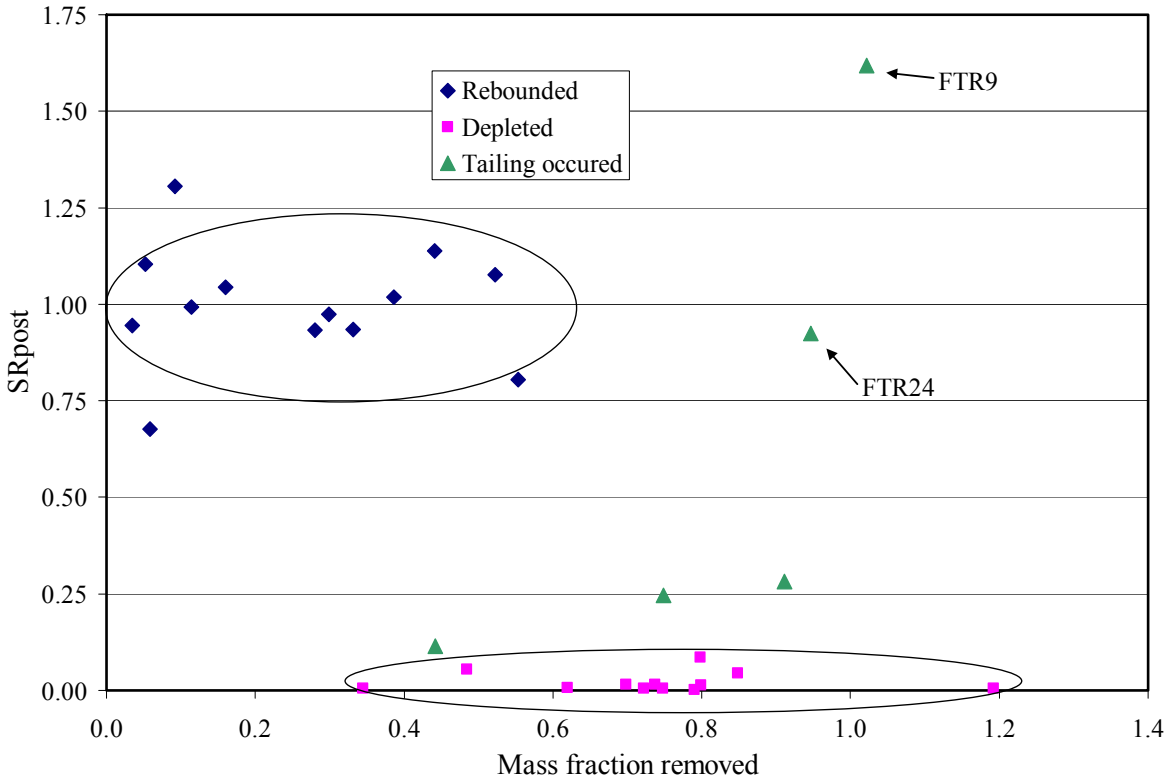

Figure 4.9. Plot of $SR_{post\text{-}ox}$ versus mass fraction depleted.

From Figure 4.9, it can be observed that there are two distinct groupings of data points, which are split according to the trend noted at the time of experiment shutdown. The first grouping of points is the "rebound" trend points, which had lower mass depletions and tended to group around an SR value of 1, indicating that when rebound occurred, it occurred at a rate comparable to the pre-oxidation rate. The second major grouping were the "depleted" trend data points and had higher mass removals and tended to be grouped at values near 0, indicating that DNAPL dissolution had nearly stopped, most likely due to removal of nearly all the DNAPL. In between these two groupings, lay the "tailing" systems, most of which were close to exhibiting a "depleted" trend and near zero. The clear separation between the former two groupings indicate that within this system, mass depletion rates, and therefore mass flux rates, either rebounded to their initial rate, or near complete removal of the DNAPL mass occurred and DNAPL concentrations were low or non-detectable. This suggests that DNAPL residuals are likely to be depleted before any significant encapsulation by MnO_2 solids occurs.

However, two notable outliers were noted from Figure 4.9. The first, FTR24, was a system where significant gas generation had occurred, resulting in possible error in the mass balance, which may explain why such a large rebound occurred in a system with a large mass removal. The other outlier was FTR9, which was a large ganglia oxidation system with high oxidant concentrations. In this system, it is possible that the more heterogeneous nature of the source resulted in the post-oxidation increase in concentrations. In this system, DNAPL was located only in the bottom half of the source zone, while most of the advective flow was forced through the top half. A large amount of MnO_2 solids were deposited in this top area during the oxidation of this system, possibly diverting flow closer to the

DNAPL ganglia during the post-oxidation phase, which may explain why the contaminant mass flux in this system increased after oxidation. Since the scale of this cross section of the FTR is only about 0.5 cm, and this source zone represents a very simple heterogeneity, it is possible that heterogeneities on the order of millimeters may still have impacts on DNAPL mass transfer on a larger scale.

A number of important efficiency impacts and other observations were noted as part of the FTR studies as well. Lower velocities were found to increase the efficiency of oxidant use as well as the efficiency of flushing indicating that fewer pore volumes of oxidant would be required at low velocities. However, the mass depletion rates are much slower at low velocities indicating that longer clean up times may be required. In addition, lower velocity systems resulted in CO_2 generation, which was observed to mobilize DNAPL and vapor phase contaminant, as well as reduce hydraulic conductivity. Higher oxidant concentrations reduced the number of pore volumes that would be needed for DNAPL depletion; however, both oxidant waste and gas generation increased with increasing oxidant concentrations. Gas generation was worsened in TCE systems with high oxidant concentration, due in part to a large pH drop that occurred, effectively forcing dissolved CO_2 into the gas phase.

4.4.2. Two-Dimensional Flow Cell Studies

The two-dimensional flow cell experiments were conducted according to the methods described in Section 3.5.2, and completed as part of a collaborative group effort. A detailed report including all relevant methods, data, findings and conclusions from this work is attached to this document in Appendix A. Below is a summary of results and discussion from this work.

The 2-D flow cell experiments were analyzed with respect to both qualitative and quantitative performance criteria. Toward the former, each 2-D flow cell experiment was analyzed for the effectiveness of oxidant delivery and distribution, contaminant concentration and distribution reductions, as well as impacts to system chemistry. For quantitative performance evaluation, analysis of the 2-D flow cell systems focused on the same 6 efficiency and effectiveness response variables described in Section 3.2.5, including K_{ox}, K_{DNAPL}, RTE, oxidant demand, media demand, and % DNAPL destroyed. The discussion that follows is broken into a discussion of these qualitative and quantitative performance analyses.

The effectiveness of the delivery and distribution of oxidant was found to vary with the oxidant type. Hydrogen peroxide was found to decompose rapidly upon introduction into the flow cell. Several different methods were utilized for activation of CHP, including addition of ferrous iron (5mM $FeSO_4$) with pH adjustment, pH adjustment alone relying on natural iron content in the media to activate the reaction, and the addition of citric acid as a chelating agent to mobilize natural iron into the aqueous phase. Regardless of activation method, hydrogen peroxide was found to rapidly decompose upon introduction into the porous media, with all CHP systems experiencing greater than 60% oxidant depletion prior to reaching the A sample port, which is located up-gradient of the source zone, and only 4 cm into the cell. This was evidenced by hydrogen peroxide concentration data as well as extensive gas generation in the up-gradient end of the flow cell. Pressurized injection was found to improve penetration of oxidant into the media, possibly due to the higher velocity associated with this injection technique, which reduces contact time with the media. Hydrogen peroxide injection achieved a relatively uniform oxidant front that swept across the 25 cm long flow cell, but concentrations never exceeded 20% of the injected concentration in the effluent of the pressurized injection systems, and was never detectable in the effluent of the gravity feed system effluents. The permanganate oxidant distribution results were much different than hydrogen peroxide systems. The permanganate systems exhibited much slower oxidant decomposition rates, with much greater oxidant penetration into the cell, despite a much lower oxidant concentration by mass. This was evidenced by a much more gradual depletion of oxidant as the oxidant flushed across the cell, with approximately 7% oxidant depletion at the A sample port up-gradient from the source zone, and effluent concentrations depleted to 20% of the injected concentration for the gravity

feed injection system. The permanganate systems achieved much deeper oxidant penetration into the media, but the oxidant front was less uniform than for peroxide. This was due to a significant density driven advection effect, where oxidant migrated downward upon introduction to the tank, resulting initially in faster velocities in the lower half of the flow cell.

Several interesting observations were made with respect to the contaminant concentrations during the oxidation phase of the experiment. In general, concentrations of contaminant were high during the pre-oxidation phase of the experiment, followed by a reduction to low or non-detectable levels during the oxidant flush, and followed by rebound to varied levels as not enough oxidant was injected to deplete the DNAPL. However, in several cases, the aqueous contaminant concentrations at certain observed locations actually increased during oxidation. The first observation of this effect was in hydrogen peroxide cell 3, in ports located above and down-gradient of the source. It is possible that the extensive gas generation associated with this system mobilized DNAPL or vapor phase contaminant upward, resulting in contaminant concentrations rising in these areas. However, as oxidant flushing continued, the concentrations dropped, possibly indicating destruction by the oxidant. A similar effect was observed in permanganate cell 5, with concentrations rising in the same area. With permanganate, gas generation due to oxidation of organics to CO_2 is possible and could have a similar effect; however it is more likely that deposition of manganese oxide (MnO_2) solids resulted in a reduction in permeability in the source area, and may have diverted flow of contaminated ground water to this area. Rises in contaminant concentrations were also noted during the oxidation phase from permanganate cell 6, but in a much different manner from cell 5. Here, a slug of increased concentrations was noted to move across the flow cell as soon as oxidant entered the tank. The exact cause of this is unknown, but it was postulated that the density driven permanganate flow observed in this system may have displaced the less dense contaminated aqueous phase upward, possibly causing a momentary alteration in the flow paths across the cell and increasing concentrations over the pre-oxidation phase. However, this hypothesis was not tested, and concentrations in the cell reduced after subsequent oxidant flushing.

System chemistry effects were also noted. pH observations in the hydrogen peroxide flow cells reflect the CHP activation methods used, with pH drops in cells 1-3 associated with the addition of acids for pH adjustment, and momentary drop in cell 4 due to citric acid addition. With the permanganate cells, a drop in pH was also noted during oxidation, with lowest pH associated with the up-gradient areas of the tank where oxidation was most actively occurring, indicating proton production by contaminant destruction. The mobility of major metal cations in the effluent was also observed. In general, hydrogen peroxide systems observed the most metals mobility, with the citric acid cell demonstrating the greatest differences in metals concentrations, probably due to the chelating ability of this organic acid. In the permanganate cells, the only major cations observed in the effluent were potassium (from permanganate addition), as well as some increase in sodium, possibly indicating ion exchange with sodium in the media. No manganese mobility was observed in the effluent, except for excess permanganate ion.

Presented in Table 4.11 are the results of the quantitative performance analysis based on the efficiency and effectiveness parameters previously described. The controls cells were not included here as many of these values are not applicable to controls. Please note that the depletion rates differ from those calculated from earlier batch studies as they were calculated based on horizontal concentration profile data, which do not separate effects of dilution. Therefore, these are effective rate constants.

Table 4.11. Efficiency and effectiveness results obtained during 2-D cell studies.

Cell ID	PCE destruction rate k' (day^{-1})	Oxidant depletion rate k' (day^{-1})	Media demand (mg/kg)	Oxidant demand (mol/mol)	% DNAPL destroyed	Relative treatment efficiency (RTE)
1	-11.1	Not available [a]	7273	2257	1.2	Not available[a]
2	-14.8	-11	24773	812	11	0.74
3	-3.3	-2.3	6136	223	9.9	0.7
4	-3.6	-9	6136	1817	1.2	2.5
5	-7.5	Not available[a]	Not available[a]	Not available[a]	66.5	Not available[a]
6	-1.8	-1.4	1818	4	32.3	0.78

[a] Not available due to inability to calculate from existing data values.

Based on the data observed in Table 4.11, and supported by observations of oxidant distribution, the oxidant depletion rate for hydrogen peroxide systems was higher than for permanganate systems. Furthermore, the oxidant demand and media demand in hydrogen peroxide systems increased with higher concentrations of oxidant, and were much higher overall than for permanganate. The permanganate systems also were much more effective in terms of DNAPL mass destroyed. It is also apparent that the pressurized injection method for permanganate resulted in a larger mass removal, possibly due to the higher velocity of this system. The RTE values were similar for cells 2 and 3 (hydrogen peroxide) and cell 6 (permanganate) indicating that oxidation was efficient. However, the lower DNAPL mass destruction associated with the CHP systems, as well as the higher oxidant demand and media demand, indicate that CHP was not very effective in this system, due to delivery and activation challenges.

4.4.3. Two-Dimensional Intermediate-Scale Tank Experiments

Two-dimensional intermediate-scale tank experiments were conducted to investigate how permanganate flushing impacted contaminant mass transfer from more complex DNAPL source architectures and evaluate permeability changes due to MnO_2 deposition. The two-dimensional intermediate-scale tank experiments were completed as part of a doctoral dissertation, and detailed results are available in Heiderscheidt (2005). A large amount of sampling data was taken during the 2-D intermediate-scale tank experiment, including aqueous phase PCE, chloride and permanganate concentrations, as well as pH, pressure data and manganese core extraction data. The intermediate-scale tank experiments consisted of a pre-oxidation phase where natural PCE dissolution was established, followed by an oxidation phase where permanganate was introduced to the tank, and a post-oxidation phase where impacts to DNAPL source zone flux resultant of oxidation were noted. Aqueous phase PCE concentration distribution data are presented in Figure 4.10 at select time points throughout the 2-D tank experiment, based on concentration data from the two vertical and one horizontal sampling transects. Plots a-d represent concentrations during the pre-oxidation phase, e-h during oxidant flushing period, and i-l represent the post-oxidation phase.

As revealed in the plots, PCE concentrations were high throughout the tank down-gradient of the source zone during the pre-oxidation phase. During oxidant flushing, PCE concentrations reduced dramatically down-gradient of the source, as can be best discerned from Figure 4.10h, where PCE concentrations were below the detection limit (<0.05 mg/L) everywhere in the sampled areas of the tank. PCE concentrations then rebounded during the post-oxidation phase, which was expected as the mass of permanganate flushed was less than needed to destroy the DNAPL. However, the rebound of each source was different, as concentrations remained low in the top half of the tank, which were down-gradient of pool 1 and residual 1, while concentration down-gradient of pool 2 actually increased relative to the pre-oxidation phase. PCE and chloride data were integrated to achieve a mass balance on the DNAPL within the tank. Figure 4.11a estimates the total mass depleted from the tank versus time using effluent concentration data, while the slope of the mass depletion curve represents the average rate of mass

depletion across the tank. Using PCE concentration data from sampling array G, which was shortly down-gradient of the source zone, it is possible to more specifically estimate the contaminant mass flux from each specific source, which is presented in Figure 4.11b. Three assumptions were made in this estimation, which are that the concentrations at the array G port correspond to the contaminant flux from the specific source located immediately up-gradient, that this concentration represents the average concentration in the cross-sectional area of flow emanating from that source, and that flow is uniformly distributed at array G. Residuals 3 & 4 could not be separated because they are in series with each other. Figures 4.10c and 4.10d highlight the variation in the mass depletion rates by presenting the instantaneous mass depletion rate for both the tank as a whole and for each individual source.

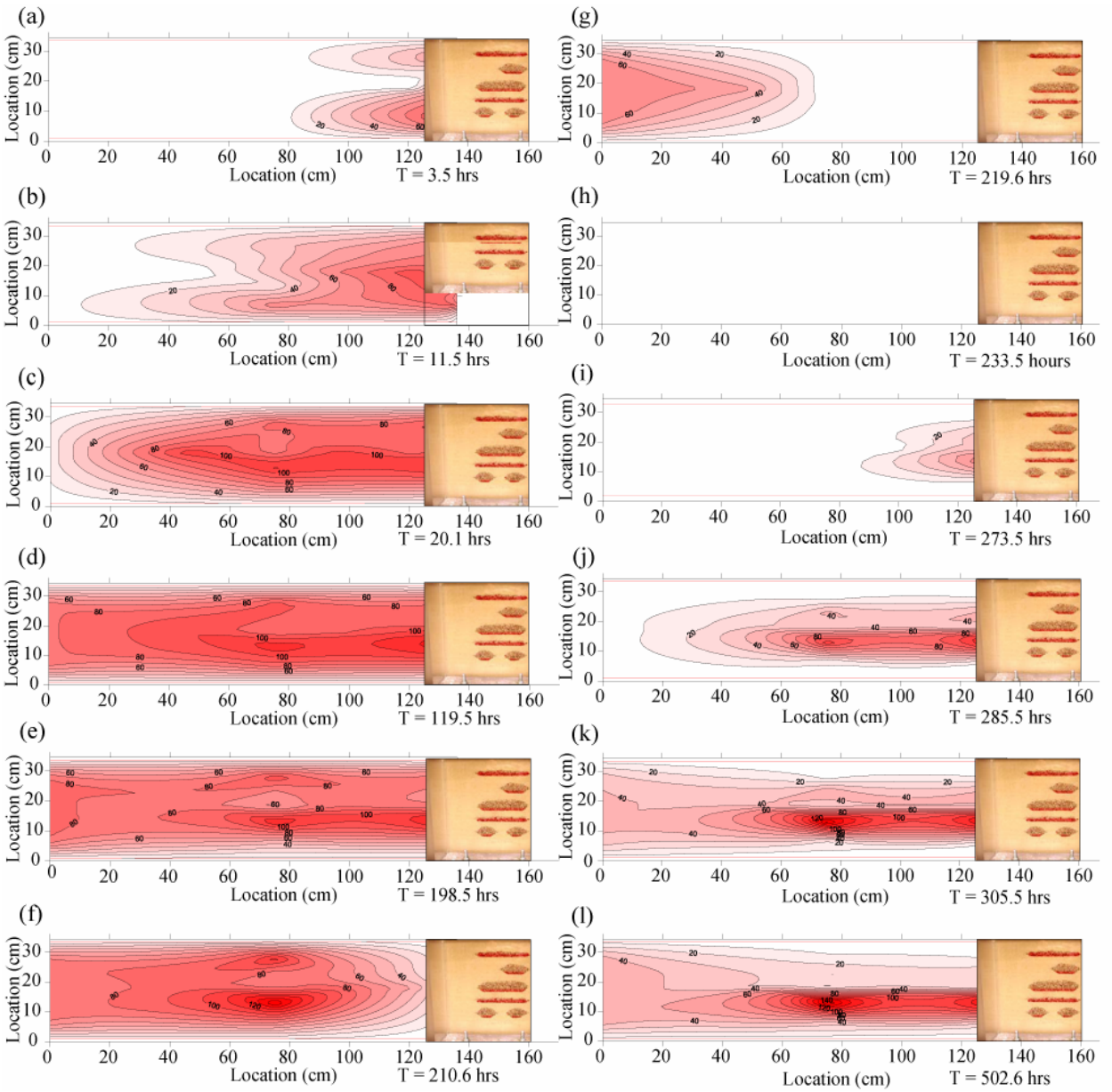

Figure 4.10. PCE concentration distributions during the intermediate-scale tank experiments during select time points: a-d are pre-oxidation phase, e-h are oxidation phase, and i-l are post-oxidation phase.

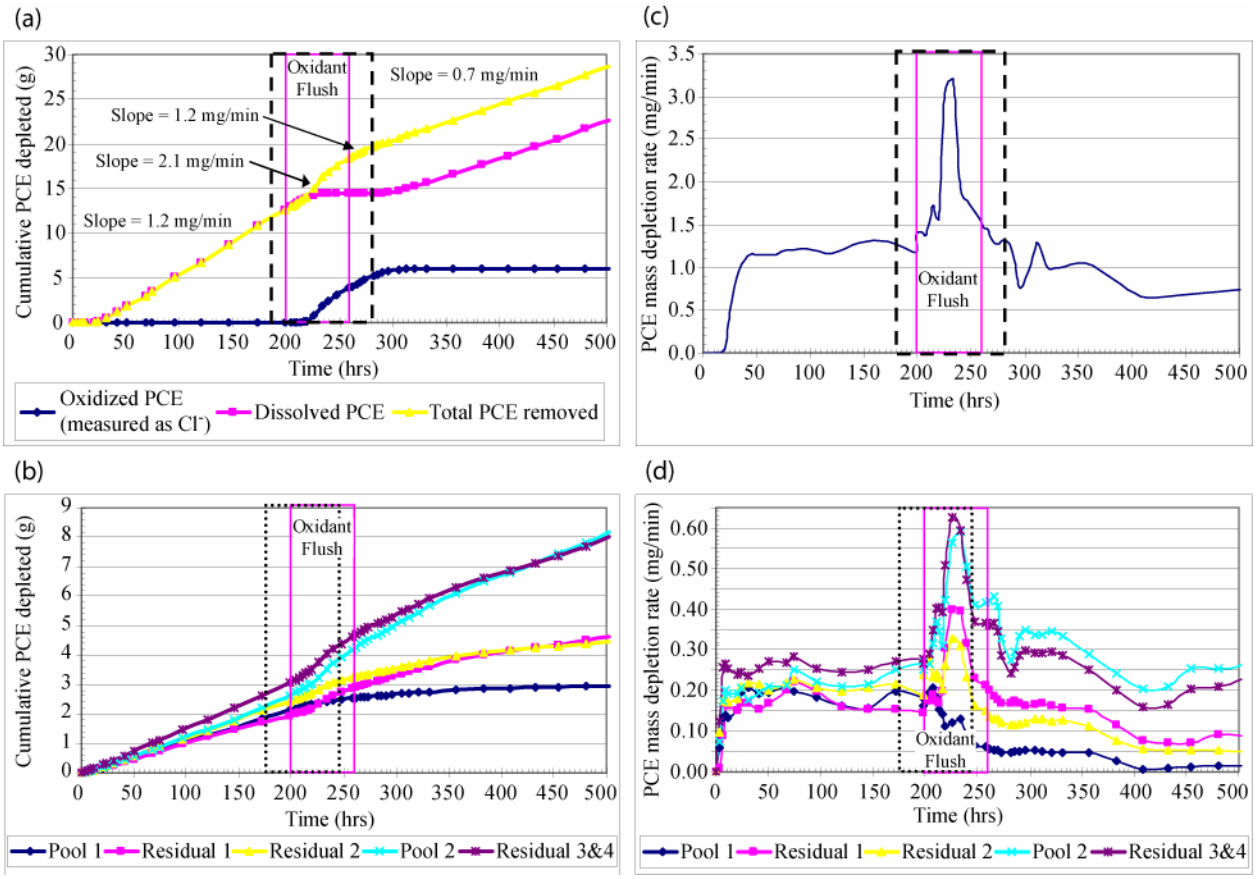

Figure 4.11. Mass depletion data from the intermediate-scale tank study: (a) cumulative mass depletion vs. time for the entire tank, including aqueous and oxidized (Cl^- data) contaminant fractions, (b) total cumulative mass depletion vs. time for each source, (c) instantaneous mass depletion rate for entire tank, and (d) instantaneous mass depletion rates for individual sources. Note: the solid red-line box represents the period of oxidant injection; the dashed black-line box represents the period with chloride in the effluent.

As can be noted from the slopes of the lines in Figure 4.11a, the aqueous PCE mass flux in the effluent decreased to zero during oxidation, but the total mass flux initially increased as PCE was oxidized to chloride. This initial rate eventually decreased to a rate similar to the pre-oxidation phase. Looking at Figure 4.11d, it is interesting to note that increases in instantaneous mass fluxes are noted in every source except for pool 1, which immediately observed a gradual decrease in mass flux. Conversely, pool 2 observed one of the highest mass flux increases. Later during the oxidation phase, the mass flux rates sharply dropped, and then gradually decreased mirroring the decrease observed in pool 1. The initial increase in mass flux was attributed to increased DNAPL dissolution due to oxidation reaction with permanganate. However the corresponding decrease in mass flux rates during oxidation could be attributed to three possible mechanisms, or a combination of all three. These are (1) decreased mass flux associated with the depletion of residual ganglia, (2) possible loss of aqueous-DNAPL interfacial area for dissolution due to deposition of MnO_2 solids at the interface, and (3) changes in permeability resultant of MnO_2 deposition causing deflection of flow around contaminated areas. The sudden drop in mass depletion rates was probably due to the depletion of ganglia, as at the beginning of the experiment, about 2g of PCE was estimated to be present as ganglia, and based on the initial increased mass depletion rate, this mass was estimated to be destroyed in about 10 hours, which is roughly when this drop occurred.

After oxidant flushing ceased, residuals 1, and 3&4, rebounded to pre-oxidation levels while residual 2 did not. Pool 1 did not rebound while pool 2 rebounded to levels exceeding pre-oxidation. The lack of rebound in pool 1 and residual 2 was likely due to the deposition of MnO_2 solids around these sources, causing reduced contact and flow bypassing. The largest concentrations of MnO_2 solids were also noted around these sources, as well as pool 2, also partially explaining the rebound in residuals 1 and 3&4, as flow may be diverted toward these residuals. The large enhancement in pool 2 mass depletion rates during oxidation, as well as increased mass flux post-oxidation are also interesting. One possibility is an artifact of DNAPL emplacement, as pool 2 has a larger transition zone above it than pool 1, possibly explaining a higher flux rate. However, pool 2 also had a residual zone above it, and two residuals below it, and the deposition of MnO_2 solids during oxidation may have the effect of blocking flow paths such that flow paths may be concentrated and caused more mixing than occurred during the pre-oxidation phase. The resulting flow path changes and mixing may have resulted in the increased mass flux observed in this system.

After experiment shutdown, the distribution of manganese oxides was evaluated by extracting manganese from soil cores. Based on mass balance, 3.7g of MnO_2 were deposited in the tank, while another 0.38 g flushed from the tank effluent, based on ICP-AES analysis of tank effluent. This corresponds to approximately 5.87g of PCE oxidized, which is similar to PCE destruction estimated based on chloride data. Thus of the total of 110.4g of permanganate flushed through the tank, only about 5.61g contributed to oxidation of PCE, with 93.6% of the injected permanganate accounted for with oxidant and manganese concentration data.

Data were also taken to evaluate the impact of oxidation on the permeability of the subsurface. Impacts to permeability, such as reduction of permeability due to deposition of manganese oxides solids (MnO_2) or increases due to DNAPL depletion may cause impacts to source zone flux, by altering the fluid flow pathways and velocities within the source zone. A plot of the MnO_2 distribution within the tank was generated with particular detail in locations near the DNAPL source zones. This is presented in Figure 4.12.

To evaluate the impact of the deposition of MnO_2 solids, hydraulic pressures were measured continuously throughout the experiment, and were processed to determine the head loss versus time at various locations throughout the tank. Figure 4.13 demonstrates the changes in hydraulic pressure versus time in the tank, for pressure measurement locations corresponding to the change in head across the various source zones. As can be seen in Figure 4.13, the head drops across residual 2, as well as pools 1 and 2, are the largest, which was anticipated as these sources had the largest MnO_2 deposits, seen in Figure 4.12d. Interestingly, the head loss at residual 4 continues to increase after oxidation, possibly indicating that MnO_2 solids may be continuing to migrate into source 4 after oxidation has ceased.

As a final step in evaluating the impact to permeability resulting from MnO_2 deposition, the head drops were converted to changes in hydraulic conductivity, using the newly developed CORT3D model. The CORT3D model incorporates a modified version of Wyllie's (1962) power law relation of relative aqueous permeability to water saturated pore space, to accommodate the change in permeability resultant of MnO_2 deposition. The model was first calibrated to pre-oxidation conditions, then applied to the post oxidation conditions. The density of the MnO_2 solids used as a fitting parameter, as the density of MnO_2 solids is anticipated to be much less than dry solid manganese oxide due to its hydrous nature. A density of 9.5 mg/mL was found to provide the best fit to the experimental data, which is 530 times less than that of dry MnO_2. It was found that MnO_2 deposition was only likely to impact permeability in areas of the tank with a solids concentration greater than 0.1 g MnO_2(s) / kg soil, which were generally located only in close proximity to the source (less than 15 cm down-gradient).

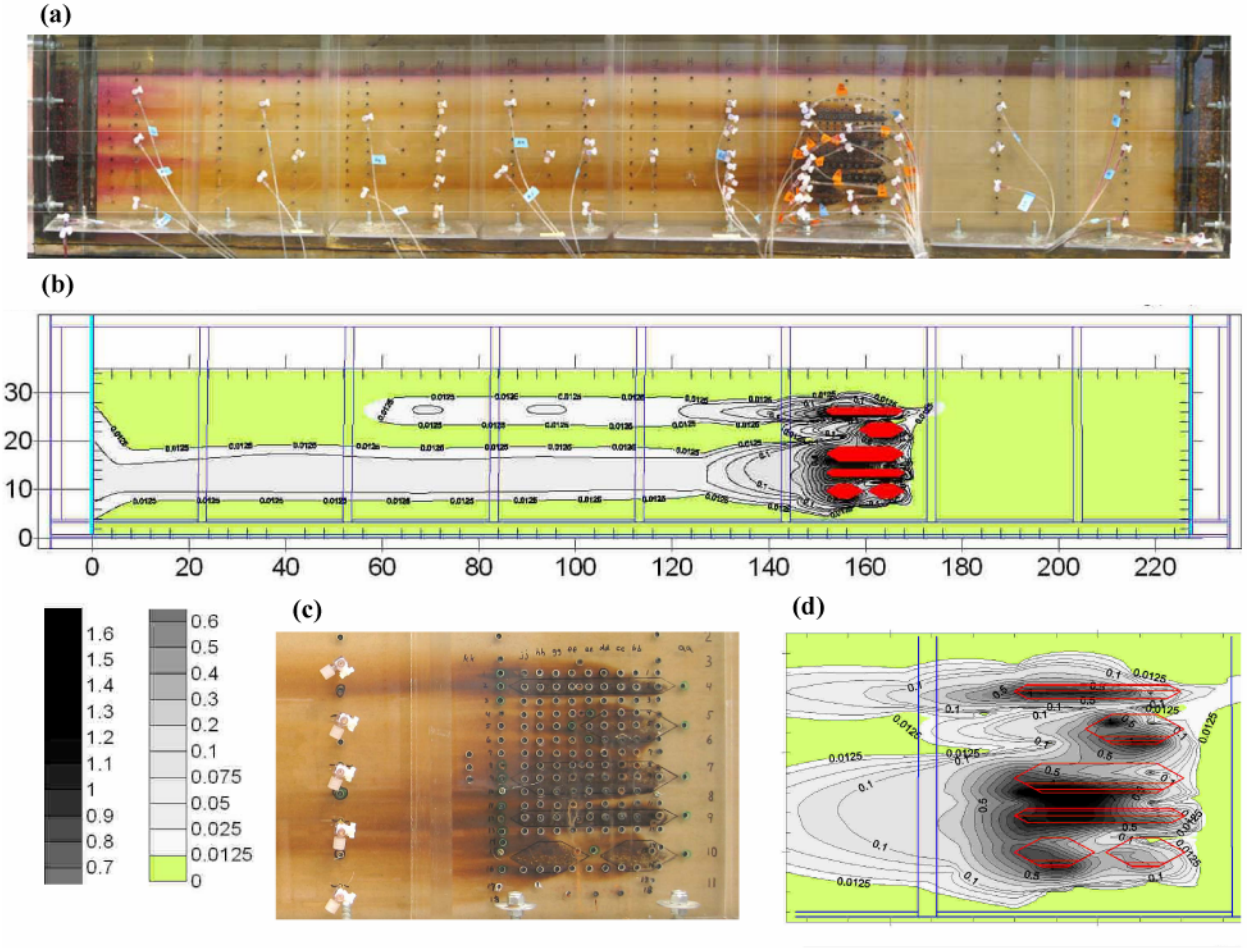

Figure 4.12. Plot of MnO_2 distribution across the tank: (a) photo the entire tank after oxidation, (b) measured MnO_2 concentration distribution across the entire tank (units of g MnO_2 / kg soil), (c) photo close-up of DNAPL source area, and (d) concentration plot of area around sources.

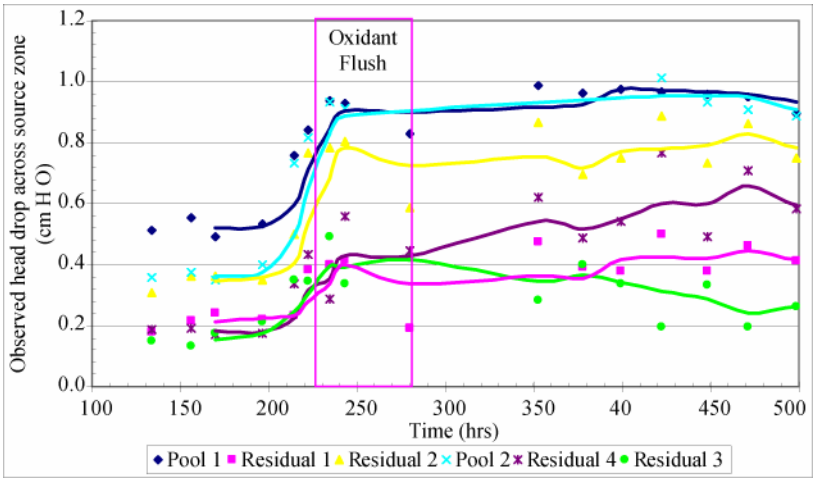

Figure 4.13. Change in head drop across source zones during oxidation.

4.4.4. Large-Scale Tank Experiments

The large-scale tank experiments were performed according to the methods described in Section 3.5.4. These experiments were conducted in cooperation with another CSM SERDP project: "CU-1294: Mass Transfer from Entrapped DNAPL Sources Undergoing Remediation: Characterization Methods and Prediction Tools." These large-scale tank studies were conducted to evaluate how several different remediation technologies impact DNAPL mass transfer from aquifers of varying degrees of heterogeneity. These tank studies consisted of an initial natural dissolution phase, a surfactant flush using Tween-80, and an oxidant flush with permanganate. Before and after the surfactant flush, a partitioning tracer test (PTT) was performed, and the tank was scanned with a dual energy gamma attenuation system to determine the DNAPL distribution between each experimental phase. The following is a summary of results from the oxidation phase of the experiment. For more information regarding the natural dissolution, surfactant flushing, and partitioning tracer test portions of the experiment the reader is referred to the final project report for SERDP project CU-1294 while additional information regarding the application of permanganate to these tank studies can be found in Heiderscheidt (2005).

The large-scale tank studies involved two experiments. Experiment 1 investigated a system with a high degree of heterogeneity and experiment 2 investigated a system with a low degree of heterogeneity. Photos from the oxidation phases of these two experiments are presented in Figure 4.14. A large volume of data was taken from the large-scale experiments. Plots of PCE mass depletion versus time, based on tank effluent data, are presented in Figure 4.15.

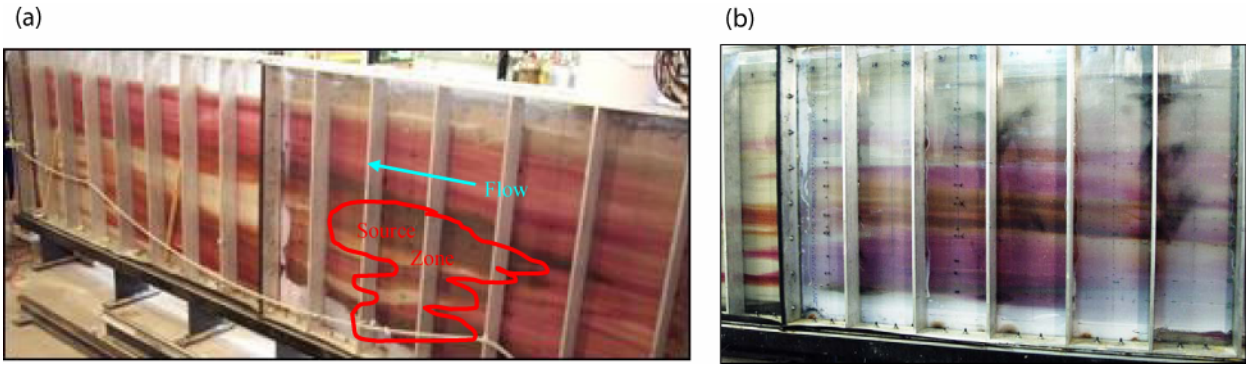

Figure 4.14. Photographs of the heterogeneous large-scale 2-D experiments: (a) experiment 1, and (b) experiment 2.

Mass transfer enhancement resultant of oxidation was observed in both experiments, evidenced by an increase in the slope of the mass depletion curve during the oxidation phase. It is interesting to note that experiment 1 had a much larger degree of mass transfer enhancement (330% over pre-oxidation) than experiment 2 (72% over pre-oxidation), despite the higher degree of heterogeneity in this system. Based on data from the gamma scans, and verified by visual observations, experiment 1 had a DNAPL ganglia to pool ratio (GTP) of 3.5, while experiment 2 had a ratio of 4.7. A larger GTP would be anticipated to have a larger mass flux due presumably to a larger DNAPL-aqueous interfacial area for dissolution to occur across. A saturation value of 0.3 was used to determine GTP, based on gamma data evaluation and comparison to visual observations. Although experiment 1 had a much larger initial PCE mass at the beginning of the experiment, this mass was distributed over a 60% larger cross sectional area orthogonal to the flow direction. As such, despite the differences in source zone characteristics, these characteristics would probably have some canceling effect, and do not appear to account for the dramatic differences in performance. Thus, the higher enhancements may be resultant of the flow heterogeneity, as well as the higher oxidant concentration used in experiment 1.

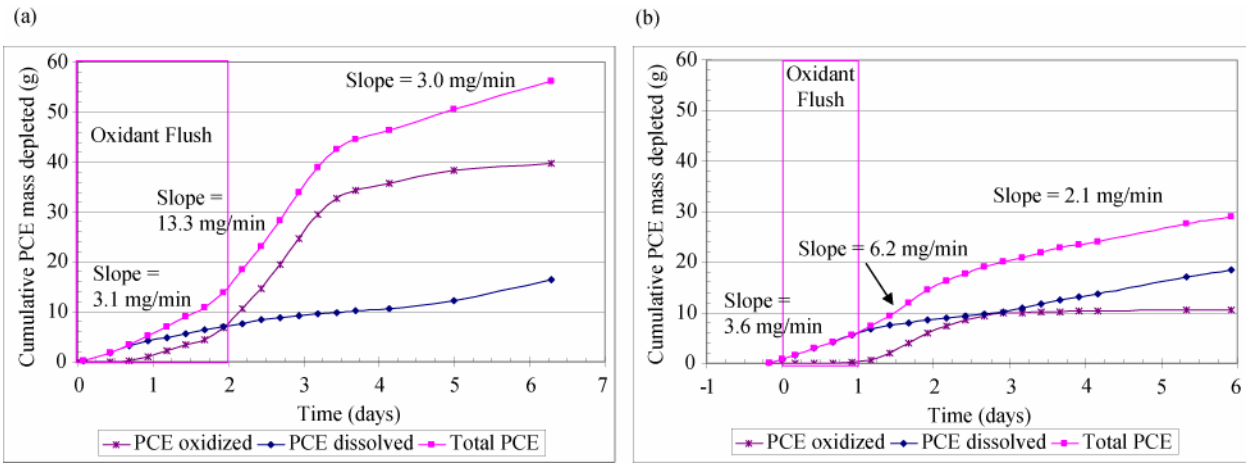

Figure 4.15. Plots of PCE mass flux vs. time from large-scale tank experiments: (a) experiment 1, and (b) experiment 2.

Observations of changes to the DNAPL source zone configuration obtained by comparing gamma scans can yield information about oxidation performance as well. Results from the dual energy gamma scan from both experiments from before and after the oxidant flush are presented in Figure 4.16.

The GTP was calculated again post-oxidation to determine the impact to the source zone mass distribution. Interestingly, the GTP increased in both experiments. Visual examination of the plots in Figure 4.16 indicates that much of the lower saturation areas have been reduced. However, evidently oxidation during both experiments reduced the pool mass even more, causing the GTP to increase. A summary of results from the large-scale tank experiments is presented in Table 4.12.

Table 4.12. Large-scale tank oxidation performance summary.

Parameter	Experiment 1 (high heterogeneity)	Experiment 2 (low heterogeneity)
Approximate PCE mass at start of oxidation (g)	509.2	273.3
Approximate cross-sectional area of all sources (cm^2)	225	150
Ganglia-to-pool ratio at start of oxidation (-)	3.45	4.67
Percent change in GTP following oxidation (%)	87%	70%
Maximum PCE oxidation possible (g)	146.6	46.3
PCE oxidized (measured as Cl^- at effluent) (g)	40.2	10.6
Percent of possible PCE oxidized (%)	27.4%	22.9%
Change in mass depletion rate (oxidation vs pre-oxidation)	4.4 times	1.7 times
Change in mass depletion rate (post- vs pre-oxidation)	1.0 times	0.6 times

It should be noted that while the enhancement of the mass depletion rate for experiment 1 is much larger than for experiment 2, the contaminant mass flux after oxidation from experiment 1 was no different than the pre-oxidation rate. This indicates that despite the reduction in DNAPL mass, no appreciable change in contaminant plume mass loading was observed. However, experiment 2 observed a 40% reduction in mass loading, despite the much smaller reduction in contaminant mass.

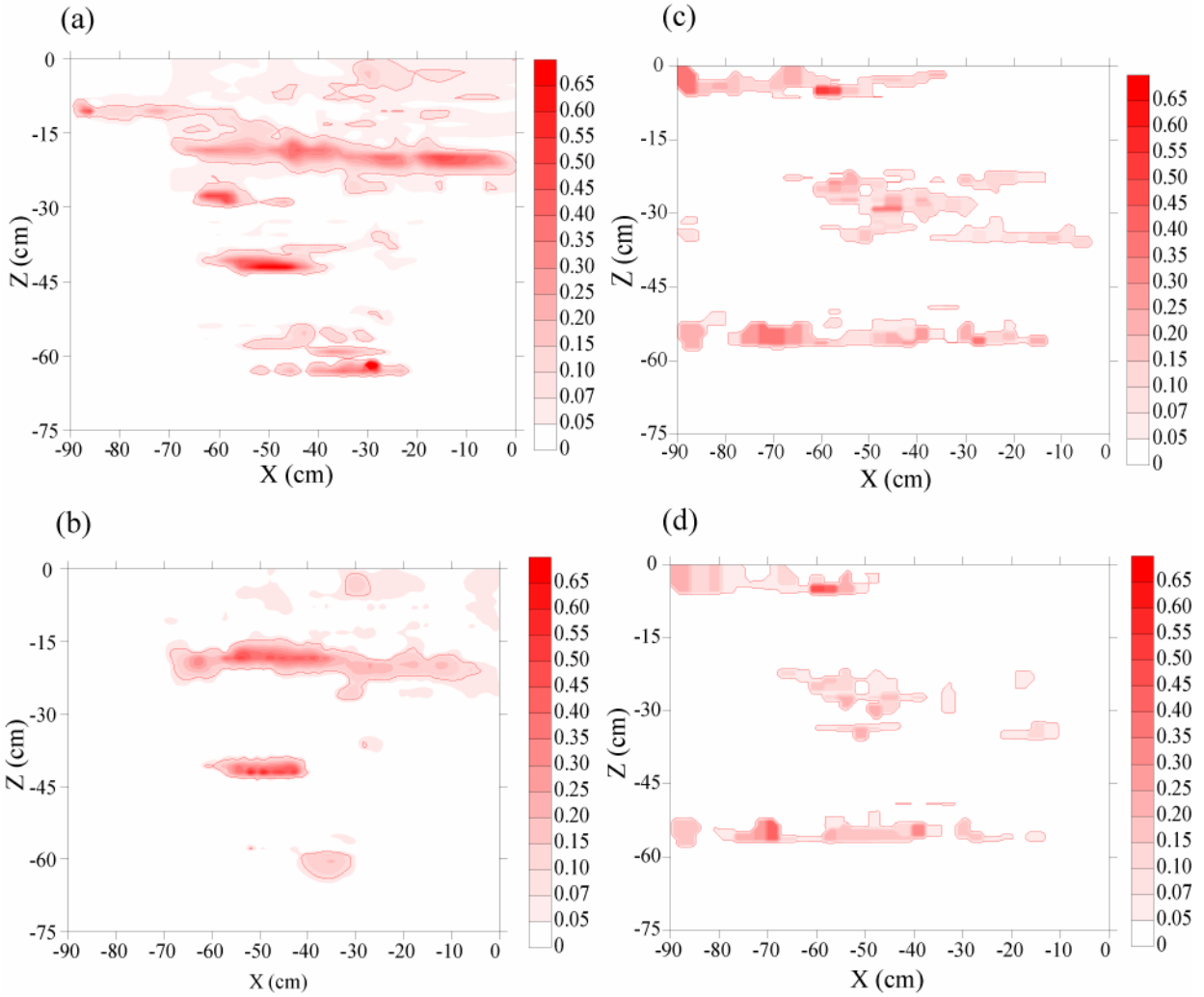

Figure 4.16. PCE source zone DNAPL saturation profile from large-scale tank oxidation experiments: (a) experiment 1 source zone prior to oxidant flushing, (b) experiment 1 source zone after oxidant flushing, (c) experiment 2 source zone prior to oxidant flushing, and (d) experiment 2 source zone after oxidant flushing.

In conclusion, significant mass transfer enhancements resulting from oxidation are possible in large-scale heterogeneous systems, and a larger degree of heterogeneity may even cause increased mass transfer due to the interaction of the oxidant with the more complex source zone. Conversely, reduced heterogeneity may not result in as large of an increase to the mass depletion rate, but may have better overall performance due to reductions in plume mass loading. This also agrees with results from the intermediate-scale tank experiments where a more complex source zone architecture observed large mass depletion enhancements, but also rebounded to higher mass loading rates than less complex source architectures.

4.4.5. Evaluation of the CORT3D Model for Performance Prediction and Evaluation of ISCO Using Permanganate

The development of the CORT3D model was part of a doctoral dissertation and is described in detail in Heiderscheidt (2005). The model was evaluated against experiment data and field applications as described by Section 3.5.5. Described here are the results of comparison of the model to the experimental data of Schroth *et al.* (2001), Schnarr *et al.* (1998), and Crimi and Siegrist (2004). The model was then applied to investigate the impact of natural oxidant demand (NOD) on permanganate distribution at the Naval Training Center in Orlando, FL. For additional detail regarding comparison of CORT3D to experimental data, see Heiderscheidt (2005).

A unique feature of CORT3D is the ability to determine the impact to permeability as a result of MnO_2 solids deposition resulting from permanganate oxidation. This data set allows for comparison of pressure data to determine if the CORT3D model is able to capture the trends in pressure data during oxidation. Schroth *et al.* (2001) evaluated a 1-D column system containing residual TCE DNAPL and collected hydraulic pressure as well as concentration data. The study included a DNAPL dissolution only control, and column in which permanganate (790 mg/L) was applied. Due to a very fast velocity in these columns, and pressure buildup in the oxidation column, the experiment ran only 30 hours before a pump failed. Several other issues regarding the pressure build up within this system also merit some discussion. Presented in Figure 4.17a are pressure data from three locations in the column, where T1, T2 and T4 are located progressing down-gradient of each other. In this column system, precipitation of MnO_2 was great enough to cause pore throat blockages. However, the pressure buildup was severe enough to dislodge MnO_2 solids, and transport them down-gradient, evidenced by the gradual buildup in pressure, followed by reaching a steady value as MnO_2 were forced down-gradient. This may have also caused preferential flow paths to form causing permanganate to advance at a faster rate. Eventually, after 25 hours, the pressures exceeded the transducer limits, and the data become unreliable. However, comparison of this data to CORT3D is still valuable to determine if the model could indicate the same trends in permeability reduction.

The model was first calibrated to the natural dissolution control column using inverse modeling. The parameters determined from inverse modeling were then used in application of the model to the oxidized system. Data from these simulations are presented in Figure 4.17. The density of MnO_2 solids must be used as a fitting parameter, as it includes reductions in pore throat sizes, coating of soil grains, and deposition of colloids in pore spaces. The best fit in this system was found to be 105 mg/mL (about 48× less than dry MnO_2 solids). Looking at the observed values in Figure 4.17 versus the simulated values, the model captured the trends in the data very well. However, it is important to note that the purpose of comparison to the experimental data was to determine if CORT3D could capture specific processes observed in the data, rather than reproduce the experimental data. The most deviation was with the pressure data, but this may largely be explained by the aforementioned issues with the pressure buildup in the column. It should be noted that the TCE concentration and total mass depletion versus time is predicted well by the model, despite differences between the head pressure data. However, this is a 1-D column system where flow is forced through the source. In 2-D or 3-D systems, flow bypassing may occur, and changes to pressure would be more likely to impact the TCE mass depletion behavior.

Comparison was also made to data from Schnarr *et al.* (1998), who conducted 1-D column experiments involving a PCE DNAPL and a soil with some NOD content, using two oxidant concentrations (7500 and 10000 mg/L $KMnO_4$) and two Darcy velocities (42 and 65 cm/day), as well as a dissolution only control. Simulation was only applied to the higher velocity experiments, and the model was calibrated to the dissolution only system. Again, the purpose of the modeling studies was to determine if CORT3D could capture specific trends in the experimental data. Additional information would be needed that was not provided to exactly reproduce the data, such as sorption characteristics, flow rate variability and DNAPL source emplacement technique. The specific processes CORT3D was evaluated for using data from Schnarr *et al.* (1998) are: increased DNAPL mass transfer (enhancement)

resultant of oxidation, the effect of fast NOD on PCE oxidation and permanganate breakthrough, the effect of slow NOD on PCE oxidation and permanganate breakthrough, simultaneous existence of permanganate and PCE in the column effluent, PCE concentration rebound after oxidant flushing ceased, and chloride generation resultant of oxidation. The slow and fast NOD rates, and amounts were estimated using inverse modeling from the low oxidant concentration, high velocity experiment, and the high concentration, high velocity experiment was used for modeling.

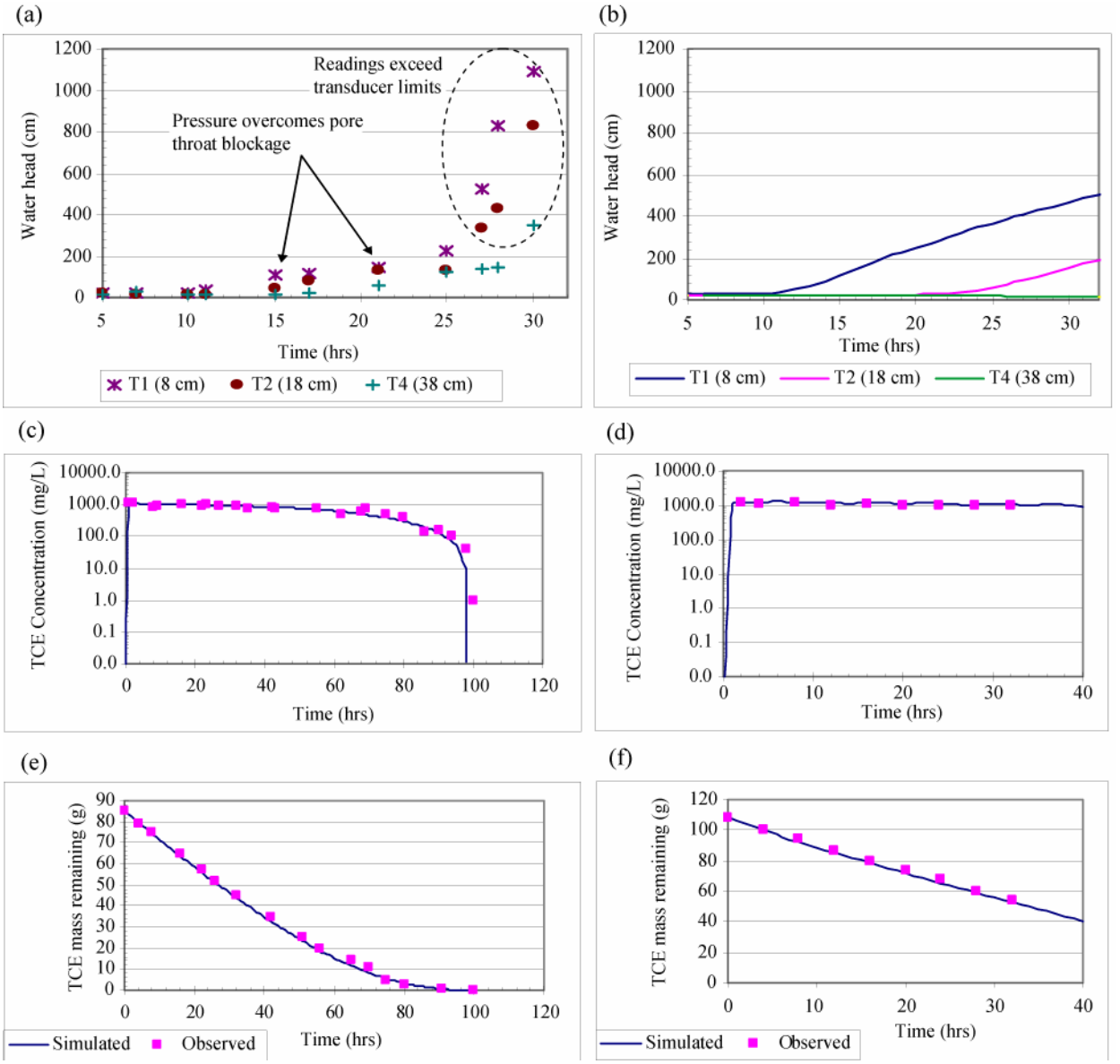

Figure 4.17. Application of the CORT3D model to data from Schroth *et al.* (2001): (a) water head data from 1-D TCE oxidation column, (b) simulated water head data from the 1-D TCE oxidation column, (c) TCE concentration data from the 1-D TCE dissolution only column, (d) TCE concentration from the 1-D TCE oxidation column, (e) TCE mass depletion curve from the 1-D TCE dissolution only column, and (f) TCE mass depletion curve from the 1-D TCE oxidation column.

The results of the CORT3D simulation and observed concentrations at the column effluent from the low and high oxidant concentration experiments are presented in Figures 4.18 and 4.19 respectively. It can be noted from these simulations that there are tailing PCE concentrations that the simulation did not reproduce, and the PCE concentration rebound was not exactly reproduced. There are several reasons for this, which include that the source zones may have been configured differently between column experiments, that the initial PCE mass may have differed between experiments, and that the sorption characteristics are unknown, as it is possible that sorption and desorption may have altered the transport of PCE in the columns.

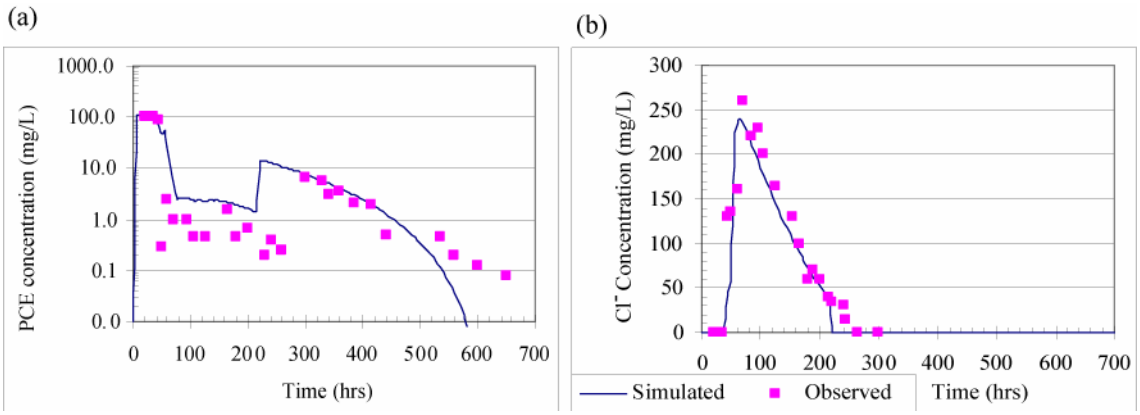

Figure 4.18. Comparison of simulated and observed results for 1-D PCE oxidation – low oxidant concentration: (a) PCE concentration vs. time, and (b) chloride concentration vs. time.

Interestingly, it was found that the mass transfer fitting parameter (α_1), had to be increased during the oxidation phase in order to fit the model to the data from the oxidation experiments, which indicates that mass transfer during oxidation was enhanced more than the model could attribute to bulk phase reaction alone. Figure 4.20 compares the results if this increase in α_1 was applied to the entire experiment including the post-oxidation flush, as well as if the increase in α_1 was ignored the natural dissolution α_1 from the control column experiment was used for the entire experiment. As can be seen, neither applying the increased α_1 to the entire experiment that over predicts the time until PCE depletion, nor using the dissolution only α_1 that under predicts the PCE removal rate, captures the system processes. This potentially indicates that the mass transfer was enhanced by flushing with permanganate.

Another observation from the PCE 1-D oxidation modeling studies was that accounting for MnO_2 precipitation was important to capturing system performance. Figure 4.21 compares PCE simulation data when the porosity changes due to MnO_2 are accounted for and when permeability reduction is ignored. Due to the 1-D column system, flow is effectively forced through the source zones, whereas in 2-D and 3-D environments, flow may be diverted away causing a reduction in mass transfer. However, due to the porosity reduction, there is an increase in velocity, and thus there is less residence time within the DNAPL source zone for reaction with permanganate to occur, causing increased effluent PCE concentrations in the system where permeability changes are accounted for.

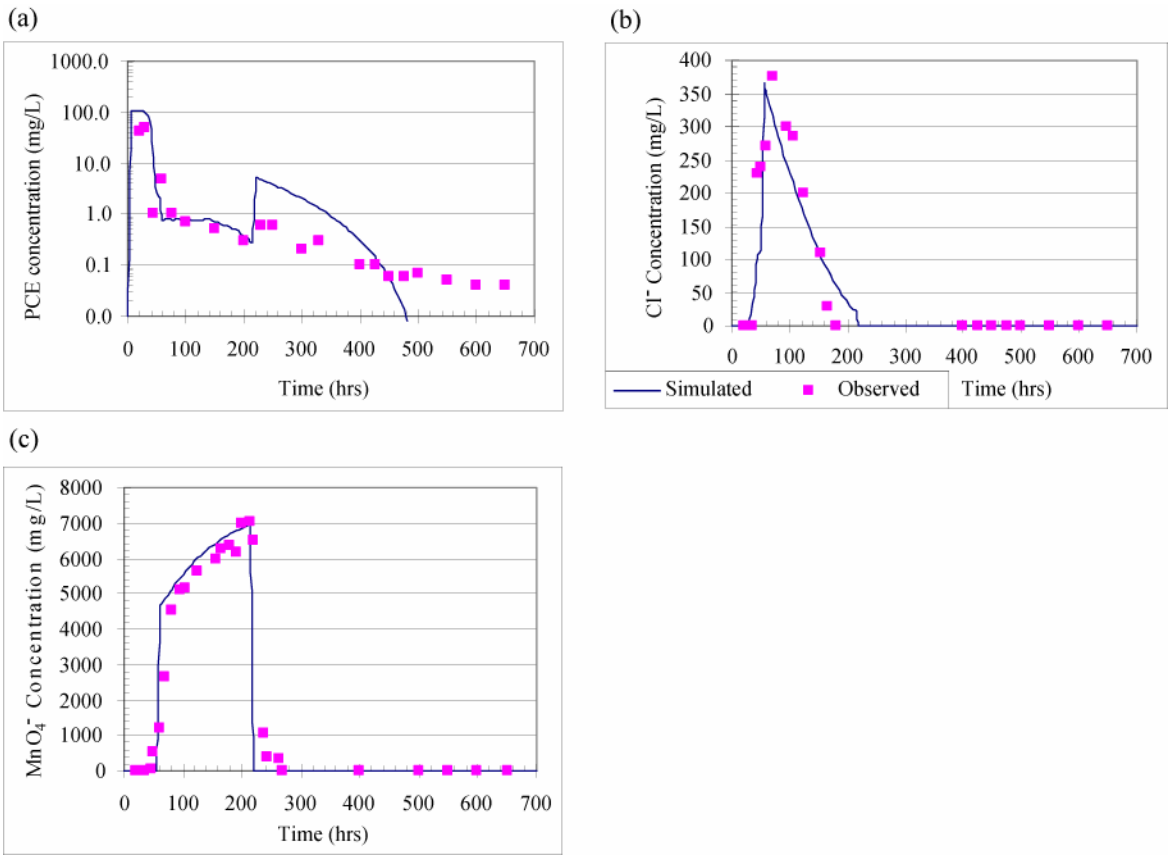

Figure 4.19. Comparison of simulated and observed results for 1-D PCE oxidation – High oxidant concentration: (a) PCE concentration vs. time, (b) chloride concentration vs. time, and (c) permanganate concentration vs. time.

A final series of simulations was run on data from Schnarr *et al.* to determine the impact of slow NOD on PCE and permanganate concentrations. Figure 4.22 compares a system where slow NOD is included in the simulation to one where slow NOD is neglected. The plots indicate that without including slow NOD, the concentrations of permanganate are over predicted, resulting in an under prediction of PCE concentrations, and an under prediction of the time needed to deplete the PCE mass. Thus slow NOD may impact DNAPL mass depletion rates during ISCO by limiting permanganate delivery.

One limitation of the data of Schnarr *et al.* (1998) was that the NOD was unknown, and had to be estimated from their experimental data. To further test the ability of CORT3D to model oxidant transport, another simulation was run using data generated at the Colorado School of Mines by Crimi and Siegrist (2004). In this study, duplicate columns were packed with NTC soil, and flushed with potassium permanganate at 1000 and 4000 mg/L. The mass fraction and rates for the fast and slow NOD were estimated from data from the high concentration experiment. It was determined that the NOD was 34% fast rate component with a first order degradation rate of 2.0 min^{-1} and the slow component had a rate of $4.3x10^{-2}$ min^{-1}. Simulations were run to determine if CORT3D could capture the system effluent permanganate concentrations versus time. No contaminant was present during this study. Simulations and observed data from these 1-D column studies are included in Figure 4.23.

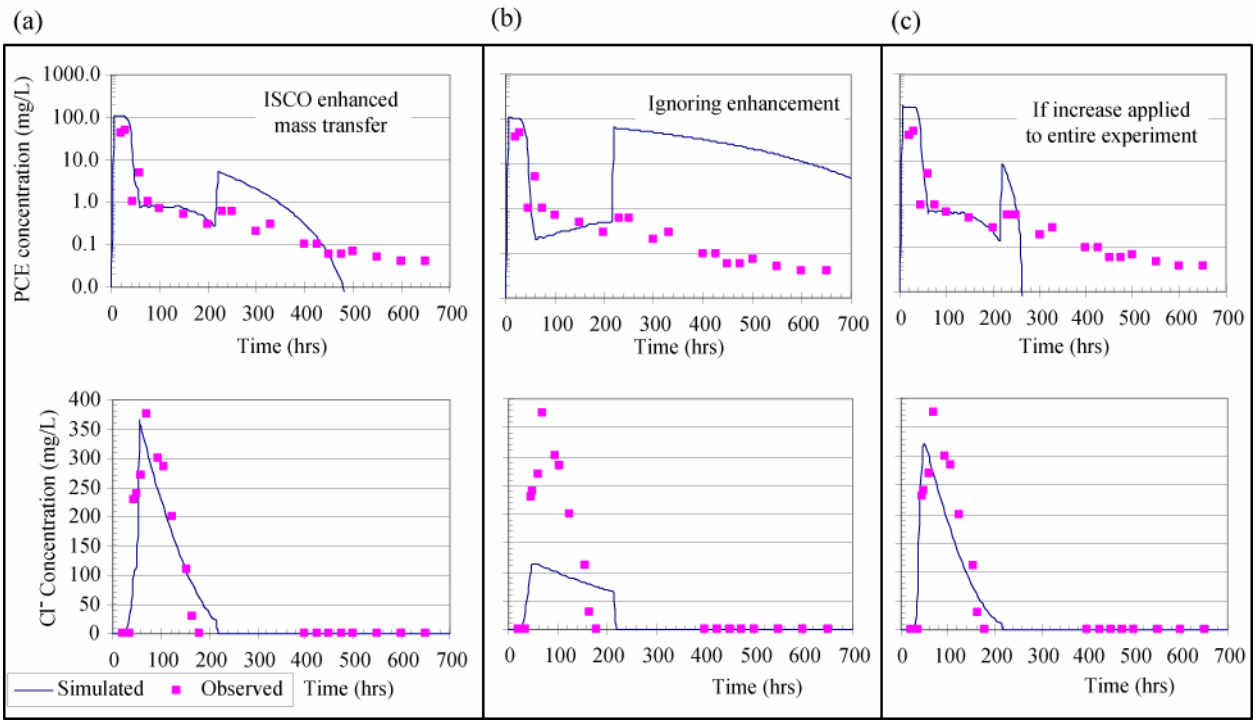

Figure 4.20. Comparison of simulations and observed results using varied mass transfer fitting parameters to account for mass transfer enhancement due to oxidation: (a) PCE and chloride concentration using increased α_1 only during oxidation phase, (b) using the natural dissolution only α_1 for the entire experiment (ignoring enhancement), and (c) using the enhanced α_1 value for the entire experiment.

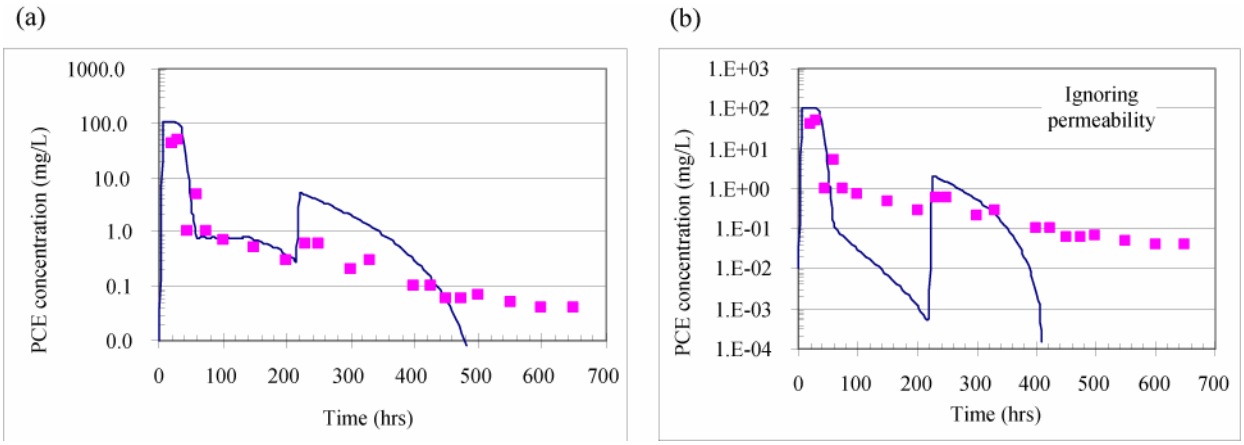

Figure 4.21. Comparison of simulations and observed results accounting for changes in permeability resultant of MnO_2 precipitation: (a) simulation with permeability change, and (b) simulation without permeability change.

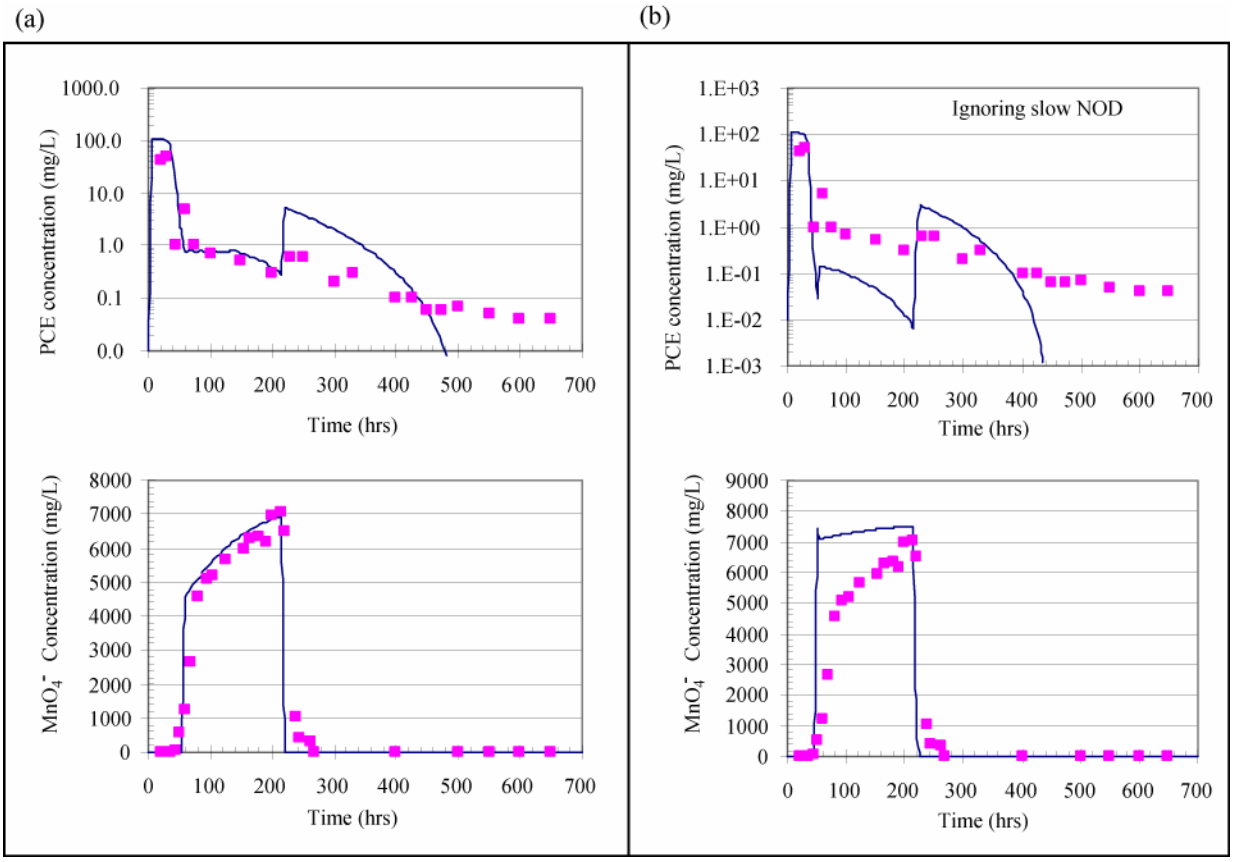

Figure 4.22. Comparison of simulations and observed results considering the impact of slow NOD: (a) with slow NOD fraction included, and (b) ignoring the slow NOD fraction.

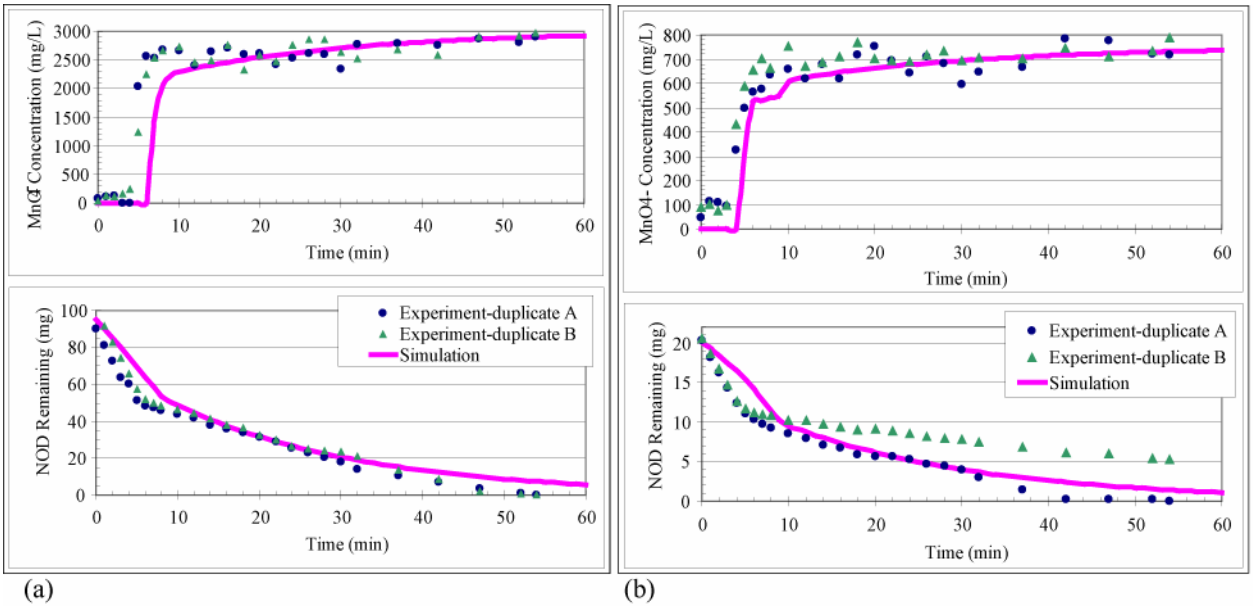

Figure 4.23. Simulated and observed permanganate transport in 1-D NOD column tests: (a) high oxidant concentration columns, and (b) low oxidant concentration columns.

As can be seen from the data, the model captured the two different rates of NOD oxidation. However, from the high oxidant concentration system, there appears to be an increase in the NOD oxidation rate towards the end of the experiment, based on the observed concentration data. Due to the complex nature of NOD, it is possible that some fast components of NOD were shielded from oxidation until the slower NOD counterparts were oxidized, possibly explaining the relatively fast loss of oxidant in the last 20 minutes of the high concentration experiment.

A final application of the CORT3D model was to evaluate and optimize oxidation transport at the Naval Training Center (NTC) field site in Orlando, Florida. A number of model simulations were run using varied oxidant concentrations, varied oxidant injection flow rates, and assumptions about NOD. This application of the model generated a large number of figures depicting simulation results, which are available in Heiderscheidt (2005). To illustrate the impact of NOD on permanganate distribution, two simulations were first run with and without NOD. Figure 4.24 compares the results of these two simulations, which dramatically show how NOD can limit permanganate transport.

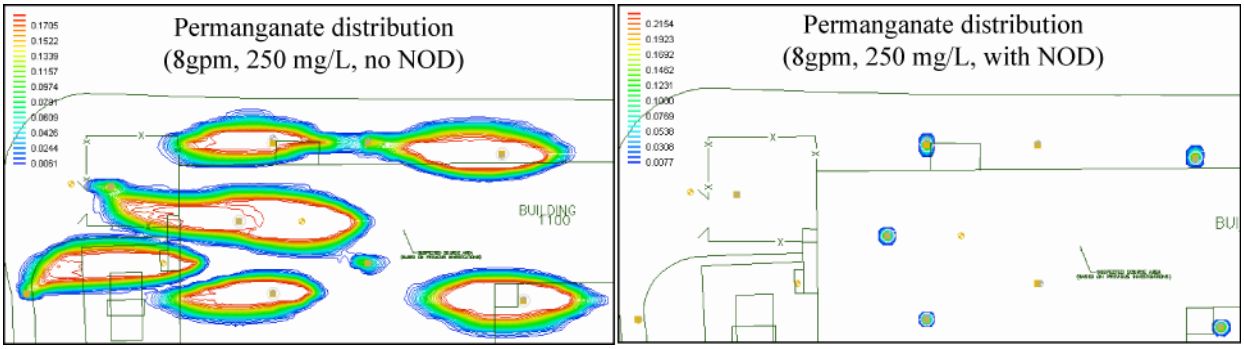

(a) (b)

Figure 4.24. Evaluation of the impact of NOD on oxidant transport simulation results: (a) No NOD, and (b) with NOD.

To determine design parameters for optimized permanganate transport within this field setting, simulations were then run utilizing varied permanganate concentrations and varied injection rates. Selected results from these simulations are presented in Figure 4.25, which includes permanganate concentrations and significant MnO_2 generation.

From these simulations, increasing the permanganate concentration from 250 to 4000 mg/L increased the oxidant transport distance by 240%; however, the extent of significant manganese generation increased by 1000%. Conversely, increasing the injection rate from 5 to 15 gpm increased the transport distance by 200%, while the extent of significant manganese generation increased by 500%. This suggests that lower oxidant concentrations at higher velocities may optimize permanganate delivery to this field site. To further evaluate this conclusion, additional simulations were run at a much higher injection rate (48 gpm), using the same two oxidant concentrations. The results of these simulations are presented in Figure 4.26.

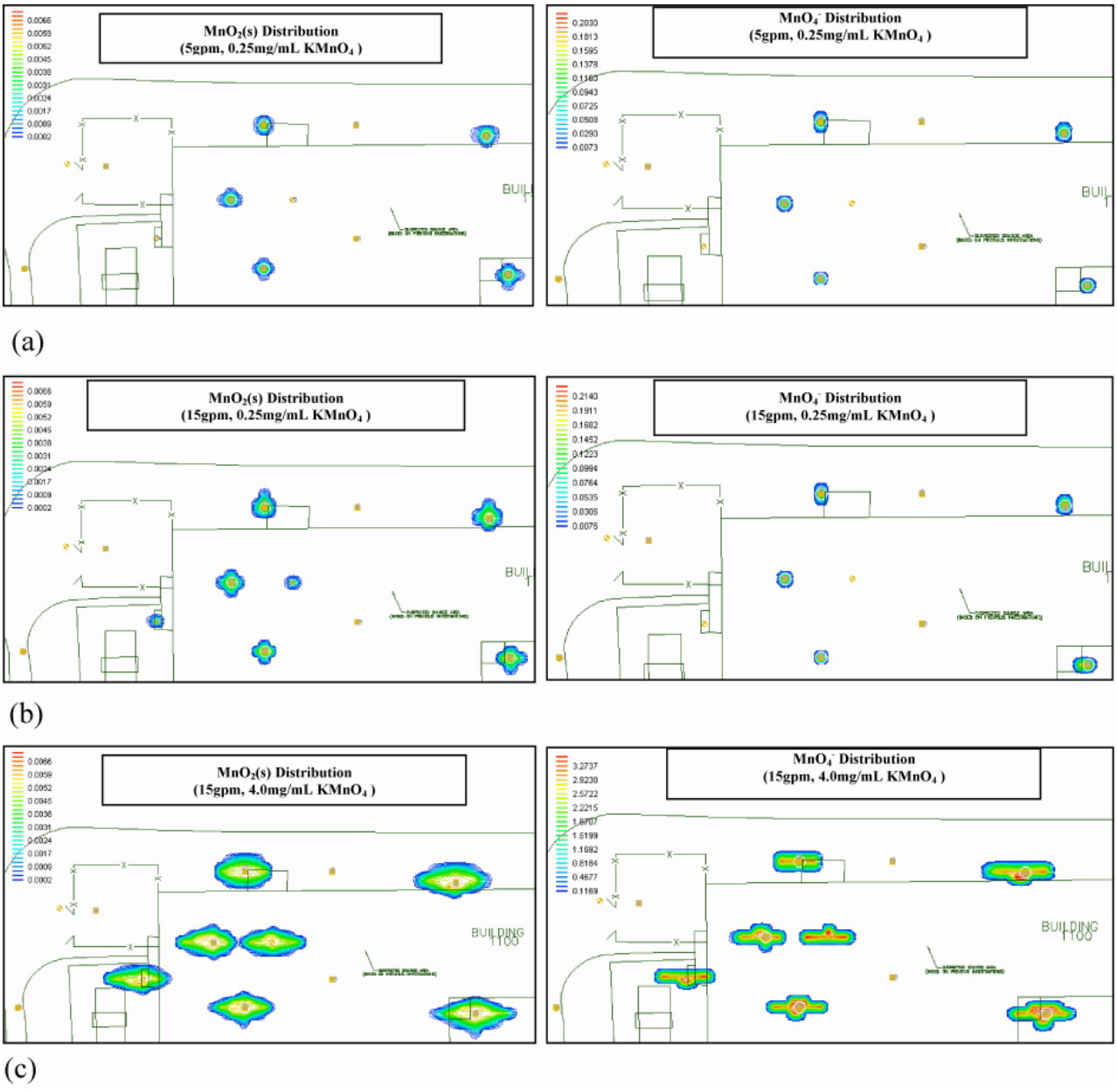

Figure 4.25. Comparison of design parameters for optimized oxidation transport: (a) 5 gpm and 250 mg/L $KMnO_4$, (b) 15 gpm and 250 mg/L $KMnO_4$, and (c) 15 gpm and 4000 mg/L $KMnO_4$. (Note: the left graph of each pair represents the simulated distribution of $MnO_2(s)$ and the right graph represents the simulated distribution of MnO_4^-.)

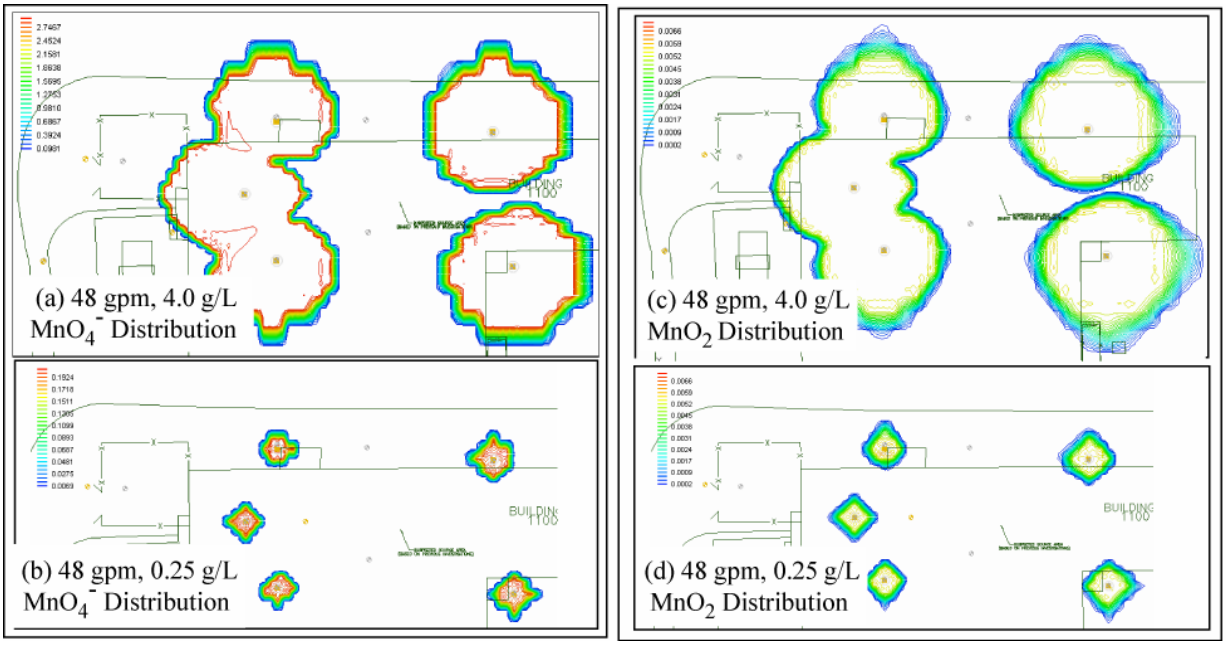

Figure 4.26. Comparison of high velocity oxidant injection simulations: (a) permanganate distribution from high concentration injection, (b) permanganate distribution from low concentration injection, (c) manganese distribution from high concentration injection, and (d) manganese distribution from low concentration injection.

As anticipated, the permanganate transport distance for the higher oxidant concentration system resulted in the largest permanganate transport distances. However, with this increased distance, the extent of significant MnO_2 deposition also increases. Although the reduction in porosity associated with these hydrous manganese solids may be as little as 0.6% based on an assumed density of 1000 mg/mL, results from the 2-D intermediate-scale tank studies and modeling of data from Schroth *et al.* (2001), the permeability reduction is likely to be as much as 10-20 times this amount. Such a permeability reduction at the field scale may result in flow bypassing the targeted contaminant source zone, as well as cause operational difficulties such as excessive pumping pressures.

Additional simulations were also run holding oxidant concentration and velocity constant, and evaluating differing rates and amounts of NOD to determine the sensitivity of these parameters. It was found that decreasing the rate of the fast NOD by a factor of 10 did not appreciably increase permanganate transport distance. However, this is presumably because the fast NOD rate is nearly instantaneous. Increasing the fast NOD mass fraction by 50% had little effect; however, decreasing the NOD mass fraction resulted in a 50% increase in oxidant transport distance.

The importance of these findings can be understood by considering remediation of a hypothetical DNAPL source zone, where the impact of NOD is neglected. This source zone contains 10000 kg of PCE evenly distributed at a 20% NAPL saturation, and assumes all permanganate that enters the source zone reacts with the contaminant. Figure 4.27 plots the predicted number of pore volumes of oxidant needed, as well as the system operation time needed to inject these pore volumes, to completely destroy the DNAPL. Because the operational timeframe is often one of the key contributors to remediation cost, due to staffing, sampling, and analysis requirements, a remediation approach that minimizes the operation timeframe may be selected. Based on this criterion only, and neglecting the role of NOD, injection at high oxidant concentration and high flow rate may appear the best operational conditions. However, based on the conclusions of modeling studies of NOD, possible operation problems and flow bypassing

may result due to the large amount of MnO_2 solids that may deposit within the source, whereas a low oxidant concentration at high flow rate may improve performance, despite the longer operational time frame.

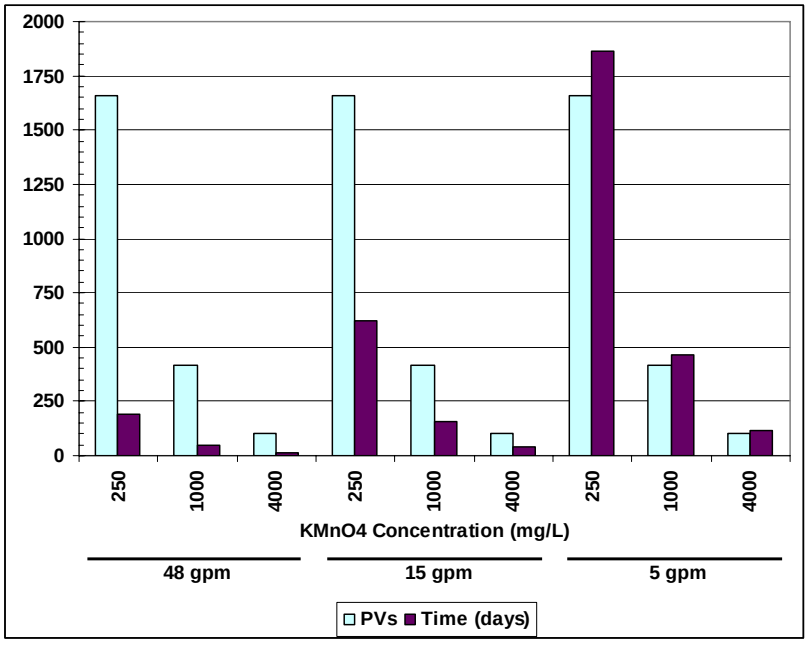

Figure 4.27. Comparison of time and pore volumes needed to treat a hypothetical DNAPL source zone.

4.5. EXPERIMENTAL EVALUATION OF COUPLING ISCO WITH OTHER REMEDIATION TECHNOLOGIES

The viability of coupling ISCO using permanganate or catalyzed hydrogen peroxide with surfactant/cosolvent flushing or in situ bioremediation were evaluated using batch reactor studies, and 1-D columns, and 2-D flow-through cells.

4.5.1. Coupling ISCO with Surfactant/Cosolvent Flushing

The evaluation of surfactant-enhanced aquifer restoration was performed as part of a doctoral dissertation, which is planned for completion in December 2006. Some preliminary results for a portion of the studies completed prior to preparation of this project final report are presented in this section. A detailed description of the methods and complete results will be reported in a forthcoming dissertation (Dugan 2006) and subsequent publications.

The coupling of ISCO with surfactant/cosolvent flushing was conceptualized as occurring in two possible scenarios. In case one, a high weight percentage of surfactant contacts a high weight percent of oxidant, which may occur if oxidant is applied shortly after surfactant flushing, or potentially oxidant and surfactants/cosolvents are co-injected. Under case two, a low weight percentage of surfactants are present in the subsurface at residual levels, after a surfactant and subsequent water flush have occurred. Oxidant is then applied to destroy residual contaminant as a polishing step.

Toward this goal, a number of surfactant/cosolvent and oxidant compatibility tests were conducted, in accordance with the methods presented in Section 3.6.1.

Initial screening tests were conducted using catalyzed hydrogen peroxide to assess reactivity with 28 surfactants with respect to case one conditions, where high concentrations of oxidant contacted typical flushing solution concentrations. Initial results indicated that this particular oxidant is not suitable for pairing with surfactants in this context due to gas and foam generation, as well as an increases in temperature ranging from 5˚C to as high as 20˚C.

Further screening tests were conducted on a sub-sample of 72 surfactants to determine whether CHP could potentially be coupled with case two application, with lower surfactant and oxidant concentrations. Six surfactants consisting of 3 nonionic and 3 anionic surfactants were selected. All six surfactants have been widely used in field remediation efforts. Screening was conducted with surfactants at 1.0 and 3.5-wt% and 3-wt% CHP. None of the six surfactants at 1.0-wt% or 3.5-wt% were compatible with 3.0-wt% H_2O_2 with 5mM $FeSO_4$ in that there was significant consumption of the oxidant, however there was no gas or foam generated. Although color change was not used as an indicator of a compatible, favorable pairing it is interesting to observe that there was a color change when surfactants were coupled with CHP. This color change is apparent in Figure 4.28 (note that all three of the surfactants were deemed to be incompatible with CHP under the conditions tested).

Figure 4.28. Photo of surfactant solution color change after reaction with CHP.

The surfactants Aerosol MA-80I and Alfoterra 23 were both compatible with CHP at relatively low surfactant concentrations indicating that co-injection would not be a suitable remediation treatment, however sequential application of surfactant followed by CHP might be possible with appropriate experimental design and engineering. Figure 4.29 illustrates a dose response relationship where increasing surfactant concentrations result in less favorable performance when CHP is applied sequentially. Anionic surfactants appear to be more resistant to oxidation.

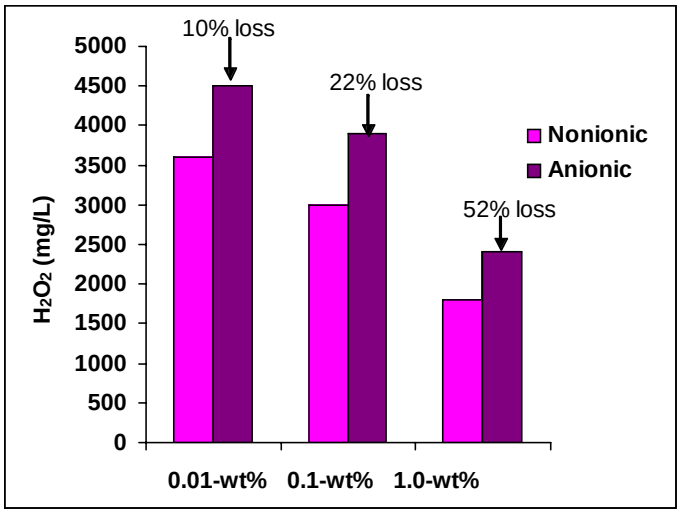

Figure 4.29. Hydrogen peroxide remaining after contacting residual concentrations of surfactant.

Coupling of ISCO using $KMnO_4$ with SEAR appeared more favorable based on compatibility test results. Table 4.13 lists results from initial studies of compatibility of surfactants with high and low concentrations of permanganate, and varied concentrations of surfactants alone, or surfactants in the presence of a cosolvent. Favorable couplings with permanganate were identified as having the ability to enhance the solubility of PCE, low oxidant demands, little or no observable color change, and minimal solids (MnO_2) generation. Favorable couplings are indicated in Table 4.13 by a simple yes while unfavorable couplings are indicated by a no.

Based on the initial studies, two surfactants, Dowfax 8390 and sodium dodecyl sulfate (SDS), and two cosolvents, acetone and tert-butanol, were found to be compatible at relatively higher concentrations (1.0-5.0-wt%) as well as residual concentrations (0.01-0.1-wt%) with a 5000 mg/L $KMnO_4$ solution. Several surfactants were compatible with permanganate at lower surfactant concentrations (i.e., 0.01-to-0.1-wt%) (e.g., Dowfax 2A1, Dowfax 3B2, Dowfax C10L, Tergitol 15-S-20, Tergitol TMN-6, Tergitol TMN-10, Aerosol MA-80I (sodium dihexyl sulfosuccinate), sodium dodecyl benzene sulfonate (SDBS). Figures 4.30a and 4.30b below demonstrate the important differences observed in the compatibility of the surfactants with permanganate. These figures illustrate the concentration of permanganate remaining in solution for three initial concentrations (0.01, 0.1, and 1.0-wt%) of the oxidation resistant surfactant Dowfax 8390, and the oxidant degradable Tween 80, at reaction time points of 3 and 24 hours. The amount of permanganate consumed after 24 hours for the surfactants Dowfax 8390, and Tween 80 was 4% and 83%, respectively.

Follow-on studies were then conducted for 24 surfactants (compatible and incompatible). Six of these surfactants were not included in the initial screening studies (i.e., Alfoterra 23, Aerosol-OT, Calfax 10L-45, Calfax 16L-35, Calfax DB-45, and Calfax DBA-70). For these studies duplicate samples were prepared and analyzed as described previously. Table 4.14 presents the permanganate concentrations measured after reaction with different surfactants for periods of 3- or 24-hours. It is important to point out that many of the surfactants that appeared to be compatible after 3-hours of reaction with permanganate became incompatible after 24-hours.

Table 4.13. Compatibility of surfactants and cosolvents with permanganate.

Surfactant		Cosolvent		$KMnO_4$ conc. (mg/L)	Favorable coupling?	Surfactant		Cosolvent		$KMnO_4$ conc. (mg/L)	Favorable coupling?
Name	Conc. (wt.%)	Name	Conc. (wt.%)			Name	Conc. (wt.%)	Name	Conc. (wt.%)		
SDS	3.5	None	-	500	Yes	Brij 97	3.5	TBA	5.0	5000	No
SDS	3.5	IPA	3.5	500	No	Brij 97	3.5	IPA	5.0	5000	No
SDS	3.5	TBA	3.5	5000	Yes	Igepal CA-630	3.5	None	-	5000	No
Aerosol MA-80I	5.0	IPA	-	500	No	Igepal CA-630	3.5	TBA	5.0	5000	No
Tween-80	5.2	None	-	5000	No	Igepal CA-630	3.5	IPA	5.0	5000	No
HPCD	10.0	None	-	500	No	Triton X-100	3.5	None	-	5000	No
None	-	IPA	3.5	500	No	Triton X-100	3.5	TBA	5.0	5000	No
None	-	TBA	3.5	5000	Yes	Triton X-100	3.5	IPA	5.0	5000	No
Aliquat	3.0	None	-	5000	No	Flo-Mo	3.5	None	-	5000	No
Span-80	3.0	None	-	5000	No	Flo-Mo	3.5	TBA	5.0	5000	No
Teepol 610S	1.0	None	-	5000	Yes	Flo-Mo	3.5	IPA	5.0	5000	No
Tergitol NP	1.0	None	-	5000	Yes	Witconol SN 120	3.5	None	-	5000	No
Dowfax 8390	1.0	None	-	5000	Yes	Witconol SN 120	3.5	TBA	5.0	5000	No
Siponic L-7-90	1.0	None	-	5000	No	Witconol SN 120	3.5	IPA	5.0	5000	No
Rhodafac RA-600 phosphate ester	1.0	None	-	5000	No	Novell II	3.5	None	-	5000	No
Katapol VP-532 SPB	1.0	None	-	5000	No	Novell II	3.5	TBA	5.0	5000	No
Alcodet HSC-1000	1.0	None	-	5000	No	Novell II	3.5	IPA	5.0	5000	No
Glycoside APG 300	1.0	None	-	5000	No	SDBS	3.5	None	-	5000	No
Zonyl	1.0	None	-	5000	Yes	SDBS	3.5	TBA	5.0	5000	No
Rexophos 25/97	1.0	None	-	5000	No	SDBS	3.5	IPA	5.0	5000	No
Adsee 799	1.0	None	-	5000	No	Aerosol MA-80	3.5	None	-	5000	No
Katapol PN-430	1.0	None	-	5000	No	Aerosol MA-80I	3.5	TBA	5.0	5000	No
Hyonic PE-90	1.0	None	-	5000	No	Aerosol MA-80I	3.5	IPA	5.0	5000	No
T-DET N9.5 (N)	1.0	None	-	5000	No	Tergitol min-foam 1X	3.5	None	-	5000	No
Glycoside APG 325	1.0	None	-	5000	No	Tergitol min-foam 1X	3.5	TBA	5.0	5000	No
Makon 12	3.0	None	-	5000	No	Tergitol min-foam 1X	3.5	IPA	5.0	5000	No
Tergitol min-foam 1-X	1.0	None	-	5000	Yes	Tergitol TMN-3	3.5	None	-	5000	Yes

Table 4.13 (cont.). Compatibility of surfactants and cosolvents with permanganate.

Surfactant		Cosolvent		$KMnO_4$	Favorable	Surfactant		Cosolvent		$KMnO_4$	Favorable
Name	Conc. (wt.%)	Name	Conc. (wt.%)	conc. (mg/L)	coupling?	Name	Conc. (wt.%)	Name	Conc. (wt.%)	conc. (mg/L)	coupling?
Cyclomide DC 212-M	1.0	None	-	5000	No	Tergitol TMN-3	3.5	TBA	5.0	5000	Yes
Aerosol MA-80	1.0	None	-	5000	Yes	Tergitol TMN-3	3.5	IPA	5.0	5000	Yes
SDBS	1.0	None	-	5000	Yes	None	-	1-butanol	5.0	5000	Yes
Dowfax 8390	3.5	None	-	5000	Yes	None	-	2-butanol	5.0	5000	No
Dowfax 8390	3.5	TBA	5.0	5000	Yes	None	-	1-pentanol	5.0	5000	No
Dowfax 8390	3.5	IPA	5.0	5000	No	None	-	Ethyl alcohol	5.0	5000	No
Teepol 610S	3.5	None	-	5000	No	Dowfax 2A1	1.0	None	-	5000	Yes
Teepol 610S	3.5	TBA	5.0	5000	No	Dowfax 3B2	1.0	None	-	5000	Yes
Teepol 610S	3.5	IPA	5.0	5000	No	Dowfax C10L	1.0	None	-	5000	Yes
Calsoft	3.5	None	-	5000	No	Cyclodextrin	1.0	None	-	5000	No
Calsoft	3.5	TBA	5.0	5000	No	Tergitol TMN6	1.0	None	-	5000	Yes
Calsoft	3.5	IPA	5.0	5000	No	Tergitol TMN10	1.0	None	-	5000	Yes
Pluronic L-43	3.5	None	-	5000	No	Tergitol XD	1.0	None	-	5000	Yes
Pluronic L-43	3.5	TBA	5.0	5000	No	Tergitiol 15-S-20	1.0	None	-	5000	Yes
Pluronic L-43	3.5	IPA	5.0	5000	No	Glucopon 425N	1.0	None	-	5000	No
Brij 97	3.5	None	-	5000	No						

Note: SDS = sodium dodecyl sulfate, SDBS = sodium dodecyl benzene sulfonate.

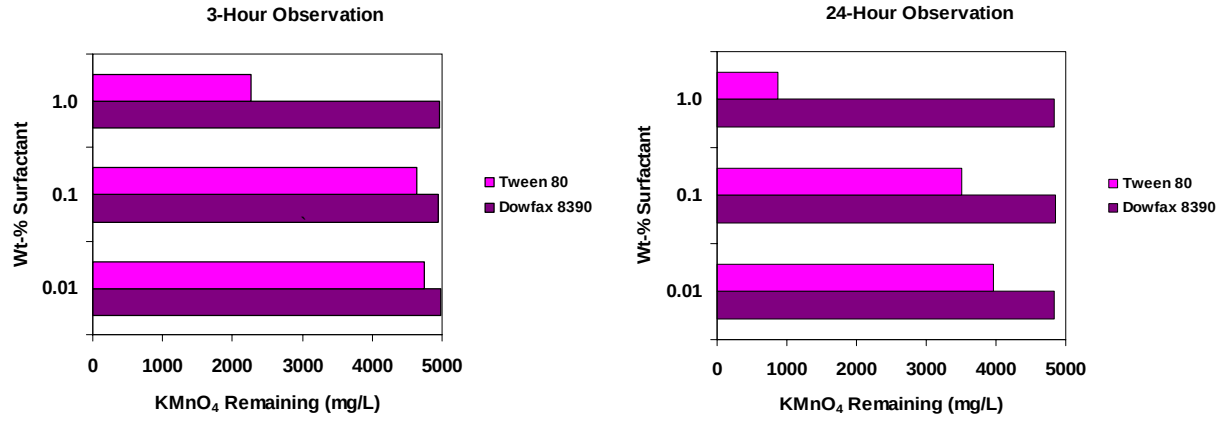

Figure 4.30. Example data of oxidant degradation versus surfactant concentration: (a) left, 3 hr observation, and (b) right, 24 hr observation.

Table 4.14. Permanganate remaining after a 3-hr or 24-hr period of reaction of 3.5 wt.% surfactant with 5000 mg/L $KMnO_4$.

Surfactant no.	Surfactant trade name	Rxn. period (hr)	Average $KMnO_4$ (mg/L)	Std. Dev. $KMnO_4$ (mg/L)	Mass loss of $KMnO_4$ (%)
1	Adsee 799	3	1219	1.0	76%
		24	1219	1.0	77%
2	Aerosol MA80-I	3	1891	2.4	63%
		24	0	0.0	100%
3	Aerosol OT	3	4865	0.4	4%
		24	4379	0.6	14%
4	Alfoterra 23	3	2417	2.9	52%
		24	4430	0.7	92%
5	Brij 97	3	* [a]	*	100%
		24	*	*	100%
6	Calsoft LAS-99	3	377	0.1	93%
		24	*	*	100%
7	Calfax 10L-45	3	3883	2.8	23%
		24	950	0.3	82%
8	Calfax 16L-35	3	4340	1.3	14%
		24	4183	2.0	15%
9	Calfax DB-45	3	3887	2.0	23%
		24	1939	0.4	61%
10	Calfax DBA-70	3	*	*	100%
		24	*	*	100%
11	Dowfax 8390	3	4458	1.5	10%
		24	3980	2.6	23%
12	Dowfax C10L	3	3863	0.1	22%
		24	1090	1.1	76%
13	Dowfax 3B2	3	4277	0.1	13%
		24	988	0.1	80%
14	Dowfax 2A1	3	4088	1.1	19%
		24	2057	3.8	64%
15	HPCD	3	*	*	100%
		24	*	*	100%
16	Flo-Mo	3	*	*	100%
		24	*	*	100%
17	Glucopon 425N	3	*	*	100%
		24	*	*	100%
18	Novell II 1012-21	3	471	0.9	91%
		24	34	0.4	99%
19	Pluronic L-43	3	*	*	100%
		24	*	*	100%
20	SDBS	3	3442	0.1	29%
		24	1896	0.5	61%
21	SDS	3	4523	0.4	6%
		24	4393	2.5	20%
22	Teepol 610S	3	4012	0.2	17%
		24	3039	0.1	38%
23	Tween 80	3	*	*	100%
		24	*	*	100%
24	Witconol SN-120	3	193	0.8	96%
		24	*	*	100%

[a] An "*" indicates that there was no permanganate remaining in solution.

Further screening studies were then conducted on the 4 surfactants that were found to be most compatible at lower concentrations (i.e., 0.5-1.0 wt.%) and were being considered for use in the 2-D cell studies involving coupling SEAR with ISCO for DNAPL removal. Duplicate samples were prepared as described previously and these results are illustrated in Table 4.15.

Table 4.15. Permanganate remaining after a 24-hr period of reaction of 0.5 to 1.0 wt.% surfactant with 5000 mg/L $KMnO_4$.

Surfactant and wt.% used	Average $KMnO_4$ (mg/L)	Std. Dev. $KMnO_4$ (mg/L)	Mass loss of $KMnO_4$ (%)
Aerosol AOT at 1 wt.%	4572.5	3.6	16%
Calfax 16L-35 at 0.5 wt.%	4952.5	3.6	8%
Dowfax 8390 at 0.5 wt.%	5077.5	3.8	6%
SDS at 0.5 wt.%	4922.5	3.7	9%

In that most SEAR or ISCO field applications would likely not be concluded after 24-hours, further studies were conducted with a select group of 24 surfactants (both nonionic and anionic) and all 7 cosolvents prepared in duplicate to measure MnO_4^- depletion and observe $MnO_{2(s)}$ formation after reaction for periods of 3-, 24-, 120-, and 336-hours. Figure 4.31 illustrates the short- and longer-term results for permanganate depletion for the following three surfactants that were judged to be compatible based on the initial batch test results (3- and 24-hr reaction periods): Aerosol-OT, SDS, and Dowfax 8390.

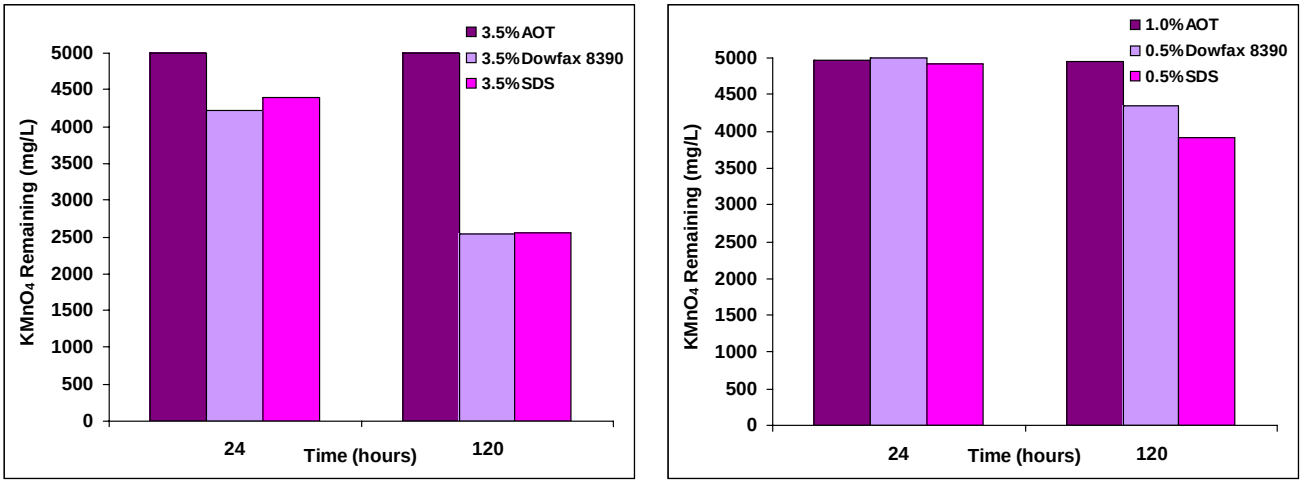

Figure 4.31. Results of short- and longer-term reaction of three different surfactants with $KMnO_4$ (5000 mg/L).

4.5.2. Coupling ISCO with Bioremediation

The evaluation of coupling ISCO with bioremediation was conducted as part of a master's thesis project and is documented in detail in an M.S. thesis (Sahl 2005) and two journal papers (Sahl and Munakata-Marr 2006, Sahl *et al.* 2006). The study included evaluation of aerobic and anaerobic degradation of TCE and PCE when coupled with permanganate using column studies, and batch microcosms evaluating the impact of oxidized ground water on anaerobic PCE degrading microbes after porous media treatment with permanganate and CHP.

4.5.2.1. Evaluation of Permanganate Oxidation Impacts on Contaminant Degrading Cultures Using 1-D Column Studies. The first series of column studies evaluated the impact of permanganate oxidation on the aerobic G4 culture which can cometabolically degrade TCE when the toluene ortho mono-oxygenase (TOM) enzyme is expressed. The TOM enzyme may be expressed when an aromatic compound such as toluene or phenol is present and being degraded by the culture. During the pre-oxidation phase of the aerobic column experiments, phenol was fed to both an inoculated column and a control. Phenol concentrations were observed in the effluent of the control, but not in the inoculated column, indicating that the culture was actively degrading phenol. After both columns were treated with potassium permanganate (1000 mg/L), phenol concentrations were non-detectable in both columns, and residual permanganate was observed in the effluent, indicating that permanganate was oxidizing phenol. After oxidant flushing ceased, phenol concentrations in the influent were increased to determine whether or not the G4 culture was still active. Phenol concentrations in the effluent remained non-detectable until several pore volumes of phenol solution had been flushed, and then phenol concentration rebounded in the control, but not the inoculated column. The rebound of phenol in the control, but not in the inoculated column may indicate that the G4 culture was active, but is not conclusive because residual oxidant may have been oxidizing phenol. Due to problems with analytical detection limits, as well as possible sorption to the media, TCE, which was present at 8 mg/L in the influent, was never observed in the effluent of either the control or the inoculated column, inhibiting the ability to determine contaminant degradation rates. As a final step, TFMP analysis was performed on both columns to determine if the TOM enzyme was expressed. When TOM is expressed, TFMP is degraded to TFMA, which is bright yellow in color. After the introduction of TFMP to the columns, the effluent of the control remained clear, while the inoculated column turned yellow, indicating that TOM was being expressed, and the G4 culture is capable of degrading TCE. However, further work is needed to determine the impact of permanganate oxidation on G4 culture TCE degradation rates, as TCE degradation was not conclusively observed in this study.

The second series of column experiments focused on anaerobic degradation of DNAPL phase PCE by the KB-1 mixed culture. The anaerobic column experiments were conducted according to the conditions outlined in Table 3.13. The experiments consist of a pre-oxidation phase to observe the initial rate of PCE dechlorination, followed by a permanganate flush at varied velocities and concentrations, and then a post-oxidation phase to determine the impact to microbial activity. To determine whether the original KB-1 culture would rebound with activity, the columns were not re-inoculated after oxidant flushing ceased.

The KB-1 culture has the ability to reductively dechlorinate PCE completely to ethene. Low concentrations of vinyl chloride (VC) and ethene were observed during this study, but the concentrations of these compounds were very low and not reliably quantified due to analytical detection limits. TCE and cis-1,2-dichloroethene (DCE) were observed in larger concentrations, but TCE was found to be a transient byproduct with generally low concentrations, and due to a contamination problem with the GC method used, the data from TCE could not be used to determine dechlorination rates. Most of the dechlorinated mass of contaminant accumulated as DCE, which is not surprising as complete dechlorination to VC and ethene requires extensive contact time which was not provided by the column experiments, as has been observed by others (Adamson *et al.* 2003, Isalou and Sleep 1998, Yang and McCarty 2000). Table 4.16 presents the average PCE, TCE, DCE and total chloroethene concentrations observed during both the pre-

oxidation and post oxidation phases of the experiments. Note that the saturation concentration for PCE is about 1.1 mmol/L.

Table 4.16. Average concentrations of chloroethenes from the anaerobic column experiments.

Column	KB-1 presence	Pre-oxidation (all units mmol/L)				Post-oxidation (all units mmol/L)			
		PCE	TCE	DCE	Total chloroethenes	PCE	TCE	DCE	Total chloroethenes
MM	Inoculated	0.378	0.009	0.383	0.761	0.594	0.008	0.340	1.220
LL	Inoculated	0.129	0.008	0.577	0.714	0.439	0.030	0.384	0.853
LL-2	Inoculated	0.131	0.011	0.994	1.140	0.508	0.005	0.443	0.956
HH	Inoculated	0.453	0.018	0.518	1.620	0.307	0.033	0.591	0.930
LH	Inoculated	0.231	0.026	0.911	1.390	0.870	0.004	0.514	1.390
NOOX-C	Inoculated	0.968	0.001	0.559	1.530	1.090	0.007	0.015	1.120
MM-C	Un-inoculated	0.660	0.000	0.002	0.663	0.565	0.000	0.000	0.663
LH-C	Un-inoculated	0.433	0.000	0.000	0.433	0.294	0.000	0.000	0.294

In all inoculated columns, a rebound in reductive dechlorination activity was observed after oxidant flushing at varied concentrations and velocities, as evidenced by TCE and DCE generation in the column effluent, without any re-inoculation. Also of note in Table 4.16, the total chloroethenes concentrations are higher in the inoculated systems than in the uninoculated controls, indicating a higher PCE mass depletion rate due to the degradation of PCE by KB-1 and therefore biologically enhanced mass transfer. In several systems, the total chloroethenes concentrations exceed the solubility of PCE, which can be the result of increased mass transfer due to bulk phase PCE dechlorination (i.e., degradation products are more soluble).

Pre-oxidation average total chloroethene concentrations and *cis*-DCE:PCE ratios (see Table 4.17) varied between some column runs. The rate of PCE dechlorination in each batch was not determined at the point of inoculation, but differences in the rate of dechlorination, especially in the dechlorination of vinyl chloride, existed between the column inocula. However, total chloroethene concentrations and *cis*-DCE:PCE ratios varied between duplicate columns (LL-1 and LL-2) inoculated with the same batch, indicating some variability in NAPL-nutrient medium contact.

During oxidation, no dechlorination daughter products were detected, suggesting that reductive dechlorination ceased. Additionally, aqueous PCE concentrations did not significantly differ between experimental conditions, or between the control column MM-C between pre-oxidation and oxidation conditions. Columns run under low oxidant concentration were likely stoichiometrically limited by permanganate concentrations; only 0.57 moles of $KMnO_4$ were provided per mole of PCE (assuming saturation concentration), compared with 1.3 moles $KMnO_4$ required for complete PCE oxidation. Column HH run under excess oxidant concentration and high oxidant application velocity showed limited PCE-$KMnO_4$ reaction, due possibly to the short column detention time (1.8 hours vs. 19 or 28 hours for low or medium velocities). Interestingly, column MM received excess $KMnO_4$ (5.7 moles per mole PCE) but permanganate was not observed in the column effluent, possibly due to competing oxidation targets (e.g., FeS_2 in growth medium).

Following the permanganate flush, a relatively rapid rebound of significant PCE dechlorination activity was observed in every inoculated column. These column studies used a nutrient medium to promote pre-oxidation PCE dechlorination activity as well as the rebound of bioactivity post-oxidation. The columns were not re-inoculated following oxidation, indicating that the original culture rebounded following oxidant application. Although other studies have reported the rebound of biological activity

following permanganate application (Hazen *et al.* 2000, Klens *et al.* 2001, Azadpour-Keeley *et al.* 2004), only one other study (Hrapovic *et al.* 2005) showed PCE dechlorination following oxidation. In the other study, only one column showed dechlorination activity after flushing for over two months with site ground water containing dehalorespiring organisms and biostimulating with acetate and ethanol; dechlorination was observed after a significant lag time (222 days after oxidation), and concentrations of dechlorination by-products were very low (0.24 μM).

Other observations of note are whether oxidant was observed to breakthrough to the effluent of the column, the number of pore volumes of anaerobic growth medium that were flushed until the rebound of dechlorination activity in the column, the total reduction in pH during oxidation, and the location and amount of manganese solids that deposit in the column resultant of oxidation. These observations may indicate how the KB-1 culture responds to oxidation with permanganate and are presented in Table 4.17.

Table 4.17. Observations that indicate performance of the KB-1 culture during oxidation.

Column	Pre-oxidation DCE/PCE	Post-oxidation DCE/PCE	M [a]	Oxidant breakthrough?	Time to activity rebound (Pore volumes)	Change in pH	MnO_2 (% penetration of column)
MM	1.01	1.04	1.03	no	3.10	3.5	50
LL	4.48	0.87	0.20	no	7.00	3.7	35
LL-2	7.57	0.87	0.19	no	6.50	3.5	35
HH	1.14	1.92	1.68	yes	2.75	4.2	85
LH	3.95	0.59	0.15	yes	1.05	3.9	100
NOOX-C	0.58	0.01	0.01	NA	NA	0.0	NA
MM-C	0.00	0.00	0.00	no	NA	3.9	55
LH-C	0.00	0.00	0.00	yes	NA	4.2	100

[a]M = post-oxidation DCE:PCE ratio divided by the pre-oxidation DCE:PCE ratio.

The pH during the oxidation phase reduced dramatically, due to the reaction between permanganate and PCE. In all columns, the effluent pH ranged from 3-4. The change in pH resultant of permanganate would be anticipated to disrupt anaerobic reductive dechlorination (Kastner *et al.* 2000). During the oxidation phase, no DCE was observed in the effluent of any of the columns. After the oxidation phase ceased and the flushing with anaerobic growth media resumed, microbial activity rebounded with an increase in chloroethene concentrations, but the time (pore volumes) to rebound varied depending on the permanganate concentration used and the delivery velocity.

Manganese dioxide deposition was clearly visible in all columns (Figure 4.32), the extent of which depended directly on the concentration as well as the velocity of oxidant application. Columns with a high oxidant application velocity (LH, HH) showed MnO_2(s) deposition throughout the entire length of the column, with visual permanganate breakthrough in the column effluent. In columns with a high oxidant application velocity, the shorter column retention time limited permanganate reaction in the NAPL source zone, allowing the permanganate solution to travel further in the column. Conversely, MnO_2(s) deposition was limited to the bottom half of the columns with a lower oxidation application velocity (LL-1, LL-2, MM, MM-C), with no permanganate ever visually observed in column effluent.

Manganese dioxide concentrations for each 5 cm section (A-E) in the dissected columns are shown in Figure 4.33. The measured concentrations quantify the visual observations described above. The average concentration of MnO_2(s) was highest in the two columns (MM, LH) that received a greater mass of $KMnO_4$ and lowest in columns (LL-1, LL-2) that received a lower $KMnO_4$ mass. In column HH, complete reduction of manganese dioxide solids was visually observed during the post-oxidation phase and therefore MnO_2(s) concentrations were not measured. Furthermore, MnO_2(s) concentrations were not

quantified in the control column (MM-C) because investigating the relationship between MnO_2(s) concentrations and bioactivity was the primary goal of MnO_2(s) quantification.

Concentrations of dissolved manganese were only elevated over the nutrient medium concentration (2.2 μM) in column HH following oxidation. Once MnO_2(s) was visually absent from column HH, concentrations of dissolved Mn^{2+} decreased to levels observed in the uninoculated control. The highest Mn^{2+} concentration observed in the column effluent of column HH was 6.0 μM.

Column LH showed the most rapid rebound of PCE dechlorination activity and had the highest average concentration of MnO_2(s), distributed throughout the column. MnO_2(s) is a moderate oxidant (Xie and Barcelona 2003) and the rebound of anaerobic activity in the presence of these solids is surprising. However, the presence of bioavailable Mn (IV) has been shown to induce the mineralization of *cis*-DCE in manganese reducing conditions (Bradley *et al.* 1998), demonstrating that anaerobic processes may proceed in the presence of an oxidant.

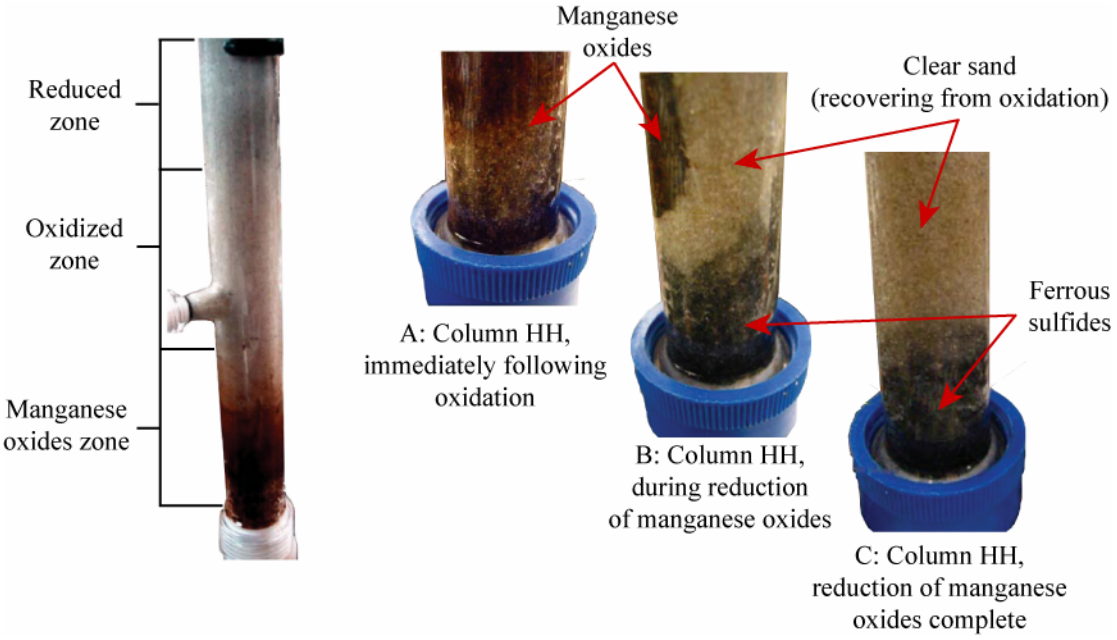

Figure 4.32. Manganese dioxide fronts observed during anaerobic column studies.

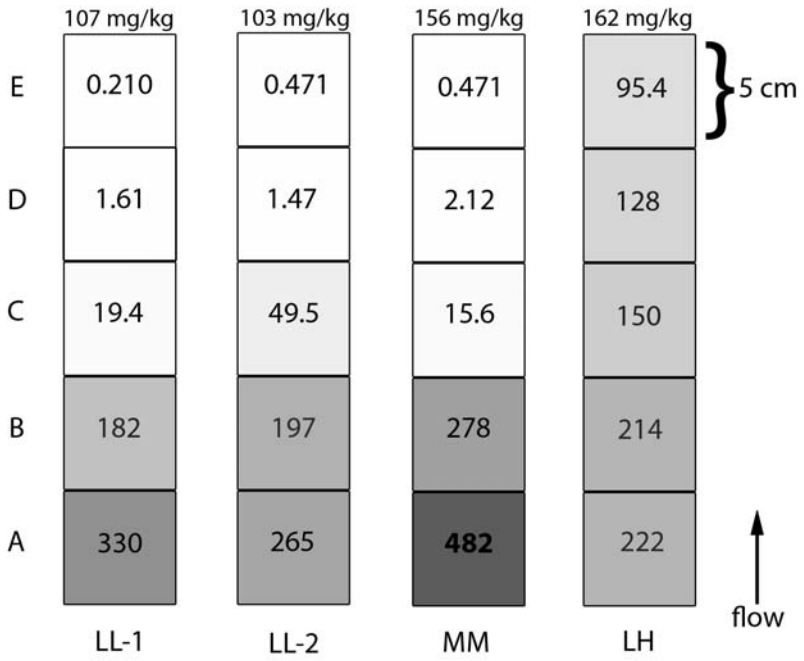

Figure 4.33. Manganese dioxide concentrations (mg-Mn as MnO_2/kg-dry sand) in each dissected column. Average MnO_2(s) concentrations are included above each column.

Dissolution of MnO_2(s) was visibly evident and elevated effluent concentrations of dissolved manganese were observed in column HH immediately following the rebound of post-oxidation reductive dechlorination; MnO_2(s) dissolution appeared complete following 3 pore volumes of media applied. It is unclear why MnO_2(s) dissolution was only visible in column HH, but it may have been due to a lower redox potential than was present in other columns. Manganese dioxide reduction usually results from a drop in redox potential due to bacterial metabolism (Gounot 1994). The redox potential was not monitored in these studies so the relationship between reductive dechlorination activity and manganese reduction could not be determined. The reduction of manganese dioxides was reported in another laboratory study using dechlorinating organisms (Hrapovic *et al.* 2005), but a direct link between reductive dechlorination activity and manganese reduction has not been established. However, the reduction of Mn (IV) has been associated with increased DCE mineralization (Bradley *et al.* 1998), suggesting a potential relationship between anaerobic remediation processes and manganese reduction.

Also possibly important to the time of reductive dechlorination activity rebound is the length of time that the microbes are exposed to the oxidant. Figure 4.34 presents the number of hours of oxidant application versus the time to activity rebound in pore volumes. This plot shows that a potentially positive linear correlation may be made, as longer oxidant exposure times resulted in longer times to activity rebound. However, it also important to note that oxidant concentration may also impact the rebound, as higher oxidant concentrations may be anticipated to be more disruptive to the KB-1 culture than low oxidant concentrations.

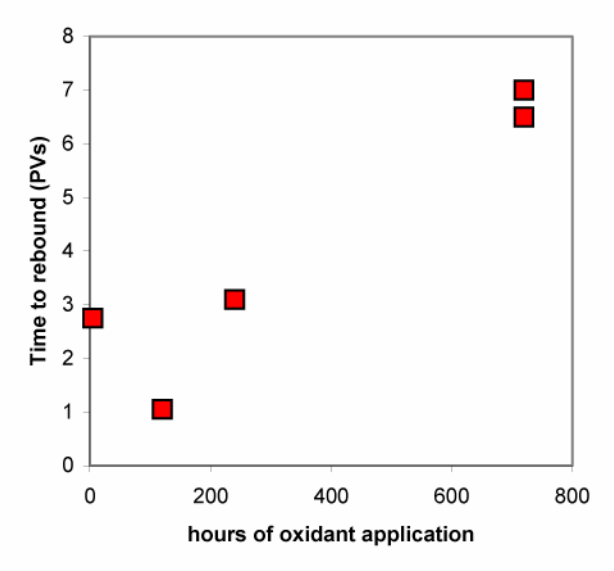

Figure 4.34. Time to activity rebound vs. hours of oxidant application.

4.5.2.2. Anaerobic Batch Microcosm Studies. Three series of anaerobic batch microcosm studies were performed to evaluate how the oxidation of porous media, and resulting byproducts may impact the reductive dechlorination behavior of the KB-1 culture. When porous media containing significant natural organic matter content is oxidized, the oxidant may break up complex organic matter into lower molecular weight, dissolved organic compounds. The goal of these microcosm experiments was to determine if these dissolved organics may enhance reductive dechlorination of PCE by the KB-1 culture, by acting as a growth substrate. The first batch microcosm employed the NTC field soil, from which concentration data are presented in Figure 4.35.

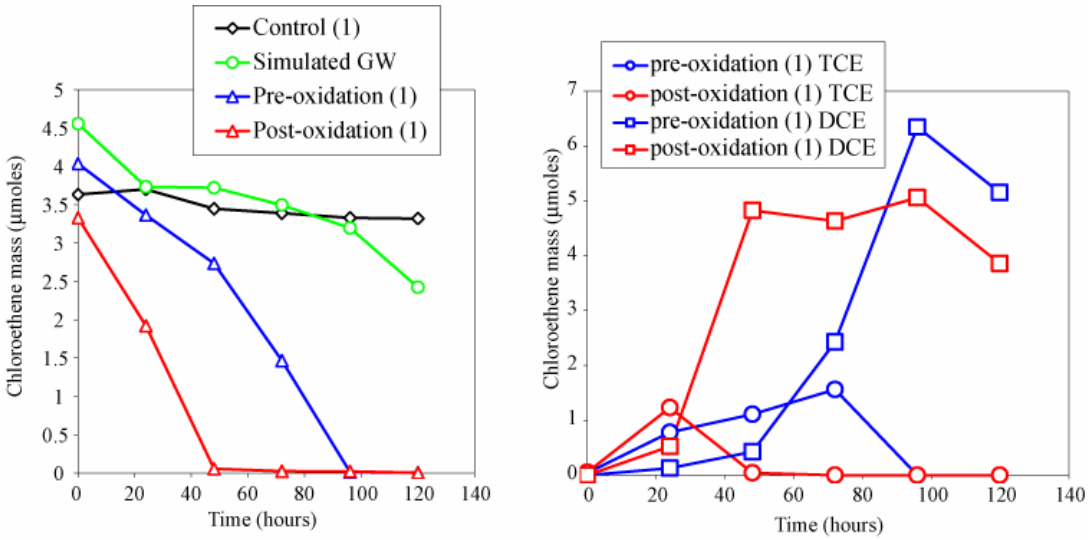

(a) Total PCE mass in NTC microcosm study (b) Total by-product mass in NTC study

Figure 4.35. Chloroethene data from NTC batch microcosm study.

From Figure 4.35a, it can be noted that the KB-1 culture was able to deplete PCE in the post-oxidation ground water at a faster rate than the pre-oxidation ground water. A corresponding increase in TCE and DCE byproduct formation is also noted in Figure 4.35b. The TCE and DCE byproduct masses begin to decrease towards the end of the experiment due to degradation to VC and ethene, which were detected but not quantified. Dechlorination activity and resulting byproduct formation was detected in the simulated ground water microcosm, but was much more limited than in either pre- or post-oxidation NTC ground water. No byproduct formation or PCE mass degradation was observed in the control.

The second and third batch microcosm studies evaluated the Mines Park (MP) sandy loam field soil, with respect to the ability of oxidation to enhance KB-1 activity by liberating dissolved organic carbon. The second batch evaluated the ability of permanganate to liberate DOC into post-oxidation ground water, generated by a flow through column experiment, and the third batch evaluated the use of catalyzed hydrogen peroxide (CHP) to liberate DOC using a batch oxidation system. PCE mass data from the second and third microcosm studies are presented in Figure 4.36.

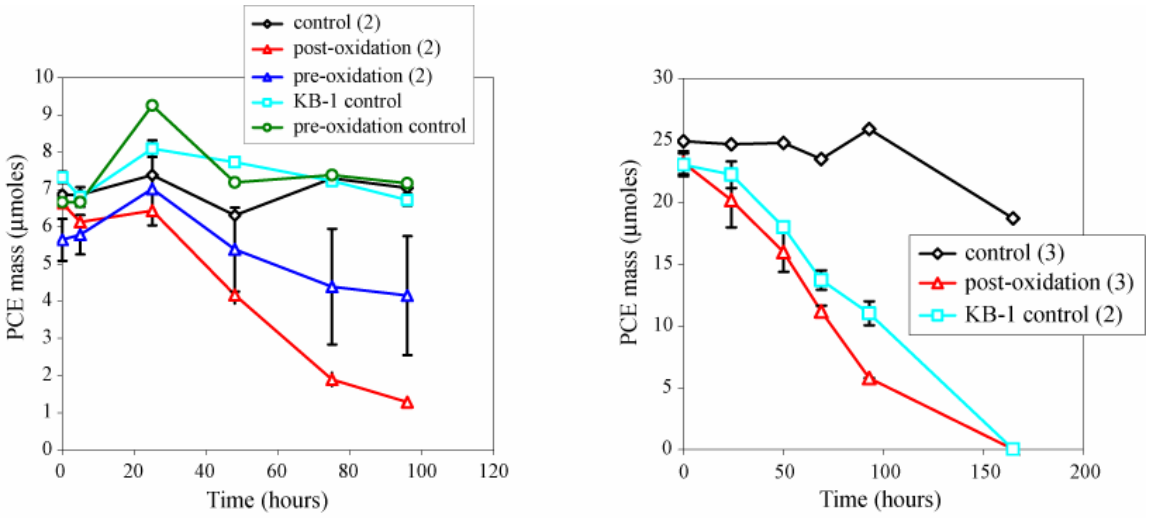

(a) Permanganate batch microcosms (b) CHP batch microcosms

Figure 4.36. Total PCE mass in Mines Park batch microcosms.

The data in Figure 4.36a indicate that the rate of reductive dechlorination by KB-1 was greatest in systems containing byproducts of permanganate oxidized porous media. TCE, DCE, VC and ethene data also supported this conclusion as the permanganate post-oxidation system accumulated dechlorination byproducts at the fastest rate (Sahl 2005). The pre-oxidation control system was run without KB-1 inoculation, showed no significant PCE degradation and no TCE or DCE generation indicating that the MP sandy loam soil used for this study probably does not have PCE-dechlorinating organisms present. With regard to the CHP oxidation system (Figure 4.36b), the post-oxidation ground water containing byproducts from CHP treated soil appeared to degrade PCE at a slightly faster rate than the KB-1 control. Unfortunately, the pre-oxidation microcosm became aerated rendering data from that microcosm inconclusive, so that comparison could not be made to the pre-oxidation system.

From the raw PCE dechlorination data, dechlorination rates were estimated assuming zero order kinetics (Maymo-Gatell *et al.* 1999) by fitting a linear regression line to the data. The R^2 value is also reported, as well as the ratio of the post-oxidation ground water rate to the same corresponding pre-oxidation ground water rate. These rates are presented in Table 4.18.

Table 4.18. Dechlorination rates in batch microcosm studies.

Sample	Oxidant	Site	k (μmol/hr)	R^2	k_{post}/k_{pre}
Culture control (1)			0.414	0.956	
Culture control (2)			1.25	0.987	
Pre-oxidation (1)		NTC	0.923	0.973	
Pre-oxidation (2)		MP	0.959	0.995	
Post-oxidation (1)	$KMnO_4$	NTC	1.33	0.994	1.44
Post-oxidation (2)	$KMnO_4$	MP	1.97	0.994	2.05
Post-oxidation (3)	CHP	MP	1.45	0.974	1.51[a]
Artificial groundwater			0.212	0.994	

[a] The pre-oxidation rate from the second batch had to be used due to aeration of the third pre-oxidation microcosm.

The rates in these studies cannot be directly compared to each other, as the rates in the culture controls from each set of microcosms are significantly different. However, as can be seen by the ratios, the post-oxidation ground waters had higher rates of reductive dechlorination than the pre-oxidation ground waters in each batch, indicating that oxidation generally had a stimulatory effect. In all three post-oxidation ground waters, DOC was found to increase by an order of magnitude over the corresponding pre-oxidation ground water. In the two permanganate post-oxidation ground water systems, the rate of dechlorination was statistically greater than the value of the pre-oxidation ground water alone, indicating that permanganate has a stimulatory effect. A stimulatory effect may have been observed in the CHP system, though problems with the pre-oxidation (3) microcosm forced comparison to the pre-oxidation (2) microcosm batch. Because the KB-1 control rates differed significantly between runs, this comparison is speculative. Relative to the KB-1 control (2) in the CHP oxidation microcosms, the post-oxidation ground water had a similar rate, possibly indicating that CHP oxidation may not have had any significant stimulatory effect. In other studies, CHP has not been shown to significantly increase the level of dissolved organic carbon (Siegrist *et al.* 2003). However, one study showed an increase in one system, attributed to partial oxidation of humic substances (Gates and Siegrist 1995).

4.6. EXPERIMENTAL INVESTIGATION OF PARTITIONING TRACER TEST (PTT) METHODS FOR PERFORMANCE EVALUATION AT ISCO TREATED SITES

Partitioning tracer test (PTT) methods have been applied at DNAPL sites as a means to estimate DNAPL mass in the subsurface, as well as characterize performance of remediation technologies such as surfactant / cosolvent flushing. However, ISCO presents unique challenges to PTT methods, as residual oxidant in the subsurface may destroy or alter partitioning organic compounds used as tracers. Furthermore, with permanganate, alterations to the subsurface environment at the DNAPL interface resulting from deposition of manganese oxide solids (MnO_2) can potentially alter the partitioning behavior of the tracers, impacting the ability to estimate remediation performance. This part of the project involved two sets of experiments, which are (1) batch studies of interactions between oxidants and partitioning tracers, and (2) evaluation of partitioning tracer methods in a 2-D flow cell for remediation performance assessment.

4.6.1. Batch Studies of Interactions Between Oxidants and Partitioning Tracers

These studies were conducted to evaluate several suites of partitioning tracers with differing chemical structures to identify tracers that are: (1) capable of partitioning into DNAPL mass for quantification of contaminant mass, (2) resistant to destruction or alteration by oxidants permanganate or catalyzed hydrogen peroxide, and (3) to evaluate the impact of MnO_2 deposition at the DNAPL aqueous

phase interface on partitioning behavior. These experiments were conducted according to the methods described in Section 3.7.1. This work was completed as part of a doctoral dissertation, which is scheduled to be defended in December 2006. A final description of the methods employed and results obtained will be presented in the dissertation (Dugan 2006) and forthcoming papers. Preliminary results for some studies completed as of the preparation of this final report are presented in this section.

The PTT test quantifies subsurface NAPL saturations (S_N). The laboratory-measured NAPL-water partitioning coefficient (K_{NW}) is required to calculate the S_N. Thus alterations to the K_{NW} value as a result of oxidation will impact the estimation of DNAPL mass, and therefore remediation performance assessment. The K_{NW} values in water for PCE and TCE DNAPLs were determined with batch tests for the alcohols in Group 1 and Group 2, as well as the ketones in Group 5. These values are presented in Table 4.19.

These values provide a baseline for comparison to K_{NW} values that would be used to determine DNAPL mass at a site undergoing natural dissolution before oxidant flushing. To determine how residual levels of permanganate remaining in the subsurface impact these K_{NW} values, batch studies were conducted with low concentrations of permanganate (440 mg/L) in the presence of tracers. Group 1 alcohol tracers consisting of primary alcohols (2M1B, 4M2P, 2,4DM3P, 2E1B, and 2E1H) were selected for this series of batch tests, the results of which are presented in Table 4.20.

Table 4.19. Partitioning tracer K_{NW} values in water, without oxidation.

Alcohol tracers	TCE K_{NW} values	PCE K_{NW} values
~ Group 1 ~		
2-methyl-1-butanol (2M1B)	3.71	1.47
2-ethyl-1-butanol (2E1B)	13.4	6.74
2-methyl-1-pentanol (2M1P)	14.5	9.12
2,4-dimethyl-3-pentanol (2,4DM3P)	71.3	31.6
2-ethyl-1-hexanol (2E1H)	202	146
~Group 2 ~		
Isopropyl alcohol (IPA)	0.361	not measured
1-hexanol (HEX)	19.5	10.0
2,2-dimethyl-3-pentanol (2,2DM3P)	57.2	37.3
6-methyl-2-heptanol (6M2H)	203	107
~Group 5 ~		
Acetone	1.1	0.9
3-methyl-2-butanone	22.3	5.9
3,3-dimethyl-2-butanone	74.6	23.2
2-methyl-3-pentanone	95.2	28.3
2,4-dimethyl-3-pentanone	133.7	57.1
5-methyl-2-hexanone	134.2	38.4
2,6-dimethyl-4-pentanone	144.1	94.5
2-octanone	164.5	127.6

Table 4.20. K_{NW} values for Group 1 tracers after exposure to residual permanganate.

Alcohol tracers	TCE K_{NW} values			PCE K_{NW} values		
	Water only	After 24 hrs $KMnO_4$ exposure	After 48 hrs $KMnO_4$ exposure	Water only	After 24 hrs $KMnO_4$ exposure	After 48 hrs $KMnO_4$ exposure
2-methyl-1-butanol (2M1B)	3.71	12.6	19.5	1.7	5.35	5.9
4-methyl-2-pentanol (4M2P)	10.3	8.73	11.4	4.77	8.02	8.35
2-ethyl-1-butanol (2E1B)	13.4	38.7	58.5	6.02	10.1	11.4
2,4-dimethyl-3-pentanol (2,4DM3P)	71.3	76.4	99.8	31.6	44.8	39.7
2-ethyl-1-hexanol (2E1H)	202	398	387	146	159	175

The PCE and TCE K_{NW} values for the five tracers studied increased in the presence of low permanganate concentrations. This effect can result in error in the PTT-estimated S_N and as a consequence may result in an underestimation of remediation effectiveness if not corrected. Studies indicate that residual concentrations of remedial agents (i.e., surfactants, cosolvents, complexing-agents) may remain in the ground water during a post-remediation PTT (e.g., Cho *et al.* 2000) and that aqueous remedial agent concentrations result in erroneous estimations of K_{NW} values and subsequent assessment of the success of the remedial effort.

To assess the impact of oxidant on tracer mass loss, batch studies were conducted to determine the amount of degradation that occurs as a function of permanganate and tracer concentration. The effects of 5, 50, and 500 mg/L $KMnO_4$ on the alcohol tracers were studied in 8 serial dilutions of the Group 1 primary alcohols. Example data are presented in Table 4.21, for 2-methyl-1-butanol, a low partitioning tracer, and 2-ethyl-1-hexanol, a high partitioning tracer, from oxidation studies conducted at 5.0 mg/L $KMnO_4$.

Table 4.21. Example data of tracer mass loss after exposure to 5.0 mg/L $KMnO_4$.

Dilution levels	2-methyl-1-butanol (2M1B)			2-ethyl-1-hexanol (2E1H)		
	Concentration in water (mg/L)		% Mass loss	Concentration in water (mg/L)		% Mass loss
	Initial	After 24 hrs of reaction		Initial	After 24 hrs of reaction	
1	12.7	11.5	9	7.2	6.8	6
2	27.5	25.6	7	16.6	15.5	7
3	51.7	53.8	8	32.0	30.0	6
4	86.1	79.0	8	54.0	49.0	9
5	158.1	142.5	10	102.3	91.6	10
6	333.9	280.8	16	214.3	181.2	15
7	565.8	399.3	30	355.0	251.7	29
8	635.9	272.5	57	383.5	165.5	57

Results indicate that the tracer concentrations decreased at potassium permanganate concentrations of 5, 50, and 500 mg/L, indicating an unfavorable reaction of the oxidant with the tracers. The results show that for samples with higher tracer concentrations, a greater mass loss occurred. The two tracers exhibit relatively similar %-mass losses with increasing tracer concentrations (e.g., less than 10% at lower concentrations and greater than 55% at the highest concentration).

Similar batch studies were conducted on tracer Groups 2 to 5 with exposure to 500 mg/L $KMnO_4$. Alcohols are organic compounds containing one or more hydroxyl functional groups attached to carbon atoms. These compounds have the general formula R-OH, where R stands for a saturated carbon chain with a hydroxyl group attached. Groups 1 and 2 consist of primary alcohol tracers that have been used previously in field applications, and only one carbon is bonded to the carbinol carbon. The carbinol carbon is the carbon atom to which the alcohol's hydroxyl group is bonded. Group 3 includes diol alcohols, which contain two hydroxyl groups, potentially making them chemically more resistant to oxidation. Group 4 includes tertiary alcohols which have three carbons bonded to the carbinol group. This potentially reduces the oxidants ability to react with the alcohol. Group 5 includes ketones, which are organic compounds that contain the carbonyl group (C=O). Preliminary results indicate a 58% mass loss of primary alcohol tracers, 30% mass loss for diol alcohols, a 20% mass loss for ketones, and 2% mass loss of tertiary alcohol tracers.

The outcome of oxidation reactions of alcohols depends on the physical chemistry of the groups present on the carbinol carbon. In a primary alcohol, one carbon is attached to the carbinol carbon; secondary alcohols have two carbons attached while tertiary alcohols have three. In order for each oxidation step to occur, there must be a hydrogen atom attached to the carbinol carbon. With primary and secondary alcohols, the oxidizing agent removes the hydrogen from the hydroxyl group, and another hydrogen atom from the carbon atom attached to the hydroxyl. Primary alcohols (e.g., 2-ethyl-1-hexanol) will tend to oxidize easily to form aldehydes or carboxylic acids. Secondary alcohols (e.g., 1,2-butanediol) are less reactive with a relatively slower oxidation process with the eventual formation of ketones. Tertiary alcohols (e.g., tert-butanol) resist oxidation with all known oxidizing agents except under forcing conditions such as elevated temperature. This is because there are no hydrogens bonded to the carbinol group for the oxidizing agent to remove. Since tertiary alcohols do not possess this particular hydrogen, it is reasonable to expect there will be little or no reaction except under forcing conditions.

A study conducted Bromley (2001) investigated the use of ketones as potentially oxidation resistant partitioning tracers for use in a post-remediation PTT after permanganate had been applied to a poly aromatic hydrocarbon (PAH) contaminated site. The study predicted that the double bond found in the carbonyl group could make ketones more resistant to oxidation than alcohols. Aliphatic ketones are usually liquid and are resistant to oxidation, but will oxidize under strongly oxidizing conditions. Molecular weight and the number of substitutions also influence a molecule's resistance to oxidation (Strassner and Busold 2001). The reasoning given in the study for using ketones as partitioning tracers was that molecules with the carbonyl group (i.e., ketones) rather than the hydroxyl group (i.e., alcohols) may potentially be more resistant to oxidation, but little was known how ketones might partition into NAPL phases. The study by Bromley (2001) provided the motivation to measure the ketone partitioning coefficients for DNAPLs PCE and TCE, as well as evaluate whether ketones were more resistant to oxidation in the presence of potassium permanganate.

For the batch studies investigating the influence of MnO_2 solids on the K_{NW} values, 4-wt% permanganate was allowed to react fully with a TCE or PCE DNAPL after which tracers were added and allowed to equilibrate. The goal of this experiment was to evaluate the effect of MnO_2 solids formation on the partitioning behavior of alcohol tracers in the presence of TCE and PCE. In order to have sufficient DNAPL for the tracers to partition into still remaining in the samples, only 1/12 and 1/20 of permanganate's total stoichiometric demand necessary to oxidize all the PCE and TCE DNAPL was used. The results of the batch tests to determine the impact of MnO_2 generation on Group 1 alcohol partitioning behavior are presented in Table 4.22.

Table 4.22. Batch tests of MnO_2 film formation impacts to K_{NW} values for Group 1 tracers.

Alcohol tracers	TCE K_{NW} values			PCE K_{NW} values		
	Water only	With MnO_2 film	Increase in TCE K_{NW}	Water only	With MnO_2 film	Increase in PCE K_{NW}
2-methyl-1-butanol (2M1B)	3.71	7.69	2.07x higher	1.47	5.92	4.02x higher
4-methyl-2-pentanol (4M2P)	10.3	17.5	1.69x higher	4.77	9.12	1.91x higher
2-ethyl-1-butanol (2E1B)	13.4	33.6	2.51x higher	6.74	11.0	1.63x higher
2,4-dimethyl-3-pentanol (2,4DM3P)	71.3	128	1.80x higher	31.6	47.5	1.50x higher
2-ethyl-1-hexanol (2E1H)	202	245	1.21x higher	146	164	1.12x higher

The batch test results indicated an increase in the TCE and PCE DNAPL partitioning coefficients for the Group 1 alcohol tracers investigated. The magnitude of the increase in K_{NW} values for the alcohols after MnO_2 film formation in an aqueous system with TCE or PCE DNAPL present ranged from about 1.1 to 4.0 times higher. This range of increases is not as large in magnitude as the increase observed from the studies of the impact of permanganate on the K_{NW} values. If this range of increases in K_{NW} was not accounted for during performance assessment using PTT, it would likely result in overestimation of the total amount of DNAPL mass present after remediation and therefore an underestimation of the effectiveness of remediation performance.

Table 4.23 provides the K_{NW} values in water for the six tertiary tracers investigated as well as the K_{NW} values for PCE after MnO_2 "film" formation. For all the tertiary tracers evaluated there is an increase in the K_{NW} value for PCE after oxidation and MnO_2 solids have formed. The magnitude of the increase observed for the Group 4 tracers (Table 4.23) is similar to that observed with the Group 1 tracers (Table 4.22).

Table 4.23. Batch tests of MnO_2 film formation impacts to K_{NW} values for Group 4 tracers.

Alcohol tracers	PCE K_{NW} values (in water alone)	PCE K_{NW} values (after all 4-wt.% $KMnO_4$ reacted)	Increase in PCE K_{NW}
Tert-butanol (TBA)	3.06	5.14	1.68x higher
2-methyl-2-butanol (2M2B)	3.74	4.16	1.11x higher
2-methyl-2-pentanol (2M2P)	6.82	13.26	1.94x higher
3-methyl-3-pentanol (3M3P)	6.95	14.41	2.07x higher
2-methyl-2-hexanol (2M2H)	11.7	33.58	2.87x higher
3-ethyl-3-pentanol (3M3P)	21.6	42.67	1.96x higher

4.6.2. Evaluation of Partitioning Tracer Methods for Remediation Performance Assessment Using a Flow-through System

This portion of the investigation was conducted to determine whether performance measured from the batch studies could be up-scaled to a 1-D or 2-D flow-through system. Comparison of DNAPL mass estimated from core extraction data can be compared to mass estimations from application of the PTT method to the cell to determine the viability of using PTT as a remediation performance indicator. These experiments were planned to follow the methods described in Section 3.7.2. This work is being completed as part of a doctoral dissertation, which is scheduled to be defended in December 2006. Data analysis was ongoing at the time of preparation of this final project report and no results were available for inclusion. A detailed description of methods employed and results obtained will be provided in the forthcoming dissertation (Dugan 2006) and subsequent publications.

4.7. SUMMARY OF MAJOR FINDINGS COMMON TO MULTIPLE RESEARCH ELEMENTS

A number of findings have evolved from the work conducted under SERDP CU-1290. Details for specific elements of the research may be found in the published M.S. theses and Ph.D. dissertations produced during the course of the project (Jackson 2004, Seitz 2004, Sahl 2005, Heiderscheidt 2005, Petri 2006, Dugan 2006). In this section, findings common to multiple experimental studies completed as part of this project are summarized.

4.7.1. Oxidant Type

Research conducted under this project focused on utilization of two oxidants for ISCO, catalyzed hydrogen peroxide and permanganate. CHP oxidation requires the catalytic breakdown of hydrogen peroxide into free radicals, which are then able to further catalyze radical generation, oxidize organic contaminants, or may be scavenged by the media or excess catalyst. Because of this free radical process, CHP has reactivity with a wide range of compounds and aquifer material surfaces. Permanganate achieves oxidation by direct electron transfer, and has reduced reactivity in the subsurface. The results of this study highlight the differences in performance between these two oxidants, which may largely be attributable to these different oxidation processes, and their interactions with the subsurface environment.

4.7.1.1. Catalyzed Hydrogen Peroxide. CHP was found to have very fast rates of reaction, and subsequently fast rates of oxidant decomposition. As such, the oxidant persistence as evaluated in these studies was poor. This was found to hold true in all systems of varying experimental scale that evaluated the use of CHP. In general, systems that provided effective contact of CHP with the contaminant appeared to be highly efficient with regard to contaminant destruction and oxidant use (i.e., RTE values in the VRs, MVRs and ZHRs). However, the effectiveness (rate and extent) of contaminant mass depletion of CHP was generally lower than in equivalent permanganate systems in every experimental series CHP was evaluated in (VRs, MVRs, ZHRs, diffusion cells, 2-D flow cells). The lower effectiveness of CHP is largely due to difficulties that arise in optimizing oxidant delivery and oxidant activation. Hydroxyl radicals are highly reactive, and in the subsurface, transport of radicals is negligible as they will readily react with dissolved species or particle surfaces. As such, in order for CHP remediation to be effective, free radical generation must occur in areas in close proximity to the targeted contaminant, requiring rapid oxidant delivery and activation within the contaminant source zones. Thus, CHP activation must occur in areas close to the DNAPL source. Based on the CHP stabilization studies, any system that added iron resulted in rapid activation of the oxidant. pH adjustment in concert with natural iron present in the media was also capable of activating oxidant. Systems performed well when activation occurred with direct contact with the contaminant, such as in the well mixed VR, MVR and ZHR systems. However, both advective and diffusive hydrogen peroxide transport are challenged by contact time with the porous media, resulting in poor oxidation effectiveness, as seen in the 2-D flow cell and diffusion cell experiments. In the MVR and 2-D flow cell experiments, rapid gas generation was also observed to

occur, which can cause reductions in hydraulic conductivity or mobilize volatile contaminants. The CHP stabilization and diffusion cell studies indicate that amending hydrogen peroxide with phosphate may improve hydrogen peroxide distribution in the subsurface. However, the phosphate ion may also interfere with oxidant activation resulting in reduced performance.

4.7.1.2. Permanganate. Permanganate, in contrast to CHP, was much more effective in reducing contaminant mass in the experimental systems evaluated. Due to the reduced reactivity of permanganate, significant advective and diffusive transport of oxidant is possible, as evidenced in all experimental transport studies, because permanganate will persist in the subsurface much longer than hydrogen peroxide. However, significant natural oxidant demand still occurs, as observed in both well-mixed batch tests and flow-through transport studies.

4.7.2. Oxidant Concentration and Subsurface Delivery

The applied oxidant concentration and method of delivery was found to impact oxidation efficiency and effectiveness in a number of systems as well.

4.7.2.1. Oxidant Type. For CHP systems, oxidation efficiency and effectiveness were observed to vary with oxidant concentration. In the aqueous contaminant phase VR systems and DNAPL-containing ZHR systems, efficiency and effectiveness increased with higher concentrations, with the exception that higher oxidant demand was observed at higher concentrations. However, in the DNAPL-containing MVR and 2-D flow cell systems, efficiency and effectiveness were improved at lower concentrations. The reasons for this apparent contradiction are not clear, but may be indicators of the sensitivity of CHP to environmental factors, particularly involving activation. The 2-D cell experimental studies demonstrated the most challenging performance of all of the CHP experimental systems. Regardless of activation method, the oxidant was found to readily decompose upon introduction to the media. With the high concentration system, the rate of decomposition increased with the oxidant concentration, but with no increase in remedial performance, indicating lower concentrations may perform better.

For permanganate systems, remediation effectiveness was improved in well mixed or diffusive transport systems (VRs, MVRs, ZHRs, diffusion cells) by using higher oxidant concentrations, which resulted in larger contaminant removals and faster rates of DNAPL destruction. Higher concentrations of permanganate also promoted diffusive transport of oxidant into low permeability media, and is more efficient from a site flushing perspective as fewer pore volumes may be required to destroy a given contaminant source.

However, a number of significant disadvantages to using high permanganate concentrations were also identified. In advective transport systems (FTRs, NOD model simulations), the role of oxidant concentration in remediation effectiveness interacted with velocity of the system. In low velocity systems, high oxidant concentrations were more effective in terms of contaminant removal, but were associated with adverse impacts, such as reduced hydraulic conductivity due to increased MnO_2 deposition in source zones as well as CO_2 gas generation resulting from pH changes related to DNAPL destruction. When velocity was increased, oxidant concentrations had less impact on rate and extent of contaminant destruction, indicating that moderate or low concentrations of oxidant could achieve remediation effectiveness that was similar to that observed at high oxidant concentrations. These systems were advantageous as they also resulted in less MnO_2 deposition within source zones and were less likely to result in CO_2 gas generation. High concentrations also increase the rate and amount of natural oxidant demand (NOD and ZHR studies). Based on the modeling studies, when low or moderate permanganate concentrations were utilized, the NOD and associated MnO_2 production were reduced. When high permanganate concentrations were used under identical conditions, the distribution of permanganate within porous media systems improved; however, MnO_2 deposition was more likely to cause pore clogging, and the increased NOD reduced the efficiency of oxidant use. Furthermore, low to moderate

oxidant concentrations may improve the performance of subsequent bioremediation using anaerobic reductive dechlorinating microbes, as high concentration may have been more toxic. Based on the 1-D anaerobic column experiments, lower concentrations appear to reduce the amount of time necessary for rebound of microbial activity after oxidation has ceased. The best balance for optimization of oxidant concentration ultimately depends on site specific conditions and remediation goals. An optimal moderate concentration of oxidant may be used, so that some of the benefits of high oxidant concentration systems are realized, but the negative impacts of high oxidant concentrations are minimized to achieve optimum performance.

4.7.2.2. Oxidant Solution Delivery Velocity. A common theme among the experiments that evaluated multiple velocities during oxidant delivery was that higher velocities led to more effective remediation performance, evidenced by increased DNAPL mass depletion, and frequently reduced adverse impacts. In the FTR experiments, increased permanganate delivery velocities had more of an effect on contaminant mass depletion rates than oxidant concentration did, indicating that for faster clean up times, higher velocity flushing should be considered. While the efficiency of permanganate was reduced at these high velocities, the reduced oxidant-contaminant contact time in the DNAPL source zone resulted in considerable oxidation reaction occurring outside of the source, resulting in MnO_2 solids being distributed over a wider volume, potentially reducing pore clogging. Also, higher velocity systems may have reduced other potentially adverse impacts such as gas generation in permanganate systems, which appeared to be reduced in faster systems. Based on modeling studies of oxidant transport, higher velocities also improve oxidant distribution, which may also improve the distribution of MnO_2 solids. Higher velocities reduce contact time with the porous media, allowing for better oxidant distribution before oxidant is nonproductively depleted by natural oxidant demand, particularly in porous media with a high NOD. Higher velocity permanganate delivery was also observed to improve performance when coupling permanganate remediation with anaerobic bioremediation. Based on the 1-D anaerobic column experiments, higher velocities shortened the contact time between the oxidant and the KB-1 mixed culture, and this may have reduced the amount of time needed for reductive dechlorination activity to rebound after oxidation. This could be due to reduced microbe toxicity due to the shorter period of exposure.

For CHP systems, higher velocity injection also improved performance, based on results from 2-D flow cells. As mentioned earlier, CHP is an efficient oxidant when it is activated and contacts the contaminant. Thus higher delivery velocities will achieve deeper penetration of the oxidant into porous media surrounding injection points, prior to oxidant decomposition.

4.7.3. Subsurface Environmental Characteristics

4.7.3.1. Natural Oxidant Demand. Natural oxidant demand increased with increasing complexity of porous media, such as with more reduced mineral content, NOM, or clay / silt particle fractions, increasing oxidant concentration, and increased contact time. Based on observations from NOD studies, as well as modeling of experimental data with CORT3D, at least two distinct NOD fractions are observed to impact permanganate transport. A fast kinetic rate fraction acts as a nearly instantaneous sink of oxidant, and a slow kinetic rate fraction that gradually consumes oxidant over time. Permanganate NOD challenges both advective and diffusive oxidant transport, both by retarding the initial permanganate front due to depletion of the initial fast NOD, and also acting as a slow oxidant sink over time from the slow NOD component. However, characterization of NOD in a way that allows for prediction of permanganate transport in the subsurface is difficult. This is due to the fact that conditions used during NOD testing frequently do not mirror oxidant transport in the subsurface (i.e., well mixed batch reactors vs. well to well flushing of porous media). Well mixed batch reactors typically provide an estimate of the ultimate NOD of the media, as every grain surface is inevitably exposed to oxidant. However, in flushing of porous media, contact areas and dead end pores can reduce the amount of porous media exposed to oxidant, and thus field measured NOD values are almost always lower than lab measured NOD.

4.7.3.2. DNAPL Source Zone Characteristics. TCE was found to be depleted and destroyed faster than PCE in every experimental system that evaluated both DNAPL types (VRs, MVRs, ZHRs, diffusion cells and FTRs). This is due to the order of magnitude higher solubility limit for TCE versus PCE, as well the faster kinetic rate of reaction between TCE over PCE in permanganate systems. However, the solubility limit can have secondary impacts on system performance. Based on the FTR experiments, TCE was more likely to result in CO_2 gas generation from permanganate ISCO than PCE. This is largely due to the fact that the higher contaminant concentrations in TCE systems result in more concentrated proton generation, as well as higher concentrations of aqueous CO_2. The resulting pH change, if the system is not adequately buffered, can result in off-gassing, which may mobilize DNAPL or vapor phase contaminant, as well as reduce hydraulic conductivity. However, such effects may be compound-specific. Permanganate oxidation of *cis*-DCE generates alkalinity instead of acidity, and would be less likely to observe this problem, despite the higher solubility limit of *cis*-DCE.

Important observations were made with respect to the impact of DNAPL source morphology. DNAPL present in the subsurface as residual ganglia are highly amenable to depletion and destruction by permanganate flushing. However, when pooled DNAPL was present, oxidation effectiveness was more variable. Residuals are depleted much faster than pools due to their high surface area to volume ratio. Mass transfer was observed to be enhanced from residuals by permanganate oxidation by bulk aqueous phase contaminant oxidation, as well as possibly other impacts to mass transfer processes, based on FTR and CORT3D modeling study results. If a system contained both residual and pooled DNAPL, then after residuals were depleted, contaminant mass flux declined to a slower rate, indicating that pool mass flux was being reduced. This is likely due to the deposition of MnO_2 solids around pool interfaces, causing flow bypassing of the DNAPL, and reducing mass transfer. MnO_2 solids were not observed to hinder mass transfer from residual DNAPL sources under the conditions of these studies. This is in part because residuals were likely to be depleted before significant MnO_2 deposition could reduce permeability. However, when more heterogeneous and complex sources were investigated, the effect of MnO_2 was more variable. Oxidation in the 2-D intermediate- and 2-D large-scale tanks resulted in some systems demonstrating higher contaminant mass fluxes than prior to oxidation. This may be due to MnO_2 deposition in more heterogeneous flow fields and sources, causing flow to increase locally, sometimes near pool surfaces, and resulting in higher concentrations. MnO_2 deposition was not observed to impact diffusive transport of oxidant into low permeability media.

4.7.3.3. Organic and Mineral Composition. The role of natural organic matter present in porous media was found to complicate ISCO efficiency and effectiveness in several ways. In this series of experimental studies, humic acid was used as a surrogate for NOM to provide experimental control. In the aqueous phase contaminant VR systems, the addition of humic acid resulted in reduced oxidation efficiency and effectiveness for both permanganate and CHP. However, when DNAPL phase contaminant was present, as in the MVR and ZHR systems, the addition of humic acid had an opposite effect, causing increased effectiveness in terms of the percent DNAPL destroyed, using either oxidant. This indicates that the presence of NOM in the subsurface may impact DNAPL mass transfer via enhanced sorption and desorption. When no reaction is present in a subsurface system with DNAPL contaminant, sorption of contaminant to media has a retarding effect on contaminant transport. However, when an oxidation reaction is present, it is possible that mass transfer could be impacted by sorption. Sorption of contaminant to the media reduces bulk aqueous phase concentrations, which allows for increased DNAPL dissolution. Then oxidation of sorbed contaminant may vacate contaminant sorption sites, allowing for additional sorption. It is also possible that the oxidants reacted with the humic acid, altering and possibly creating additional sorption sites. Although it is unknown how the humic acid utilized in this study compares to NOM that is encountered in field soils, the results of this study indicate that the role of NOM in porous media during ISCO has a more complex effect on remediation performance than simply increasing natural oxidant demand (NOD).

Several interesting observations were made in experiments evaluating the presence of goethite in an oxidation system. Goethite was used as a surrogate for natural iron-bearing minerals, which may be present in porous media systems. Geothite was expected to have the most impact to CHP oxidation as iron is used as catalyst for hydroxyl radical production. The MVR experiments reflect this effect. CHP oxidation effectiveness improved with greater rate and extent of contaminant destruction, but with reduced efficiency. However, impacts were also noted in the permanganate systems as well. The MVR experiments found that effectiveness of contaminant destruction increased with permanganate and goethite present, but again at reduced efficiency. The ZHR experiments found that permanganate in the presence of goethite improved effectiveness for oxidation of PCE, but not for TCE. The reasons for the apparently increased effectiveness of permanganate remediation when goethite is present are not known, but more research into the role of mineralogy in permanganate system performance is merited.

4.7.4. Coupling ISCO with Other Remediation Methods

Coupling ISCO with other remediation technologies may be advantageous as site remediation goals may not be attainable using one technology application alone.

4.7.4.1. Coupling ISCO with Bioremediation. One low cost remediation method that has been applied to contaminants such as TCE and PCE is anaerobic reductive dechlorination, which can use PCE as an electron acceptor. However, several considerations need to be made for how ISCO may impact such a remediation approach, whether it has been applied before or after oxidant application. In general, CHP oxidation is disruptive to anaerobic microbes due to oxygenation of the subsurface environment. Based on batch microcosm studies, there is evidence that oxidation of porous media by CHP will generate higher concentrations of dissolved organic carbon, which could provide a substrate for anaerobic microbes growing in down-gradient areas where conditions remain anaerobic. However, it was inconclusive if this had any effect on remediation effectiveness.

Permanganate oxidation appears to be more amenable to coupling with anaerobic reductive dechlorination processes. However, permanganate systems have to consider interactions with the microbes to identify operational requirements. For the anaerobic mixed culture KB-1, reductive dechlorination behavior ceased after oxidant flushing began, but rebounded after oxidation under every set of conditions tested in 1-D column experiments. However, the amount of time until activity rebound varied between systems, and appeared to depend on the total time and concentration of permanganate to which the microbes were exposed. Higher concentrations and longer exposures required more time for activity rebound, possibly due to increased toxicity under these conditions. Thus, higher velocities and lower oxidant concentrations were more favorable for coupling of permanganate flushing with anaerobic reductive dechlorination, as these reduce contact time and oxidant exposure. Potential beneficial effects of permanganate ISCO were also investigated through 1-D column experiments and batch microcosms. When permanganate reacts with NOM in soil, low molecular weight organic compounds may be liberated as DOC. This DOC may represent a growth substrate that microbes located down-gradient of permanganate oxidation zones may utilize to enhance their contaminant degradation rates. Thus, simultaneous application of ISCO and bioremediation may be possible, with permanganate flushing of DNAPL source zones to reduce source mass, and reductive dechlorination in down-gradient plume zones. Another potential benefit of anaerobic bioremediation is that manganese reducing bacteria may reduce or eliminate MnO_2 after permanganate application. This was observed in the 1-D column experiments, and is potentially beneficial as MnO_2 deposition may cause pore clogging within source zones, reducing oxidant delivery and leaving DNAPL pools behind. Alternating applications of permanganate and anaerobic bioremediation with manganese reduction could potentially achieve complete source removal over time, which may be advantageous at sites where large source masses and complex heterogeneity preclude the ability to achieve complete mass removal with one technology alone.

4.7.4.2. Coupling ISCO with Surfactant / Cosolvent Flushing. The ability to couple ISCO with surfactant enhanced aquifer restoration (SEAR) methods is appealing. Combining ISCO with SEAR in a combined injection or sequential injection scheme were both investigated, initially through compatibility tests with two different concentrations of both permanganate and CHP, as well as different concentrations of a wide range of surfactants and cosolvents. While the final results of this work are pending final analysis and publication of a Ph.D. dissertation (Dugan 2006), the preliminary findings reveal that a more robust coupling is more likely using permanganate ISCO combined with a carefully selected anionic surfactant system. Coupling of CHP is more constrained in that only low concentrations of hydrogen peroxide can be used with some surfactants since higher concentrations tend to react with the surfactant system causing substantial gas and foam generation. The results of this research do point out that use of ISCO with SEAR should only be done with due consideration of the compatibility of the oxidant type and concentration with the surfactant system used (or planned for use).

4.7.4.3. Compatibility of ISCO with PTT Methods. The research concerning the viability of applying PTT methods to assess the performance of ISCO applied to DNAPL sites was not fully completed at the time this final report was prepared. Preliminary findings indicate that certain PTT tracers are compatible with oxidants but that the partitioning properties of the tracers may change as a result of the oxidant-DNAPL interactions (e.g., MnO_2 film formation during permanganate ISCO).

4.8. PRACTICAL IMPLICATIONS

Practical implications and guidance have been derived based on the research completed during the course of SERDP project CU-1290. Given below are some general implications and guidance insights for application of ISCO to DNAPL sites followed by some site-specific observations.

4.8.1. General Implications

Oxidant selection is a major factor in remediation design as the two oxidants evaluated as part of this study (potassium permanganate versus catalyzed hydrogen peroxide) have differing performance in different kinds of subsurface environments, contaminant types and distributions. The application of catalyzed hydrogen peroxide appears to be favorable when rapid introduction and activation of the oxidant can be achieved directly in the targeted contaminant source zone. This is most effectively accomplished with either a direct push injection probe or possibly with deep soil mixing equipment. With probe injections, hydrogen peroxide as well as any activation aids must be delivered rapidly under pressure to achieve oxidant distribution in as large a radius of influence as possible before the oxidant decomposes. This tends to mirror the current standard of practice for CHP application in the industry. However, success or failure of this approach depends on site specific conditions. Decomposition rates may be media- and contaminant-specific, as natural organic matter, iron, and other mineralogical content in porous media have the potential to impact oxidant decomposition. Rapid oxidant decomposition can reduce the injection point radius of influence while improved oxidant stability can increase the radius of influence. Thus the distance between injection points will be site-specific depending on this radius, but generally spacing needs to be close (typically several feet) to apply the necessary oxidant coverage. CHP oxidation does not appear to be viable for diffusive transport into low permeability media (LPM). Thus if contaminant is present in LPM lenses, CHP is unlikely to persist long enough in the subsurface to diffuse into and destroy contaminant in such lenses. Therefore, CHP performance will be challenged at sites with a large degree of heterogeneity or when contaminated LPM lenses are targeted for remediation. This is due to the difficulty of effectively providing contact of the contaminant with the activated oxidant, as delivery may only occur through direct advection, and heterogeneous sites will not have uniform oxidant injection profiles. Deep soil mixing may improve the application of CHP to heterogeneous sites. Sites requiring minimal surface activity disruption will also be challenging for CHP application due the numerous oxidant introduction points. One definite advantage of CHP is that if successful delivery of

activated oxidant to the contaminant is achieved, contaminant destruction is rapid, and the time required for oxidant application may be minimized.

With permanganate, due to its increased persistence in the subsurface, more delivery methods are available, and thus permanganate is a more flexible oxidant for application to sites of varied characteristics. Delivery methods that have been used for permanganate include push probe injection, well to well flushing, fracture emplaced permanganate solids, soil mixing and treatment walls. However, permanganate reacts with fewer contaminants of concern than CHP, reducing its applicability to sites with contaminants that permanganate can target. These are most commonly chloroethenes present either as aqueous and sorbed phase contamination, or DNAPL. Current common practices for oxidant application to DNAPL sites involve injection of high concentrations of permanganate (10000 - 60000 mg/L $KMnO_4$, or up to 40% $NaMnO_4$) via probe injections or well to well flushing, typically using as few pore volumes of injection fluid as possible. After the initial oxidant application, there are typically repeat applications to contamination "hot spots" until concentrations are tamped down across the entire remediation site. However, problems have arisen from this approach. Sites with a large NOD or high masses of DNAPL have suffered from permeability reductions, usually attributed to MnO_2 deposition, but occasionally to CO_2 generation as well. The result may be excessive backpressures at injection points. Also, occasional overdosing of oxidant has been observed, resulting in persistent concentrations of permanganate in groundwater that must be remediated with a reducing agent. Other concerns that may arise from typical practices are the timeframe of active remediation and repeat oxidant applications as this increases cost and may hold up property title transfers or other similar site owner activities.

Based on the results from these studies, remediation effectiveness or efficiency may be bolstered by several possible new approaches. With applications of permanganate, deposition of MnO_2 has been attributed to pore clogging in close vicinity to DNAPL dissolution interfaces, reducing mass transfer and resulting in incomplete removal of the DNAPL. Furthermore, high NOD may challenge oxidant delivery, and slow groundwater velocities result in low rates of mass depletion from DNAPL sites. One common theme identified throughout the project, but particularly from the FTR studies and the CORT3D natural oxidant demand simulations, was that higher permanganate delivery velocities coupled simultaneously with lower permanganate concentrations (i.e., 100 - 5000 mg/L $KMnO_4$) appears to be promising for increased DNAPL source remediation effectiveness, as well as reduced delivery challenges arising from NOD. An effective way to achieve this may be with a well to well flushing system, especially if a 5-spot recirculation system is used. The velocity profile of the 5-spot pattern may result in the most efficient way of increasing velocity in the subsurface, and oxidant waste is minimized as extracted water with excess oxidant is reinjected. Increased velocities result in faster rates of DNAPL mass depletion, and the reduced permanganate concentrations may allow for formation of "reaction clouds" within and down-gradient of DNAPL sources, dispersing MnO_2 over wider spatial volumes, and thus reducing negative impacts to permeability. The NOD is reduced by the lower oxidant concentrations and decreased contact time, minimizing nonproductive oxidant use. Also, at lower concentrations, oxidant overdosing is less likely to occur. In heterogeneous formations, this approach may still be viable as reductions in permeability from MnO_2 over time in high permeability layers may eventually route more flow through lower permeability layers.

Increasing research has also focused on dissolved and sorbed phase contamination entrapped in low permeability media (LPM) formations or lenses, which may remain after DNAPL has been depleted. This contaminant may then back diffuse out of the low permeability layers resulting in contamination that may exceed remedial action levels. Oxidant application methods that have been used for such sites may be fracture emplacement of permanganate solids, or probe injection. Targeted probe injection may result in direct application of oxidant into a LPM lens. However, to achieve complete contaminant removal in such a site, diffusive oxidant transport would likely be relied upon to contact all contaminated media. Based on results from the diffusion cell studies, diffusive transport of permanganate is viable, but depends on site specific conditions. If the low permeability media has a low NOD, diffusive transport may be

rapid through the LPM. However, if significant NOD is present, reaction with NOD may control the rate of permanganate diffusion, even if the diffusive properties of the media are favorable. One possible delivery method that may increase rates of diffusion into LPM is utilization of high concentrations of oxidant, and injection of oxidant directly above LPM layers. The high concentration results in a stronger concentration gradient promoting diffusion, and due to the increased density of the permanganate solution, a density driven advection effect may speed diffusion into the LPM.

4.8.2. Site Specific Implications

The implications of the research described herein can provide insights concerning the application of ISCO to a specific site. A summary of key implications is given in Table 4.24.

Table 4.24. Summary of key implications for different aspects of ISCO application.

Activity	Considerations to help achieve successful application of ISCO at a specific site
Site characterization	The comprehensive and integrated results of these studies suggest that the following parameters are key factors in ISCO system design and are thus critical to site characterization efforts if ISCO is to be considered for DNAPL treatment: • Aquifer matrix characteristics (i.e., porous media and groundwater) o Contaminant type and presence of co-contaminants o Organic carbon content (both nature and extent) o Key mineral components (e.g., iron and manganese-based minerals, carbonate based minerals) o Groundwater ionic content (e.g., key components iron, manganese, oxidizable metals, radical scavengers) o Acidity / alkalinity o pH / temperature • Site hydrogeology o Hydraulic conductivity / porosity o Hydraulic gradient / groundwater velocity profile o Site heterogeneity o DNAPL source zone architecture (pools of contaminant vs. residual distribution) • Additional key site characteristics o Pre-oxidation microbial activity o Presence of naturally-occurring metals that may be mobilized upon ISCO application
Technology screening	The following factors must be considered when evaluating ISCO compared to other technologies, in considering oxidant type, and in considering oxidant delivery feasibility and options: • Amenability of contaminant to oxidation via permanganate and/or CHP • Ability to inject and deliver oxidant to the subsurface o CHP ▪ Injection can occur in close proximity to contaminant source ▪ Injection points can be spaced closely ▪ Subsurface formation allows for rapid oxidant delivery and activation o Permanganate ▪ Appropriate design can be achieved for site-specific characteristics (e.g., a diffusion-based system can be implemented for a tight formation; a circulation system can be implemented where above-ground characteristic may impede direct delivery to source zone)

Table 4.24 (cont.). Summary of key implications for different aspects of ISCO application.

Activity	Considerations to help achieve successful application of ISCO at a specific site
Treatability testing	Laboratory bench-scale treatability testing must be conducted to not only evaluate the amenability of the contaminant for destruction by oxidant(s), but to also determine specific parameters that aid in design of full-scale ISCO application systems. • Permanganate NOD o Bench-scale tests should reflect potential field application approaches ▪ Varied concentrations – to find balance between oxidation rate and contaminant dissolution rate ▪ Greater mixing and longer contact time for diffusive transport ▪ Less mixing and shorter contact time for faster advective transport ▪ Determination of extent *and* rate of NOD o Determine optimum oxidant loading based on contaminant dissolution and destruction kinetics o Determine optimum oxidant loading to minimize NOD while achieving complete contaminant destruction • CHP stability o Compare rate of contaminant destruction to rate of oxidant depletion in presence of site porous media and groundwater o Compare contaminant destruction and oxidant stability for varied activation and stabilization approaches • Secondary effects o Observations of MnO_2 formation/accumulation for permanganate o Mobilization of metals and/or co-contaminants o Gas generation o pH changes
Modeling	Appropriate modeling tools allow for the anticipation of the effects of varied design parameters on potential ISCO performance, as well as potential secondary effects of ISCO application. Modeling tools can allow for aid in system design when appropriate ISCO-specific factors are considered as highlighted below: • Design support o Evaluate influence of varied oxidant concentrations and delivery rate on oxidant distribution, contaminant destruction, and secondary effects o Evaluate influence of varied design approaches on oxidant distribution and contaminant destruction efficiency and effectiveness (e.g., multiple injection points vs. circulation delivery) o Evaluate potential ISCO effectiveness for varied DNAPL mass distributions • Key parameters – with respect to space and time o Advection, dispersion, diffusion o Contaminant dissolution characteristics o Contaminant sorption/desorption o Rate of reaction of oxidant and contaminant o Rate of reaction of oxidant and NOD (fast initial and slow later rates) o Porosity effects ▪ Increased porosity due to DNAPL dissolution/destruction ▪ MnO_2 generation and pore filling (when using permanganate)

Table 4.24 (cont.). Summary of key implications for different aspects of ISCO application.

Activity	Considerations to help achieve successful application of ISCO at a specific site

Field-scale implementation	Field-scale implementation of ISCO first involves conducting the appropriate treatability tests and applying relevant design tools. From these results an oxidant delivery approach can be selected and implemented, as generally highlighted below. Appropriate monitoring must occur during ISCO to allow for system optimization to further enhance treatment efficiency and effectiveness.
	• Delivery approaches
	  o Permanganate
	  ▪ Low oxidant concentration, rapid delivery rate – appropriate for:
	  • High NOD systems
	  • Permeable formations
	  • Rapid contaminant dissolution
	  • Rapid contaminant destruction kinetics
	  • Residual DNAPL contamination
	  • DNAPL pool configuration
	  ▪ High oxidant concentration, rapid delivery rate – appropriate for:
	  • Low NOD systems
	  • Permeable formations
	  • Rapid contaminant dissolution
	  • Rapid contaminant destruction kinetics
	  • Residual DNAPL contamination
	  ▪ Low oxidant concentration, slower delivery rate – appropriate for:
	  • Moderately permeable formations
	  • Low to moderate NOD systems
	  • Slower contaminant dissolution
	  • Slower contaminant destruction kinetics
	  • Higher efficiency of oxidant use
	  ▪ High oxidant concentration, slower delivery rate – appropriate for:
	  • Low permeability media/diffusive transport
	  • Low NOD systems
	  • Slower contaminant dissolution
	  • Slower contaminant destruction kinetics
	  • Smaller flushing volume
	  o Catalyzed hydrogen peroxide
	  ▪ Multi-point injection, low to moderate concentration
	  • Permeable formations
	  • Rapid contaminant dissolution
	  • Contaminant destruction kinetics exceed oxidant depletion kinetics
	  • Low concentration of radical scavengers
	• Site monitoring
	  o Oxidant distribution and concentrations
	  o Contaminant concentrations
	  o Co-contaminant concentrations
	  o Key metals that may be mobilized (based on site characterization information)
	  o Subsurface pressure distribution (indicative of MnO_2 deposition and possibility of resulting pore-filling, flow bypass, and/or excessive system backpressure)
	  o Groundwater quality – pH, alkalinity/acidity, ORP
	• Optimization
	  o Adapt system design real-time in response to site monitoring information
	  o Optimize delivery concentration, volume and delivery rate based on remediation goals (e.g., time, cost, treatment effectiveness).

Table 4.24 (cont.). Summary of key implications for different aspects of ISCO application.

Activity	Considerations to help achieve successful application of ISCO at a specific site
Coupling ISCO	Results of ISCO coupling experimentation indicate several key factors, which must be considered where coupling ISCO with bioprocesses and/or surfactant cosolvent flushing might be advantageous. • Coupling ISCO - advantageous o Highly heterogeneous site o Heavy contamination with DNAPL pools and residual architectures o Cost-benefit analysis indicates economic viability and advantages • Key factors for coupling ISCO and bioprocesses o Presence of bio-recalcitrant co-contaminants where bioremediation/natural attenuation are otherwise viable approaches o Low permeability sites with some areas of higher permeability o Lower concentrations of oxidant delivered to minimize subsurface contact time can provide more rapid microbial activity rebound o High NOD sites may benefit from focused ISCO application to high contaminant density areas – resultant dissolved organic carbon can be favorable for co-treatment of less contaminated areas via bioprocesses • Key factors for coupling surfactant/cosolvent flushing and ISCO o Highly permeable sites with limited areas of low permeability o Compatibility of oxidant and surfactant/cosolvent o MnO_2 generation and deposition with permanganate

4.9. REFERENCES

Adamson, D.T., McDade, J.M., and Hughes, J.B. (2003). Inoculation of a DNAPL Source Zone to Initiate Reductive Dechlorination of PCE. *Environmental Science and Technology*, 37:2525-2533.

Bromley, S.M. (2001). Ketones as Partitioning Tracers: Laboratory Experiments and Quantitative Modeling. Eberhard-Karls Universität, Tübingen, Germany.

Crimi, M.L., and Siegrist, R.L. (2004). Experimental Evaluation of In Situ Chemical Oxidation Activities at the Naval Training Center (NTC) Site, Orlando, Florida. Final project report submitted to the Navy by the Colorado School of Mines, Golden, CO.

Crimi, M.L., and Siegrist, R.L. (2005). Factors Affecting Effectiveness and Efficiency of DNAPL Destruction Using Potassium Permanganate and Catalyzed Hydrogen Peroxide." *Journal of Environmental Engineering*, 131(12):1724-1732.

Cussler, E.L. (1997). Diffusion: Mass Transfer in Fluid Systems. Cambridge University Press, Cambridge, UK.

Gates, D.D., and Siegrist, R.L. (1995). In-Situ Chemical Oxidation of Trichloroethylene Using Hydrogen Peroxide. *Journal of Environmental Engineering*, 121(9):639-644.

Goldstone, J.V., Pullin, M.J., Bertilsson, S., and Voelker, B.M. (2002). Reactions of Hydroxyl Radical with Humic Substances: Bleaching, Mineralization, and Production of Bioavailable Carbon Substrates. *Environmental Science and Technology*, 36:364-372.

Heiderscheidt, J.L. (2005). DNAPL Source Zone Depletion During In Situ Chemical Oxidation (ISCO): Experimental and Modeling Studies. Ph.D. dissertation, Colorado School of Mines, Golden, CO.

Imhoff, P.T., Jaffé, P.R., and Pinder, G.F. (1993). An Experimental Study of Complete Dissolution of a Nonaqueous Phase Liquid in Saturated Porous Media. *Water Resources Research*, 30(2):307-320.

Isalou, M., and Sleep, B.E. (1998). Biodegradation of High Concentrations of Tetrachloroethene in a Continuous Flow Column System. *Environmental Science and Technology*, 32:3579.

Jackson, S.F. (2004). Comparative Evaluation of Potassium Permanganate and Catalyzed Hydrogen Peroxide During In Situ Chemical Oxidation of DNAPLs. M.S. thesis, Colorado School of Mines, Golden, CO.

Kastner, J.R., Santo Domingo, J., Denham, M., Molina, M., and Brigmon, R. (2000). Effect of Chemical Oxidation on Subsurface Microbiology and Trichloroethene Biodegradation. *Bioremediation Journal*, 4(3):219-236.

MacKinnon, L.K., and Thomson, N.R. (2002). Laboratory-Scale In Situ Chemical Oxidation of a Perchloroethylene Pool using Permanganate. *Journal of Contaminant Hydrology*, 56(1-2):49.

Maymo-Gatell, X., Anguish, T., and Zinder, S.H. (1999). Reductive Dechlorination of Chlorinated Ethenes and 1,2-Dichloroethane by *Dehalococcoides Ethenogenese* 195. *Appl. Environ. Microbiol.*, 65(7):3108-3113.

Miller, C.T., Poirier-McNeill, M.M., and Mayer, A.S. (1990). Dissolution of Trapped Nonaqueous Phase Liquids: Mass Transfer Characteristics." *Water Resources Research*, 26(11):2783-2796.

Petri, B.G. (2006). Impacts of Subsurface Permanganate Delivery Parameters on Dense Nonaqueous Phase Liquid Mass Depletion Rates. M.S. thesis, Colorado School of Mines, Golden, CO.

Powers, S.E., Abriola, L.M., and Weber, W.J., Jr. (1994). An Experimental Investigation of Nonaqueous Phase Liquid Dissolution in Saturated Subsurface Systems: Transient Mass Transfer Rates. *Journal of Contaminant Hydrology*, 30(2):321-332.

Sahl, J. (2005). Coupling In Situ Chemical Oxidation (ISCO) with Bioremediation Processes in the Treatment of Dense Non-Aqueous Phase Liquids (DNAPLs). M.S. thesis, Colorado School of Mines, Golden, CO.

Sahl, J., and J. Munakata-Marr (2006). The Effects of In Situ Chemical Oxidation on Microbial Processes: A Review. *Remediation Journal*, 16(3):57-70.

Sahl, J., J. Munakata-Marr, M.L. Crimi, and R.L. Siegrist (2006). Coupling Permanganate Oxidation with Microbial Dechlorination of Tetrachoroethene. *Water Environment Research*, in press.

Schnarr, M., Truax, C., Farquhar, G., Hood, E., Gonullu, T., and Stickney, B. (1998). Laboratory and Controlled Field Experiments Using Potassium Permanganate to Remediate Trichloroethylene and Perchloroethylene DNAPLs in Porous Media. *Journal of Contaminant Hydrology*, 29(3):205.

Schroth, M.H., Oostrom, M., Wietsma, T.W., and Istok, J.D. (2001). In-Situ Oxidation of Trichloroethene by Permanganate: Effects on Porous Medium Hydraulic Properties. *Journal of Contaminant Hydrology*, 50(1-2):79.

Seitz, S.J. (2004). Experimental Evaluation of Mass Transfer and Matrix Interactions During In Situ Chemical Oxidation Relying on Diffusive Transport. M.S. thesis, Colorado School of Mines, Golden, CO.

Siegrist, R.L., Crimi, M.L., Illangasekare, T.H., and Munakata-Marr, J. (2003). SERDP Annual Report: Reaction and Transport Processes Controlling In Situ Chemical Oxidation of DNAPLs. Colorado School of Mines, Golden, CO.

Siegrist, R.L., Urynowicz, M. A., Crimi, M. L., and Lowe, K. S. (2002). Genesis and Effects of Particles Produced During In Situ Chemical Oxidation Using Permanganate. *Journal of Environmental Engineering*, 128(11):1068-1079.

Siegrist, R.L., Urynowicz, M.A., West, O.R., Crimi, M.L., and Lowe, K.S. (2001). Principles and Practices of In Situ Chemical Oxidation Using Permanganate, Battelle Press, Columbus, Ohio.

Strassner, T., and Busold, M. (2001). A Density Functional Theory Study on the Mechanism of the Permanganate Oxidation of Substituted Alkenes. *Journal of Organic Chemistry*, 66(3):672-676.

Struse, A. M. (1999). Mass Transport of Potassium Permanganate in Low Permeability Media and Matrix Interactions. M.S. thesis, Colorado School of Mines, Golden, CO.

Tchobanoglous, G., and Schroeder, E.D. (1987). Water Quality, Addison-Wesley Publishing, Menlo Park, CA.

Urynowicz, M. A. (2000). Dense Nonaqueous Phase Trichloroethene Degradation with Permanganate Ion. Ph.D. dissertation, Colorado School of Mines, Golden, CO.
Wyllie, M.R.J. (1962). Relative Permeability. In: Petroleum Production Handbook, Reservoir Engineering. T. C. Frick, ed., McGraw-Hill, New York, NY.
Yang, Y., and McCarty, P.L. (2000). Biologically Enhanced Dissolution of Tetrachloroethene DNAPL. *Environmental Science and Technology*, 34:2979-2984.

CHAPTER 5

SUMMARY, CONCLUSIONS, AND RECOMMENDATIONS

This project encompassed an extensive array of experimental work and modeling efforts to enhance the understanding of the pore/interfacial scale DNAPL reactions and porous media transport processes that govern the delivery of oxidant to a DNAPL-water interface and the degradation of the DNAPL present in the subsurface at a contaminated site. Numerous conclusions have been reached based on the findings of the research. Specific conclusions are presented in the M.S. theses and Ph.D. dissertations completed during the course of this project (Jackson 2004, Seitz 2004, Sahl 2005, Heiderscheidt 2005, Petri 2006, Dugan 2006) while a summary is provided below.

5.1. SUMMARY AND CONCLUSIONS

In summary, for application of potassium permanganate or catalyzed hydrogen peroxide for remediation of PCE or TCE DNAPL contamination, quantitative understanding has been improved and mathematical expressions and a numerical model have been developed and/or tested in this research, the scope of which has included:

- Bench-scale studies involving aqueous phase vial reactors were used to determine how dissolved phase reaction kinetics for PCE and TCE are affected by the composition of the bulk aqueous phase (i.e., oxidant type and concentration and NOM, mineralogy, pH,). Additional studies conducted in multiphase vial reactors investigated the impact of ISCO on TCE and PCE DNAPL mass transfer rates as a function of aqueous phase compositions. A series of response variables, described in Section 3.2.5, were developed to evaluate the efficiency and effectiveness of ISCO under the varied phase compositions investigated.
- Bench-scale studies involving slurry reactors and 1-D diffusion cells were used to determine the effects of porous media of varying properties on oxidant transport and degradation of DNAPLs. These were conducted under contrasting transport regimes of either completely mixed systems or static, diffusion-controlled systems. Zero-headspace reactors were utilized to investigate the impact of differing conditions (e.g., PCE vs. TCE at different mass levels, presence and composition of NOM, oxidant type and loading) on the efficiency and effectiveness of ISCO within well-mixed soil slurry systems. Steady-state diffusion tests were performed to determine the viability of diffusive transport of oxidants for contaminant destruction in low permeability media. Impacts to porous media properties due to of oxidation were also determined. As part of these studies, it was necessary to evaluate the oxidant persistence in porous media (i.e., NOD or oxidant decomposition) and determine if CHP could be readily stabilized to promote subsurface transport.
- Bench and intermediate-scale flow-through studies were used to evaluate the reaction and transport processes that occur at the pilot-scale, including the effects of ISCO systems of varied designs on different DNAPL mass and entrapment architectures. Bench scale 1-D flow-through tube reactor studies were utilized to investigate the impact of varied oxidant delivery velocities and concentrations on DNAPL mass depletion rates and efficiencies in systems with varied DNAPL types and entrapment architectures. Further experimentation was conducted in 2-D flow cells, which investigated varied oxidant types and delivery techniques on an experimental system with a more complex source architecture and flow field.

- Several intermediate-scale and large-scale 2-D tank systems were used to investigate complex DNAPL entrapment architectures and complex heterogeneous flow fields to determine impacts to DNAPL mass depletion and mass flux resultant of ISCO using permanganate, including the potential reduction in permeability due to manganese dioxide deposition. These experiments enabled the testing of a new model, which was developed as part of this project, as well as in cooperation with SERDP project CU-1294: Mass Transfer from Entrapped DNAPL Sources Undergoing Remediation: Characterization Methods and Prediction Tools. This CSM model is named CORT3D, and its based on the RT3D modeling code. CORT3D was developed to account for permanganate oxidation chemistry, multiple rate-limited NOD fractions, DNAPL mass transfer, and changes in porous media flow properties resulting from permanganate oxidation.
- Batch and flow-through experiments were completed to evaluate the viability and effectiveness of coupling ISCO with other remediation technologies. Studies were conducted to investigate the feasibility and design considerations of coupling ISCO with both anaerobic and aerobic bioremediation technologies, utilizing batch microcosm studies and 1-D column experiments. Experimentation also investigated coupling ISCO with surfactant and cosolvent remediation. Batch screening studies were conducted to determine which surfactants and cosolvents were most compatible with the oxidants in this study, and follow up experimentation was conducted within a 2-D flow cell to determine the effectiveness of various coupling regimes (i.e., sequential versus combined delivery of surfactants/cosolvents and oxidants).
- A final aspect of the project included experiments designed to evaluate whether partitioning tracer test methods provide a viable way to measure DNAPL mass removals after ISCO has been applied to a DNAPL site. Experiments were conducted to determine how residual oxidant, including MnO_2 deposition at the NAPL-water interface, might impact alcohol and ketone tracers and their respective NAPL-water partitioning coefficients. Effective tracers were then applied in 2-D flow cell systems to determine how effective the tracers might be at measuring performance at ISCO treated sites.

The findings of this project are diverse and difficult to summarize in a succinct listing. Section 4.7 of Chapter 4 provides a summary and discussion of the major findings of the research with respect to PCE and TCE DNAPL degradation as affected by oxidant type and concentration, delivery method, and subsurface conditions. The viability of coupling ISCO with other remediation technologies is also addressed. Listed below are several generalized conclusions concerning the application of ISCO to DNAPL sites.

- CHP was found to have very fast rates of reaction, and subsequently fast rates of oxidant decomposition. As such, the oxidant persistence as evaluated in these studies was poor. This was found to hold true in all systems of varying experimental scale that evaluated the use of CHP. In general, systems that provided effective contact of CHP with the contaminant appeared to be highly efficient with regard to contaminant destruction and oxidant use (i.e. RTE values in the VRs, MVRs and ZHRs). However, the effectiveness (rate and extent) of contaminant mass depletion of CHP was generally lower than in equivalent permanganate systems in every experimental series CHP was evaluated in (VRs, MVRs, ZHRs, diffusion cells, 2-D flow cells). The lower effectiveness of CHP is largely due to difficulties that arise in optimizing oxidant delivery and oxidant activation.
- Permanganate, in contrast to CHP, was much more effective in reducing contaminant mass in the experimental systems evaluated. Due to the reduced reactivity of permanganate, advective and diffusive transport of oxidant is possible, as evidenced in all experimental transport studies (e.g., 1-D diffusion cells, FTRs, 2-D cells).

- When considering remediation effectiveness, oxidant concentration can interact strongly with the velocity of oxidant delivery into a porous media system. For either oxidant studied in this project, with application into porous media systems where delivery to the DNAPL depended on advective transport of the oxidant (e.g., FTRs or 2-D cells), the use of lower concentrations of oxidant delivered at higher fluid velocities appeared preferable. A common theme among the experiments that evaluated multiple velocities was that higher velocities led to more effective remediation performance, evidenced by increased DNAPL mass depletion, and frequently reduced adverse impacts and enhanced potential for bio-coupling. However, higher oxidant concentrations can promote diffusive transport of oxidant into low permeability media, and be more time-efficient from a site flushing perspective as fewer pore volumes may be required to destroy a given DNAPL contaminant source.
- Natural oxidant demand (permanganate) and oxidant decomposition (peroxide) increased with increasing complexity of porous media (e.g., higher reduced mineral content, NOM, or clay/silt particle fractions), increasing oxidant concentration, and increased contact time. NOD and oxidant decomposition challenge both advective and diffusive oxidant transport. However, site-specific characterization in a way that allows for prediction of transport in the subsurface is difficult. Conditions used during lab testing of oxidant-subsurface interactions need to mirror the planned oxidant delivery and transport in the subsurface.
- TCE was found to be depleted and destroyed faster than PCE in every experimental system that evaluated both DNAPL types (VRs, MVRs, ZHRs, diffusion cells and FTRs). This is likely due to the order of magnitude higher solubility of TCE versus PCE, as well the faster kinetic rate of reaction between TCE over PCE in permanganate systems. However, the solubility limit can have secondary impacts on ISCO system performance. Based on the FTR experiments TCE was more likely to result in CO_2 gas generation from permanganate ISCO, than PCE. This is largely due to the fact the higher contaminant concentrations in TCE systems result in more concentrated proton generation, as well as higher concentrations of aqueous CO_2. The resulting pH change, if the system is not adequately buffered, can result in off-gassing, which may mobilize DNAPL or vapor phase contaminant, as well as reduce hydraulic conductivity. However, such effects may be compound-specific. Permanganate oxidation of *cis*-DCE generates alkalinity instead of acidity, and would be less likely to observe this problem, despite the higher solubility limit of *cis*-DCE.
- DNAPL present in the subsurface as residual ganglia are highly amenable to depletion and destruction by permanganate flushing. However, when pooled DNAPL was present, oxidation effectiveness was more variable. Residuals are depleted much faster than pools due to their high surface area to volume ratio. Mass transfer was observed to be enhanced from residuals by permanganate oxidation by bulk aqueous phase contaminant oxidation, as well as possibly other impacts to mass transfer processes, based on FTR and CORT3D modeling study results.
- The role of natural organic matter and certain minerals (i.e., goethite) present in the subsurface can complicate the understanding of ISCO efficiency and effectiveness. For example, the results of this study revealed that the role of NOM in porous media during ISCO has a more complex effect on remediation performance than simply increasing natural oxidant demand.
- Coupling ISCO with anaerobic reductive dechlorination for destruction of contaminants such as TCE and PCE is a viable approach. In general, CHP oxidation is disruptive to anaerobic microbes due to oxygenation of the subsurface, but chemical oxidation of porous media by CHP can generate higher levels of DOC, which can provide a substrate for anaerobic microbes growing in down-gradient areas where conditions remain anaerobic. Permanganate oxidation appears to be more amenable to coupling with anaerobic reductive dechlorination processes. For the anaerobic mixed culture KB-1, reductive dechlorination behavior ceased after oxidant flushing began, but

rebounded after oxidation ceased. The amount of time until activity rebound varied between systems, and appeared to depend on the total time and concentration of permanganate to which the microbes were exposed.

- Coupling ISCO with surfactant enhanced aquifer restoration (SEAR) and use of PTT test methods for performance assessment appear viable, but only with careful evaluation and design to ensure that the ISCO-SEAR and ISCO-PTT systems are compatible.

5.2. RECOMMENDATIONS

While the research completed during this SERDP project has enhanced the understanding of the processes controlling the effective application of ISCO using potassium permanganate or catalyzed hydrogen peroxide, further work is warranted to explore other oxidant systems (i.e., use of oxidants other than those studied in this project (e.g., persulfates) as well as combinations of oxidants) and to develop modeling and decision support tools for full-scale system design.

The fundamental research described in this report provides a knowledge base for the future development of guidance on the principles and practices of ISCO so that it can be selected as a preferred remedy when appropriate and can be implemented to reliably achieve performance goals. Decision aids and design tools will enable cost-effective implementation of ISCO for remediation of DNAPLs at a given site, using ISCO either as a stand-alone method or by coupling it with a pre- or post-ISCO operation. This needed guidance is being developed by the CSM project team under the follow-on ESTCP project, ER-0623: “In Situ Chemical Oxidation for Remediation of Groundwater: Technology Practices Manual”.

APPENDIX A

SUPPLEMENTARY EXPERIMENTAL STUDIES

A.1. INTRODUCTION

This appendix describes experimental work completed during the course of SERDP project CU-1290 that is not captured in detail in the M.S. theses or Ph.D. dissertations completed in support of the project. The methods and results of the experiments are described and where appropriate conclusions and implications are noted. The complete citation for references included in this Appendix may be found in the reference list provided for Chapter 2 within the body of this report.

A.2. LABORATORY EXPERIMENTS TO EXPLORE THE INFLUENCE OF PARTICLE SIZE/SURFACE AREA ON THE INTERACTIONS OF THE OXIDANT WITH POROUS MEDIA

A.2.1. Introduction

One of the many questions with respect to the specific interactions of the oxidants with natural porous media involves the influence of soil particle size, or surface area, on the extent and kinetics of oxidant depletion. It is well known that interactions of the oxidant with porous media can impact overall contaminant destruction efficiency and effectiveness through competition of the contaminant and the media for the oxidant. Studies examining the influence of surface area on catalyzed hydrogen peroxide (CHP) oxidation have conflicting results. The findings of Lin and Gurol (1998) and Kwan and Voelker (2003) note dependence of hydrogen peroxide decomposition on the surface area of iron-based minerals, indicating that a lower surface area can result in mass transfer limitations with respect to the interaction of the hydrogen peroxide with the mineral surface. However Ravikumar and Gurol (1994) noted no influence of surface area in the sand systems they examined. This indicates that further experimentation is necessary to determine if a specific relationship between particle size/surface area and oxidant depletion does exist. Additionally a review of the literature indicates a lack of information with respect to the impact of particle surface area on oxidation kinetics in permanganate systems.

A.2.2. Experimental Approach

Soil slurries in 160-mL zero-headspace reactors (ZHRs) were employed in this study, manufactured by Associated Design and Manufacturing Company, and similar to those used for TCLP analysis (US Environmental Protection Agency (USEPA) Method SW846) (see Figure 3.2).

The experimental conditions encompass variations in oxidant type and loading, and DNAPL type and loading, as summarized in Table A.1. Two sets of experiments were conducted: (1) “no oxidant” systems to examine the influence of particle surface area on DNAPL partitioning behavior, and (2) “no DNAPL” systems to examine the influence of particle surface area on oxidant depletion rate and extent. (Table 3.3 includes the characteristics of the base sand material used as system solids (soil/sediment), as well as the base simulated groundwater). A difference in soil surface area was achieved by crushing the base sand media, via a BICO UA V-Belt Driven Pulverizer Model 242-53, to a smaller particle size (d_{10}/d_{60} = 0.19/0.53 mm), resulting in a greater surface area (approx. 25% more surface area) available for interaction with the oxidant and DNAPL.

Table A.1. Experimental conditions evaluated in surface area studies.

Oxidant	Oxidant load	DNAPL	DNAPL mass	Media
$KMnO_4$	2.5% concentration by mass	TCE	0.2x capacity of soil and groundwater*	Sand
CHP**	0.25% concentration by mass	PCE	2x capacity of soil and groundwater	
			3x capacity of soil and groundwater	

*Capacity of soil and groundwater determined based on fugacity-based partitioning model (Dawson, 1997)
**CHP generated with design H_2O_2 concentration and 5mM $FeSO_4$

For each experimental run, duplicate reactors were prepared. First, 100 g of the appropriate solids media were added to the reactor, which was then sealed. The vessels were then pressurized from the bottom, while open at the top to remove air from the system. Next, the requisite type and volume of DNAPL was added directly to the soil with a syringe and the reactor was immediately capped and sealed. DNAPL addition was followed immediately by addition of 30 mL of simulated groundwater through the top cap. "No DNAPL" systems were prepared with the 30 mL of simulated groundwater only. The top cap was then closed, and the ZHRs were allowed to equilibrate while tumbling 360^o for 24 hours at 20^{o}C. After the equilibration period, the reactors were sampled (time = 0) through the top cap using a syringe. Sampling parameters, volumes, and methods are included in Table A.2. Then, the vessel bottom pressure was released, and 30 mL of the oxidant solution, prepared in deionized water, was added through the top cap with a fitted syringe (final solids to liquid ratio = 1:1 vol.). The vessels were then sealed at the top and pressurized through the bottom. The pressure within the chamber allowed for direct sampling of the aqueous phase by release through the top cap, minimizing loss to the gaseous phase, while the valve is opened. During a 24-hour reaction period, the ZHRs were continuously tumbled, and again sampled at 2, 8, and 24 hr, at which time the reaction was discontinued. At this time, 30 mL of hexane were introduced through the top cap while pressure was released from the bottom of the reactor. The ZHRs were tumbled for an additional 2 hours to allow for transfer of any DNAPL remaining in the system (solids or groundwater) into the hexane for measurement.

Table A.2. Analyses performed on ZHR materials.

Groundwater (at time = 0, 2hr, 8hr):		
Analysis	Sample vol.	Method
DNAPL concentration	1.0 mL	HP 6890 Capillary GC-ECD with hexane extraction
Oxidant concentration		
Permanganate (MnO_4^-)	0.1 mL	Spectrophotometry: Hach DR 4000 at 525 nm
Hydrogen peroxide (H_2O_2)		Hach method: idometric titration

Three data parameters were compared in the systems to evaluate the impact of particle size/surface area in these systems. (1) DNAPL distribution between aqueous and sorbed/DNAPL phase in "No oxidant" systems. (2) Media demand in "No DNAPL" systems, which is the mass of oxidant depleted per mass of solids present (mg/kg), and (3) Pseudo-1st order reaction kinetic rate constants for oxidant depletion (K_{ox}), also measured in "No DNAPL" systems.

A.2.3. Results and Discussion

The sorption/distribution of the study DNAPLs were examined in "no oxidant" systems with the two different particle surface areas available. These systems demonstrated no significant loss of DNAPL in the 24 hr reaction period. No difference in DNAPL distribution or system DNAPL capacity was demonstrated in the higher surface area systems as compared to the lower surface area systems. Table A.3 presents the media demand and K_{ox} results with respect to oxidant type, oxidant load, and media surface area in "no DNAPL" systems.

Table A.3. Media demand and oxidant depletion rates with variable oxidant type, oxidant load, and media surface area.

Oxidant type	Oxidant load	Surface area	Media demand (mg/kg)	K_{ox} (min^{-1})
MnO_4^-	2.5%	Lower	6351	0.0005
MnO_4^-	2.5%	Higher	6752	0.0065
CHP	2.5%	Lower	11934	0.0052
CHP	0.25%	Lower	1109	0.0032
CHP	2.5%	Higher	2412	0.0112
CHP	0.25%	Higher	243	0.0220

Note: Experimental error led to the lack of comparison of surface area in 0.25% permanganate load systems.

Generally in these studies, the oxidant load demonstrated the greatest impact of the variables on media demand, however surface area had the greatest influence on the oxidant depletion rate. Permanganate systems' media demand was not notably impacted by particle size/surface area at the higher oxidant load examined. However, CHP systems demonstrated a lower media demand in the higher surface area control systems. This effect was relatively consistent with oxidant loading (i.e., a 25% increase in surface area decreased media demand by a factor of approximately five for both oxidant loads). Additionally, CHP systems demonstrated a higher media demand in higher oxidant load systems, which was relatively consistent with surface area (i.e., a tenfold increase in oxidant demand resulted in approximately a tenfold increase in media demand for both the low and high surface areas).

The *interactive* effects of surface area and oxidant load were more evident in the K_{ox} response for CHP systems. The increased oxidant load had a stronger effect (increased K_{ox} by a factor of about 1.6) in the lower surface area systems, than in the higher surface area systems (decreased K_{ox} by a factor of about 2). Also, the 25% increase in surface area had a stronger effect in the lower oxidant load system (increased K_{ox} by a factor of 6.9) than in the higher oxidant load system (increased K_{ox} by a factor of about 2). Unfortunately, the interactive effect of oxidant load and surface area could not be examined in permanganate systems. However, in comparing the two oxidants (high oxidant load), the change in K_{ox} as a function of surface area was greater for permanganate systems than for CHP systems under these reaction conditions. The higher surface area increased the permanganate depletion rate by a factor of

approximately 13, whereas this change only increased the hydrogen peroxide depletion rate by a factor of about 2.

The actual values measured for media demand are consistent with reported values in the literature for both laboratory and field application (Watts 1991, Siegrist et al. 2001). Many studies have also been conducted with respect to the impact of oxidant load in both permanganate and CHP systems (e.g., Watts *et al.* 1991, Khan and Watts 1994, Gates *et al.* 1995, Watts and Dilly 1996, Watts *et al.* 1996, Watts and Stanton 1999, Gates-Anderson *et al.* 2001, Siegrist *et al.* 2001, Siegrist *et al.* 2002). These studies indicate that increasing oxidant load results in faster oxidation, as well as a greater media demand.

The results of these studies, with respect to surface area effects in CHP systems, are consistent with the findings of Lin and Gurol (1998) and Kwan and Voelker (2003), which note dependence of hydrogen peroxide decomposition on the surface area of minerals. These authors attributed their results to the possibility that a lower surface area can result in mass transfer limitations with respect to the interaction of the hydrogen peroxide with the mineral surface. This same effect was observed with respect to permanganate reactions (at the higher oxidant load), and in theory, this same mass transfer explanation may apply. It is important to acknowledge that although differences in media demand and oxidant depletion rates differed with porous media surface area, these results were measured in completely mixed systems. It is possible that in flow-through experimental systems, the more important variable will be the surface area actually contacted by the oxidant and not necessarily the grain-size surface area of the media.

A.3. LABORATORY EXPERIMENTS USING 2-D FLOW-THROUGH CELLS

A.3.1. Introduction

While initial bench-scale laboratory studies investigated the interactions between dense nonaqueous phase liquid (DNAPL) contaminants and oxidants, oxidants and porous media, and contaminants and porous media in batch and 1-D flow-through systems, this experimentation incorporates an analysis of these interactions collectively in two dimensional space at the intermediate scale. The 2-D cells employed in these studies enable the evaluation of reaction and transport processes, as well as oxidation efficiency and effectiveness, under a variety of experimental conditions. The particular studies described herein focus on the effects of important oxidant delivery characteristics.

There are numerous oxidant delivery approaches, all with the goal of facilitating contact between the oxidant and contaminant for reaction to occur. Two important aspects with respect to delivery include the oxidant concentration and the delivery velocity (e.g., gravity-feed well delivery vs. direct-push pressurized delivery). It is ideal to optimize the oxidant delivery concentration in DNAPL systems to (1) maximize DNAPL depletion and destruction rates affording faster cleanup times, while (2) accounting for, yet minimizing, undesirable impacts such as nonproductive demand of the oxidant by the porous media, source zone clogging by reaction byproducts and oxidant waste by distribution into uncontaminated areas. It is ideal to optimize the oxidant delivery velocity in DNAPL systems to (1) "replace" the oxidant volume available to react with contaminant based on contaminant reaction and dissolution rates, and (2) minimize contact with porous media because less contact results in less nonproductive oxidant demand.

These approaches to delivery optimization are inter-related and specific to site conditions including contaminant type, mass distribution, and heterogeneity, as well as porous media characteristics such as hydraulic conductivity and the rate and extent of natural oxidant demand (NOD), all of which can impact delivery capabilities. They must be considered collectively because considering them individually may lead to conflicting design guidance. For example, if a contaminant is present in a complex DNAPL source architecture, and time to clean-up is not a concern, a slower oxidant delivery velocity may be more efficient as oxidant has more contact time with the contaminant, resulting in less oxidant waste by

preventing oxidant from flowing unreacted past the contaminant. Conversely, if this same contaminant is located in a high NOD porous media, a faster delivery velocity reduces oxidant waste through nonproductive consumption by the porous media and potentially reduces the permeability loss associated with reaction byproducts. A balance is necessary to optimize the system based on contaminant dissolution and oxidant transport and reaction kinetics.

The 2-D cell studies were conducted to better understand the interactive relationship of different processes occurring during ISCO that dictate optimized system delivery conditions. Tetrachloroethene (PCE) was the representative contaminant employed in these systems. ISCO with $KMnO_4$ and CHP were evaluated with respect to space and time. The oxidants were delivered at varying oxidant concentrations and delivery velocities. Analyses were conducted on samples within the 2-D cells in both vertical and horizontal cross-sections located down-gradient of the PCE source, as well as on effluent samples. Measurements included PCE and oxidant concentrations, pH, chloride, and common cations. Additionally, 2-D cells were dissected post-treatment. Pore water was analyzed for oxidant concentrations, and porous media cores were analyzed for cation exchange characteristics.

A.3.2. Materials and Methods

The primary element of the 2-D transport cell is a 30 cm x 30 cm x 2.5 cm Delrin box. One box face is left open, and is covered by a tempered glass plate to allow visual observation of cell processes (cell front). The opposite cell face (cell back) contains 100 pin-sized sample ports in a 2.5 cm grid with alternating rows offset from the row above and below by 1.25 cm. The sample ports are lined with Hamilton layered septa with Teflon interior to prevent any system leaking or off-gassing through the ports. The cell interior is accessed by needles inserted through the septa and sample port into the cell. On each end of the cell (influent and effluent) is a 1.25 cm diameter port. These ports are accessed through quick disconnect fittings that provide a 0.3 cm opening to collect influent and effluent samples.

Two porous media (laboratory base sand, and fine-grained silica sand) and a simulated ground water are used to pack the cells. The characteristics of each are included in Table A.4. The laboratory base sand is passed through a #20 sieve to remove large material from the media. Ground water used during packing is de-aired by vacuum removal while vigorously mixing on a magnetic stirrer for approximately 30 min/L, or until no visible bubbles are observed escaping the system. The removal of air from the ground water decreases the possibility of air entrapment during packing and ensures the cell is fully saturated.

The 2-D cell is wet packed via gradual horizontal layering of the fine-grained silica sand in the cell in lifts of approximately 15 grams each distributed horizontally across the cell. Approximately 0.6 to 1.2 cm of water is maintained above the sand level at all times. The coarse laboratory base sand is used to create a higher permeability lens within the lower permeability silica sand. To create the lens, place holders are used to maintain the shape of the lens as a stretched hexagon shape (long rectangle with equilateral triangles at each end). This shape is utilized as it reduces vertical ground water flow that results from the contrast in hydraulic conductivity between the coarse and fine media. The length of the lens is approximately 7.9 cm long and approximately 2.5 cm in height. Once the lens is emplaced, the remainder of the cell is filled with the base sand using the same wet packing procedure.

To ensure uniform flow through the cell, gravel influent and effluent chambers (approximately 1-1.5 cm wide each) span the vertical length of the cell. The gravel is separated from the porous media by stainless steel wire cloth wrapped around stainless steel wire mesh for improved stability. A saturated bentonite layer (approx. 1.25 cm thick) is added across the top of the cell to ensure that no air layer forms at the top of the cell and the flow field behaves as a confined aquifer. Figure A.1 provides schematics of the front and back of the 2-D cell.

Design flow conditions are achieved in the cell by delivering flushing solutions (simulated ground water or oxidant) via peristaltic pump, and a constant head chamber is connected to the effluent port to maintain positive pressure within the cell.

Eight experimental runs were conducted in the 2-D cells. These are summarized in Table A.5 and include runs with both oxidants $KMnO_4$ and CHP, varied oxidant concentrations or oxidant activation approaches (for catalyzed hydrogen peroxide), and two different oxidant delivery velocities designed to simulate gravity feed conditions (ambient ground water linear velocity of 12 cm/d) and pressurized injection (approximately 4x ambient flow, or 45 cm/d). Two control runs were conducted with no oxidant, but with matching velocities by flushing simulated ground water under gravity feed and pressurized injection.

Table A.4. Characteristics of porous media and simulated ground water.

~ Composition of Base Sand Material ~		
Parameter	Units	Value
pH		6.8
Total organic carbon	Dry wt.%	0.017
Grain size, d_{10} and d_{60}	mm	0.22, 0.60
~ Composition of Fine-Grained Silica Sand ~		
Parameter	Units	Value
pH		7.37
Total organic carbon	Dry wt.%	0.019
Grain size, d_{10} and d_{60}	mm	0.025, 0.079
~ Composition of Simulated Ground water ~		
Component	Concentration (g/L)	Volume added (mL)
KCl	0.83	1.0
$NaNO_3$	1.00	1.0
$FeCl_3$	1.28	1.0
$MgCl_2$	34.4	2.0
$CaSO_4$	2.5	56
Deionized water		939
~ Characteristics of Simulated Ground water ~		
Parameter	Units	Value
pH	-	5.0
Alkalinity	mg-$CaCO_3$/L	40
Conductivity	mohms	277

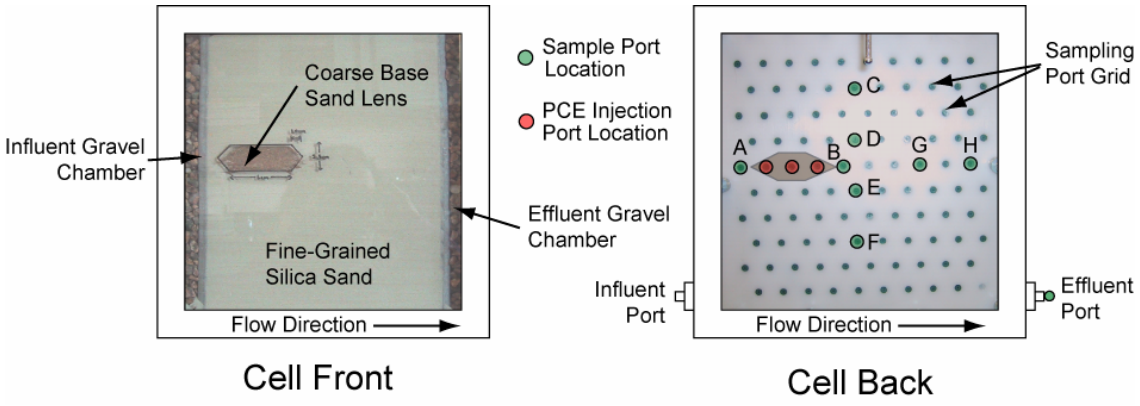

Figure A.1. Diagram of 2-D cell layout.

Table A.5. 2-D Experimental run conditions.

Cell ID	Oxidant system	Oxidant concentration	Oxidant delivery
1	Catalyzed hydrogen peroxide	3% H_2O_2 w/5 mM $FeSO_4$, pH 3	Pressurized
2	Catalyzed hydrogen peroxide	10% H_2O_2 w/5 mM $FeSO_4$, pH 3	Pressurized
3	Catalyzed hydrogen peroxide	3% H_2O_2, pH 3	Gravity feed
4	Catalyzed hydrogen peroxide	3% H_2O_2 w/pre-ox citric acid flush	Gravity feed
5	Potassium permanganate	1% $KMnO_4$	Pressurized
6	Potassium permanganate	1% $KMnO_4$	Gravity feed
7	None – control	None – control	Pressurized
8	None – control	None – control	Gravity feed

Each experimental run is conducted in three phases; pre-oxidation, oxidation, and post-oxidation. During the pre-oxidation phase for each run, first a dye test is conducted at a rapid delivery velocity (approx 75 cm/d) to ensure uniform fluid delivery in the cell (Figure A.5). Then, the cell is flushed for an additional 24 hours with simulated ground water to ensure complete removal of all tracer dye. PCE is then emplaced into the coarse lens by slow delivery through cell back face ports (Figure A.1) via syringe pump to achieve 18-20% NAPL saturation of the lens. Simulated ground water is delivered to the cells at 12 cm/d (ambient ground water flow condition) for 72 hours (approximately 3 pore volumes (PVs) of delivery). Sampling during this time establishes the baseline PCE dissolution profile, with sampling occurring at the 0, 12, 24, 48, and 72 hour time points.

During the second phase of each experimental run, the oxidation phase, oxidant is delivered for approximately 1 PV at the design oxidant delivery velocity, 12 cm/d (ambient) to simulate gravity feed conditions (for 24 hours), or 45 cm/d to simulate a pressurized injection (for 8 hours). Samples are collected at 0, 2 hr, 4 hr, 8 hr, 12 hr, and 24 hr starting with oxidant injection (as appropriate for design condition).

The final phase of the experiment, the post-oxidation phase, consists of the resumption of simulated ground water flow, which is delivered for 7 PVs (1 week) at the ambient delivery velocity of 12 cm/d to establish the post-oxidation PCE profile within the cell. Samples are collected at 0, 4 hr, 8 hr, 12 hr, 24 hr, and every 24 hours thereafter for up to one week.

For each phase of the experimental runs, several measurements are made on samples collected from cell ports and cell effluent. The sampling array included vertical and horizontal profiles of sample ports (ports A-H, 8 total) along with cell effluent measurements (Figure A.1). At selected times points during each experimental phase of operation, the 8 back ports are sampled by inserting a needle into the appropriate sample port. Pore water is passively collected at the cell's fluid delivery velocity into sampling tubes to avoid disruption of the flow field. A 0.1 mL aliquot of sample is removed and placed into a gas chromatography (GC) vial containing 1.0 mL of hexane for extraction of PCE into the hexane phase. The hexane phase is subsequently analyzed by gas chromatography with electron capture detection (Hewlett Packard 6890 with ECD). Another 0.1 mL aliquot of sample is removed and placed into an ion chromatography (IC) vial for chloride analysis via IC (Dionex DX-600). For more detail regarding the analytical methods used for GC and IC analysis, see Petri (2006). pH is measured in this sample aliquot via microprobe measurement (Thermo Orion microprobe) prior to IC analysis. An additional 0.1 mL aliquot of sample is prepared for oxidant measurements. For measurement of hydrogen peroxide concentrations, this aliquot is diluted to 30 mL and H_2O_2 is measured using a standard Hach iodometric titration kit. For measurement of MnO_4^-, the aliquot is diluted to 10 mL and absorbance is measured spectrophotometrically (Hach DR 4000) at 525 nm, which is then equated to concentration via 5-point calibration.

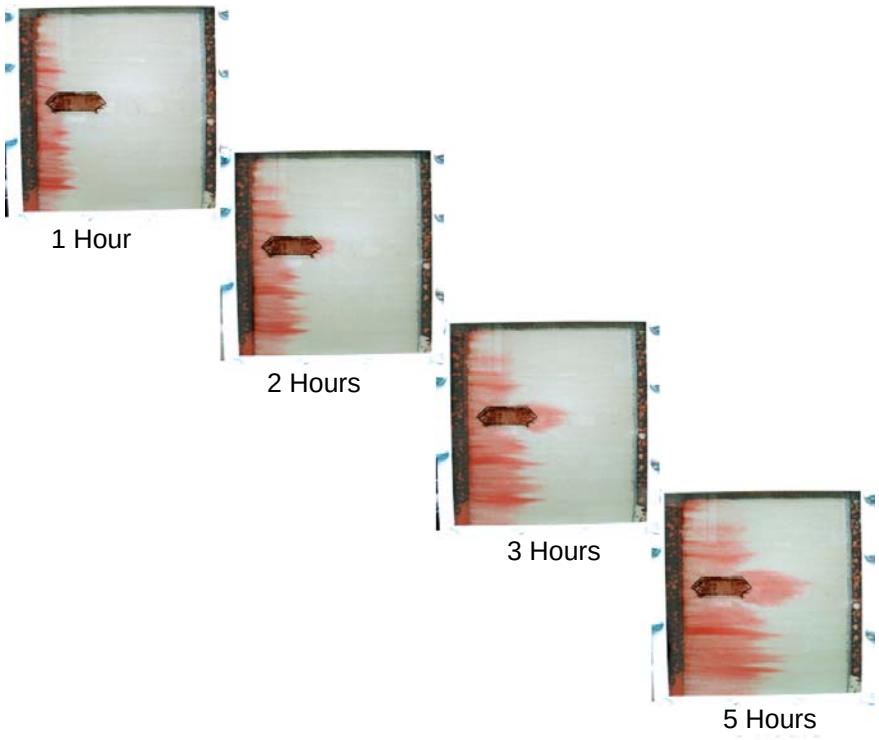

Figure A.2. Example dye test results in 2-D cell.

Sample effluent is collected by opening quick disconnect fittings and first purging 10-15 drops of fluid. Effluent is then collected into sample vials. GC, IC, pH, and oxidant measurements are made on effluent samples as described above. Additionally, 4.0 mL of effluent are prepared for cation analysis via inductively coupled plasma – atomic emission spectrometry (ICP-AES; Perkin Elmer Optima 3000). It was not possible to collect the necessary volume of fluid for ICP analysis from the cell's back sample ports, because doing so would severely impact the flow field within the cell.

Upon completion of the post-oxidation experimental phase, the cell is dissected (Figure A.3). Five 9 cm long, 1.25 cm diameter hollow tubes are driven into the porous media at equal levels in the cell. Three cores are taken to span the source zone, along with 2 down-gradient cores. Once fully inserted, the face of the cell is removed and the coring devices are unearthed from the porous media. The media is removed from the coring device by pushing the core with a solid tube slightly smaller than the tube's diameter. The cores are sectioned into two sub-cores. One core is analyzed for the concentration of residual oxidant in the pore water. The other sub-section is prepared for measurement of cation exchange characteristics by sequential extraction with DI water (water-exchangeable), BaCl (barium-exchangeable), and finally a hydroxylamine hydrochloric acid and nitric acid solution to dissolve any MnO_2 potentially deposited during permanganate oxidation. Each extraction solution was measured by ICP-AES for resulting cation concentrations.

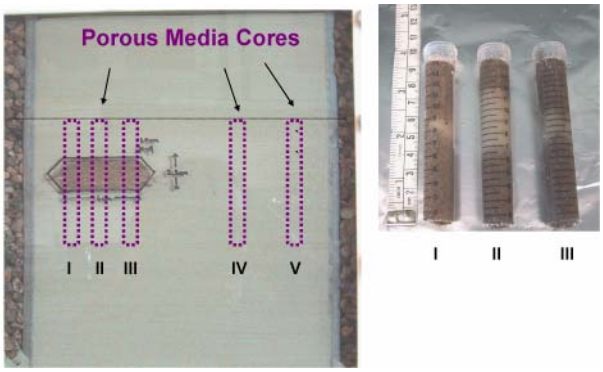

Figure A.3. Schematic of 2-D cell core dissection.

A.3.3. Results and Discussion

The presentation and discussion of results are provided in several sections. First, a qualitative discussion of performance is presented to evaluate the performance of the oxidant flushing regime by analyzing oxidant and contaminant distribution as well as system chemistry effects. A more quantitative analysis then follows, which evaluates the cell's efficiency and effectiveness parameters that have been introduced by earlier work as part of this SERDP project and are used to identify optimal operational parameters.

A.3.3.1. Remediation Performance - Oxidant Distribution. Table A.6 provides values for the total oxidant mass addition and the estimated percentage of oxidant consumed during each of the 2-D cell runs based on data from the effluent sampling location (aside from no oxidant control runs 7 and 8). The mass additions of hydrogen peroxide were substantially larger than the additions of permanganate, yet with both oxidants, the majority of oxidant was consumed within the cell, which has a hydraulic retention time of 6-8 hours during a pressurized injection and ~24 hours during a gravity feed flush.

Table A.6. Oxidant consumed within 2-D cells based on effluent measurements.

Cell ID	Oxidant type	Activation method	Delivery	Mass oxidant introduced (g)	Percentage of oxidant consumed*
1	Hydrogen peroxide	5 mM $FeSO_4$, pH3	Pressurized	33.7	95
2	Hydrogen peroxide	5 mM $FeSO_4$, pH3	Pressurized	112	97
3	Hydrogen peroxide	pH3	Gravity feed	27	100
4	Hydrogen peroxide	Citric acid flush	Gravity feed	27	100
5	Permanganate	Not applicable	Pressurized	unknown	CBD**
6	Permanganate	Not applicable	Gravity feed	9.2	87

*Approximate values based on known influent concentration and delivery velocity and measured effluent concentrations vs. time;
**CBD = cannot be determined – incomplete data set

Table A.6 indicates that 95-100% of hydrogen peroxide was consumed within the cells to which it was delivered (Cells 1-4), whereas 87% of permanganate was consumed in the cell to which it was delivered at the slower delivery velocity (Cell 6). All of the hydrogen peroxide cells witnessed a relatively rapid decomposition of the oxidant, which is demonstrated by the large oxidant consumption in these systems. On the basis of data from the hydrogen peroxide cells, the presence of a small amount of hydrogen peroxide at the effluent for the pressurized injection experiments may indicate better penetration of the oxidant into the cell at these higher delivery velocities. This improved penetration may be due to the higher velocity in these systems, which reduces the contact time with the media allowing for oxidant distribution over larger spatial distances. One note of interest is that there does not appear to be a significant difference between the percentages of oxidant consumed versus the oxidant mass loadings for hydrogen peroxide. This is particularly striking in Cell 2, which utilized a 10% hydrogen peroxide flush resulting in nearly four times as much oxidant mass addition as the other three hydrogen peroxide cells, yet 97% of the injected mass was consumed, indicating that the higher oxidant loading resulted in higher oxidant consumption. Permanganate was much more persistent than hydrogen peroxide with a much smaller overall mass delivered, yet a lower total amount consumed. Unfortunately the data do not allow for a comparison of oxidant delivery velocity vs. oxidant consumption for permanganate, due to the incomplete data set from Cell 5. However, it is expected that less permanganate would be consumed at the pressurized delivery in Cell 5 as the reduced contact time with the porous media and contaminant would result in less oxidant demand.

Additionally, oxidant concentrations are considered in both the vertical and horizontal profiles established for cell sampling (see Figure A.1) to give a more detailed understanding of the oxidant distribution within the 2-D cell. Table A.7 demonstrates the maximum oxidant concentration measured in each port for each cell (except Cell 5 which had an incomplete data set). Table A.8 uses these values to calculate the smallest percent difference between the injected and achieved concentrations of oxidant at each location in the cell, expressed as a percentage of the injected oxidant concentration. For example, if the value at the B location is 28 percent, then highest concentration of oxidant at that location was 28 percent less than the injected concentration. While this value does not separate out impacts in oxidant concentration caused by dilution, the dye test indicated a relatively uniform flow field with a dye sharp front, and thus these values provide an estimation of the percentage of oxidant that was consumed prior to reaching each location. Since these are the smallest values, they represent the best case scenario for oxidant penetration into the cell, with smaller numbers being ideal for better oxidant distribution. Table A.5 is separated by horizontal and vertical profile data, and effluent data are presented separately, as they represent a composite of flushing solution concentrations across the entire cross section of the cell.

Table A.7. Maximum oxidant concentrations measured in sample ports and cell effluent.

Cell and injected conc. = Port	Maximum oxidant concentration (mg/L)				
	Cell 1 - peroxide	Cell 2 - peroxide	Cell 3 - peroxide	Cell 4 - peroxide	Cell 6 - permanganate
	30000	100000	30000	30000	10000
A	8700	42000	12000	6600	9320
B	6000	11700	12000	600	7155
C	8400	17100	9600	0	0
D	6900	58100	12000	1800	1280
E	13200	34200	9600	1200	5125
F	14700	32400	6000	600	6960
G	8700	7200	4200	600	3260
H	6000	4500	3000	0	2105
Effluent	5700	4500	0	0	1825

*Sample ports correspond with horizontal and vertical sampling profiles and correspond to figure to the right of the table. The brown area in the figure indicates the PCE source zone.

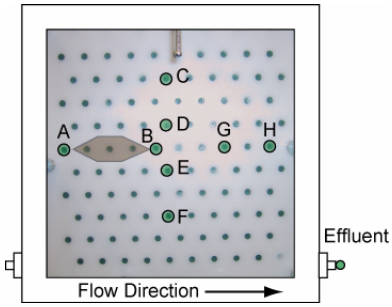

Table A.8. Smallest percent difference in oxidant concentration.

Smallest percentage difference between injected and observed concentrations					
Sample Location	Cell 1 - peroxide	Cell 2 - peroxide	Cell 3 - peroxide	Cell 4 - peroxide	Cell 6 - permanganate
~ Horizontal profile ~					
A	71	58	60	78	7
B	80	88	60	98	28
G	71	93	86	98	67
H	80	95	90	100	79
~ Vertical profile ~					
C	72	83	68	100	100
D	77	42	60	94	87
E	56	66	68	96	49
F	51	68	80	98	30
~ Effluent composite ~					
Effluent	81	95	100	100	82

Tables A.7 and A.8 demonstrate that a greater percentage of hydrogen peroxide was consumed (58-78%) prior to reaching the A measurement port than permanganate (7%), indicating that hydrogen peroxide undergoes decomposition rapidly upon contact with the media (gravel influent chamber and fine-grain silica sand). This extensive hydrogen peroxide consumption cannot be attributed to reaction with PCE because the A port occurs up-gradient of the coarse lens that contains the PCE, and data from the no-oxidant control cells indicated that there was little dissolved phase PCE here. The hydrogen peroxide decomposition was evidenced by extensive gas generation in each of these cells upon contact with the gravel influent chamber. Because the cells were run as confined aquifers, gas generation within

the cell during the hydrogen peroxide experiments resulted in a buildup of pressure within the cell. This pressure buildup would force a drop in the water table and also result in faster fluid movement. In order to prevent this from occurring, each of the hydrogen peroxide cells was vented to release gas throughout oxidant delivery.

The vertical profile data are indicative of the uniformity of oxidant delivery through the 2-D cell. Each of the hydrogen peroxide cells (Cells 1-4) demonstrate relatively uniform delivery in the cell from a vertical perspective; however, the permanganate cell demonstrates significantly greater oxidant concentrations in the lower E and F ports than in the higher C and D ports. This may be indicative of density-driven permanganate flow as permanganate solutions are denser than water, especially at the 1% concentration level.

From the horizontal profile data, for all of the cells, it can generally be seen that oxidant consumption increases as it moves down-gradient from A to H. This is expected as more oxidant is anticipated to be consumed as contact time with the porous media and contaminant increase. However, lower numbers along this profile indicate deeper oxidant penetration, thus permanganate Cell 6 achieved the deepest oxidant penetration of any of the cells.

The data from sampling location B are also important to consider for each of the cells, which indicate the concentration of oxidant located immediately down-gradient of the PCE source zone. Considering the hydrogen peroxide systems first, a strong drop in oxidant concentrations from location A to B across the PCE source zones may potentially indicate oxidant consumption caused by destruction of the contaminant. The data from Table A.7 indicate such a drop in Cells 1, 2 and 4. Furthermore, in these same cells, the hydrogen peroxide concentrations at the vertical profile (locations C though F) are higher than at the B location, despite the vertical profile being located down-gradient of this location. Because the vertical-profile sampling array is offset slightly from the B port (see diagram next to Table A.7), it does not necessarily capture impacts directly down-gradient of the source zone, like sampling port B does. Thus, the larger oxidant concentration drop across the source zone from A to B, and the higher concentrations at the vertical profile despite their longer contact time with the media, indicate a larger oxidant demand across the coarse-grained PCE source than the rest of the cell. This is important to note as it may indicate hydrogen peroxide consumption during oxidation of PCE.

A.3.3.2. Remediation Performance - Contaminant Mass Distribution. Figures A.4 (hydrogen peroxide Cells 1-4) and A.5 (permanganate and control Cells 5-8) demonstrate PCE concentration versus time for each sampling port for each 2-D cell run to give a visual impression of aqueous PCE mass distribution in the cells throughout the experiments. For Cells 1, 2, 5, and 7, the oxidation phase is the period between 72 and 80 hours (x-axis). For Cells 3, 4, 6, and 8, the oxidation phase is the period between 72 and 96 hours (x-axis). Note that post-oxidation ground water delivery velocities are equivalent for all cells, allowing for comparison of remediation performance between cells (12 cm/d). For ease of viewing, the experimental phases are approximately demarcated on the graphs, the pre-oxidation phase marked in grey, the oxidation phase in purple, and the post-oxidation phase in yellow.

A number of interesting trends can be discerned from this data. The vertical profile data (center of figure) demonstrate that in all 8 cells, the PCE mass is centralized near the source zone (i.e., limited vertical migration). In general, PCE concentrations decrease or remain stable when oxidant flushing begins, which is expected. However, in a few notable instances, they actually increase. The first instance was observed in Cell 3, along the vertical profile. A very noticeable rise in concentrations occurs at the C and D sampling locations, and a smaller but detectable rise also occurs within the cell effluent. However, sharp drops in concentrations occur all along the horizontal profile, indicating oxidation was destroying PCE. This rise in the C and D ports could potentially be caused by the upward migration of gas bubbles, which result from the decomposition of the oxidant. Gas bubbles can mobilize both DNAPL as well as vapor phase contamination, and the resulting mass transfer from the altered contaminant source can cause contaminant concentrations to rise where they were previously undetectable. However, in the case of Cell

3, the concentrations quickly drop again, potentially indicating that oxidation was destroying the contamination that it had mobilized. In permanganate Cell 5, a similar trend is noted, but only at sample port D and to a smaller degree than Cell 3. With permanganate, precipitation of manganese oxide solids, as opposed to gas generation, may have been responsible for alterations in the aqueous PCE distribution. Port D is located down-gradient, and slightly above the PCE source. Since the DNAPL is confined to a coarse sand lens, deposition of solids in this lens may potentially force more ground water to flow through surrounding fine grained media, resulting in vertical flow of contaminated ground water. If this occurred, this vertical flow might have reached sample port D, causing the elevation in concentrations. However, like Cell 3, these elevated concentrations quickly dropped again as the oxidation phase continued, probably due to oxidation of the contaminant.

Permanganate Cell 6 also witnessed elevated PCE concentrations during the oxidation phase, but behaved much differently than these previous two. This cell had a large spike in the aqueous PCE concentrations which began at the start of the oxidation phase, and moved along the horizontal profile. It was not observed at the A port, but seen at the B port and a little later at the G and E ports. The H port notices the spike almost immediately into the oxidation phase, as does the effluent, despite these ports being well down-gradient of the oxidant influent chamber. The exact cause of this spike is unknown. One possible theory results from the fact that this same cell saw significant density driven advection of permanganate downward during the initiation of the oxidant flush, as was mentioned earlier with respect to oxidant delivery. Because of this downward movement of fluid at the beginning of the oxidation phase, it may have subsequently displaced the less dense contaminated aqueous phase upward, potentially causing a momentary alteration in the flow paths through the cell during oxidant flushing initiation. This resulting alteration of the flow field may have caused the spike by moving contaminated ground water through the sampling array in ways which are atypical in comparison to the pre-oxidation phase. Regardless of the cause, at all sampling locations, after this initial spike had passed, the concentrations rapidly drop, indicating oxidation was occurring.

Figures A.4 and A.5 also give information about remediation performance, such as the rebound of contamination after the oxidation phase. Comparing the permanganate systems, a more rapid and extensive rebound in the horizontal profile data (left-hand side of figure) was observed in the slower oxidant delivery system (Cell 6) than the fast oxidant delivery system (Cell 5). The vertical profile data in this figure (center) and the effluent data (right) also demonstrate this effect. This may be explained by DNAPL mass removal data, which are presented later (Table A.10). Cell 5 resulted in a much higher percentage of DNAPL mass destruction than Cell 6, which in turn may have reduced the magnitude and spatial distribution of the contamination rebound that occurred after oxidant flushing ceased. However, an opposite effect was noted in the hydrogen peroxide cells, with a more rapid and extensive rebound observed in the horizontal profile data (left-hand side of figure) under faster oxidant delivery systems (Cells 1 and 2) than the slower delivery systems (Cells 3 and 4). In comparing of the oxidant systems to the no oxidant controls, permanganate appears to have had a greater impact on the PCE mass distribution than hydrogen peroxide as evidenced by more pronounced differences in permanganate data vs. control than in hydrogen peroxide data vs. control. This is due to permanganate appearing to have slower and less rebound than the hydrogen peroxide systems, as well as the complex reactive transport discussed earlier concerning the concentration spikes in permanganate Cell 6.

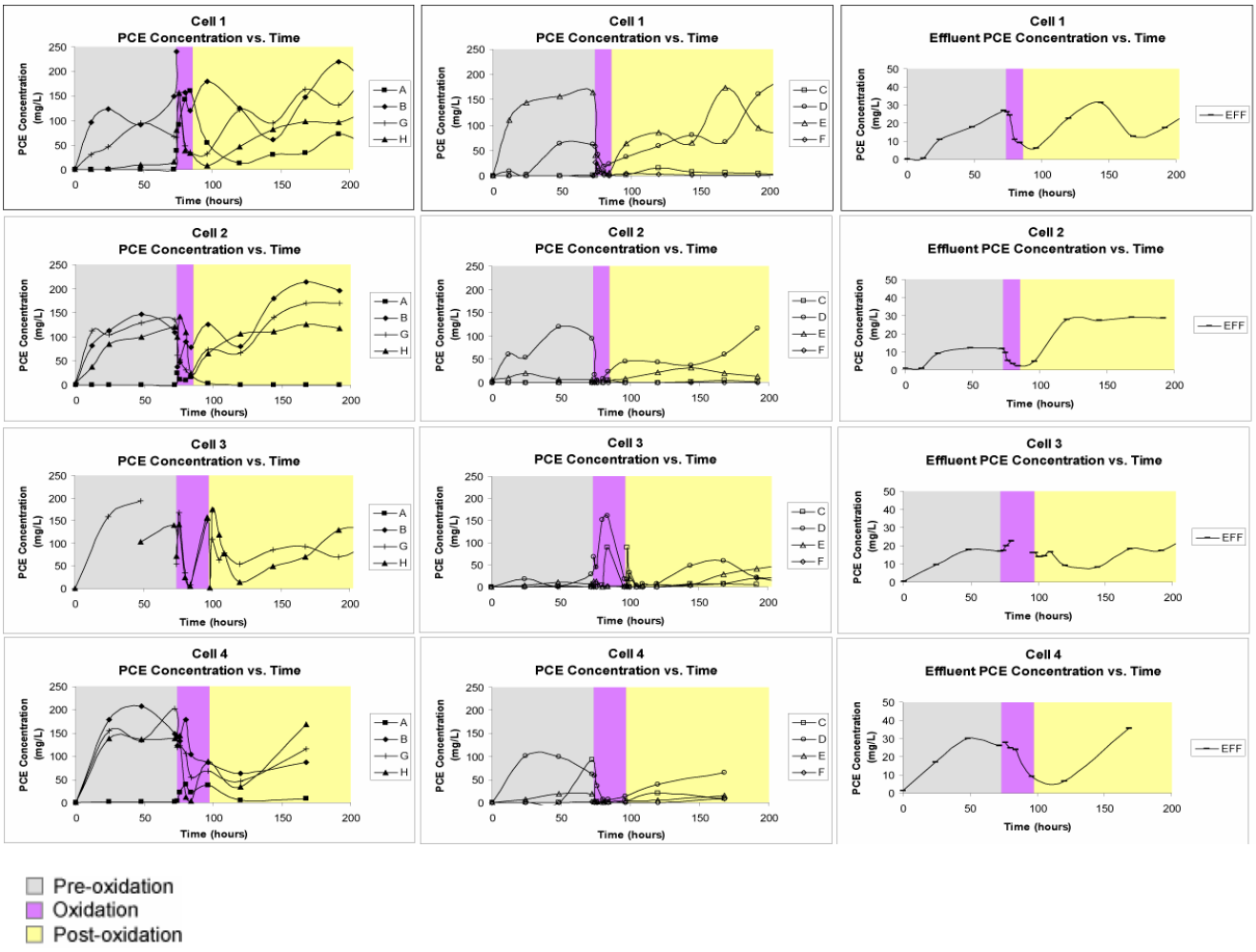

Figure A.4. PCE distribution for CHP cells (Cells 1-4). Left side graphs present horizontal profile data, center graphs present vertical profile data, and right graphs present cell effluent data. For Cells 1 and 2, "during oxidation" is the period between 72 and 80 hours (x-axis). For Cells 3 and 4, "during oxidation" is the period between 72 and 96 hours (x-axis).

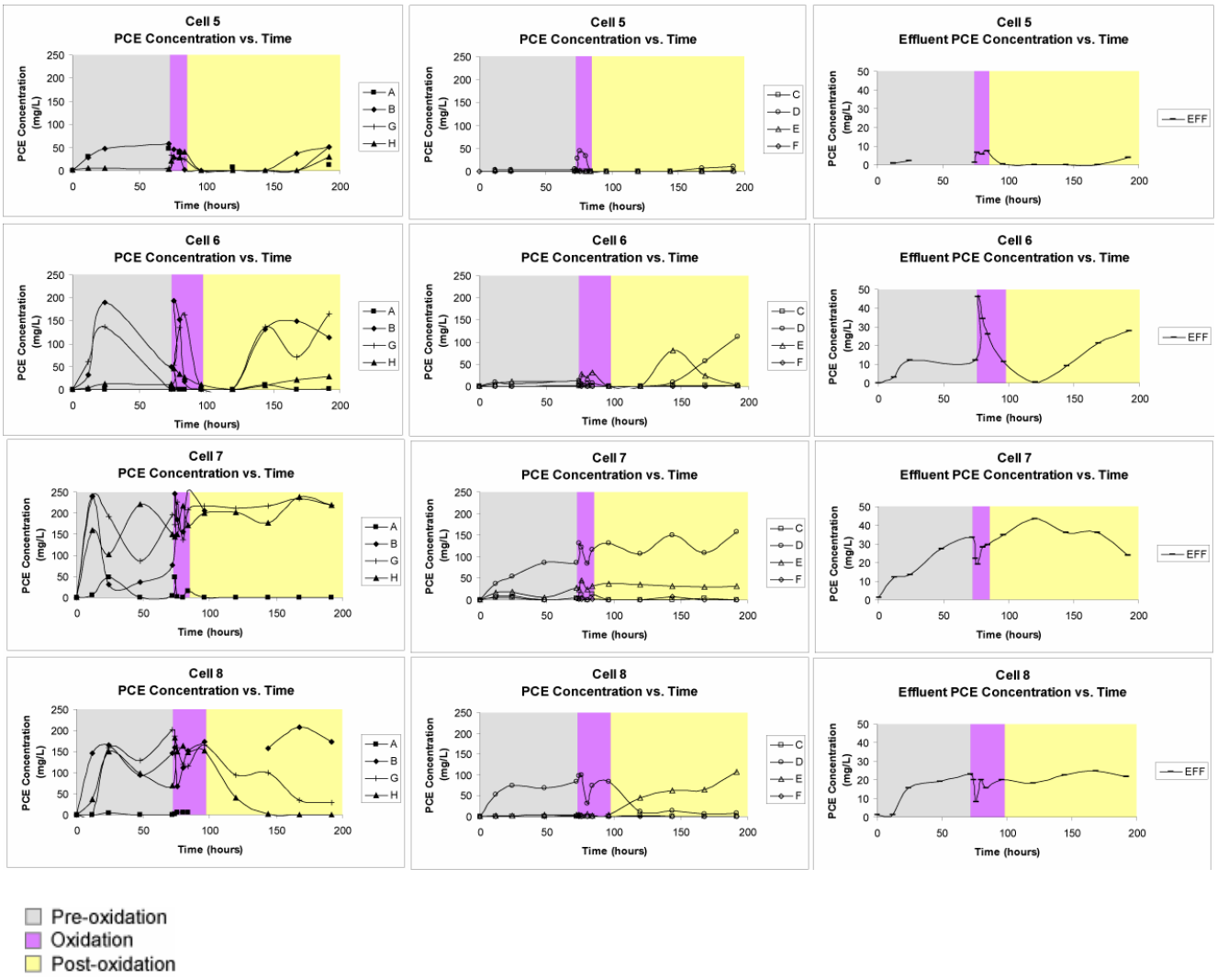

Figure A.5. PCE distribution for permanganate and no oxidant control cells (Cells 5-6). Left side graphs present horizontal profile data, center graphs present vertical profile data, and right graphs present cell effluent data. For Cells 5 and 7, "during oxidation" is the period between 72 and 80 hours (x-axis). For Cells 6 and 8, "during oxidation" is the period between 72 and 96 hours (x-axis).

A.3.3.3. Remediation Performance - System pH. Figure A.6 includes pH data from hydrogen peroxide Cells 1-4 and permanganate Cell 6. Cell 5 data were incomplete and are not shown here. Control Cells 7 and 8 are not presented, but both controls had a less than 1.5 pH unit difference between maximum and minimum pH over the course of the experiment from all ports, with pH very slowly increasing with time. Hydrogen peroxide Cells 1-3 implemented a pH adjustment approach using a strong acid flush to reduce the cell pH to assist with hydrogen peroxide activation. Cells 1 and 2 involved mixing a pH 3 $FeSO_4$ solution with the hydrogen peroxide directly at the influent port just before moving into the 2-D cell. Cell 3 was implemented similarly, however the pH 3 solution contained no $FeSO_4$ and

natural iron present in the porous media was relied upon to activate the oxidant. Cell 4 employed a citric acid flush for chelation of iron associated with the porous media to aid in oxidant activation and control. A drop in pH in Cell 4 during the oxidation phase is indicative of the citric acid flush, but the pH of the hydrogen peroxide flushing solution was not adjusted prior to introduction into the cell, and thus the pH rebounded when this solution entered the cell. Potassium permanganate Cell 6 involved no pH adjustment. The pH within this cell remained fairly constant throughout the pre-oxidation and most of the oxidation phases, but late in the oxidation phase, the pH reduced along the horizontal profile, with its lowest point at location A, and gradually increasing pH down-gradient toward location H. During the post-oxidation phase in this cell, some of the ports on this horizontal profile actually saw an increase in pH to levels higher than during the pre-oxidation phase. However, the pH always remained lowest at A and increased moving down-gradient.

The pH effects were as anticipated for all 2-D cells, considering the pH adjustments made to Cells 1-3, the small changes observed in Cell 4, and the competing potential pH effects in permanganate systems. In permanganate systems, both increases and decreases in pH can occur – a decrease as a byproduct of reaction between permanganate and PCE (as observed in some ports), and an increase as a result of the interaction of permanganate with carbonate materials (as observed in other ports).

A.3.3.4. Remediation Performance - Cation Concentrations. Figure A.7 presents concentrations of major cations over time from the effluent for each 2-D cell for which data was available (Cells 5 and 8 had incomplete data sets). Concentrations were measured for calcium, magnesium, iron, manganese, zinc, sulfur, sodium and potassium. Iron increased in the effluent of Cells 1 and 3, but not in Cells 2 and 4. In all of the hydrogen peroxide cells, regardless of activation method, calcium, magnesium and zinc increased in the effluent. Sodium and potassium increased in Cells 1 and 2, while sodium decreased and potassium remained constant in Cells 3 and 4. Sulfur remained steady in Cells 1-3, but strongly increased in citric acid activated Cell 4. In permanganate Cell 6, potassium and sodium strongly increased, as would be expected by the addition of $KMnO_4$ and possible resulting ion exchange (sodium) within the media. A slight decrease in calcium concentrations was noted from Cell 6, while iron, zinc, sulfur, and magnesium were all relatively constant. A small increase in potassium mobility was noted in no oxidant control Cell 7, while all other metals were constant. No appreciable manganese mobility in the effluent was observed in any of the cells.

The hydrogen peroxide cells demonstrated the greatest extent of metals mobility, as almost all cation concentrations measured in cell effluent in were greater than those measured in control Cell 7. These elevated metals concentrations may be attributable to interactions between the oxidant, the contaminant and the porous media, or delivery of the oxidant itself (i.e. iron in the case of CHP, potassium and manganese in the case of $KMnO_4$). Of the hydrogen peroxide cells, Cell 4 demonstrated the greatest differences in cation concentrations compared to control systems. This cell employed the metal chelator, citric acid, to aid in oxidant activation and stabilization, therefore these differences were anticipated to an extent.

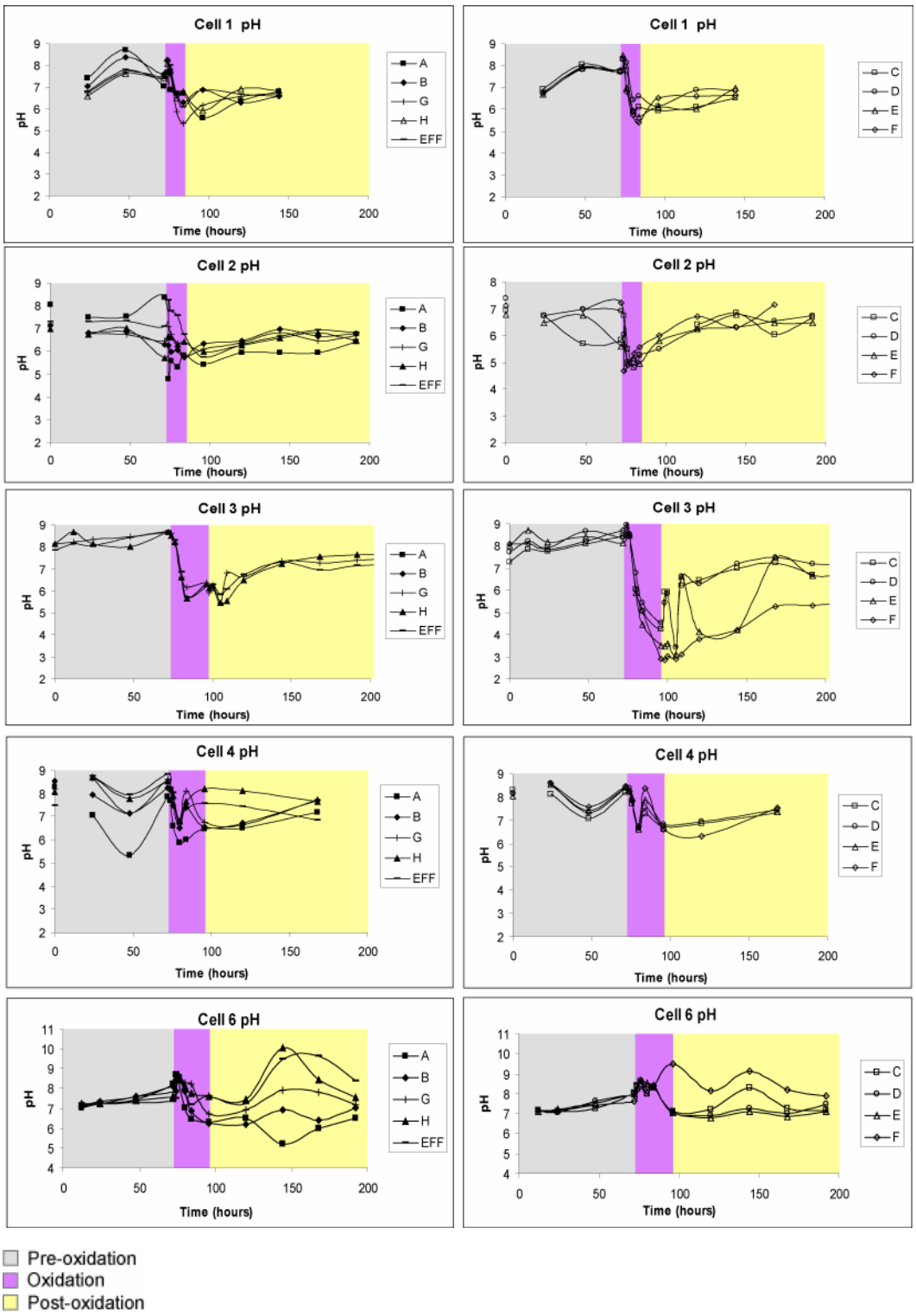

Figure A.6. pH data from hydrogen peroxide Cells 1-4 and permanganate Cell 6. Cell 1-3 involved a strong acid flush to drop the pH to activate the hydrogen peroxide. Cell 4 utilized a citric acid flush with no deliberate pH adjustment for activation. The permanganate Cell 6 involved no pH adjustment. Please note the change in scale for Cell 6.

There are also differences between permanganate and control systems, although not as pronounced as differences between CHP systems and control systems. The most significant difference is with potassium. This was anticipated due to the introduction of permanganate as $KMnO_4$. Note that little excess Mn was observed in permanganate Cell 6 compared to controls. Because the pH remained relatively neutral, the Mn would be anticipated to be primarily in the MnO_2 form, either depositing within the 2-D cell or filtered from the effluent samples as solids.

Unfortunately instrumentation difficulties led to incomplete data sets for many of the 2-D cell's cation extraction procedure performed on soil cores post-treatment. Two complete data sets are available for Cells 3 and 4. Data for major cations for these cells are displayed in Figure A.8. One additional 2-D cell has complete data sets for only DI-exchangeable and BaCl-exchangeable cations – Cells 6. These data are presented in Figure A.9. Refer to Figure A.3 for the coring diagram.

Hydrogen peroxide Cell 4 results show substantially greater DI- and BaCl-extractable cations than hydrogen peroxide Cell 3. Again, citric acid, a metal chelator, was employed in Cell 4 so these results are not unexpected. Cell 3 has greater cation concentrations, in general, in the acid dissolution solution than Cell 4, further indicating they are less extractable without the citric acid flush. The results for DI- and BaCl-extractable cations of permanganate Cell 6 are more similar to those of hydrogen peroxide Cell 3 than those of Cell 4 (which employed citric acid). The primary difference in the results between Cells 3 and 6 is the higher extractable sulfur in the permanganate cell. Clearly further research is necessary with respect to the mechanisms of interaction of the oxidants with porous media in order to determine the predictability of these observed effects, as well as research with respect to the geochemical impacts of the use of chelates in free-radical reaction pathways such as those in CHP systems (and the oxidant persulfate).

A.3.3.5. Parameters Impacting Efficiency and Effectiveness. There have been 5 terms employed throughout SERDP project CU-1290 to describe oxidation efficiency and effectiveness. These include (1) reaction rate constants for oxidant and DNAPL depletion ($time^{-1}$), (2) media demand (mg-oxidant/kg-porous media), (3) oxidant demand (mol-oxidant/mol-DNAPL), (4) the percent (%) DNAPL destroyed, and (5) the relative treatment efficiency (RTE), which compares the rate of oxidant depletion to the rate of DNAPL destruction. The rate constants give information about how fast contaminant is being depleted within the subsurface, also as providing quantitative information about the persistence of the oxidant. The media demand and the oxidant demand give quantitative design information about how much oxidant dosing is required overcome the demand of the media and to treat the DNAPL. The percent DNAPL destroyed indicates the overall performance of the remedial action in terms of mass removal, and the RTE gives an idea of how efficient the system is performing by relating the oxidant persistence to the DNAPL destruction rate. A lower RTE indicates better performance with RTE values of 1 or less being considered efficient because contaminant is being destroyed faster than oxidant is being depleted.

A.3.3.5.1. Oxidant and PCE degradation rates. The oxidant concentration data from the horizontal profile in Table A.8 allow for estimation of the rate of oxidant degradation within each cell. By calculating the cell retention time associated with each sampling point based on the oxidant delivery velocity, a first order oxidant depletion effective rate constant (k') can be calculated. These are effective rate constants because they do not separate the effects of oxidant dilution from oxidant degradation. Similarly, concentrations for PCE along the horizontal profile allow for estimation of the DNAPL depletion rate, using the same approach. These rate constants are presented in Table A.9.

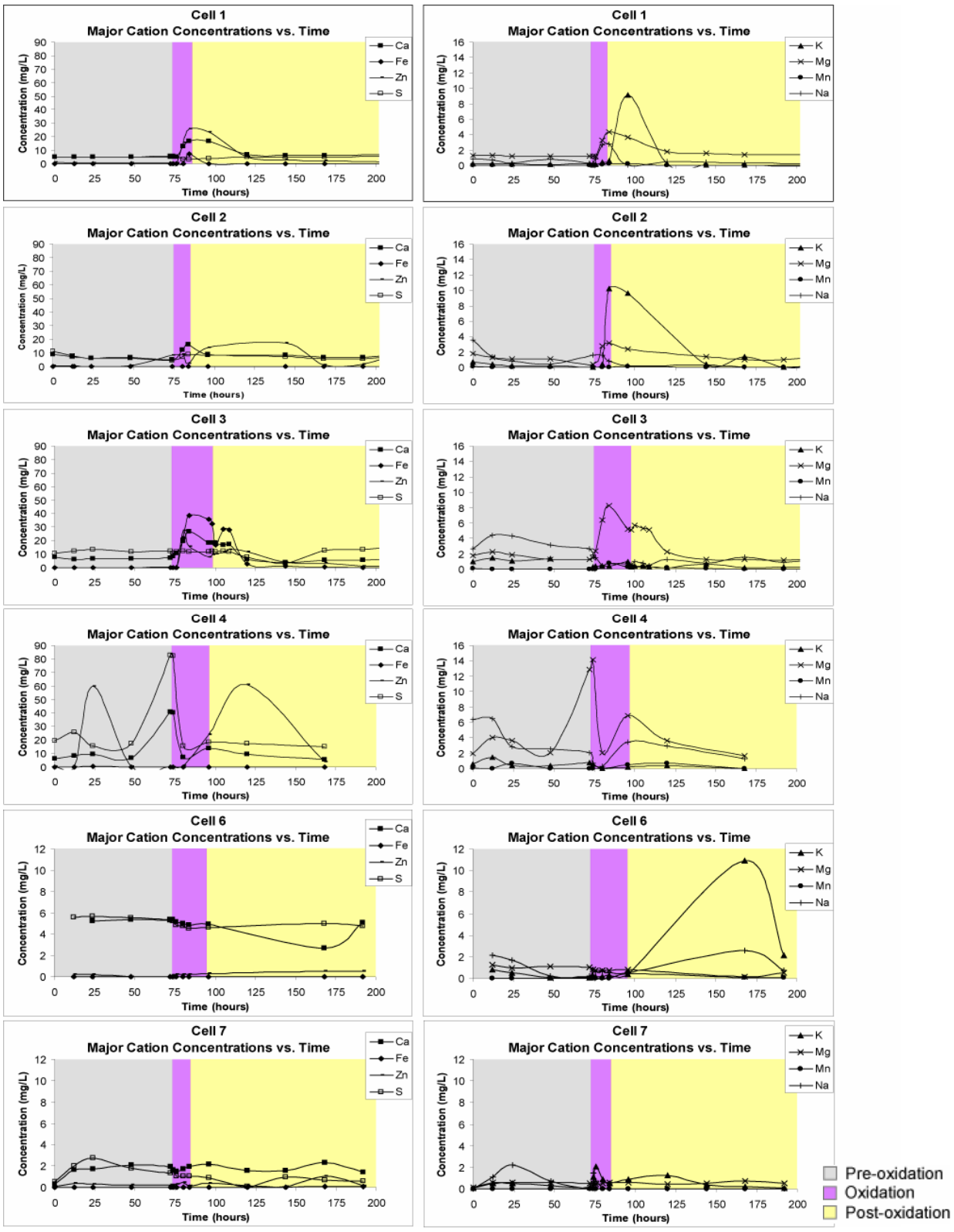

Figure A.7. Major cations in the effluent for Cells 1-4 and 6-7. For Cells 1, 2, and 7, "during oxidation" is the period between 72 and 80 hours (x-axis). For Cells 3, 4, and 6, "during oxidation" is the period between 72 and 96 hours (x-axis).

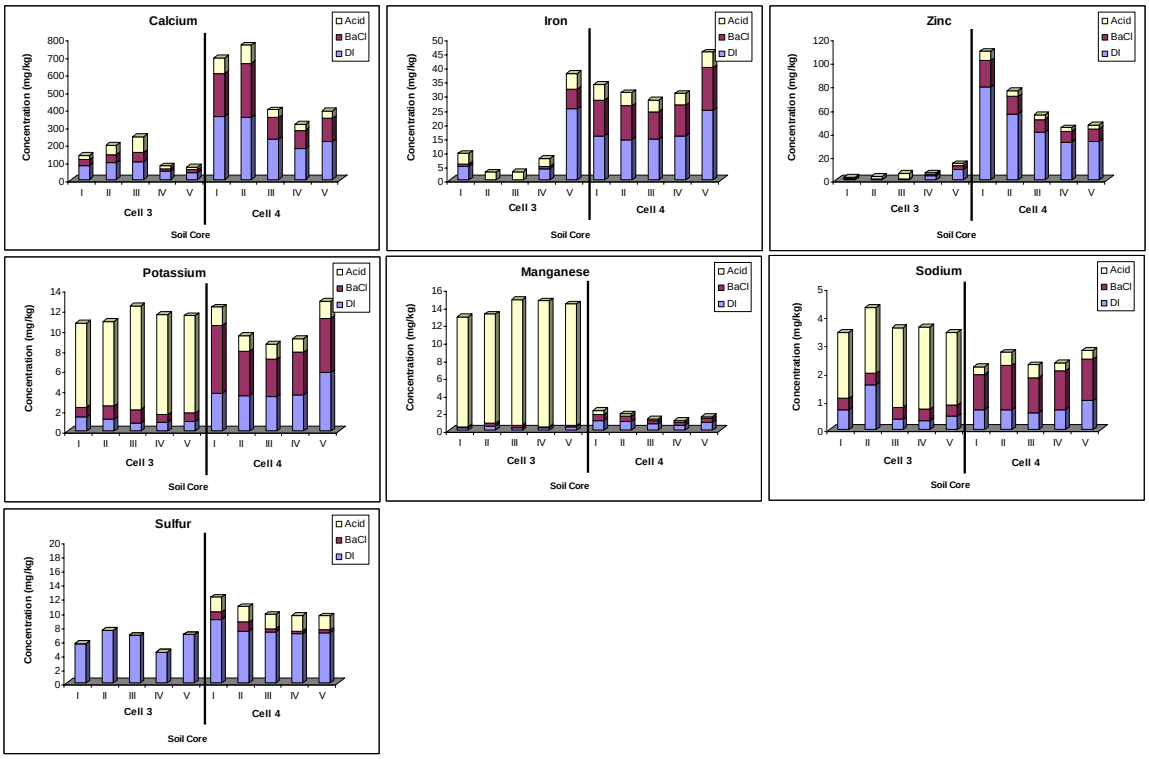

Figure A.8. DI-exchangeable and BaCl exchangeable cation concentrations and cation concentrations resulting from extraction with hydroxylamine hydrochloric acid plus nitric acid for 2-D Cells 3 and 4.

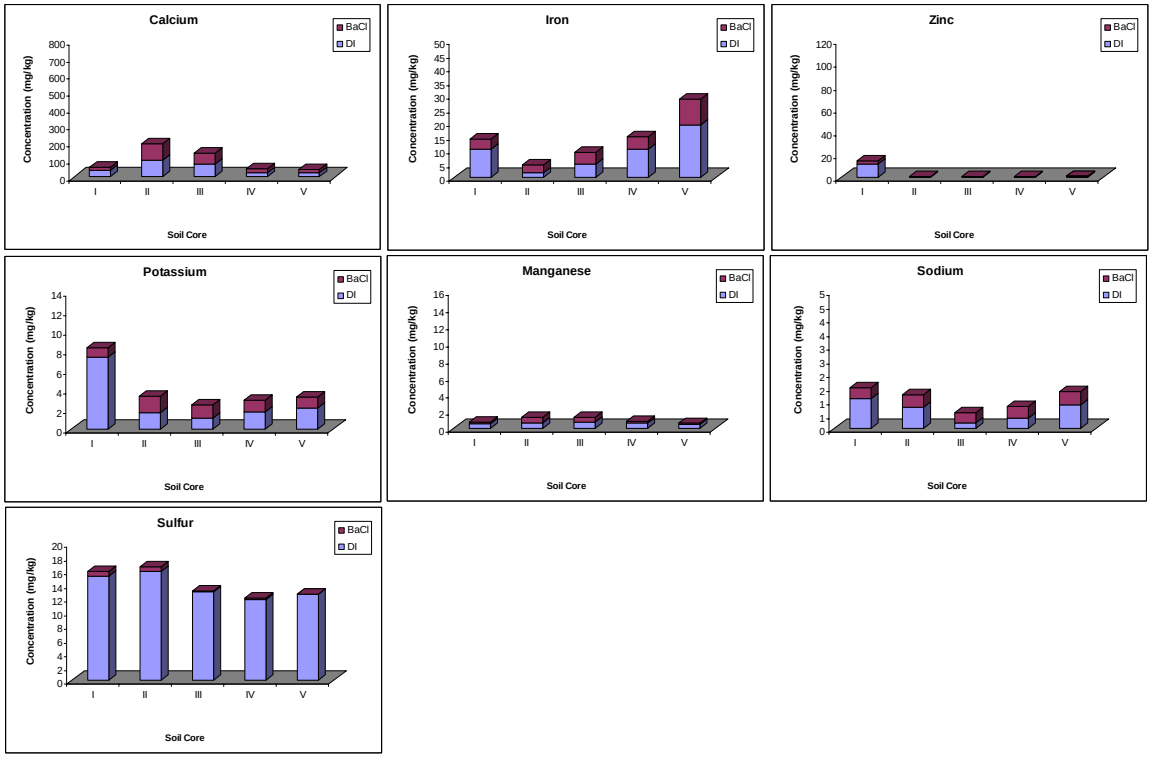

Figure A.9. DI-exchangeable and BaCl exchangeable cation concentrations for Cell 6.

Table A.9. PCE and oxidant depletion rates within the 2-D cell.

Cell ID	Oxidant delivery	PCE depletion rate k' (day^{-1})	R^2 for k' linearization	Oxidant depletion rate k' (day^{-1})	R^2 for k' linearization
1	Pressurized	-11.1	0.94	Not available*	
2	Pressurized	-14.8	0.96	-11	0.63
3	Gravity feed	-3.3	0.97	-2.3	0.87
4	Gravity feed	-3.6	0.66	-9	0.95
5	Pressurized	-7.5	0.67	Not available*	
6	Gravity feed	-1.8	0.82	-1.4	0.99
7	Pressurized	-3.2	0.99	Not applicable**	
8	Gravity feed	+1.4	0.85	Not applicable**	

*Not available due to inability to calculate based on available data values
**Not applicable to control systems with no oxidant introduction

Oxidant depletion after the A port measurement can be attributed both to reaction with the PCE as well as interaction with the porous media. The lower the k' value, the more persistent the oxidant is within the 2-D cell. Oxidant persistence is desirable; however it is important to be aware that a lower oxidant depletion rate may also be indicative of slower or less contaminant destruction. The rate of permanganate depletion was slower than the rate of hydrogen peroxide consumption. Also, the higher concentration hydrogen peroxide cell experienced more rapid oxidant decomposition than equivalent lower concentration systems. The k' values for oxidant depletion will be discussed further below with respect to contaminant destruction efficiency (RTE values).

The data shows that PCE depletion was fastest in Cells 1 and 2, the hydrogen peroxide cells with the faster oxidant delivery velocity. Recall that the slower oxidant delivery velocity cells had very little oxidant present at the B port (source zone), which likely impacted this depletion rate. The same effect is observed in permanganate systems, where faster PCE depletion occurred with the faster oxidant delivery velocity. Note that the rate calculations are a function of cell retention time, which accounts for the oxidant delivery velocity itself, therefore the differences can be attributed to actual differences in the PCE destruction rate. It is probable that the faster delivery velocity allowed for a rapid supply (due to delivery velocity) of a higher concentration of oxidant (due to lower NOD as a result of less contact time) with respect to the ability of PCE to transfer to the dissolved phase (rate and extent). Increased velocity also increases the DNAPL mass transfer rate, which can then make more aqueous phase PCE available for degradation. Further studies are necessary with even greater delivery velocities to determine if a point exists at which an increased velocity reaches a "point of diminishing returns" where increased velocity no longer increases the PCE mass depletion rate. For more insight into the relationships between velocity and oxidant concentrations on DNAPL mass depletion rates, see Petri 2006. It is anticipated that a "too fast" delivery velocity would be achieved where the oxidant bypasses the PCE at a rate faster than it is able to dissolve.

A.3.3.5.2. Other Measures of Oxidation Efficiency and Effectiveness. Table A.10 contains values for the other four measures of remediation efficiency and effectiveness. The media demand calculations assume an estimated average porous media bulk density for the entire cell (gravel influent and effluent, coarse base sand lens, fine-grained silica sand) of 1.5 g/cm^3 (reported by Seitz (2004)). Oxidant demand results are based on estimates of oxidant depletion as described above, along with estimates of PCE destruction based on chloride measurements. The percent DNAPL destroyed is also based on chloride measurements. The RTE values were calculated based on the oxidant and PCE depletion rate values presented in Table A.9.

Table A.10. Efficiency and effectiveness values based on 2-D cell results.

Cell ID	Media demand (mg/kg)	Oxidant demand (mol/mol)	Percentage DNAPL destroyed	Relative treatment efficiency (RTE)
1	7273	2257	1.2	Not available*
2	24773	812	11	0.74
3	6136	223	9.9	0.7
4	6136	1817	1.2	2.5
5	Not available*	Not available*	66.5	Not available*
6	1818	4	32.3	0.78
7	1802***	Not applicable**		
8	1802***	Not applicable**		

*Not available due to inability to calculate based on existing data values
**Not applicable to control systems with no oxidant introduction
***Background, clean (no PCE) media demand values based on NOD studies conducted for Task 2

It is important to consider the relative rate of oxidant depletion and PCE destruction. The ideal system will have relatively slow oxidant depletion with rapid PCE destruction (low RTE value). Table A.10 provides the RTE values for Cells 2, 3, 4, and 6. Cells 2 and 3 demonstrate a similar RTE value for slower and faster oxidant delivery velocities, however these two cells also differ in oxidant concentration (10% for 2 and 3% for 3), which make these values difficult to compare. It is interesting to note the similarity between two of the hydrogen peroxide cell values (Cells 2 and 3) and the permanganate system value (Cell 6), and also that these values are all less than 1, which indicates very efficient oxidation.

The media demand and oxidant demand values further represent oxidation efficiency, with lower values indicative of more efficient oxidation. The CHP systems demonstrate significantly higher values for both media demand and oxidant demand compared to the permanganate values calculated. In fact, the permanganate system shown in Table A.10 had an oxidant demand value of 4, which is not substantially different from the theoretical value of 1.33.

The ultimate measurement of oxidation effectiveness is the % PCE destroyed. Permanganate demonstrated greater contaminant destruction than the CHP systems. Hydrogen peroxide delivered at a higher initial concentration demonstrated more extensive PCE destruction (comparing Cells 1 and 2). There is not an apparent velocity effect with respect to the CHP systems. There is, however, an apparent velocity effect for permanganate, with more extensive PCE oxidation occurring in the faster delivery systems. This might be due in part to the effectiveness of delivery of the permanganate during the oxidation phase. Cell 6 had the lower delivery velocity, and also had downward density driven advection of permanganate in the cell. If a larger mass of this permanganate was able to sink below the PCE source due the lower delivery velocity, then despite similar mass additions of permanganate to Cells 5 and 6, Cell 6 may have received less oxidant contact in the contaminated areas.

A.3.4. Conclusions and Implications

A.3.4.1. Conclusions. In summarizing the conclusions of these studies, it's important to note that there are a wide variety of approaches for delivery of oxidants. These studies evaluated a limited number of approaches, with primary differences in delivery velocity (two conditions), two different oxidants ($KMnO_4$ and CHP), delivery concentration (two conditions for CHP), and three means of activating or

stabilizing hydrogen peroxide (low pH soluble iron, low pH natural mineral, neutral pH citric acid-iron chelation).

Oxidant delivery and distribution:

- A greater percentage and mass of hydrogen peroxide was consumed within the 2-D cells than permanganate.
- Hydrogen peroxide consumption was more rapid than permanganate based on effective 1st order depletion rate constant calculations.
- A greater mass and rate of hydrogen peroxide consumption results with slower delivery velocities and higher initial oxidant concentration.
- Extensive hydrogen peroxide decomposition occurred prior to reaching the PCE source located 2.5 to 5.0 cm into the cell (1.25 to 10 hours of media contact time, depending on the delivery velocity).
- Extensive gas generation resulting from hydrogen peroxide decomposition can affect the flow field under confined aquifer conditions.
- Permanganate was subject to density-driven flow within 15 cm of delivery distance, and this flow may have altered contaminant transport within the cell.

PCE mass distribution:

- Faster oxidant delivery conditions with CHP resulted in more extensive and rapid rebound of PCE during the post-oxidation phase, despite equivalent ground water velocities during this phase.
- More extensive and rapid rebound of PCE occurred post-oxidation with permanganate under slower delivery conditions, possibly due to the lower mass removal at lower velocities, again despite equivalent ground water delivery velocities.
- Increases in PCE concentration occurred during permanganate delivery, indicative of enhanced DNAPL mass transfer due to oxidation.
- Permanganate exerted a greater positive impact on PCE mass distribution than CHP as evidenced by comparison to control systems.

PCE oxidation efficiency and effectiveness:

- PCE was degraded more rapidly in CHP systems than in permanganate systems.
- Faster delivery of both oxidants resulted in more rapid PCE destruction than slower delivery.
- Efficient oxidation of PCE resulted with both CHP and permanganate as evidenced by comparing the rate of oxidant depletion to the rate of contaminant destruction (relative treatment efficiency < 1).
- Permanganate resulted in more efficient oxidation of PCE than CHP as evidenced by media demand and oxidant demand values.
- Permanganate resulted in more effective oxidation of PCE than CHP as evidenced by % DNAPL destroyed values.
- Faster permanganate delivery resulted in more effective PCE destruction than slower permanganate delivery.

Geochemical effects:

- Elevated cation concentrations occurred in 2-D cell effluent during and post-oxidation with both permanganate and CHP systems compared to no oxidant control systems.
- CHP systems had greater cation concentrations in cell effluent during and post-oxidation than permanganate cells.
- The CHP system with citric acid had the most pronounced elevation in effluent cation concentrations.

- Porous media core extraction data emphasize the important impacts the use of citric acid can have on system geochemistry, with higher values of extractable cations resulting in the citric acid system.

A.3.4.2. Implications. The results of these 2-D cell studies provide evidence of the important interactive relationship of oxidant delivery velocity and concentration with respect to oxidation efficiency and effectiveness. An important next step is to employ these data in system modeling efforts to evaluate optimum delivery conditions and to understand the boundary conditions with respect to the extrapolation of the findings of these studies to the field scale. The important general implications of the findings of these studies include:

- DNAPL oxidation, in general, can be efficient with both oxidants with respect to the relative rates of oxidant consumption and contaminant destruction.
- Permanganate offered more efficient PCE DNAPL oxidation in the 2-D cells studies as evidenced by the media demand, oxidant demand, and % contaminant destroyed values for these systems.
- One pore volume (1 PV) of oxidant delivered at 2-10x the stoichiometric demand of the oxidant for the contaminant is simply not enough – the maximum extent of PCE destruction this approach offered was 66.5% in the permanganate cell under faster delivery conditions.
- Several pore volumes of post-oxidation ground water flow through the contaminant source zone may be necessary to observe PCE rebound even under conditions of minimum PCE destruction.
- The key to successful CHP implementation is control of the oxidant decomposition rates, which would, in turn, positively impact gas generation issues and extensive oxidant depletion before contact with the contaminant.
- The key to successful permanganate delivery is matching the oxidant delivery velocity and concentration to contaminant type and dissolution characteristics.
- The use of metal chelates and low pH conditions with hydrogen peroxide results in geochemical changes that warrant further study and are important to monitor at the field scale.

APPENDIX B

LIST OF TECHNICAL PUBLICATIONS

B.1 INTRODUCTION

This Appendix provides a listing of technical publications that were produced under SERDP project CU-1290. Additional conference proceedings papers, journal papers, and book chapters are also in preparation but not included herein in the listing provided herein.

B.2 TECHNICAL PUBLICATIONS PRODUCED DURING THE COURSE OF PROJECT CU-1290

B.2.1. Articles or Papers Published in Journals and Magazines

B.2.1.1. Peer-Reviewed Journal Articles

Crimi, M.L. and R.L. Siegrist (2003). Geochemical Effects Associated with Permanganate Oxidation of DNAPLs. *Ground Water,* 41(4):458-469.

Crimi, M.L. and R.L. Siegrist (2004). Association of Cadmium with MnO_2 Particles Generated During Permanganate Oxidation. *Water Research,* 38(4):887-894.

Crimi, M.L. and R.L. Siegrist (2004). Impact of Reaction Conditions on MnO_2 Genesis During Permanganate Oxidation. *Journal Environmental Engineering*, 130(5):562-572.

Crimi, M.L. and R.L. Siegrist (2005). Factors Affecting Effectiveness and Efficiency of DNAPL Destruction Using Potassium Permanganate and Catalyzed Hydrogen Peroxide. *Journal of Environmental Engineering*, 131(12):1724-1732.

Haselow, J.S., R.L. Siegrist, M.L. Crimi, and T. Jarosch (2003). Estimating the Total Oxidant Demand for In Situ Chemical Oxidation Design. *Remediation Journal*, 13(4):5-16.

Petri, B.G., R.L. Siegrist, and M.L. Crimi (2006). Effects of Groundwater Velocity and Permanganate Concentration on DNAPL Mass Depletion Rates during In Situ Oxidation. *Journal of Environmental Engineering*, submitted and in review.

Sahl, J.W., J. Munakata-Marr, M.L. Crimi, and R.L. Siegrist (2006). Coupling Permanganate Oxidation with Microbial Dechlorination of Tetrachloroethene. *Water Environment Research.* Accepted and in press.

Sahl, J., and J. Munakata-Marr (2006). The Effects of In Situ Chemical Oxidation on Microbial Processes: A Review. *Remediation Journal*, 16(3):57-70.

Siegrist, R.L., K.S. Lowe, M.L. Crimi, and M.A. Urynowicz (2006). Quantifying PCE and TCE in DNAPL Source Zones: Effects of Sampling Methods Used for Intact Cores at Varied Contaminant Levels and Media Temperatures. *J. Ground Water Monitoring and Remediation,* 26, no. 2, Spring 2006, pp. 114–124.

B.2.1.2. Articles in Trade Journals and Magazines

Siegrist, R.L. (2005). In Situ Chemical Oxidation (ISCO) and Coupled Technologies for Remediation of Contaminated Groundwater. *Thai Environmental Engineering Magazine*, Vol.2, No.6 / November-December 2005. pp. 20-24. Text prepared in Thai by Professor Pongsak Noophan, Silpakorn University, Nakom Pathom, Thailand.

B.2.2. Technical Reports

Siegrist, R.L., M. Crimi, J. Munakata-Marr, T. Illangasekare, S. Van Cuyk, K. Lowe, S. Jackson, S. Seitz, J. Heiderscheidt, P. Dugan, B. Petri, and J. Sahl. *Reaction and Transport Processes Controlling In Situ Chemical Oxidation of DNAPLs*. Quarterly reports and annual progress report to the DOD Strategic Environmental Research and Development Program, April, July, October, and December 2002-2005.

B.2.3. Conference/Symposium Proceedings and Papers

See Section B.2.4. for published abstracts.

B.2.4. Published Technical Abstracts

Crimi, M.L., and R.L. Siegrist (2003). Bench-Scale Studies of Reaction Processes Controlling In Situ Chemical Oxidation (ISCO) of DNAPLs. 6th Intern. Symp. and Exhibition on Environmental Contamination in Central and Eastern Europe and the Commonwealth of Independent States. Sept. 1, 2003, Prague, Czech Republic.

Crimi, M.L., R.L. Siegrist, and S. Jackson (2004a). Chemical Oxidation of Aqueous-Phase vs. DNAPL-Phase Contaminants. Battelle's 4th Intern. Conf. on Remediation of Chlorinated and Recalcitrant Compounds. May 24, 2004, Monterey, CA.

Crimi M., R.L. Siegrist, S. Jackson, S. Seitz, T.A. Palaia, and M.A. Singletary (2004b). Optimization of Field Scale Permanganate Injection for PCE Treatment. 3rd Intern. Conf. on Oxidation and Reduction Technologies for In Situ Treatment of Soil and Groundwater. October 2004, San Diego, CA.

Crimi, M., S. Seitz, J. Sahl, J. Kopp, J. Heiderscheidt, P. Dugan, B. Petri, R. Siegrist, J. Munakata-Marr and T. Illangasekare (2005a). ISCO of DNAPLs: Applicability Based on 2-Dimensional Transport Studies of DNAPL Entrapment and Oxidant Delivery Techniques. European Conference on Oxidation and Reduction Technologies for Ex-Situ and In-Situ Treatment of Water, Air and Soil, Göttingen Germany, June 12-15 2005.

Crimi M., S. Seitz, J. Sahl, J. Kopp, J. Heiderscheidt, P. Dugan, B. Petri, and R.L. Siegrist (2005a). ISCO of DNAPLs: Applicability Based on 2-Dimensional Transport Studies of DNAPL Entrapment and Oxidant Delivery Techniques. The 21st Annual Intern. Conf. on Soils, Sediments, and Water. Oct. 17-21, 2005, Amherst, MA.

Crimi, M.L., P. Block, B., and McGinnis (2005a). Experimental Evaluation of the Use of Activated Persulfate to Destroy Lindane. The 4th Intern. Conf. on Oxidation and Reduction Technologies for In Situ Treatment of Soil and Groundwater. Oct. 23-27, 2005, Chicago, IL.

Crimi, M.L., and J. Taylor (2005). Remediation Protocol for Oxidative Destruction of BTEX Contaminants. The 1st Intern. Conf. on Challenges in Site Remediation: Proper Site Characterization, Technology Selection and Testing, and Performance Monitoring. Oct. 23-27, 2005, Chicago, IL.

Dugan, P.J., R.L. Siegrist, M.L. Crimi, and C.E Divine (2004a). Coupling flushing reagents with oxidants: effects on remediation and characterization. Battelle's 4th Intern. Conf. on Remediation of Chlorinated and Recalcitrant Compounds. May 24, 2004, Monterey, CA.

Dugan, P.J., R.L. Siegrist, M.L. Crimi, and C.E. Divine (2004b). Coupling Surfactants/Cosolvents with Oxidants: Effects on Remediation and Performance Assessment. 3rd Intern. Conf. on Oxidation and Reduction Technologies for In Situ Treatment of Soil and Groundwater. Oct. 2004, San Diego, CA.

Dugan, P.J., Siegrist, R.L., and Crimi, M.L. (2004c). Coupling surfactants/cosolvents with oxidants: Effects on site characterization and DNAPL remediation, *Eos Trans. AGU. 85*(47), Fall Meet. Suppl. Abstract H42A-07.

Dugan, P.J., R.L. Siegrist, and M.L. Crimi (2005a). Coupling Surfactants/Cosolvents with Permanganate for DNAPL Removal: Comparison of Co-Injection and Sequential Application. 4th Intern. Conf. on Oxidation and Reduction Technologies for In Situ Treatment of Soil and Groundwater. Oct. 23-27, 2005, Chicago, IL.

Dugan, P.J., R.L. Siegrist, and M.L. Crimi (2005b). Partitioning Tracer Tests: Effects on Performance Assessment After Coupling Surfactant with Oxidant for DNAPL Remediation. 4th Intern. Conf. on Oxidation and Reduction Technologies for In Situ Treatment of Soil and Groundwater. Oct. 23-27, 2005, Chicago, IL. p.77.

Heiderscheidt J.L., T.H. Illangasekare, R.L. Siegrist, and M.L. Crimi (2004). Use of Chemical Oxidation to Reduce Rate-Limited Matrix Diffusion of PCE from Low Permeability Materials and Effects on Natural Oxidant Demand. 3rd Intern. Conf. on Oxidation and Reduction Technologies for In Situ Treatment of Soil and Groundwater. Oct. 2004, San Diego, CA.

Munakata-Marr, J., P. Dugan, J. Sahl, M. Crimi, R. Siegrist and T. Illangasekare. (2005). Coupling In situ Chemical Oxidation with Pre- and Post-Oxidation Mass Removal/Mass Destruction Technologies. European Conference on Oxidation and Reduction Technologies for Ex-Situ and In-Situ Treatment of Water, Air and Soil, Göttingen Germany, June 12-15 2005.

Petri, B.G., R.L Siegrist, and M.L. Crimi (2004). Mass Transfer Impacts of Oxidant Flushing Parameters During In Situ Chemical Oxidation of Dense Non-aqueous Phase Liquids. 3rd Intern. Conf. on Oxidation and Reduction Technologies for In Situ Treatment of Soil and Groundwater. Oct. 2004, San Diego, CA.

Petri, B.G., R.L. Siegrist, and M.L. Crimi (2005). Impacts of Permanganate Flushing Parameters on Mass Transfer from Dense Non-Aqueous Phase Liquid Residuals. The 4th Intern. Conf. on Oxidation and Reduction Technologies for In Situ Treatment of Soil and Groundwater. Oct. 23-27, 2005, Chicago, IL. p.31.

Sahl, J., S. Van Cuyk, M.L. Crimi, J. Munakata-Marr, and R.L. Siegrist (2004a). Impact of Chemical Oxidation on Microbial Communities in Contaminated Ground Water Aquifer Sediments. Battelle's 4th Intern. Conf. on Remediation of Chlorinated and Recalcitrant Compounds. May 24, 2004, Monterey, CA.

Sahl, J., J. Munakata-Marr, M. Crimi and R.L. Siegrist (2004b). The impact of in situ chemical oxidation (ISCO) on DNAPL biodegradation. Accelerated Bioremediation of Chlorinated Solvents ITRC/RTDF Training Course, Denver CO, September 2004.

Sahl J., J. Munakata-Marr, M.L. Crimi, and R.L. Siegrist (2004c). Coupling In Situ Chemical Oxidation (ISCO) With Bioremediation for DNAPL Treatment. 3rd Intern. Conf. on Oxidation and Reduction Technologies for In Situ Treatment of Soil and Groundwater. Oct. 2004, San Diego, CA.

Sahl, J., M.L. Crimi, J. Munakata-Marr, and R.L. Siegrist (2005). The Impact of In Situ Chemical Oxidation on Bioremediation Processes in the Treatment of Chloroethenes. 4th Intern. Conf. on Oxidation and Reduction Technologies for In Situ Treatment of Soil and Groundwater. Oct. 23-27, 2005, Chicago, IL. p.4.

Seitz, S.J., M.L. Crimi, and R.L. Siegrist (2003). Diffusive Mass Transport Limitations for In Situ Chemical Oxidation (ISCO) of DNAPLs. 6th Intern. Symp. and Exhibition on Environmental Contamination in Central and Eastern Europe and the Commonwealth of Independent States. Sept. 1, 2003, Prague, Czech Republic.

Seitz, S.J., M.L. Crimi, and R.L. Siegrist (2004a). Diffusive Transport during In Situ Chemical Oxidation (ISCO) of DNAPL Sites. Battelle's 4th Intern. Conf. on Remediation of Chlorinated and Recalcitrant Compounds. May 24, 2004, Monterey, CA.

Seitz, S., M.L. Crimi, and R.L. Siegrist (2004b). In Situ Chemical Oxidation Applicability at DNAPL Sites with Diffusion-Dominated Low Permeability Media. The 3rd Intern. Conf. on Oxidation and Reduction Technologies for In Situ Treatment of Soil and Groundwater. Oct. 2004, San Diego, CA.

Siegrist, R.L. (2002). Fundamentals of In Situ Chemical Oxidation. USEPA workshop on In Situ Treatment of Groundwater Contaminated with Non-aqueous Phase Liquids. Dec. 10, 2002, Chicago, IL.

Siegrist, R.L. (2003). In Situ Chemical Oxidation (ISCO): Principles and Practices for Source Zone Treatment. Invited presentation to NRC Committee on Source Removal of Contaminants in the Subsurface. Apr. 14, 2003, Washington, D.C.

Siegrist, R.L., M.L. Crimi, N. Thomson, and R. Watts (2004). In Situ Chemical Oxidation for DNAPL Source Zone Treatment. SERDP/ESTCP Symposium on Meeting DOD's Environmental Challenges. Dec. 2, 2004, Washington, D.C.

Siegrist, R.L. (2005a). In Situ Chemical Oxidation for DNAPL Source Zone Treatment. Invited Seminar, Danish Technical University. Jan. 2005, Lynnby, Denmark.

Siegrist, R.L. (2005b). Remediation of Contaminated Sites Using In Situ Chemical Oxidation and Coupled Technologies. Invited Seminar, Kasekart University. Mar. 2005, Bangkok, Thailand.

Siegrist, R.L. (2006a). Site Remediation Using Chemical Oxidation Techniques. Invited presentation at the NATO/CCMS Pilot Study meeting, "Prevention and Remediation in Selected Industrial Sectors: Small Sites in Urban Areas." June 4-7, 2006, Athens, Greece.

Siegrist, R.L. (2006b). Chemical Oxidation for Clean Up of Contaminated Groundwater. Invited presentation at the NATO Advanced Research Workshop, "Environmental Security Threats in Urban Settings", June 8-9, 2006, Athens, Greece.

Siegrist, R.L., M.L. Crimi, J. Munakata-Marr, T. Illangasekare, P. Dugan, J. Heiderscheidt, B. Petri, and J. Sahl (2006). Remediation of Contaminated Sites Using In Situ Chemical Oxidation and Coupled Technologies. Invited presentation at the NATO Advanced Research Workshop on "Methods and Techniques for Cleaning Up Contaminated Sites", October 9-11, 2006, Sinaia, Romania.

Taylor, S., M.L. Crimi, and R.L. Siegrist (2002). Comparative Evaluation of Contaminant Degradation Kinetics and Efficiency during In Situ Chemical Oxidation of DNAPLS. 2nd Intern. Conf. on Oxidation and Reduction Technologies for In Situ Treatment of Soil and Groundwater. Nov. 17, 2002, Toronto, Ontario.

B.2.5. Published Book Chapters and Student Theses/Dissertations

B.2.5.1. Book Chapters

Siegrist, R.L., M.L. Crimi, J. Munakata-Marr, T. Illangasekare, P. Dugan, J. Heiderscheidt, B. Petri, and J. Sahl (2006). Chemical Oxidation for Clean Up of Contaminated Groundwater. Invited book chapter for "Methods and Techniques for Cleaning Up Contaminated Sites", proceedings of the NATO Advanced Research Workshop in Sinaia, Romania, October 9-11, 2006.

B.2.5.2. M.S. Theses or Ph.D. Dissertations

Dugan, P. (2006). Coupling In Situ Technologies for DNAPL Remediation and Viability of the PTT for Post-Remediation Performance Assessment. Ph.D. Dissertation, Environmental Science and Engineering Division, Colorado School of Mines, Golden, CO. December 2006.

Heiderscheidt, J.L. (2005). DNAPL Source Zone Depletion During In Situ Chemical Oxidation (ISCO): Experimental and Modeling Studies. Ph.D. Thesis, Environmental Science and Engineering Division, Colorado School of Mines, Golden, CO. August 2005.

Jackson, S.F. (2004). Comparative Evaluation of Potassium Permanganate and Catalyzed Hydrogen Peroxide during In Situ Chemical Oxidation of DNAPLs. M.S. Thesis, Environmental Science and Engineering Division, Colorado School of Mines, Golden, CO. January 2004.

Petri, B.G. (2006). Impacts of Subsurface Permanganate Delivery Parameters on Dense Nonaqueous Phase Liquid Mass Depletion Rates. M.S. Thesis, Environmental Science and Engineering Division, Colorado School of Mines, Golden, CO. January 2006.

Sahl, J. (2005). Coupling In situ Chemical Oxidation (ISCO) with Bioremediation Processes in the Treatment of Dense Non-aqueous Phase Liquids (DNAPLs). M.S. Thesis, Environmental Science and Engineering Division, Colorado School of Mines, Golden, CO. April 2005.

Seitz, S.J. (2004). Experimental Evaluation of Mass Transfer and Matrix Interactions during In Situ Chemical Oxidation Relying on Diffusive Transport. M.S. Thesis, Environmental Science and Engineering Division, Colorado School of Mines, Golden, CO. December 2004.

APPENDIX C

OTHER TECHNICAL MATERIAL

C.1 INTRODUCTION

This Appendix provides a listing of patents, protocols, EPA/State regulatory permits, Awards, and scientific/technical honors received during and as a result of SERDP project CU-1290.

C.2. OTHER MATERIALS

C.2.1. Patents

Dugan, P.J., R.L. Siegrist, and M.L. Crimi (2006). "Methods and Compositions for Treatment of Subsurface Contaminants". Non-provisional patent application 187105-US-2 filed with the United States Patent Office on October 21, 2006.

C.2.2. Awards and Honors

1. SERDP Project CU-1290, "Reaction and Transport Processes Controlling In Situ Chemical Oxidation of DNAPLs", was awarded "The Outstanding Project of the Year Award" by the DOD Strategic Environmental Research and Development Program (SERDP) during a ceremony in Washington, D.C. in December 2005. Drs. Crimi, Munakata-Marr, and Illangasekare were co-PI's on this project, which supported 2 Ph.D. and 4 M.S students and provided undergraduate research experiences for 4 B.S. students. This CSM project was selected from a pool of over 60 projects funded within DOD's environmental research program.